IN THE UNITED STATES PATENT AND TRADEMARK OFFICE

In re Inter Partes Review of	§
	§
U.S. Patent No. 10,027,184	§
	§
Issue Date: July 17, 2018	§
	§
Filing Date: June 1, 2016	§
	§

DECLARATION OF INGRID HSIEH-YEE, PH.D.

Table of Contents

I. Introduction 3
A. Qualifications and Professional Experience 4
B. MARC, OCLC and WorldCat 5
C. WorldCat on OCLC FirstSearch 8
D. Library Catalogs 9
E. Information Systems Consulted 10
F. Scope of This Declaration 10
G. Evidence Considered in Forming My Opinions 10
II. Authenticity and Public Availability of *Wang* (Ex. 0001) 12
A. Authentication 12
B. Bibliographic and MARC Records 14
C. Internet Archive Records of Library Online Catalog 17
D. WorldCat Record 20
E. OCLC FirstSearch Record 21
F. Summary of My Opinion on *Wang* 22
III. Conclusion 24

InductEV, Inc.
Exhibit 1010
Page 002

I. Introduction

I, Ingrid Hsieh-Yee, Ph.D., do hereby declare as follows:

1. I am over the age of eighteen (18) and otherwise competent to make this declaration.

2. I have been retained as an independent expert witness on behalf of InductEV, Inc. ("INDUCTEV") for proceedings before the United States Patent and Trademark Office ("PTO") regarding the authenticity and public availability of certain prior art reference in relation to US Patent No. 10,027,184.

3. I am being compensated for my work in this matter at my customary hourly rate of $300 per hour. I am also being reimbursed for any reasonable expenses associated with my work and testimony in this investigation. My compensation is not contingent on the results of my study, the substance of my opinions, or the outcome of this matter.

4. I reserve the right to supplement or amend my opinions in response to any additional evidence, testimony, discovery, argument, and/or other additional information that may be provided to or obtained by me after the date of this declaration.

InductEV, Inc.
Exhibit 1010
Page 003

A. Qualifications and Professional Experience

5. My complete qualifications and professional experience are described in my academic curriculum vitae (**Appendix A**). The following is a brief summary of my relevant qualifications and professional experience.

6. I was a professor in the Department of Library and Information Science at the Catholic University of America for 32 years, retired at the end of August 2022, and was conferred the title of Professor Emerita in December 2022. I have experience working in an academic library, a medical library, and a legislative library. I hold a Masters and a Ph.D. in Library and Information Studies from the University of Wisconsin-Madison.

7. I am an expert on library cataloging and classification and have published two editions on this subject, *Organizing Audiovisual and Electronic Resources for Access*: *A Cataloging Guide* (2000 and 2006). I taught a variety of courses, including Cataloging and Classification, Advanced Cataloging and Classification, Organization of Internet Resources, Organization of Information, Metadata, Digital Content Creation and Management, Internet Searches and Web Design, Information Literacy Instruction, Advanced Information Retrieval and Analysis Strategies, and The Information Professions in Society. I am familiar with metadata schema design and implementation. In my teaching I covered the design and implementation of metadata in databases, search engines, digital repositories,

InductEV, Inc.
Exhibit 1010
Page 004

digital libraries, and digital archives. I also covered how information organization affects the discovery and access to digital resources on the Internet. My research interests cover cataloging and classification, information organization, metadata, information retrieval, information architecture, digital collections, scholarly communication, social media, user interaction with information systems, and others.

B. MARC, OCLC and WorldCat

8. I am very familiar with a library cataloging encoding standard known as the "Machine-Readable Cataloging" standard, also known as "MARC," which became the national standard for sharing bibliographic data in the United States by 1971 and the international standard by 1973. MARC is the primary communications protocol for the transfer and storage of bibliographic metadata in libraries. Experts in my field reasonably rely upon MARC records when forming their opinions.

9. A MARC record consists of several fields, each of which contains specific data about the work. Each field is identified by a standardized, unique, three-digit code corresponding to the type of data that follows. **Appendix B** is a true and correct copy of Parts VII to X of "Understanding MARC Bibliographic: Machine-Readable Cataloging" (http://www.loc.gov/marc/umb/um07to10.html) from the Library of Congress that explains commonly used MARC fields. For example, the personal author of a work is recorded in Field 100, the title is recorded in Field 245, publisher information is recorded in Field 260, the physical volume and

InductEV, Inc.
Exhibit 1010
Page 005

characteristics of a publication are recorded in Field 300, and topical subjects are recorded in Fields 650.

10. The Online Computer Library Center (OCLC) is the largest bibliographic network of the world, with more than 548 million records and thousands of member institutions (many of which are libraries of some type) in more than 100 countries. OCLC was founded in 1967 to promote and support library cooperation. According to the "Third Article, Amended Articles of Incorporation of OCLC Online Computer Library Center, Inc.," OCLC was created "to establish, maintain and operate a computerized library network and to promote the evolution of library use, of libraries themselves, and of librarianship, and to provide processes and products for the benefit of library users and libraries, including such objectives as increasing availability of library resources to individual library patrons and reducing the rate of rise of library per-unit costs, all for the fundamental public purpose of furthering ease of access to and use of the ever-expanding body of worldwide scientific, literary and educational knowledge and information" (source: https://www.oclc.org/content/dam/oclc/membership/articles-of-incorporation.pdf).

11. OCLC members can contribute original cataloging records in MARC to the system or derive cataloging records from existing records, an activity referred to as "copy cataloging." When an OCLC participating institution acquires a work, it can create an original MARC record for the work in OCLC's Connexion system (a

InductEV, Inc.
Exhibit 1010
Page 006

system for catalogers to create and share MARC records), and the system will automatically generate a code for the date of record creation in the yymmdd format, and the creating library's OCLC symbol is recorded in subfield "a" of the 040 field. Once the MARC record is in Connexion, it becomes available to other OCLC members for adoption to their local online catalogs (*i.e.*, copy cataloging).

12. After a MARC record is created in Connexion, it also becomes searchable and viewable on WorldCat, which is a free web portal for users to explore more than 10,000 libraries worldwide. Records in WorldCat, however, are not presented in MARC fields. Instead, the data elements are labeled to help users interpret the records. Thus, the information stored in MARC records in Connexion is available to the interested public through the user-friendly WorldCat web portal.

13. WorldCat (http://www.worldcat.org) is "the world's largest network of library content and services" and its features are summarized in "What is WorldCat" (https://www.worldcat.org/about). WorldCat began operation in January 1998 as a free web portal to more than 10,000 libraries worldwide. Through WorldCat, users can search for information resources in their local libraries and libraries around the world. WorldCat allows users to search for books, CDs, videos, and many new types of digital content, such as audiobooks, in many languages. Users can also retrieve research materials and article citations with links to their full text. After an item is retrieved, WorldCat helps users identify a library nearby that holds the item or all

InductEV, Inc.
Exhibit 1010
Page 007

the libraries that hold the item. WorldCat is an efficient way to explore the content held by more than 10,000 libraries around the world. WorldCat is publicly accessible, and there is no fee to perform a search on WorldCat.

C. WorldCat on OCLC FirstSearch

14. WorldCat is an information system of OCLC that contains more than 548 million records representing holdings of many libraries around the world. OCLC has provided three ways for users to access the WorldCat system. For the general public, OCLC provides WorldCat as a free web portal to facilitate the discovery and access to works held by more than 10,000 libraries worldwide. For libraries, OCLC provides a more technical system, the Connexion system, for catalogers to create and share MARC records to expedite copy cataloging and facilitate interlibrary loans. For reference librarians and researchers, OCLC provides OCLC FirstSearch for these users to explore the WorldCat database. OCLC FirstSearch provides online access to six OCLC databases including WorldCat. A key difference between WorldCat the free portal and the WorldCat database on OCLC FirstSearch is that FirstSearch records display holdings information and more technical details on publications, such as the date when a record was added to the WorldCat system, and the latest date when the record was updated. OCLC FirstSearch requires institutional subscriptions for user access.

InductEV, Inc.
Exhibit 1010
Page 008

D. Library Catalogs

15. Library online catalogs gained acceptance in the early 1980s and many libraries migrated their systems to the World Wide Web in the mid-1990s. Library online catalogs are based on MARC records that represent their collections in order to help the public understand what materials are publicly accessible in those libraries. Most libraries with online catalogs have made their catalogs freely available on the Web. These online catalogs offer user-friendly search interfaces. Strong user interest in keyword searches and the popularity of Google have led to the "googlization" of library search systems. As a result, many library catalogs nowadays provide a single search box for users to conduct keyword searches, with additional support for searches by author, title, subject terms, and other data elements such as ISBN (International Standard Book Number). Library catalogs these days also offer features for users to narrow their search results by language, year, format, and other elements. Many libraries display MARC records on their online catalogs with labels for the data elements to help the public interpret MARC records. Many libraries also offer the option to display MARC records in MARC fields.

InductEV, Inc.
Exhibit 1010
Page 009

E. Information Systems Consulted

16. I am personally familiar with many online catalogs, databases, and search engines. In preparing for this declaration, I used the following authoritative information systems to search for records:

- Internet Archive (https://archive.org/)
- OCLC FirstSearch (https://firstsearch.oclc.org/)
- Online catalog of the University of Auckland Library (https://auckland.primo.exlibrisgroup.com/discovery/search?vid=64UAUCK_INST:NEWUI)
- WorldCat (https://www.worldcat.org/)

F. Scope of This Declaration

17. I have been asked to offer an opinion on the authenticity and public availability date of the following document:

> Wang, C. S. (2004). Design considerations for inductively coupled power transfer systems, Doctoral dissertation, Electrical and Computer Engineering, University of Auckland, **Ex. 0001** ("*Wang*").

G. Evidence Considered in Forming My Opinions

18. In the preparation of this declaration, I have reviewed the documents referenced below and any other documents I reference herein, and each of these is a

InductEV, Inc.
Exhibit 1010
Page 010

type of material that experts in my field would reasonably rely upon when forming their opinions:

(1) The document referenced above in Section I.F;

(2) Bibliographic and MARC records for *Wang*, available at https://auckland.primo.exlibrisgroup.com/permalink/64UAUCK_INST/13vfdcn/alma99154109314002091 from the online catalog of the_University of Auckland Library, accessed and obtained on October 12, 2023, **Appendix 0001A**;

(3) "Statute & Guidelines for the Degree of Doctor of Philosophy (PHD)" of the University of Auckland, archived on December 18, 2005, by the Internet Archive, and available at https://web.archive.org/web/20051218124139/http://www.postgrad.auckland.ac.nz/postgraddegree/PolicyGuidelines/PDF/2003statuteguide.pdf, accessed and obtained on October 16, 2023, **Appendix 0001B**;

(4) Archived copies of the online catalog of the University of Auckland Library, including the search screen archived by the Internet Archive on February 2, 2001, available at https://web.archive.org/web/20010202154200/http://voyager.auckl

InductEV, Inc.
Exhibit 1010
Page 011

and.ac.nz/; the online catalog website archived on October 10, 2006, available at https://web.archive.org/web/20061010050227/http://voyager.auckland.ac.nz/; and the "General Library Thesis Booking" webpage archived on June 24, 2004, available at https://web.archive.org/web/20040624051430/http://www.library.auckland.ac.nz/forms/thesis/thesis.asp, accessed and obtained on October 16, 2023, **Appendix 0001C**;

(5) WorldCat record for *Wang*, available at https://www.worldcat.org/title/156754859, accessed and obtained on October 12, 2023, **Appendix 0001D**;

(6) OCLC FirstSearch record for *Wang*, available at LINK (subscription required for access), accessed and obtained on October 12, 2023, **Appendix 0001E**.

II. Authenticity and Public Availability of *Wang* (Ex. 0001)

A. Authentication

18. **Ex. 0001** is a true and correct copy of "Design considerations for inductively coupled power transfer systems," ("*Wang*"), a doctoral dissertation completed by Chwei-sen Wang at the University of Auckland in 2004, that I received from counsel. I understand from counsel that this copy was obtained from the

InductEV, Inc.
Exhibit 1010
Page 012

University of Auckland Library via a document delivery service. This is indicated on page 1 of the document, which is a document request for the Wisconsin TechSearch (WTS) service provided by the University of Wisconsin-Madison. The webpage indicated on the request sheet (wts.wisc.edu) confirms that WTS provides an "Article Delivery and Research Services for Professionals." I am familiar with WTS, which in my experience is a reliable and well-known service for obtaining copies of documents from libraries around the world.

19. Page 1 is the document request sheet. Page 2 is the title page that shows "Design considerations for inductively coupled power transfer systems" is the title, Chwei-Sen Wang is the author, and this thesis was completed for "the degree of Doctor of Philosophy in Electrical and Computer Engineering, The University of Auckland, 2004." Page 3 shows a library date stamp of "University of Auckland Library … OCT 2005" that indicates this work was added to the library collection no later than October 2005. Pages 4 and 5 (internal pages i and ii) are the abstract, and the Acknowledgements on internal page iii shows a date of "Oct. 21, 2004." The table of contents from internal pages iv to x shows this thesis has nine chapters, 10 appendices, a section for Nomenclature, a list of figures (some in color), and a list of tables. **Ex. 0001** shows the front matter ends on internal page xxvi, each chapter (except Chapter 6) includes references, and the appendices begin on internal page 239 and end on internal page 253.

InductEV, Inc.
Exhibit 1010
Page 013

20. **Ex. 0001** is in a condition that creates no suspicion about its authenticity. Specifically, this copy is not missing any intermediate pages, the text on each page appears to flow seamlessly from one page to the next, and there are no visible alterations to the document. In addition, **Ex. 0001** is in the custody of the library at the institution that granted the doctoral degree to the author. I therefore see no reason to question the authenticity of this copy of *Wang* (**Ex. 0001**).

21. I note that the document submitted as Exhibit 1008 in this *inter partes* review is the same copy of *Wang* as **Ex. 0001**, simply with the vendor's document retrieval form on page 1 removed.

B. Bibliographic and MARC Records

22. **Appendix 0001A** is a true and correct copy of the bibliographic and MARC records for *Wang*. I personally located, identified, and obtained these records from the online catalog of the University of Auckland Library. They are the type of record experts in my field would reasonably rely upon when forming their opinions. I used screen captures to produce this appendix.

23. Pages 1 to 4 of **Appendix 0001A** are the bibliographic record that shows the author, title, and publication year of this work and identifies it as a thesis completed for the Electrical and Electronic Engineering Department of the University of Auckland. The record indicates the full text of *Wang* is available from the university's institutional repository and a link to "e-Theses University of

InductEV, Inc.
Exhibit 1010
Page 014

Auckland" is provided for users to access it. The library bibliographic record shows the print version of *Wang* is in the "On-Demand Collection" and loanable, and users can place a request for this work. The record details area shows the title, author, thesis note, publication date ("2004"), and a contents note which is the abstract from *Wang*. It also shows three subject terms ("Electric current converters," "Electric power transmission," and "power electronics") are included to represent the subjects of this work, and to enable users to conduct subject searches to find this thesis. The Description note shows the pagination and other characteristics of this work. The link to "Display source record" leads to the MARC record. The title, author, degree and degree granting institution, publication year, abstract, and physical description match the information presented in **Ex. 0001**, confirming this record represents the *Wang* thesis.

24. Page 5 is the MARC record that shows the date of record creation. The first six digits of Field 008 show the MARC record was created on "051020" (*i.e.*, October 20, 2005), and the "s2004" code following this creation date indicates this work has a single publication date of 2004. Subfield "a" of Field 040 shows the record is from a New Zealand library, and Subfield "c" of this field shows the transcribing cataloging agency is "UV0." According to the *Directory of OCLC Members* (https://www.oclc.org/en/contacts/libraries.html), "UV0" is the OCLC library symbol for the University of Auckland Library. Field 008 and Field 040

InductEV, Inc.
Exhibit 1010
Page 015

inform my opinion that the University of Auckland Library created this MARC record for *Wang* on October 20, 2005, making this work discoverable in the library online catalog from that date on. Field 035 shows this record has an OCLC number of "156754859," meaning the record was entered into OCLC.

25. The MARC record shows the author, title, publication year, physical description, thesis note, bibliographical reference note, and a link to the online version of this thesis in Field 856. The record also shows subjects of this thesis are represented by three Library of Congress subject headings in Fields 650, including "Electric current converters," "Electric power transmission," and "Power electronics." These subject headings support users to search for this thesis by subject headings and keywords in the headings.

26. This MARC record (**Appendix 0001A**) shows *Wang* was published in 2004, and the University of Auckland Library cataloged this thesis and created a MARC record for it on October 20, 2005. By that date, interested users would have been able to conduct subject searches by the Library of Congress subject headings in this MARC record to discover this work. They would also have been able to search for this thesis by its author and title.

27. A customary library practice is to process a newly cataloged work promptly to make it publicly accessible. In most academic libraries, the processing would take no more than a week after the MARC record is completed. According to

InductEV, Inc.
Exhibit 1010
Page 016

the University of Auckland's "Statute & Guidelines for the Degree of Doctor of Philosophy (PHD)" that covers all doctorate candidates at the university from March 2003 on, the Board of Graduate Studies "has approved the submission of theses in temporary binding as an option for PhD candidates for examination purposes" and after the examination is completed, "three hardbound copies of the thesis…must be deposited with the Graduate Centre before a conferment of degree form will be issued" (see Appendix A in **Appendix 0001B**, a copy of the statute & guidelines archived on December 18, 2005, by the Internet Archive, and available at https://web.archive.org/web/20051218124139/http://www.postgrad.auckland.ac.nz/postgraddegree/PolicyGuidelines/PDF/2003statuteguide.pdf). The guidelines show that three hardbound copies of a thesis must be deposited with the university before a degree can be conferred. This document informs my opinion that after *Wang* was cataloged on October 20, 2005, the thesis would have become available for user request by October 27, 2005.

C. Internet Archive Records of Library Online Catalog

28. To demonstrate that the online catalog of the University of Auckland Library was available to the public in the early 2000s, I searched the Internet Archive for records. **Appendix 0001C** is a true and correct copy of the archived copies of the library catalog from the Internet Archive. I personally located, identified, and obtained this archived copy. This is the type of material experts in my field would

InductEV, Inc.
Exhibit 1010
Page 017

reasonably rely upon when forming their opinions.

29. Page 1 of **Appendix 0001C** is a screen capture of a WayBack Machine calendar that shows the library catalog (http://voyager.auckland.ac.nz) was archived 84 times between "16 Jan 1999" and "3 Mar 2022" and this particular copy was archived on "Feb 02 2001" by the Internet Archive and available at https://web.archive.org/web/20010202154200/http://voyager.auckland.ac.nz/. Page 2 is the PDF version of the same archived copy. These two pages show that by February 2, 2001, the Voyager online catalog of the University of Auckland would have been available to users and five types of searches were available.

30. Page 3 shows a screen capture of a WayBack Machine calendar that shows this particular copy of the Voyager catalog was archived on "OCT 10 2006" and available at https://web.archive.org/web/20061010050227/http://voyager.auckland.ac.nz/, and three types of searches were available to users. Page 4 is a screen capture of the "Main Search List" to show the search options for users. Page 5 is a PDF version of the copy of the library catalog archived on October 10, 2006, and it shows a form entitled "General Library Theses Booking" was available for theses held in the General Library. Pages 6 is a screen capture that shows a WayBack Machine calendar indicating "Booking Form for General Library Theses Only" was archived eight times, and this particular copy was archived on "JUN 24 2004" and available

InductEV, Inc.
Exhibit 1010
Page 018

at

https://web.archive.org/web/20040624051430/http://www.library.auckland.ac.nz/forms/thesis/thesis.asp. Page 7 is the PDF version of this archived copy, and it informs users how theses can be requested and used.

31. Internet Archive is a digital library that archives cultural heritage materials, scholarly research, and other web resources from the Internet and provides users with free access to its collections. I have used Internet Archive in the past and am familiar with their practice of assigning an extended URL to an archived file in the format of_http://www.archive.org/web/[Year in yyyy][Month in mm][Day in dd][Time code in hh:mm:ss]/[Archived URL] to show the point of time the archived file was captured.

32. The URLs of the archived copies in **Appendix 0001C** show that the Voyager online catalog of the University of Auckland Library was available to users no later than February 2, 2001, the General Library Theses Booking Form was available to users no later than June 24, 2004, and the Voyager catalog offered users several search options no later than October 10, 2006. Because Internet Archive may not capture web resources when they first appear on the Internet, the archive date does not represent the first time a web resource appears on the Internet, so the archive date of_Internet Archive should be interpreted as the "no later than" date, meaning the archived resource was publicly accessible on the Internet no later than that date.

InductEV, Inc.
Exhibit 1010
Page 019

The archive dates of archived copies in **Appendix 0001C** therefore mean that the Voyager catalog of the University of Auckland Library was publicly available on the Internet by February 2001, and the thesis request form was publicly accessible by June 24, 2004, and the Voyager catalog was definitely available to the public on the Internet as of October 10, 2006. These archived copies mean that the MARC record for *Wang*, which was completed on October 20, 2005, would have been publicly searchable through the University of Auckland's Voyager online catalog no later than October 10, 2006, and users would have been able to use the "General Library Theses Booking" form to request access to this thesis.

D. WorldCat Record

33. To determine whether *Wang* was discoverable on WorldCat, the free web portal, I searched WorldCat for records and found a record at https://www.worldcat.org/title/156754859. The record number of "156754859" is the same as the OCLC number in Field 035 of the MARC record created by the University of Auckland Library (**Appendix 0001A**). **Appendix 0001D** is a true and correct copy of the record for *Wang* that I personally located, identified, and obtained. This is the type of record experts in my field would reasonably rely upon when forming their opinions.

34. Page 1 of **Appendix D** shows the title, author, abstract, publication date ("2004") and degree granting institution of *Wang*, and a side box shows users can

InductEV, Inc.
Exhibit 1010
Page 020

borrow this thesis from the University of Auckland, General Library.

E. OCLC FirstSearch Record

35. The WorldCat record for *Wang* confirms that users would have been able to discover this thesis in the free web portal, but the WorldCat record alone does not provide information on when the record was added to the WorldCat system. To determine the record entry date, I searched the WorldCat database in OCLC FirstSearch. **Appendix 0001E** is a true and correct copy of the WorldCat record for *Wang* in OCLC FirstSearch. I personally located, identified and obtained this record. This is the type of record experts in my field would reasonably rely upon when forming their opinions.

36. Page 1 of **Appendix 0001E** shows the title, author, and OCLC accession number ("156754859") for *Wang*, and the "Location" area shows the University of Auckland Library (library code "UV0") is the only library holding this work. The OCLC number, location, title, author, publication year, description, dissertation note, language, abstract, and the first three subject descriptors are the same as the details presented in the library records (**Appendix 0001A**). The "Date of Entry" field shows that "20051020" (i.e., October 20, 2005) is the date when this record was entered into the WorldCat system. **Appendix 0001E** informs my opinion that the record for *Wang* was entered into the WorldCat system on October 20, 2005, and became discoverable from that date on to OCLC member libraries, OCLC

InductEV, Inc.
Exhibit 1010
Page 021

FirstSearch users, and users of WorldCat, the free web portal. After users discovered the record, they would have been able to contact the university library to borrow the Wang thesis.

F. Summary of My Opinion on *Wang*

37. The copy of *Wang* (**Ex. 0001**) obtained from the University of Auckland Library is authentic because this work has been in the custody of the library of the degree granting institution. This copy carries a library date stamp of "OCT 2005" and the library's bibliographic and MARC records (**Appendix 0001A**) show this work was cataloged on October 20, 2005, making the thesis discoverable in the library's online catalog (indexed by title, author, and subject) from that date on. The university's thesis guidelines (**Appendix 0001B**) shows that a dissertator would have to deposit three hardbound copies of their thesis before the doctoral degree could be conferred, and that means it should not take the library much time to make the thesis publicly accessible after the MARC record was created. It is therefore my opinion that *Wang* would have been discoverable in the library catalog from October 20, 2005, on, and the library copy of this work would have become publicly accessible by October 27, 2005. Archived copies of the library online catalog obtained from Internet Archive (**Appendix 0001C**) show the Voyager catalog of the library was publicly accessible to users on the Internet no later than February 2, 2001, and the General Library Theses Booking form has been publicly

InductEV, Inc.
Exhibit 1010
Page 022

available no later than June 24, 2004. The Voyager catalog archived on October 10, 2006, shows the system was still available to the general public at that time, and that means the record for *Wang* created on October 20, 2005, would have been discoverable through the online catalog of the University of Auckland Library no later than October 10, 2006. The WorldCat record for *Wang* (**Appendix 0001D**) shows this thesis can be found in WorldCat, the free web portal. The OCLC FirstSearch record for *Wang* (**Appendix 0001E**) shows the record was entered into the WorldCat system on October 20, 2005, and from that date on, the record would have made *Wang* discoverable for OCLC member libraries, OCLC FirstSearch users, and the general public who use WorldCat the free portal. After interested users discovered the record, they would have been able to contact the University of Auckland Library to request access to *Wang*. For these reasons, it is my opinion that *Wang* was published in 2004, publicly discoverable by October 20, 2005, and the library copy of this thesis would have been publicly accessible to the public no later than October 27, 2005.

InductEV, Inc.
Exhibit 1010
Page 023

III. Conclusion

38. I hereby declare that all statements made herein of my own knowledge are true and that all statements made on information and belief are believed to be true, and further, that these statements were made with the knowledge that willful false statements and the like so made are made under penalty of perjury.

Date: 10-17-2023 Executed: Ingrid Hsieh-Yee

Ingrid Hsieh-Yee, Ph.D.

InductEV, Inc.
Exhibit 1010
Page 024

Appendix 0001A

https://auckland.primo.exlibrisgroup.com/discovery/fulldisplay?context=L&vid=64UAUCK_INST:NEWUI&search_scope=MyInst_an

UNIVERSITY OF AUCKLAND Waipapa Taumata Rau NEW ZEALAND

Search all | Databases | Journals | Collection discovery | Interlibrary loan | Catalogue help | ••• | English | Māori | Sign in | Menu

Search all

Search All

Advanced Search

All | Articles | Books | Book chapters | Journals | Databases | Videos | More

Top
Send to
View online
Get it
Details
Browse shelf
Links
Tags

THESIS

Design considerations for inductively coupled power transfer systems

Wang, Chwei-sen, author.

PhD Electrical and Electronic Engineering University of Auckland 2004

2004

Available at ON-DEMAND COLLECTION Place a Request (A1b18.13). >

Available Online >

Send to

QR | EXPORT TO EXCEL | EXPORT BIBTEX | ENDNOTE | EASYBIB | ENDNOTE WEB | REFWORKS

PRINT | CITATION | PERMALINK | E-MAIL

https://auckland.primo.exlibrisgroup.com/permalink/64UAUCK_INST/13vfdcn/alma99154109314002091

COPY THE PERMALINK TO CLIPBOARD

View online

Full text availability

e-Theses University of Auckland

Found a broken link? Report it.

Get it

Please sign in to see request options and to place requests. Sign in

BACK TO LOCATIONS

LOCATION ITEMS

ON-DEMAND COLLECTION
Available , Place a Request ; A1b18.13
(1 copy, 1 available, 0 requests)

Item in place
Loanable

Details

Title	Design considerations for inductively coupled power transfer systems
Author(s)	Wang, Chwei-sen, author.
Thesis note	PhD Electrical and Electronic Engineering University of Auckland 2004
Publication date	2004
Contents	Inductively coupled power transfer (ICPT) systems use electromagnetic fields to transfer electric power from a primary source (power supply) to one or more secondary loads (pickups). Because there is no physical contact between the primary and secondary, ICPT systems are intrinsically safe and reliable. This technology has been significantly commercialised for around a decade. Present applications include material handling, public transport, and battery charging. This thesis focuses on the design of ICPT

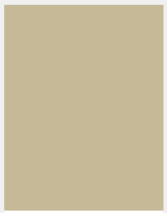
Details

Title	Design considerations for inductively coupled power transfer systems
Author(s)	Wang, Chwei-sen, author. ›
Thesis note	PhD Electrical and Electronic Engineering University of Auckland 2004
Publication date	2004
Contents	Inductively coupled power transfer (ICPT) systems use electromagnetic fields to transfer electric power from a primary source (power supply) to one or more secondary loads (pickups). Because there is no physical contact between the primary and secondary, ICPT systems are intrinsically safe and reliable. This technology has been significantly commercialised for around a decade. Present applications include material handling, public transport, and battery charging. This thesis focuses on the design of ICPT systems for high power applications where both the primary and secondary coils are compensated by capacitors. The main aim is to develop systems with smaller size, less weight, lower cost, greater power and better efficiency. Previous work in this field has concentrated on either the power supply or the pickup. This thesis instead focuses on the interactions between the power supply and the pickup. When power is transferred from the primary to the secondary, the primary is affected by the secondary loading. This can result in poor displacement power factor (DPF), reduced power transfer capability, and a loss of controllability. First, steady state linear mathematical models are developed to represent the load seen by the power supply that includes the primary compensation capacitor, the electromagnetic structure, the secondary compensation capacitor, and the pickup load. These models quantify the system behaviour in terms of the fundamental design parameters, and are used to evaluate a design procedure for ICPT systems. This evaluation provides an insight into the system, enabling suitable design decisions as well as quantification of frequency bifurcation boundaries in variable-frequency systems. Several new primary tuning schemes are also proposed, taking into account the secondary loading effects. In loosely coupled systems, the primary and secondary resonant circuits can be tuned independently as the secondary loading effect on the primary are negligible. In well-coupled systems, the secondary loading affects the primary resonance significantly, and the proposed new tuning schemes greatly improve the DPF and power transfer capability. Various sensitivity analyses to variations in the primary and secondary compensation capacitances as well as misalignment of the electromagnetic structure show that systems designed using the proposed new tuning schemes have similar sensitivities compared with the original tuning. Throughout the thesis work, an LCL resonant inverter driving a contact-less electric vehicle battery charger was used to verify the proposed theory. The operation of this inverter under discontinuous current mode is also investigated. A novel design procedure is detailed and verified that enables this inverter to deliver maximum power to the load.
Subjects	Electric current converters › Electric power transmission › Power electronics ›
Genre	Academic theses
Description	xxvi, 253 pages : illustrations (some color) ; 30 cm
Language	English

InductEV, Inc.
Exhibit 1010
Page 028

Language	English
Data Source	99154109314002091

Browse shelf



...elopment ...STEP-...pliant ...ufacturin ...tabase for ...



Development of a STEP-compliant manufacturing database for ...

2005



Real-time multiprocessor implementation of an ...

2005



Design considerations for inductively coupled power transfer ...

2004



A hierarchical Bayesian model and simulation software for ...

2005



Bridge abutment scour countermeasures ...

2005



Links

Display source record

InductEV, Inc.
Exhibit 1010
Page 029

https://auckland.primo.exlibrisgroup.com/discovery/sourceRecord?vid=64UAUCK_INST:NEWUI&docId=alma99154109314002091

```
leader  03859cam a2200277Ii 4500
001     99154109314002091
005     20201203130722.0
008     051020s2004    nz a     mb   000 0 eng d
035     ##$a(OCoLC)156754859
035     ##$a(OCoLC)ocn156754859
040     ##$aNz $beng $erda $cUV0 $dOCLCQ $dOCLCF $dOCLCO $dOCLCQ $dOCLCO $dOCL $dUV0
100     1#$aWang, Chwei-sen, $eauthor.
245     10$aDesign considerations for inductively coupled power transfer systems / $cby Chwei-sen Wang.
264     #0$c2004.
300     ##$axxvi, 253 pages : $billustrations (some color) ; $c30 cm
336     ##$atext $btxt $2rdacontent
337     ##$aunmediated $bn $2rdamedia
338     ##$avolume $bnc $2rdacarrier
502     ##$bPhD $gElectrical and Electronic Engineering $cUniversity of Auckland $d2004
504     ##$aIncludes bibliographical references.
520     3#$aInductively coupled power transfer (ICPT) systems use electromagnetic fields to transfer electric power from a primary source (power supply) to one or
650     #0$aElectric current converters.
650     #0$aElectric power transmission.
650     #0$aPower electronics.
655     #7$aAcademic theses. $2lcgft
856     41$uhttp://hdl.handle.net/2292/52289 $ze-Thesis University of Auckland
```

Appendix 0001B

https://web.archive.org/web/20051218124139/http://www.postgrad.auckland.ac.nz/postgraddegree/PolicyGuidelines/PDF/ 150%
http://www.postgrad.auckland.ac.nz/postgraddegree/PolicyGuidelines/PDF/2003statuteguide.pdf Go MAY DEC FEB
6 captures 18
17 May 2005 - 24 Aug 2007 2004 2005 2007 About this capture
1 of 40 Automatic Zoom

STATUTE & GUIDELINES FOR THE DEGREE OF DOCTOR OF PHILOSOPHY (PHD)

This document details the Statute for the Degree of Doctor of Philosophy, and includes guidelines explaining how this Statute is applied and what procedures are involved in PhD registration. These guidelines also explain how the Board of Graduate Studies interprets and applies the Statute for the degree of Doctor of Philosophy at The University of Auckland.

InductEV, Inc.
Exhibit 1010
Page 032

STATUTE & GUIDELINES FOR THE DEGREE OF DOCTOR OF PHILOSOPHY (PHD)

This document details the Statute for the Degree of Doctor of Philosophy, and includes guidelines explaining how this Statute is applied and what procedures are involved in PhD registration. These guidelines also explain how the Board of Graduate Studies interprets and applies the Statute for the degree of Doctor of Philosophy at The University of Auckland.

This document is intended for people who are registered as candidates for the PhD Degree, or who wish to register as candidates for the PhD, and for those involved with the administration, supervision and examination of the PhD at The University of Auckland.

All candidates who are registered for the degree of Doctor of Philosophy at The University of Auckland from 1 March 2003 and those who have chosen to transfer from the 1999 Statute are governed by the Statute detailed in these Guidelines.

This document can be accessed online through:
www.postgrad.auckland.ac.nz

InductEV, Inc.
Exhibit 1010
Page 033

CONTENTS

STATUTE FOR THE DEGREE OF DOCTOR OF PHILOSOPHY

CLAUSE 1 PREAMBLE **6**

CLAUSE 2 ELIGIBILITY **7**

CLAUSE 3 ADMISSION **8**

CLAUSE 4 REGISTRATION **8**

Registration Essential 8
Provisional Registration 8
Application for Registration 8
Part-time Registration 8
Non-resident Candidature 9
Concurrent Registration 9
Role of the Head of Department 9
Presentation in te reo Maori 10
Role of the Board of Graduate Studies 10
Date of Registration 10
Supervision 11
Co-Supervisors and Advisors 11
Coursework 11

CLAUSE 5 REVIEWS OF REGISTRATION **12**

Provisional Goals 12
Provisional Review 12
Annual Review of Registration 13
Specified Conditions for Registration 13
Recommendation to Terminate 13

CLAUSE 6 ENROLMENT AND FEES **13**

Enrolment 13
Refunds 14
Fees Other than Tuition Fees 14
Fees to be Paid before Thesis Accepted 14
Other Fees Payable 14

InductEV, Inc.
Exhibit 1010
Page 034

CLAUSE 7 CHANGES TO CONDITIONS OF REGISTRATION 14

Absence from the University 15
Changes in Supervision 15
Change to Part-time Registration 15
Extension of Time for Submission 15
Suspension of Registration 15
Termination of Registration 16

CLAUSE 8 SUBMISSION 16

Copies of Thesis 16
Time for Submission 17
Notification of Submission 17
Declaration as to Originality 17
Statement from Supervisors 17
Language of Thesis 17

CLAUSE 9 EXAMINATION 18

General Provisions 18
Nomination of Examiners 18
Appointment of Examiners 18
Appointment of Examination Committee 18
Examiners' Reports 19
Replacement of Examiners 19
Consideration of Examiners' Reports 20
Recommendation of the Examination Committee 20
Further Examiners 20
Oral Examination 21
Recommendation of the Oral Examination 21
When Revision and Resubmission are Permitted 22
Final Decision 23
Copies for Deposit 23

CLAUSE 10 APPEALS 23

As to Registration 23
As to Examination 24

CLAUSE 11 DISPUTE RESOLUTION PROCEDURES 25

CLAUSE 12 TRANSITIONAL ARRANGEMENTS 25

InductEV, Inc.
Exhibit 1010
Page 035

GUIDELINES

ELIGIBILITY 26

Guideline 1 26
Guideline 2 26
Guideline 3 26
Guideline 4 27
Guideline 5 27

ADMISSION 27

Guideline 6 27

REGISTRATION 28

Guideline 7 28
Guideline 8 28
Guideline 9 28
Guideline 10 28
Guideline 11 29
Guideline 12 29
Guideline 13 29
Guideline 14 29
Guideline 15 29
Guideline 16 30

REVIEWS OF REGISTRATION 30

Guideline 17 30
Guideline 18 30

ENROLMENT AND FEES 31

Guideline 19 31
Guideline 20 31

CHANGES TO CONDITIONS OF REGISTRATION 31

Guideline 21 31
Guideline 22 32
Guideline 23 32
Guideline 24 32
Guideline 25 33
Guideline 26 33

SUBMISSION 34

Guideline 27 34
Guideline 28 34
Guideline 29 34
Guideline 30 35

InductEV, Inc.
Exhibit 1010
Page 036

EXAMINATION **35**
Guideline 31 35
Guideline 32 35
Guideline 33 36
Guideline 34 36
Guideline 35 36
Guideline 36 36
APPEALS **36**
Guideline 37 36
TRANSITIONAL ARRANGEMENTS **37**
Guideline 38 37
APPENDICES **38**
Appendix A: The Temporary Binding Option for Theses 38
Appendix B: Library Access for Intending Candidates 38
Appendix C: Web Links to Relevant Postgraduate Policies and Forms 39

InductEV, Inc.
Exhibit 1010
Page 037

STATUTE FOR THE DEGREE OF DOCTOR OF PHILOSOPHY

Please note that all of the forms and most of the policy documents referred to below may be found on the University intranet at ***www.postgrad.auckland.ac.nz*** and are also available in hard copy from the Graduate Centre.

CLAUSE 1 PREAMBLE

a Candidates for the degree of Doctor of Philosophy are required to pursue an approved programme of advanced study and research as enrolled students of the University. The demands of PhD research require a significant commitment by candidates in terms of time and resources, and candidates are normally expected to be working full time on their doctoral research.

b It is expected that this programme will usually be completed within three to four years of full-time candidature. Part-time candidature may also be permitted.

c Upon completion of an approved programme of research, the PhD will be awarded to a candidate who;

i submits a thesis which meets the requirements set out in Clause 1d,

and

ii satisfies the examiners in an oral examination and any other examination that may be required on the subject of the thesis and on relevant matters in the field or fields to which the subject belongs.

d The PhD degree is awarded for a formal and systematic exposition of a coherent programme of advanced research work carried out over the period of registration for the Degree which in the opinion of the examiners and the Board of Graduate Studies satisfies all of the following criteria;

i to be an original contribution to knowledge or understanding in its field,

and

ii to meet internationally recognised standards for such work,

and

iii to demonstrate a knowledge of the literature relevant to the subject and the field or fields to which the subject belongs, and the ability to exercise critical and analytical judgement of it,

and

InductEV, Inc.
Exhibit 1010
Page 038

iv to be satisfactory in its methodology, in the quality and coherence of its written expression, and in its scholarly presentation and format.

e PhD theses may not exceed 100,000 words or 250 pages in total without the permission of the Board of Graduate Studies.

f Where a thesis includes published research papers and/or case studies, published or unpublished, these must be fully integrated into the subject matter and text of the thesis and be listed in the bibliography.

g All research for the thesis is to be conducted in accordance with the University of Auckland Guidelines for the Conduct of Research.

Guidelines for the Conduct of Research

CLAUSE 2 ELIGIBILITY

Candidates for the degree of Doctor of Philosophy are required to have;

a

i completed the requirements for the award of a Master's degree with First Class or Second Class (division I) Honours at the University of Auckland,

Guideline 1

ii completed the requirements for the award of a Bachelor's degree with First Class or Second Class (division I) Honours at the University of Auckland,

or

iii completed all the taught course work requirements for a Masters degree of the University of Auckland at the equivalent of First Class or Second Class (division I) Honours level, and have made substantial progress towards completion of the Master's research thesis,

Guideline 2

or

iv completed the requirements for the award of a qualification that the Board of Graduate Studies considers to be equivalent to a Master's degree with First Class or Second Class (division I) Honours or a Bachelor's degree with First Class or Second Class (division I) Honours from the University of Auckland,

Guideline 3

and

b demonstrated an ability to pursue doctoral level research.

Guideline 4

InductEV, Inc.
Exhibit 1010
Page 039

c In exceptional circumstances, the Board of Graduate Studies may consider for registration a person whose qualifications do not meet the requirements of Clause 2a, if it is satisfied that the person's experience in research and the results of that experience are so outstanding that the person is likely to have the ability to complete the degree successfully.

Guideline 5

CLAUSE 3 ADMISSION

Admission Essential

a Every candidate for the degree of Doctor of Philosophy must have applied for admission and been admitted to the University of Auckland.

Guideline 6

CLAUSE 4 REGISTRATION

Registration Essential

a Every candidate for the degree of Doctor of Philosophy must be registered by the Board of Graduate Studies in accordance with this Clause 4.

Provisional Registration

b Registration is provisional for all candidates for the first twelve months following the Date of Registration as defined in Clause 4k of this Statute.

Guideline 7

Application for Registration

c Application for registration must be made to the Head of the teaching Department, Division or School, Chair of the Board of Studies or the Director of the Research Centre or Institute ("the Head of Department") in the discipline in which the candidate is to be primarily registered.

Guideline 8

Part-time Registration

d Candidates who are in full-time employment in a research supportive environment at the time of first registration, and who expect to continue in that employment situation, may apply to register as part-time students.

Guideline 9

InductEV, Inc.
Exhibit 1010
Page 040

e An applicant with demanding family responsibilities which prevent attending the University and participating in research activities on a full-time basis may apply to be registered as a part-time student.

Non-resident Candidature

f Where an intending candidate is not resident in Auckland, the Head of Department must provide Board of Graduate Studies with evidence that the candidate will be provided with research resources and supervisory support at the location in which the research is to be carried out.
Guideline 10

Off-Campus Registration Policy

Concurrent Registration

g In exceptional cases a candidate may be permitted to enrol concurrently in a second degree in order to complete that degree, provided it is not the qualifying degree for entry into the PhD programme.
Guideline 11

Role of the Head of Department

h The Head of Department will make a recommendation in writing to the Faculty Associate Dean (Postgraduate) as to

i whether the Candidate;

a meets the eligibility requirements,

and

b has a preliminary research proposal capable of meeting the requirements of Clause 1 d of this Statute,

and

c has an appropriate set of goals for the provisional year of registration, agreed to by both the candidate and main supervisor.
Guideline 12

And, if the Head of Department is of that opinion, then:

ii whether their Department (in conjunction with any other Department where the field of study is interdisciplinary, or other University in the case of jointly awarded degrees) accepts the responsibility for;

a making satisfactory supervision arrangements over the whole course of the PhD,

and

InductEV, Inc.
Exhibit 1010
Page 041

b providing adequate research resources and facilities,

Guideline 13
Statement of Resources and Support for PhD Research

and

iii whether the field of study is interdisciplinary, and if so, which other Departments will be involved. In these cases, the Heads of any other Departments involved are required to endorse the recommendation,

Guideline 14

and

iv nominate suitably qualified supervisors and, where appropriate, advisers,

and

v in the case of a candidate in a Department of Languages and Literatures, or a candidate for whom joint registration with another University in a non-English speaking country is proposed, a recommendation as to the language in which the thesis is to be submitted and examined.

Guideline 30
Management of Co-supervised/Jointly Awarded PhD Degrees.

Presentation in te reo Maori

i Candidates wishing to present and defend a thesis in Maori must, before applying to the Head of Department to be registered, obtain the permission of the Pro Vice-Chancellor (Maori). When such permission is granted, the Pro Vice-Chancellor (Maori) will make a recommendation in writing to the Board of Graduate Studies as to;

i whether the candidate has adequate fluency and literacy in te reo Maori in the subject area of the thesis, and

ii the likelihood of being able to find appropriately qualified examiners for the thesis.

Role of the Board of Graduate Studies

j On receipt of the recommendation of the Faculty Associate Dean (Postgraduate), the Board of Graduate Studies will decide whether or not to register the candidate and, if so, the conditions which will apply to the registration. The Board of Graduate Studies may call for any further information it considers relevant before making its decision.

Date of Registration

k Registration takes effect on the date (the "Date of Registration") approved by the Board of Graduate Studies. Where a candidate has already started supervised

InductEV, Inc.
Exhibit 1010
Page 042

research on the PhD topic the Date of Registration may be backdated by not more than six months. For a candidate transferring from a Masters degree under Clause 2 (a)iii, the Date of Registration may be backdated not earlier than the date on which the coursework component of the Master's degree was completed.
Guideline 15
Fees Statute

Supervision

l The Board of Graduate Studies will appoint the supervisors for each candidate. The supervisors must be actively involved in research in the candidate's general field, and must either hold a doctoral degree or be appropriately qualified and experienced. Persons who are themselves candidates for the degree of PhD may not be appointed as supervisors, although they may be appointed as advisers.
Guideline 16
Guidelines on Thesis Supervision

m For each candidate the Board of Graduate Studies will appoint a suitably qualified main supervisor who takes overall responsibility for the supervision of the candidate and for assistance in the provision of research resources. The main supervisor must be a staff member of the University of Auckland.
Guideline 16
Guidelines on Thesis Supervision

Co-Supervisors and Advisers

n In addition, the Board of Graduate Studies will appoint for each candidate;
i at least one suitably qualified co-supervisor

and/or

ii an advisory committee or adviser/s.
Guideline 16
Guidelines on Thesis Supervision

Coursework

o. The Board of Graduate Studies may require the candidate to undertake coursework that is considered to be necessary for the successful completion of the programme of research. Such coursework must be completed as part of the provisional registration requirements, will not normally exceed 8 points in total and should either be at the postgraduate level or, in special cases, at Stage III level. Candidates must normally pass any such coursework at the grade of at least B+ or its equivalent.

InductEV, Inc.
Exhibit 1010
Page 043

CLAUSE 5 REVIEWS OF REGISTRATION

Provisional Goals

a During provisional registration, a candidate must;

i achieve the goals prescribed by the Board of Graduate Studies at the commencement of the registration,

and

ii complete a fully developed research proposal, including a provisional thesis title, a schedule of research, an outline of the thesis structure and a statement of the resources required to complete the research. The research proposal should be submitted for approval to the appropriate postgraduate committee of the Department and/or Faculty in which the candidate is registered. The committee may accept the proposal, or indicate changes needed to the candidate and supervisor(s) and request a resubmission, or it may decline to accept the proposal. It will inform the Head of Department of its decision.

Guideline 17

Provisional Review

b At the end of the twelve months of provisional registration, the supervisor/s and the Head of Department are to submit a formal report to the Board of Graduate Studies on the progress of the candidate. The report should clearly state whether or not the progress of the candidate has been satisfactory, the goals laid down for the provisional year have been achieved and the candidate's research proposal has been approved according to Clause 5a (ii). The report should include a recommendation that the candidate's registration be;

i confirmed,

or

ii terminated,

or

iii continued on a provisional basis for not more than six months.

Guideline 17

c Where the recommendation is to confirm the candidate's registration, the report to Board of Graduate Studies must include a copy of the candidate's full research proposal and provisional thesis title.

InductEV, Inc.
Exhibit 1010
Page 044

Annual Review of Registration

d In each year of registration each candidate must pursue a programme of advanced study and research to the satisfaction of the Head of Department and the main supervisor. At the end of each year of registration following the provisional period, the main supervisor, the candidate and the Head of Department are to submit, through the Associate Dean (Postgraduate) of the Faculty, a joint report to the Board of Graduate Studies on the candidate's progress. As part of this report the main supervisor and the Head of Department are to make one of the following recommendations;

i that the candidate's registration be continued,

or

ii that the candidate's registration be continued subject to specified conditions,

or

iii that the candidate's registration be terminated.

Guideline 18

Specified Conditions for Registration

e Where a recommendation is made under Clauses 5b (iii) or 5d (ii), the Head of Department will also recommend to the Board of Graduate Studies the specific goals and/or conditions to be met by the candidate and the time in which these are to be completed. At the end of this period the Head of Department and Main Supervisor will advise the Board of Graduate Studies whether or not these requirements have been met. Registration will terminate if the specified conditions have not been fulfilled to the satisfaction of the Board of Graduate Studies.

Recommendation to Terminate

f No decision to terminate registration may be made by Board of Graduate Studies unless the candidate has been notified in writing and given reasonable opportunity to respond.

CLAUSE 6 ENROLMENT AND FEES

Enrolment

a Candidates for the PhD Degree must be enrolled and pay fees in each academic year for which they are registered. Candidates need not pay tuition fees for any period during which their registration is suspended under Clause 7f.

InductEV, Inc.
Exhibit 1010
Page 045

b On enrolment in each academic year every candidate must pay the fee prescribed for that academic year.

Guideline 19

Refunds

c A candidate who submits a thesis or terminates their registration will receive a refund of one-twelfth of the tuition fee paid for each complete month of the period between the date of submission of the thesis or termination of registration and the end of the academic year for which fees have been paid.

Fees Other than Tuition Fees

d Unless otherwise exempted under the relevant regulations, all candidates must pay the prescribed Building Levy and Student Services fees and any other fees as may be prescribed from time to time. There is no refund of these fees.

Guideline 19
Fees Statute

Fees to be Paid before Thesis Accepted

e No thesis will be accepted for examination unless outstanding fees have been paid for the academic year in which a candidate is registered.

Other Fees Payable

f Candidates who enrol for courses other than those required as part of their programme for the PhD Degree must pay the fees prescribed for those courses on enrolment.

Guideline 20
Fees Statute

CLAUSE 7 CHANGES TO THE CONDITIONS OF REGISTRATION

a The Head of Department may, after consultation with the candidate, make a written recommendation to the Board of Graduate Studies for changes in the conditions of registration for the candidate. The candidate may express his or her written views on the recommendation to the Board of Graduate Studies if he or she wishes. After considering a recommendation from the Head of Department, Board of Graduate Studies may, after considering any submissions made by the candidate, change the conditions of registration for any candidate.

Guideline 21

InductEV, Inc.
Exhibit 1010
Page 046

Absence from the University

b Where a resident candidate intends to be absent from the University in pursuit of their research for more than two months, supervisors are to submit for approval by the Board of Graduate Studies, through the Head of Department and before the candidate's departure, suitable plans for the supervision of the candidate during their absence.

Guideline 22
Guidelines for Off-Campus Registration.

Changes in Supervision

c When necessary, the Head of Department is to recommend changes to the supervision of the candidate for approval by the Board of Graduate Studies. This will normally be required when a supervisor is granted leave, resigns or retires.

Guideline 23

Change to Part-time Registration

d Candidates who have been registered full-time for a period of two years may apply to be registered part-time.

Guideline 24

Extension of Time for Submission

e When the Postgraduate Committee is satisfied that there is sufficient reason, it may extend a candidate's submission date. Before approving an extension of submission time the Board of Graduate Studies will require the candidate, the supervisor(s) and Head of Department to agree on the programme of supervision and schedule of research considered necessary for submission by the new date proposed.

Suspension of Registration

f Where a candidate is unable to continue with their research programme because of circumstances beyond their control, the Board of Graduate Studies may suspend their registration for a specified period of time. The following conditions apply:

i The length of time for which a candidate's registration may be suspended will be in multiples of whole calendar months.

ii The Board of Graduate Studies must be satisfied that any period of suspension will not adversely affect the viability of the candidate's research.

iii Any period of suspension will be excluded from the calculation of the final submission date.

InductEV, Inc.
Exhibit 1010
Page 047

iv While registration is suspended, a candidate is exempt from fees and enrolment, and is not entitled to any tuition or supervision, or to the use of any other research resources of the University.

Guideline 25

Termination of Registration

g The Board of Graduate Studies may terminate the registration of any candidate who;

i fails to enrol for any academic year corresponding to a year of registration,

or

ii fails to make payment of any Tuition and Research fees related to the PhD registration,

or

iii applies to cease being registered,

or

iv has not made satisfactory progress while under provisional registration,

or

v has received an unsatisfactory annual report,

or

vi has not met any conditions specified under Clause 5e,

or

vii has not submitted or re-submitted the thesis in time,

or

viii has had the termination of their registration recommended by a decision of a Disputes Committee constituted pursuant to Clause 11 of this Statute,

or

ix is prohibited under the Disciplinary Statute of the University from enrolling.

Guideline 26

CLAUSE 8 SUBMISSION

Copies of Thesis

a All candidates are initially required to submit three copies of the thesis to the Graduate Centre. The thesis should have a temporary binding and a statement to examiners as specified in the Guide to Theses and Dissertations.

Guideline 27
Guide to Theses and Dissertations

InductEV, Inc.
Exhibit 1010
Page 048

Time for Submission

b Unless permitted to do otherwise by the Board of Graduate Studies under Clause 7e, a candidate must normally submit the thesis in not less than three and not more than four years from the Date of Registration if they are full time students, or not less than six and not more than eight years in the case of candidates who have been registered as part time students for the whole period of their registration. In the case of candidates who have been permitted to change between full and part time, the submission times will be calculated on a pro rata basis.

Notification of Submission

c One month prior to the expected date of submission, candidates should notify the Graduate Centre in writing of their intention to submit. If the candidate has reason to believe that any person would be unsuitable to serve as an examiner of the thesis on the grounds of conflict of interest, he or she may also submit at this time the name of this person and a statement in writing as to the nature of the conflict of interest to the Graduate Centre.

Guideline 28

Declaration as to Originality

d The thesis is to be accompanied by a statutory declaration, signed by the candidate, stating that it is the candidate's own work and that neither the thesis nor any part of it has been submitted or accepted for any other degree or diploma.

e Where the thesis contains jointly authored research papers, case studies and/or any other work, published or unpublished, the declaration is to state the extent to which the jointly authored material is the candidate's own work. Evidence that all co-authors have approved the inclusion of the joint work must be supplied.

Guideline 29

Statement from Supervisors

f When the thesis is submitted, the Graduate Centre will invite a statement from the supervisor/s regarding the context or outcome of the thesis research. This statement must be endorsed by the Head of Department and the candidate. The Graduate Centre will forward a copy of the statement to the chair of the Examination Committee for its consideration.

Language of Thesis

g The thesis is to be presented in English unless otherwise approved by the Board of Graduate Studies at the time of first registration of the candidate.

Guideline 30

InductEV, Inc.
Exhibit 1010
Page 049

CLAUSE 9 EXAMINATION

General Provisions

a The Head of Department and/or the Associate Dean (Postgraduate) of the Faculty may nominate another person to the Board of Graduate Studies to be authorised to act in his or her place in all of the provisions of this Clause 9. If either the Head of Department or the Associate Dean (Postgraduate) is a supervisor of the candidate, an alternate must be nominated and appointed.

b Neither the supervisors nor the candidate may communicate with the examiners regarding the examination at any stage of the examination process, except as specified in this Clause 9.

Nomination of Examiners

c On notification of submission or intent to submit under Clause 8c, the Head of Department will nominate at least two suitably qualified persons to the Board of Graduate Studies for selection as examiners. The nominees should each hold a doctoral degree, or have equivalent expertise and experience, and be expert in the field of study which is the subject of the thesis. At least one nominee should be from outside New Zealand. The examiners may not be staff members of the University or have been involved in either the thesis research or the preparation of the thesis.

Guideline 31

Appointment of Examiners

d The Board of Graduate Studies will consider the nominations provided by the Head of Department and any submissions made by the candidate under the provisions of Clause 8c and will appoint two suitably qualified persons who are available to act as examiners. One examiner (the Oral Examiner) must be able to attend the oral examination and will normally be resident in New Zealand or Australia.

Guideline 32

Appointment of Examination Committee

e The Board of Graduate Studies will also appoint an Examination Committee which will normally be composed of;

i the Head of Department,

ii an Associate Dean (Postgraduate), who will chair the Examination Committee, ***and***

InductEV, Inc.
Exhibit 1010
Page 050

iii one other person (the HoD Nominee) nominated by the Head of Department. This person will have thorough knowledge of the general field of the thesis, but not necessarily of the thesis topic, and will normally be a staff member of the University.

No member of the Examination Committee may be a supervisor or have been involved in either the thesis research or the preparation of the thesis. The Associate Dean will normally be from the same Faculty as the candidate, but if that person is in the same Department as the candidate then an Associate Dean from another Faculty should be substituted.

Examiners' Reports

f As suppliers of evaluative material in terms of the Privacy Act 1993, all examiners will be informed that the information and reports they supply as such will be held in confidence to supervisors and to persons involved in the formal examination process. Candidates will not be informed of the names, or other identifying information, of their examiners except that of the Oral Examiner.

Guideline 33

g Each examiner will be provided with a copy of the thesis and, acting independently, is required to provide the Graduate Centre, within two months of receipt of the thesis, with a written report in English on the quality of the thesis according to the criteria outlined in Clause 1 d. One copy of the thesis will be provided to the Examination Committee.

h The examiners will include with their reports one of the following recommendations;

i to award the degree,

or

ii to award the degree after specified minor corrections have been made to the thesis,

or

iii to permit the candidate to revise the thesis and resubmit it for examination on one further occasion only,

or

iv not to award the degree.

Replacement of Examiners

i If a report has not been received within two months, the Graduate Centre will send a reminder to the examiner and advise him or her that unless the report is received within two further months the appointment as examiner will lapse. If the report

InductEV, Inc.
Exhibit 1010
Page 051

has not been received within two months of the date of the reminder, the Board of Graduate Studies may appoint a replacement examiner.

Guideline 34

Consideration of Examiners' Reports

j Upon receipt of both of the examiners' reports, the Graduate Centre will provide copies for consideration by the Examination Committee. The examiners' reports will also be made available to the supervisor/s on a confidential basis. Supervisor/s may comment on the reports in writing to the Examination Committee on a confidential basis. The Examination Committee may also request clarification of issues raised in examiners' reports from the examiners and, if necessary, from supervisors. If the recommendations of the examiners are in conflict and the Examination Committee considers that the conflict may be resolved, the chair may invite the two examiners to consult and to provide a written report or reports on the outcome of their consultations.

Guideline 33

Recommendation of the Examination Committee

k The Examination Committee will then make a report to the Board of Graduate Studies which includes the nature and outcome of any communications with the examiners and/or supervisor/s made under Clause 9j and which recommends one of the following;

i to appoint one or more further independent Examiners to report on any areas of conflict,

or

ii to proceed to the Oral Examination,

or

iii to permit the candidate to revise the thesis and resubmit it for examination on one further occasion only,

or

iv not to award the degree.

Further Examiners

l In the event that the examiners' reports are in serious conflict the Board of Graduate Studies may appoint further independent external examiners to report on any matters which it may specify. In this event the candidate will be kept informed, and Clauses 9 f-i will apply for the reports of the further examiners.

InductEV, Inc.
Exhibit 1010
Page 052

Oral Examination

m In the event that the Board of Graduate Studies accepts a recommendation to proceed to an oral examination, the following procedures will apply.

i The Head of Department will arrange this examination.

ii The Board of Graduate Studies, on the recommendation of the Head of Department, will appoint a person to act as an independent chair of the oral examination. The chair must be a member of the academic staff of the University, but will not normally be a member of a Faculty in which the candidate is registered.

iii The examination must be attended by the candidate, the Oral Examiner, the chair and the HoD Nominee on the Examination Committee.

iv The Graduate Centre will forward copies of the examiners' reports to the supervisor/s.

The Main Supervisor may attend the oral examination, but will not act as an examiner and may only participate to the extent requested by the chair.

v During the oral examination the Oral Examiner and HoD Nominee will discuss with the candidate the subject of the thesis and relevant matters in the field or fields to which the subject belongs. The Oral Examiner will discuss with the candidate issues raised in the examiners' reports and ask questions of the candidate on behalf of the other examiner.

Guideline 35

Recommendation of the Oral Examination

n On completion of the oral examination, the chair will provide a written report and recommendation, endorsed by the HoD Nominee and the Oral Examiner, to the Board of Graduate Studies. The report will include one of the following recommendations;

either

i to award the degree,

or

ii to award the degree after specified minor corrections have been made to the thesis to the satisfaction of the Oral Examiner or nominee, who may be the Main Supervisor, and by a specified date,

or

iii to permit the candidate to revise the thesis and resubmit it for examination on one further occasion only,

or

InductEV, Inc.
Exhibit 1010
Page 053

iv not to award the degree.

In the case of recommendation iii, the report must also state clearly the nature of the revisions recommended.

Guideline 36

When Revision and Resubmission are Permitted

- In the event that the Board of Graduate Studies requires the candidate to revise the thesis for resubmission, either prior to or following an oral examination, the following provisions apply:
  - i If an oral examination has already been held, a copy of the report of the oral examination will be sent to the Examination Committee.
  - ii The Examination Committee will agree on the date by which the thesis is to be resubmitted and the nature of the revisions recommended, and will convene a meeting with the candidate and supervisors to discuss these revisions. Both the revisions and the date are then to be reported in writing by the Chair of the Examination Committee to the Graduate Centre for approval by the Board of Graduate Studies and formal communication to the candidate. The date of resubmission may not be more than twelve months from the date of the oral examination or, in the case of a recommendation under 9k (iii), not more than twelve months from the date the examiners' reports were forwarded to the Examination Committee by the Graduate Centre.
  - iii The candidate is required to enrol and pay the prescribed tuition and research fees from the month in which the decision was made to the month by which the thesis is to be resubmitted. The registration of the candidate is to continue under the conditions applying at the first date of submission.
  - iv If the thesis is not resubmitted by the prescribed date, the registration of the candidate will normally be terminated.
  - v Upon resubmission, the revised thesis is to be examined as a whole by the same examiners in accordance with the provisions of this Clause, excepting that a further resubmission may not be recommended and that the Examination Committee may recommend that a second oral examination not be held. If one or both of the original examiners is unavailable to re-examine the thesis the Board of Graduate Studies will appoint alternative examiners.
  - vi Upon receipt of both of the examiners' reports, the Graduate Centre will provide copies of the new examiners' reports, the original examiners' reports and the oral examination (if held) to the Examination Committee and to the supervisor/s on a confidential basis. The procedure followed by the Examination Committee will be that in Clause 9j. Following consideration of

InductEV, Inc.
Exhibit 1010
Page 054

all examiner's reports the Examination Committee will make a report to the Board of Graduate Studies which includes the nature and outcome of any communications with the examiners and/or supervisor/s made under Clause 9j. In the case where an oral examination has not already been held the Examination Committee report must recommend that either an oral examination be held or the degree not be awarded. In the case where an oral examination has previously been held the Examination Committee report must recommend one of the following:

a to proceed to a second oral examination,

or

b to award the degree

or

c to award the degree subject to minor corrections,

or

d not to award the degree

Final Decision

p After considering all of the reports of the examiners and the Examination Committee the Board of Graduate Studies will make the final decision as to the award of the degree.

Copies for Deposit

q On successful completion of the examination three hardbound copies of the thesis, corrected as may be required, must be deposited with the Graduate Centre. The degree will not be conferred until the candidate has complied with this requirement.

CLAUSE 10 APPEALS

As to Registration

a Candidates, Supervisors or Heads of Department may appeal against a decision of the Board of Graduate Studies made under Clauses 4,5, 7 or 8 of this statute, normally within three months of the making of the decision, on the grounds that;

i relevant information which was not available to the Board of Graduate Studies at the time of its making the decision has since become available,

InductEV, Inc.
Exhibit 1010
Page 055

and/or

ii the procedure adopted in arriving at the decision was unfair.

The appeal must state clearly all grounds relied on by the candidate and attach all relevant documentation.

b Any appeal made under Clause 10a will be considered by the Chair of the Board of Graduate Studies, or their nominee, who may seek further information relating to the grounds of the appeal and shall notify the candidate of such information before making any decision. The Chair shall give a written decision outlining the reason(s) for the decision. A decision;

i grounded on the lack of relevant information shall be final,

or

ii grounded on procedural unfairness may be further appealed, within six months after the decision is made, to the Vice-Chancellor (or nominee) whose decision shall be final.

As to Examination

c If a PhD candidate believes that he or she has been significantly disadvantaged by the examination process, or by any part of the examination process, then a written appeal may be made to the Board of Graduate Studies, setting out the grounds of the appeal. All relevant documentation relied upon must be submitted with the appeal.

d Any appeal as to examination process must be lodged within three months of the result of the examination being officially communicated to the candidate. The appeal document must state clearly all grounds relied on and include all relevant documents.

e In the case of appeals as to examination process:

i The Chair of the Board of Graduate Studies will undertake a preliminary investigation and determine if there are grounds for the appeal to be taken to a further stage.

ii If there are grounds for further consideration of an appeal, this will be undertaken by two members of the Board of Graduate Studies who have not been involved in the examination process, who will make a recommendation to the Vice-Chancellor.

iii The candidate will be provided with a copy of the recommendation to the Vice-Chancellor and will have the opportunity to respond to the recommendation.

iv The decision of the Vice-Chancellor will be final and may involve a re-examination of the work.

Guideline 37

InductEV, Inc.
Exhibit 1010
Page 056

CLAUSE 11 DISPUTE RESOLUTION PROCEDURES

a Disputes are to be resolved according to the *Policy for Resolution of Research Problems: Postgraduate Research Students.*

(see http://www.auckland.ac.nz/Docs/sa/postgraduate/download/dispute.pdf).

CLAUSE 12 TRANSITIONAL ARRANGEMENTS

a This Statute comes into force on 1 March 2003 and revokes the previous Statute for the Degree of Doctor of Philosophy.

b For candidates initially registered under a previous statute the Board of Graduate Studies may agree to vary the application of the provisions of this Statute to ensure consistency with the provisions of the statute under which the candidate was enrolled where it is satisfied that the candidate would otherwise be at a disadvantage.

c Arrangements for payments of fees for candidates who were registered before 1 March 2003 may continue until the commencement of the 2004 academic year.

Guideline 38

InductEV, Inc.
Exhibit 1010
Page 057

GUIDELINES

Please note that all of the forms and most of the policy documents referred to below may be found on the University intranet at *www.auckland.ac.nz/postgraduate* and are also available in hard copy from the Graduate Centre.

ELIGIBILITY

Guideline 1 The MBA and MMgt differ significantly in their structures and purposes to other Masters degrees and are not, in themselves, sufficient to meet the requirements for admission to the PhD.
Clause 2a(i)

Guideline 2 A candidate may apply to convert an unfinished Masters thesis into a PhD thesis, where such a conversion meets the criteria of Clause 1. Candidates will not be able to convert an unfinished Master's degree to a PhD on the basis of coursework only.

Candidates registered under this provision shall normally have achieved a minimum average of B+ for the coursework component of their Master's degree. The Head of Department must certify that the thesis work completed is at the required honours level standard, and that the thesis topic is capable of being extended to a PhD. Once they have been awarded the PhD, candidates admitted under this Clause will not be permitted to go back and complete the Master's degree that they have converted.
Clause 2a(iii)

Guideline 3 This Clause allows the Board of Graduate Studies to admit suitably qualified people who do not strictly meet the requirements of 2.a.i and 2.a.ii. It particularly applies to:

- Candidates whose Masters degree from the University of Auckland is equivalent to an Honours degree, but is subject to a different grading system, eg. the Master of Engineering.
- Candidates who have qualified for admission to the Degree of Bachelor of Medicine and Bachelor of Surgery.
- Candidates who have qualified for admission to the Degree of Bachelor of Human Biology, and a pass in Part I of the Degree of

InductEV, Inc.
Exhibit 1010
Page 058

Bachelor of Medicine and Bachelor of Surgery, and a pass with a minimum of B+ in a 2 point Master's paper, relevant to the candidate's intended field of PhD research (a candidate who has met these requirements and registers for the degree of PhD will be required, in the first year of full time research, to satisfactorily complete a further relevant Master's paper which has been approved by the Head of Department).

- Candidates who have an equivalent qualification from another New Zealand university or from an overseas university.
- Candidates registered for the degree of Doctor of Philosophy at another university who wish to complete at this University. These candidates are required to withdraw from registration at the other university and to provide the Board of Graduate Studies with a statutory declaration concerning the nature and extent of the research done and the supervision received at the other university.

Clauses 2a(iv)

Guideline 4

In order to meet this requirement intending candidates need to have successfully undertaken a substantial research project. As part of this requirement, candidates must have demonstrated a high level of proficiency in the English language.

Clause 2b

Guideline 5

For a candidate to be considered for admission under Clause 2c, the Department needs to make a case in writing to the Board of Graduate Studies providing evidence of the nature, quality and relevance of the research experience and any other supporting evidence, such as publication record.

Clause 2c

ADMISSION

Guideline 6

This process is separate from that of applying for registration. The Application for Admission form is available online at www.auckland.ac.nz and can also be obtained from the Graduate Centre. Candidates whose qualifying degree was conferred by another university need to apply to have their qualifications assessed by the University as part of this admission process. These procedures must be completed before a PhD registration can be approved.

Clause 3a

InductEV, Inc.
Exhibit 1010
Page 059

REGISTRATION

Guideline 7

The purpose of Provisional Registration is to enable the Board of Graduate Studies to confirm the ability of the candidate to complete a PhD satisfactorily and to provide guidance to the candidate regarding the rate of progress expected. Where there is doubt about a candidate's qualifying criteria, it is preferable to enrol that candidate in a Master's degree or an appropriate transitional course of study. Registration for a PhD may then be considered at a later date should the candidate's performance prove satisfactory.

Clause 4b

See also Clauses 5a and 5b

Guideline 8

Active participation in and support from an active research community is an essential part of the PhD process, and the Head of Department and the Main Supervisor have particular responsibility for ensuring that this is provided. The Board of Graduate Studies, in accordance with the NZVCC's guidelines on this matter, requires candidates to be formally associated with a teaching Department or School so as to encourage this active participation.

Clause 4c

See also Clause 4h

NZVCC Guidelines

Guideline 9

This clause would normally apply to employees, such as academics or scientists, who are required to carry out research as part of their duties. Candidates need to provide a letter from their employer stating the term and nature of the full-time employment and expressing support for the candidate's registration. The letter must also state the nature of the research support being provided by the employer, which should normally include assistance with supervision and access to appropriate research facilities.

Clause 4d

See also Clauses 1b, 4e, 4f and 7d

Off-Campus Registration Policy

Guideline 10

Conditions of non-resident candidature are outlined in the policy document Guidelines for Off-Campus Registration

Clause 4f

See also Clauses 4d, 4e, 7b

Off-Campus Registration Policy

InductEV, Inc.
Exhibit 1010
Page 060

Guideline 11 A candidate must seek approval for concurrent registration from the Board of Graduate Studies at the time of registration or re-enrolment.
Clause 4g

Guideline 12 The provisional goals, perhaps four or five in number, should be realistically and specifically framed to provide a clear indication at the end of the year of the candidate's ability to complete the PhD satisfactorily and to provide guidance to the candidate regarding the rate of progress normally expected. The goals should be measurable, and provide tangible evidence of satisfactory progress in candidates' research during the first year. Suitable goals could include achievements such as: the completion of a chapter or chapters, the completion of an initial literature review, the initial development and testing of models, the completion of preliminary field work and collection of field data, the presentation of a departmental seminar on the PhD research.
Clause 4h(i)c
See also Clause 4b

Guideline 13 The minimum levels of resources and facilities the Department must provide are outlined in the policy document *Statement of Resources and Support for PhD Research.*
Clause 4h(ii)b
Statement of Resources and Support for PhD Research

Guideline 14 To ensure that candidates undertaking interdisciplinary projects are not disadvantaged in terms of supervision and resources, one Department must be clearly designated as the primary Department in which the candidate is registered.
Clause 4h(iii)

Guideline 15 Payment of fees is always required from the Date of Registration, which will be the first day of the calendar month. This should be taken into account when recommending a Registration Date. For those candidates who have applied for and have been awarded a doctoral scholarship, payments may commence only when the registration procedure has been completed, and will be payable from the Registration Date.
Clause 4k
Fees Statute

InductEV, Inc.
Exhibit 1010
Page 061

Guideline 16 The Main Supervisor must have a contractual obligation to provide adequate supervision and is normally a member of the academic staff of a Department or School in which the candidate is registered. Honorary staff members are not eligible to be the Main Supervisor.

Co-supervisors or advisers will normally be members of the academic staff of The University of Auckland or of another tertiary institution, or full time members of staff of an appropriate research organisation. Co-supervisors are expected to be active in assisting the Main Supervisor in the supervision of the candidate. Advisers, on the other hand, are expected to assist candidates and supervisors by providing support and advice when they are requested.

An advisory committee should normally consist of not more than six members, including the supervisors. Its role is to meet at least once a year with the candidate to review and provide guidance on the progress and content of the research. This meeting may take the form of the candidate presenting a seminar to the committee and receiving written feedback.

It is expected that all supervision will be conducted in accord with the policy document *Senate Guidelines on Thesis Supervision.*
Clause 4l, 4m, 4n
Guidelines on Thesis Supervision

REVIEWS OF REGISTRATION

Guideline 17 The research proposal may be submitted and approved at any time during the provisional year.

The candidate shall be given an opportunity to make written submissions to the Board of Graduate Studies on the provisional report. Candidates and staff are advised that an extension of Provisional Registration will be approved in exceptional circumstances only. Where candidates clearly fail to meet the requirements of Provisional Registration, it is expected that termination of their registrations will be recommended.
Clauses 5a, 5b
See also Clause 4b and 4h(i)c

Guideline 18 The candidate should be given an opportunity to make written submissions to the Board of Graduate Studies on the annual report.

The report form will be provided by the Graduate Centre for confirmed candidates on the anniversary of their Registration Date. The Head

InductEV, Inc.
Exhibit 1010
Page 062

of Department then forwards the report to the Associate Dean (Postgraduate) who in turn forwards it to the Graduate Centre.

Reports must be completed in full, and should enable the Board of Graduate Studies to make a reliable assessment of the progress of the research. For candidates in their third or fourth year of registration a schedule of work still remaining should also be provided, with a timetable for its completion.
Clause 5d
See also Clauses 5e and 5f

ENROLMENT AND FEES

Guideline 19 In the first year of candidature, fees will be charged from the Date of Registration to the end of that academic year (the next 28th February). In each subsequent year, candidates are required to pay fees for the full academic year (from 1st March to 28th February) in accordance with the Clauses below. Upon submission of the thesis, a candidate will be refunded the appropriate proportion of the tuition fees paid for that year. These fees are payable for each year of enrolment at the beginning of that year.
Clauses 6b and 6d
Fees Statute

Guideline 20 Where candidates are required to undertake coursework as part of their PhD registration, the tuition fees for their thesis will be reduced by the amount of fees payable for the required papers. Heads of Department are advised that addition or alteration of required papers to a candidate's registration requires the approval of the Board of Graduate Studies and to accompany their recommendation with an appropriate justification. There is no examination fee. Candidates should be aware that fees may increase from time to time during the period of the candidate's course of study. GST is included in all fees.
Clause 6f
Fees Statute

CHANGES TO THE CONDITIONS OF REGISTRATION

Guideline 21 During the progress of the PhD it may become necessary to change various conditions of registration, such as the topic or supervisor/s. Generally, all changes require the consent of the Board of Graduate Studies, after receiving a recommendation from the Head of Department in consultation with the Main Supervisor. The normal procedure is

InductEV, Inc.
Exhibit 1010
Page 063

for the Head of Department to fill out the appropriate form or send a memo to Associate Dean (Postgraduate) of the Faculty. It will then be forwarded, via the Graduate Centre, to the Board of Graduate Studies for consideration.

Heads of Department are advised that recommendations should always be accompanied by detailed reasons in support of the change. Recommendations that contain inadequate information will be returned with a request for satisfactory information to be provided.

Appeals regarding any decision made by the Board of Graduate Studies should be carried out using the Appeals Procedures outlined in Clause 10.

Clause 7a
See also Clause 10

Guideline 22 Absence from the University is acceptable provided that it is for a clearly specified period of time, that it is to pursue field work, laboratory work, or research, and that there are suitable supervision arrangements for the duration of the absence. More information can be found in the policy document *Guidelines for Off-Campus Registration.*

Clause 7b
See also Clause 4f
Guidelines for Off-Campus Registration

Guideline 23 As far as practicable, changes in supervision due to leave or retirement should be anticipated by the advance appointment of a Co-supervisor able to take over the role of the Main Supervisor.

When supervisors retire, it is often desirable that they continue to be involved in the supervision of their PhD candidates. The Board of Graduate Studies will normally approve such involvement when candidates are likely to complete within a year or two and the retired supervisor is willing and able to assist candidates in their research. In each case, the candidate, the retired supervisor, the Main Supervisor and the Head of Department must consent to the new supervision arrangement.

Clause 7c
See also Clauses 4l, 4m, 4n
Guidelines on Thesis Supervision

Guideline 24 A change to part-time candidature will be approved only when the candidate can show good reasons for not being able to work full-time on

InductEV, Inc.
Exhibit 1010
Page 064

their PhD. Changes from full-time to part-time or from part-time to full-time will only be permitted at the time of re-enrolment.
Clause 7d
See also Clauses 1b, 4f, 7d

Guideline 25 A suspension is a concession granted by the Board of Graduate Studies to avoid disadvantaging a candidate in terms of time when they are unable to continue their research for a specified period.

When recommending a suspension, the Head of Department needs to stipulate not only the reasons, but the time required, and should comment on the possible effects of interruption on the viability of the research.

Suspensions for incapacity arising from illnesses or accidents will normally be approved, as will those arising from events such as childbirth or bereavement. Appropriate evidence of incapacity, such as a medical certificate, needs to be provided with the recommendation. Requests to suspend because of other work or personal commitments may also be considered, but part-time enrolment may be more appropriate in such cases.

Suspensions will not normally be approved for less than 3 months or more than one year at a time. Where it is necessary, a further period of suspension may be granted. Because periods of suspension may be harmful to the quality of research and hinder satisfactory completion, after three years of suspension it is more appropriate to recommend termination. Where the incapacity has no clearly foreseeable conclusion, or is likely to persist for more than three years, it is more appropriate to recommend that the registration be terminated.

When appropriate an approved period of suspension may be shortened, but where it becomes apparent that a candidate has continued to engage in research during a period of suspension the suspension will be revoked and fees charged.
Clause 7f

Guideline 26 Candidates whose registration has been terminated will not normally be permitted to resume in the same subject at a later date.

Clause 7g

InductEV, Inc.
Exhibit 1010
Page 065

SUBMISSION

Guideline 27

For details concerning the layout of theses candidates should consult their supervisor/s and the University Library's *Guide to the Presentation of Theses*, and are advised to consult *The Preparation and Style of Manuscripts* published by The Auckland University Press

The *Guide to Theses and Dissertations* is available free of charge from the Library and the Graduate Centre.

It is important that candidates consult with their supervisor/s about any specific departmental requirements for the preparation and style of theses.

Candidates will normally be allowed to submit additional material, such as CD-ROMS and audio cassettes, with their theses provided that such material is accompanied by a declaration, signed by the candidate and the Main Supervisor and endorsed by the Head of Department. This declaration is to detail the content of the additional material, explain how it is related to the thesis, and state that it does not contain any direct appeal to the examiners.

The attention of candidates and staff is drawn to the Examination Regulations printed in the Calendar concerning PhD theses and abstracts.

Reference to publications arising from the thesis research may only be made in the text and bibliography or by incorporating the papers in the thesis itself.

Clause 8a
Guide to Theses and Dissertations
Examination Regulations, Clauses 22 & 23

Guideline 28

The advance notification of submission is intended to minimise the time taken for examination.

Any statement regarding conflict of interest will normally only be considered by the Board of Graduate Studies prior to the appointment of examiners.

Clause 8c

Guideline 29

The approval of co-authors is required to satisfy Copyright laws. The recommended format and wording for this declaration is available from the Graduate Centre.

Clause 8d, 8e
Declaration

InductEV, Inc.
Exhibit 1010
Page 066

Guideline 30 A candidate who wishes to submit a thesis in a language other than English is required to request permission to do so when applying to register for the degree of Doctor of Philosophy. This request must be accompanied by the recommendation of the Head of Department or both Heads of Departments in case of joint supervised PhD. Candidates wishing to submit in te reo Maori should consult Clause 4i.

The Board of Graduate Studies will consider applications for theses to be submitted in a language other than English on a case by case basis, and give permission only where it is satisfied that:

- The field of study and topic of the thesis make this essential.
- Suitable examiners will be available for the examination of the thesis.
- All examiners' reports and recommendations will be submitted in English.

It is not a sufficient reason for permission that the candidate's first language is not English.

Clause 4h(v), 8g
See also Clause 4i

EXAMINATION

Guideline 31 Nominations of examiners are made to the Board of Graduate Studies by the Head of Department on the advice of the supervisor/s, sending the appropriate form via the Associate Dean (Postgraduate) of the Faculty. Formal requests to act as examiners are made by the Graduate Centre once the Board of Graduate Studies has approved the nominations. Candidates should not expect to be involved in the selection of examiners.

Clause 9c
See also Clauses 9a, 9b and 9d.

Guideline 32 It is not the intention of this provision to exclude the appointment of examiners who have had a minor consultative role on some aspect of the candidate's research.

It is expected that at least one of the external examiners will be resident outside New Zealand. As the University is expected to provide travel and expenses for the Oral Examiner, financial considerations make it desirable that this examiner should normally be resident in New Zealand, or on the eastern seaboard of Australia. Departments will be required to assist with the travel expenses of examiners from further afield, or when the costs exceed the amount budgeted for an examination.

Clause 9d

InductEV, Inc.
Exhibit 1010
Page 067

Guideline 33 At no stage should candidates be provided with copies of the examiners' reports.

Where any corrections or revisions are necessary, the Head of Department or Main Supervisor will be asked by the Board of Graduate Studies to provide the appropriate information extracted from the reports in a manner that preserves the confidentiality of the examiners.

Under New Zealand law, any person may request a statement of reasons for a decision made about them. This includes decisions of an academic nature. If a candidate requests a statement of reasons for the decision to award or not to award the degree, then the Head of Department will be asked to prepare a brief paper which outlines the points of agreement of the examiners. This paper must preserve the confidentiality of the examiners and should demonstrate that the decision of the University was based on the recommendations of the examiners as a whole, and not on the views of an individual examiner.
Clauses 9f and 9j

Guideline 34 All approaches to an examiner concerning submission of a report must be made through the Graduate Centre. If some unforeseen delay appears likely, the Graduate Centre should be informed. It is expected that all examiners will prepare and submit their reports independently of each other and that there will be no communication between examiners about the thesis during the reporting process.
Clause 9i

Guideline 35 The independent Chair will normally be nominated at the same time as the examiners.
Clause 9m(ii)
See also Clause 9c

Guideline 36 The candidate and the examiners shall be informed of the decision of the Board of Graduate Studies by the Graduate Centre. Confirmation that any minor corrections have been made as requested must be forwarded to the Graduate Centre with three hardbound copies of the thesis before the degree can be conferred.
Clause 9n

APPEALS

Guideline 37 Any appeal is to be made in writing through the Graduate Centre.
Clause 10

InductEV, Inc.
Exhibit 1010
Page 068

TRANSITIONAL ARRANGEMENTS

Guideline 38 To ensure that no candidate is unduly disadvantaged by the new Statute the Transitional Arrangements Clause will be applied generously.

Candidates who wish to have their registration amended under the conditions of Clause 12 should apply in writing to the Graduate Centre. This application should state clearly the grounds for the request, and needs to include the recommendation of the Head of Department concerned. This Transitional Arrangements Clause is in no way intended to remedy any disadvantage that may occur as a result of the University's normal fees setting procedures. Towards the end of each year, Council establishes a Fees Policy for the following year, and this Statute cannot cover any disadvantage caused by this. The purpose of this clause is to reduce any disadvantage arising from the new fee provisions of this Statute by allowing existing candidates some time in which to complete under their currently approved fees payment arrangements.

Clause 12c
See also Clause 6

InductEV, Inc.
Exhibit 1010
Page 069

APPENDICES

APPENDIX A: THE TEMPORARY BINDING OPTION FOR THESES

The Board of Graduate Studies has approved the submission of theses in temporary binding as an option for PhD candidates for examination purposes.

The term "temporary binding" includes the hard, temporary binding available in the School of Engineering. However, this binding is not suitable for the final hardbound copies.

In considering the option of submitting their thesis in temporary binding rather than hardbound copies, candidates should note the following:

All theses in temporary binding must contain a warning (on the cover or inside page) that the copy is for examination purposes only and not for other use or reference.

The copies in temporary binding will not necessarily be returned by examiners. This should be taken into consideration when inserting original photographs, and/or other material, in the temporary version.

Three copies of the thesis are to be submitted for examination, whether using the temporary binding or hardbound option.

On completion of the examination, three hardbound copies of the thesis (corrected, if this has been required by the decision of the Board of Graduate Studies) must be deposited with the Graduate Centre before a conferment of degree form will be issued.

Candidates are advised that the examination process usually takes several months, and in some circumstances beyond the University's control may take longer.

Candidates are also advised, when meeting a deadline for submission, to be mindful of the time required for binding the thesis, and to confirm arrangements in advance with the binder.

APPENDIX B: LIBRARY ACCESS FOR INTENDING CANDIDATES

While researching their proposals or awaiting approval of their registration, intending candidates frequently wish to access the University's Library. Normally, this is not possible unless they are enrolled.

To assist those in these situations, a procedure has been established whereby intending candidates will be given some access to the Library. Candidates who wish to do this should collect the appropriate form from the Graduate Centre and take it to the Head of the Department in which they will be primarily registered for completion. Once they return the completed form to the Graduate Centre, arrangements will then

InductEV, Inc.
Exhibit 1010
Page 070

be made for them to have access to the Library's various services while researching their proposal or commencing research while awaiting approval of their registration. Candidates will find this process easier if firstly they ensure that they have applied for admission to PhD. Once this has been processed, they will then be able to obtain an ID card if they do not already have one.

APPENDIX C: WEB LINKS TO RELEVANT POSTGRADUATE POLICIES AND FORMS

Postgraduate Policies Relevant to PhD Candidates:

Statute for the Degree of Doctor of Philosophy (PhD)
Guide to Theses and Dissertations
Guidelines for Negotiating Supervision
Senate Guidelines on Thesis Supervision
Policy for Resolution of Research Problems (Postgraduate Research Students)
Guidelines to Off-Campus Registration
Statement of Resources and Support for PhD Research
Guaranteed Scholarships for PhD Candidates

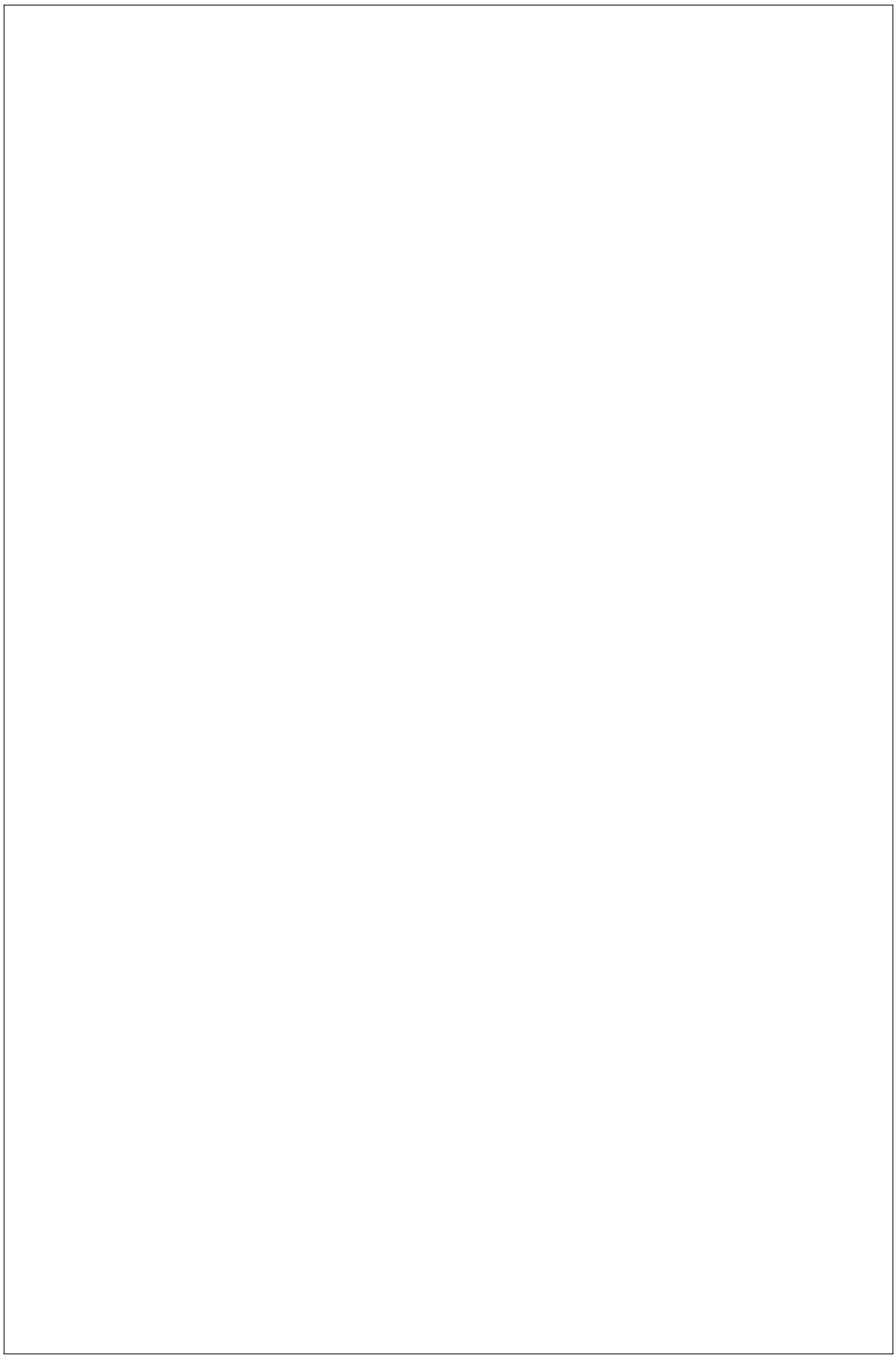
All postgraduate policies can be accessed at www.postgrad.auckland.ac.nz

Postgraduate Forms Relevant to PhD Candidates:

DOC2 Recommendation to Senate for Provisional Registration for a Doctoral Degree
DOC3 Nomination to Senate for the Appointment of Examiners for a Doctoral Degree
DOC6 Change of Conditions form
DOC7 Declaration to Accompany a Doctoral Thesis on Submission
DOC8 Application for Temporary Library Membership for Intending Doctoral Candidates
Annual Report

All postgraduate forms can be accessed at www.postgrad.auckland.ac.nz

InductEV, Inc.
Exhibit 1010
Page 071



InductEV, Inc.
Exhibit 1010
Page 072

Appendix 0001C

https://web.archive.org/web/20010202154200/http://voyager.auckland.ac.nz/ 150%

http://voyager.auckland.ac.nz/ Go DEC FEB OCT

84 captures 02

16 Jan 1999 - 3 Mar 2022 1999 2001 2006 About this capture



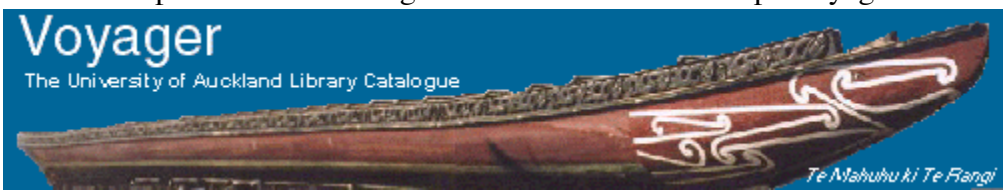
Patron | Help | Library Information | Other Libraries | LEARN | New Books Tutorial

Select Search Type:

Title/Author/Subject/Call No.	Find items by title, serial title, author, subject heading, or call number.
Relevance Keyword	Search by any word(s), phrase(s), name(s). Results are ranked by relevancy.
Guided Keyword	Fill-in-the-blank keyword search using AND, OR, NOT.
Expert Keyword	Search by keyword on command line using AND, OR, NOT.
Course Material	Search for Short Loan or Desk Copy items by lecturer, department, course.

Set Limits — You may limit your search (for example by year, or by library location) before executing the search. Limits apply only to title and keyword-type searches.

The Wayback Machine - https://web.archive.org/web/20010202154200/http://voyager.auckland.ac.nz:80/



Patron | Help | Library Information | Other Libraries | LEARN | New Books Tutorial

Select Search Type:

Title/Author/Subject/Call No.	Find items by title, serial title, author, subject heading, or call number.
Relevance Keyword	Search by any word(s), phrase(s), name(s). Results are ranked by relevancy.
Guided Keyword	Fill-in-the-blank keyword search using AND, OR, NOT.
Expert Keyword	Search by keyword on command line using AND, OR, NOT.
Course Material	Search for Short Loan or Desk Copy items by lecturer, department, course.

Set Limits	You may limit your search (for example by year, or by library location) before executing the search. Limits apply only to title and keyword-type searches.

InductEV, Inc.
Exhibit 1010
Page 075

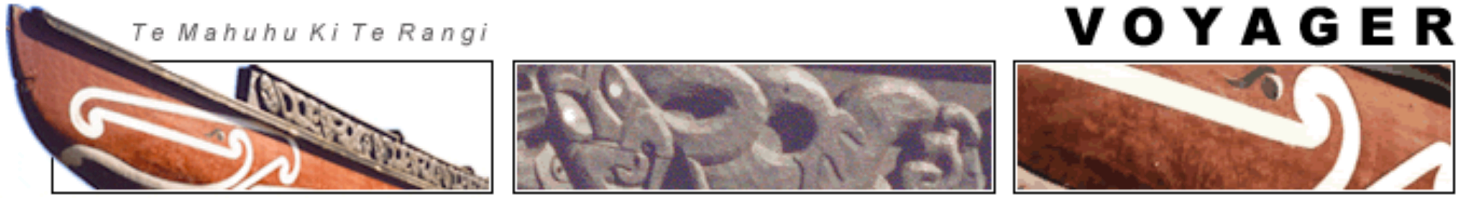
https://web.archive.org/web/20061010050227/http://voyager.auckland.ac.nz/

http://voyager.auckland.ac.nz/ Go

84 captures
16 Jan 1999 - 3 Mar 2022

FEB OCT SEP
2001 10 2008
2006

About this capture



Te Tumu Herenga | The University of Auckland Library **Catalogue**

Main Voyager Search List | **Guided Keyword Search** | **Course Material Search** | Patron

New - Intercampus Delivery From Inside Voyager
The Inter-Campus Library Delivery Service (ICLDS) is now available from Voyager. If you want an available item from another campus select the title on Voyager and use the 'Intercampus delivery' option from the Requests tab to place your request.

Voyager - the Library Catalogue
This catalogue describes material held in the University of Auckland Library system.

Voyager Tutorial - Te Punga
Te Punga is an interactive graphic novel that follows three students with an assignment, learning to use the Library and its Voyager catalogue. You can also access the online Enquiry Desk for quick access to explanations and examples of particular concepts.

- Voyager Tutorial
- Voyager courses
- General Library Theses Booking
- Endnote For Voyager
- LEARN
- New Books
- Library Hours
- Library Maps

InductEV, Inc.
Exhibit 1010
Page 076

https://web.archive.org/web/20081014034746/http://voyager.auckland.ac.nz/cgi-bin/Pwebrecon.cgi?DB=local&PAGE=Firs 150%

http://voyager.auckland.ac.nz/cgi-bin/Pwebrecon.cgi?DB=local&PAGE=First Go

6 captures
14 Oct 2008 - 24 Jan 2016

SEP OCT JUN
2007 14 2008 2010
About this capture



Database Name: The University of Auckland Library

Main Search List | Guided Keyword Search | Course Material Search

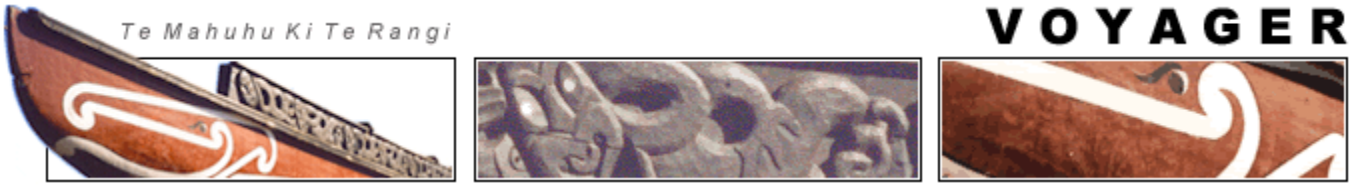
Search for:

Quick Limit: None

Search in:

- TITLE (omit the, a, nga... as the first word)
- SERIAL TITLE (includes journals and newspapers)
- AUTHOR* (enter family/last name first)
- CALL NUMBER*
- KEYWORD RELEVANCE (see Search Hints below)
- KEYWORD BOOLEAN (link words with 'and', 'or', 'not')
- SUBJECT HEADING*
- AUTHOR SORTED BY UNIFORM TITLE* (see Search Hints)

The Wayback Machine - https://web.archive.org/web/20061010050227/http://voyager.auckland.ac.nz/



Te Tumu Herenga | The University of Auckland Library **Catalogue**

Main Voyager Search List | **Guided Keyword Search** | **Course Material Search** | Patron

New - Intercampus Delivery From Inside Voyager
The Inter-Campus Library Delivery Service (ICLDS) is now available from Voyager. If you want an available item from another campus select the title on Voyager and use the 'Intercampus delivery' option from the Requests tab to place your request.

Voyager - the Library Catalogue
This catalogue describes material held in the University of Auckland Library system.

Voyager Tutorial - Te Punga
Te Punga is an interactive graphic novel that follows three students with an assignment, learning to use the Library and its Voyager catalogue. You can also access the online Enquiry Desk for quick access to explanations and examples of particular concepts.

General Library Theses Booking Form
An online booking form for theses held in the General Library is now available on Voyager. Please click on the 'General Library Theses Bookings' button.

Te Puna - NZ Catalogue
The catalogue of the National Library of New Zealand and includes; the National Bibliographic Database; Index New Zealand (journal index); and He Puna Kupu Maori, a Maori thesaurus.

Te Mahuhu Ki Te Rangi
"Te Mahuhu ki Te Rangi" was built by Ngati Whatua ki Orakei for the 150 year Waitangi Celebrations in 1990. Built from laminated kahikatea, it measures 37 metres (120ft) long, 2.7 metres (9 ft) wide and can carry 140 kaihoe. It was named after the orginal migration waka which bought Ngati Whatua (Kaipara/Auckland) to Aotearoa.

>> more

- Voyager Tutorial
- Voyager courses
- General Library Theses Booking
- Endnote For Voyager
- LEARN
- New Books
- Library Hours
- Library Maps
- Te Puna
- UoA E-Journals
- UoA E-Books
- Lending Policy
- Lending FAQ
- Other Libraries

LEARN | Contact | Suggestion Box | Subject Librarians | The University of Auckland

https://web.archive.org/web/20040624051430/http://www.library.auckland.ac.nz/forms/thesis/thesis.asp 150%

http://www.library.auckland.ac.nz/forms/thesis/thesis.asp Go MAY JUN AUG

8 captures 24 Jun 2004 - 11 Feb 2021

2003 24 2004 2008 About this capture

Booking Form for General Library Theses Only

Admin

- The Thesis booking form is to be used for theses held in the General Library.
- We do not provide on-demand retrieval for these items.
- **Theses are available for use in the General Library only i.e. cannot be taken out of the library and are required to be returned to the Lending Desk before closing time on the day of issue..**
- A second copy of most theses is available for normal loan (28 or 60 days) from Off Campus Storage. Complete an Inter-Campus Library Delivery Service form.
- Three theses may be booked for any one day.
- Bookings may be made up to three days in advance.
- Bookings for theses required the same day, will be accepted until 9.30am.
- Booked theses are available for collection from the Lending Desk from 10am, and are held until Library closing time.
- Theses should be returned 15 minutes before closing time to allow staff to discharge them for you.
- Theses are reshelved the following morning.

The Wayback Machine - https://web.archive.org/web/20040624051430/http://www.library.auckland.ac.nz:80/forms/th…

Learn Homepage

Thursday, June 24, 2004

Exit To Learn Homepage | Exit To Learn Homepage | Exit To Learn Homepage

Exit to Library Name Page

LEARN QuickLinks...

Booking Form for General Library Theses Only

Admin

- The Thesis booking form is to be used for theses held in the General Library.
- We do not provide on-demand retrieval for these items.
- **Theses are available for use in the General Library only i.e. cannot be taken out of the library and are required to be returned to the Lending Desk before closing time on the day of issue.**.
- A second copy of most theses is available for normal loan (28 or 60 days) from Off Campus Storage. Complete an Inter-Campus Library Delivery Service form.
- Three theses may be booked for any one day.
- Bookings may be made up to three days in advance.
- Bookings for theses required the same day, will be accepted until 9.30am.
- Booked theses are available for collection from the Lending Desk from 10am, and are held until Library closing time.
- Theses should be returned 15 minutes before closing time to allow staff to discharge them for you.
- Theses are reshelved the following morning.

Number of Theses To Book: 1

Continue Clear Quit

LEARN | Document Delivery Forms | Voyager

InductEV, Inc.
Exhibit 1010
Page 080

Appendix 0001D

https://www.worldcat.org/title/156754859 133%

WorldCat® Items Search for books, articles, and more Create account | Sign in

Home Libraries Topics Lists About For Librarians Annapolis, Maryland, US



Design considerations for inductively coupled power transfer systems

Author: Chwei-sen Wang (Author)

Abstract: Inductively coupled power transfer (ICPT) systems use electromagnetic fields to transfer electric power from a primary source (power supply) to one or more

Show more

Thesis, Dissertation, English, 2004
Dissertation: University of Auckland

Show more information

Borrow from **University of Auckland, General Library** near Annapolis, Maryland

Borrow

8,652 miles away

Find a Copy at a Library Filter by: Any format Any edition Distance within 200+ mi

1 edition in 1 library

Featured libraries All libraries

InductEV, Inc.
Exhibit 1010
Page 082

1 edition in 1 library

Featured libraries | All libraries

Showing 1 library near Annapolis, Maryland

Only public libraries



Academic

University of Auckland, General Library

Borrow

8,652 miles from your current location.
5 Alfred Street, Auckland, 1010, New Zealand

Favorite Library

WorldCat®

OCLC

WorldCat is the world's largest library catalog, helping you find library materials online.

Home
Libraries
Topics
Lists

About
For Librarians
Help & FAQ
Contact Us

Language

Appendix 0001E

FirstSearch University Libraries THE CATHOLIC UNIVERSITY OF AMERICA

Libraries that Own Item

| Back to CUA Libraries

- This screen shows libraries that own the item you selected.

Home Databases Searching Results Staff View | My Account | Options | Comments | Exit | Hide tips

List of Records Detailed Record Marked Records Saved Records Go to page

E-mail Print Return Help Current database: **WorldCat** Total Libraries: 1 WorldCa

Title: Design considerations for inductively coupled power transfer systems **Author:** Wang, Chwei-sen **Accession Number:** 156754859

Libraries with Item: "Design considerations for..."(Record for Item | Get This Item)

Location	Library	Code
New Zealand	UNIV OF AUCKLAND LIBR	UV0

Record for Item: "Design considerations for..."(Libraries with Item)

GET THIS ITEM

Access: http://hdl.handle.net.proxycu.wrlc.org/2292/52289

Availability: Check the catalogs in your library.

- Libraries worldwide that own item: 1

External Resources:

- Find it@CU Find or Request It at CU
- ILL@CU Request it via ILL
- Cite This Item

FIND RELATED

More Like This: Search for versions with same title and author | Advanced options ...

Title: Design considerations for inductively coupled power transfer systems /

Author(s): Wang, Chwei-sen, author.

Year: 2004

Description: xxvi, 253 pages : illustrations (some color) ; 30 cm

Dissertation: Ph. D.; Electrical and Electronic Engineering; University of Auckland; 2004

Language: English

Abstract: Inductively coupled power transfer (ICPT) systems use electromagnetic fields to transfer electric power from a primary source (power supply) to one or more secondary loads (pickups).

InductEV, Inc.
Exhibit 1010
Page 085

Because there is no physical contact between the primary and secondary, ICPT systems are intrinsically safe and reliable. This technology has been significantly commercialised for around a decade. Present applications include material handling, public transport, and battery charging. This thesis focuses on the design of ICPT systems for high power applications where both the primary and secondary coils are compensated by capacitors. The main aim is to develop systems with smaller size, less weight, lower cost, greater power and better efficiency. Previous work in this field has concentrated on either the power supply or the pickup. This thesis instead focuses on the interactions between the power supply and the pickup. When power is transferred from the primary to the secondary, the primary is affected by the secondary loading. This can result in poor displacement power factor (DPF), reduced power transfer capability, and a loss of controllability. First, steady state linear mathematical models are developed to represent the load seen by the power supply that includes the primary compensation capacitor, the electromagnetic structure, the secondary compensation capacitor, and the pickup load. These models quantify the system behaviour in terms of the fundamental design parameters, and are used to evaluate a design procedure for ICPT systems. This evaluation provides an insight into the system, enabling suitable design decisions as well as quantification of frequency bifurcation boundaries in variable-frequency systems. Several new primary tuning schemes are also proposed, taking into account the secondary loading effects. In loosely coupled systems, the primary and secondary resonant circuits can be tuned independently as the secondary loading effect on the primary are negligible. In well-coupled systems, the secondary loading affects the primary resonance significantly, and the proposed new tuning schemes greatly improve the DPF and power transfer capability. Various sensitivity analyses to variations in the primary and secondary compensation capacitances as well as misalignment of the electromagnetic structure show that systems designed using the proposed new tuning schemes have similar sensitivities compared with the original tuning. Throughout the thesis work, an LCL resonant inverter driving a contact-less electric vehicle battery charger was used to verify the proposed theory. The operation of this inverter under discontinuous current mode is also investigated. A novel design procedure is detailed and verified that enables this inverter to deliver maximum power to the load.

Access: http://hdl.handle.net.proxycu.wrlc.org/2292/52289 **Note:** e-Thesis University of Auckland

SUBJECT(S)

Descriptor:
Electric current converters.
Electric power transmission.
Power electronics.
Électricité -- Transport.
Électronique de puissance.
Electric current converters
Electric power transmission
Power electronics

InductEV, Inc.
Exhibit 1010
Page 086

Genre/Form:	dissertations. Academic theses Academic theses. Thèses et écrits académiques.
Note(s):	Includes bibliographical references.
Responsibility:	by Chwei-sen Wang.
Material Type:	Thesis/dissertation (deg); Manuscript (mss); Internet resource (url)
Document Type:	Book; Archival Material; Internet Resource
Date of Entry:	20051020
Update:	20230922
Accession No:	OCLC: 156754859
Database:	WorldCat

© 1992-2023 OCLC
Terms & Conditions
For information on how your personal data is processed when you use FirstSearch, please see your institution's privacy policy.

Exhibit 0001

WTS

ARTICLE DELIVERY

WTS Number: 275596

Order #170728

Request Date: 04/09/2021 11:07am

Rush

Requester: Maria Jamass - Latham & Watkins
Phone: 2129061200
Reference: 00826-068620-0001
Delivery email: **maria.jamass@lw.com** **Maxcost:**
Instructions: **All seem to only be available at the University of Auckland**

Citation:

THESIS
Design considerations for inductively coupled power transfer systems
Chwei-sen Wang
PhD Electrical and Electronic Engineering University of Auckland, 2004

Library/Supplier: OCLC 207535383

WTS staff contact: Karen

ISSN/ISBN/OCLC: OCLC: 156754859

Base Service Fee: $15 **Rush fee:** $15.00

Copyright: WTS will pay copyright royalties and bill me:$_____pages:_____

Shipping: $_____ **Research:** $_____ **Supplier:** $_____

THIS IS NOT AN INVOICE

DESIGN CONSIDERATIONS FOR INDUCTIVELY COUPLED POWER TRANSFER SYSTEMS

By

Chwei-Sen Wang



A thesis submitted in partial fulfillment of the requirements for the degree of Doctor of Philosophy in Electrical and Computer Engineering, The University of Auckland, 2004

InductEV, Inc.
Exhibit 1010
Page 090

UNIVERSITY of ... KLAND
LIBRARY
OCT 2005

ABSTRACT

Inductively coupled power transfer (ICPT) systems use electromagnetic fields to transfer electric power from a primary source (power supply) to one or more secondary loads (pickups). Because there is no physical contact between the primary and secondary, ICPT systems are intrinsically safe and reliable. This technology has been significantly commercialised for around a decade. Present applications include material handling, public transport, and battery charging.

This thesis focuses on the design of ICPT systems for high power applications where both the primary and secondary coils are compensated by capacitors. The main aim is to develop systems with smaller size, less weight, lower cost, greater power and better efficiency. Previous work in this field has concentrated on either the power supply or the pickup. This thesis instead focuses on the interactions between the power supply and the pickup. When power is transferred from the primary to the secondary, the primary is affected by the secondary loading. This can result in poor displacement power factor (DPF), reduced power transfer capability, and a loss of controllability.

First, steady state linear mathematical models are developed to represent the load seen by the power supply that includes the primary compensation capacitor, the electromagnetic structure, the secondary compensation capacitor, and the pickup load. These models quantify the system behaviour in terms of the fundamental design parameters, and are used to evaluate a design procedure for ICPT systems. This evaluation provides an insight into the system, enabling suitable design decisions as well as quantification of frequency bifurcation boundaries in variable-frequency systems.

Several new primary tuning schemes are also proposed, taking into account the secondary loading effects. In loosely coupled systems, the primary and secondary resonant circuits can be tuned independently as the secondary loading effect on the primary are negligible. In well-coupled systems, the secondary loading affects the primary resonance significantly, and the proposed new tuning schemes greatly improve the DPF and power transfer capability. Various sensitivity analyses to variations in the primary and secondary compensation capacitances as well as misalignment of the electromagnetic structure show that systems designed using the proposed new tuning schemes have similar sensitivities compared with the original tuning.

Throughout the thesis work, an LCL resonant inverter driving a contact-less electric vehicle battery charger was used to verify the proposed theory. The operation of this inverter under discontinuous

InductEV, Inc.
Exhibit 1010
Page 092

current mode is also investigated. A novel design procedure is detailed and verified that enables this inverter to deliver maximum power to the load.

InductEV, Inc.
Exhibit 1010
Page 093

ACKNOWLEDGEMENTS

The author sincerely appreciates the supervision of Dr. Grant A. Covic and Dr. Oskar H. Stielau. Because of their wisdom and patience, the research work is always in a natural process going in the right direction. Particular thanks go to Prof. John T. Boys. His experience and leadership enabled this work to be carried out smoothly within the research group of inductive power transfer technology. The author is grateful for the wise advice and encouragement from EmPr. Ray Meyer. Additional thanks go to the power electronic research group, in particular Dr. Patrick A. Hu, Mr. Howard Lu and Mr. Edward Xu. Finally, it is an honour to have financial support, as a Doctoral Fellow (Top Achiever Doctoral Scholarship), from the Foundation of Research, Science and Technology (FRST), New Zealand.

In memory of my father, Lien-Jiin.

To my loving, Yu (mother), Annie (wife), Ya-Ting and Ya-Wei (daughters).

Chwei-Sen Wang

Auckland, New Zealand

Oct. 21, 2004

InductEV, Inc.
Exhibit 1010
Page 094

InductEV, Inc.
Exhibit 1010
Page 095

CONTENTS

Abstract i

Acknowledgements iii

Contents v

Nomenclature xi

List of Figures xv

List of Tables xxv

Chapter 1 Introduction 1

1-1 Background of ICPT Systems 1

1-2 Fundamental Structure of ICPT Systems 4

1-3 Motivations of the Research 4

1-4 Contributions of the Thesis 6

1-5 Scope of the Thesis 8

References 9

Chapter 2 Overview of ICPT Systems 11

2-1 Introduction 11

2-2 Electromagnetic Structures 11

2-2.1 Material 12

2-2.1.1 Magnetic Cores 12

2-2.1.2 Conductor Windings 13

2-2.2 Geometry 13

2-2.2.1 Primary Electromagnetic Structures 13

2-2.2.2 Secondary Electromagnetic Structures 14

2-2.3 Electromagnetic Coupling Model 15

InductEV, Inc.
Exhibit 1010
Page 096

2-2.4 Capability of the Electromagnetic Structure 17
2-2.4.1 Load Voltage and Current 17
2-2.4.2 Power Transfer Capability 18
2-3 Compensation 20
2-3.1 Secondary Compensation 20
2-3.2 Secondary Resonance 21
2-3.3 Primary Compensation 22
2-3.4 Primary Resonance 23
2-3.5 Basic Compensation Topologies 24
2-4 Power Converters 25
2-4.1 Overview of Power Converters 25
2-4.2 Voltage-Sourced Power Converters 27
2-4.3 Current-Sourced Power Converters 28
2-4.4 Impedance Matching 30
2-5 Controllers 31
2-5.1 Power Flow Regulation 31
2-5.2 Frequency Control 32
2-5.3 Switching Control in Voltage-Sourced Full-Bridge Inverters 32
2-5.4 Switching Control in Current-Sourced Full-Bridge Inverters 33
2-5.5 Bifurcation Phenomenon 34
2-6 Future Trends 36
2-7 Conclusions 38
References 38

Chapter 3 Development of a General Load Model 47
3-1 Introduction 47
3-2 Overview of the Load Model 47
3-3 The Pickup Load 49
3-4 The Secondary Resonant Circuit 50
3-5 The Secondary Quality Factor 51
3-6 The Reflected Impedance 52
3-7 Pickup Behaviour and Influences on the Primary 54
3-7.1 Operation at the Secondary Resonant Frequency 54

InductEV, Inc.
Exhibit 1010
Page 097

3-7.2 Normalization of the Impedance Model 56
3-7.3 Influence of Frequency on the Pickup Behaviour 56
3-7.4 Influence of Frequency on the Reflected Impedance 59
3-7.5 Operating Conditions for Maximum Power Transfer 61
3-8 The Primary Coil 62
3-9 The Primary Quality Factor 65
3-10 The Power Supply Load Model 67
3-10.1 Modelling of the Power Supply Load Impedance 67
3-10.2 The Normalized Load Impedance 69
3-11 Verification of the Load Model 71
3-12 Conclusions 75
References 76

Chapter 4 Evaluation of a Design Methodology for ICPT Systems 77
4-1 Introduction 77
4-2 A Design Procedure 77
4-2.1 Design of Ordinary Transformers 78
4-2.2 Design of ICPT Systems 79
4-3 Design Options for the Pickup Regulator 86
4-4 Design Options for the Power Supply 88
4-5 Design Evaluations 92
4-5.1 Sensitivity of the Displacement Power Factor 92
4-5.2 System Behaviour using a Fixed-Frequency Controller 98
4-5.3 System Behaviour using a Variable-Frequency Controller 101
4-5.4 Design Considerations 104
4-6 A Practical Design Example 105
4-7 Conclusions 109
References 110

Chapter 5 Tuning to Improve Power Transfer for Variable-Frequency Systems 113
5-1 Introduction 113
5-2 Primary Tuning for Unity DPF at Rated Load 114

InductEV, Inc.
Exhibit 1010
Page 098

5-3 Power Transfer Capability and Bifurcation Phenomenon 117
5-4 Bifurcation Criteria 130
5-5 Discussion 139
5-6 Verification 143
5-7 Conclusions 145
References 146

Chapter 6 Tuning to Improve DPF for Fixed-Frequency Systems 149
6-1 Introduction 149
6-2 System Behaviour with Primary Tuning for Unity DPF at Rated Load 149
6-3 Primary Tuning for Load Independent Unity DPF 154
6-3.1 Primary Capacitance and Operating Frequency 155
6-3.2 Power Transfer Capability and Secondary VA Rating 156
6-4 Discussion 163
6-5 Design Examples 164
6-6 Verification 167
6-7 Conclusions 170

Chapter 7 A Sensitivity Analysis of Systems Using the Proposed Primary Tuning Schemes 171
7-1 Introduction 171
7-2 Fundamentals of the Sensitivity Analysis 172
7-3 Compensation Capacitor Selection 173
7-4 The Influence of Variations in Primary Capacitance 177
7-4.1 Fixed-Frequency Systems 177
7-4.2 Variable-Frequency Systems 182
7-5 The Influence of Variations in Secondary Capacitance 184
7-5.1 Fixed-Frequency Systems 184
7-5.2 Variable-Frequency Systems 188
7-6 The Influence of Misalignment in the Electromagnetic Structure 190
7-6.1 Coupling Parameter Variations in an Electric Vehicle Battery Charger ... 191
7-6.2 Fixed-Frequency Systems 192

InductEV, Inc.
Exhibit 1010
Page 099

7-6.3 Variable-Frequency Systems 199
7-7 Discussion 206
7-8 Conclusions 209
References 209

Chapter 8 Investigating an LCL Resonant Inverter for ICPT Applications ... 211
8-1 Introduction 211
8-2 Overview of the System 212
8-2.1 Operating Modes of the LCL Resonant Inverter 212
8-2.2 An Analytical Procedure for System Design 214
8-3 Capability of the Inverter 214
8-3.1 The Inverter Model 214
8-3.2 Waveform of the Inverter Current 215
8-3.3 Inverter Power Delivery Capability 218
8-3.4 Fundamental Component of the Inverter Current 219
8-4 Capability of the Resonant Tank 221
8-4.1 The Resonant Tank Model 221
8-4.2 Operating Frequency 222
8-4.3 Power Absorption Capability 223
8-5 Steady State Power Flow Analysis 225
8-5.1 An Analytical Procedure for Steady State Analysis 225
8-5.2 The Switching Instants and the Series Inductance 225
8-5.3 Behaviour at Light Load 228
8-6 Verification 229
8-7 Conclusions 230
References 231

Chapter 9 Conclusions and Future Work 233
9-1 Conclusions 233
9-1.1 Variable Frequency Systems 233
9-1.2 Fixed Frequency Systems 235
9-2 Future Work 235
References 237

InductEV, Inc.
Exhibit 1010
Page 100

Appendices 239

A. Primary Voltage and Current Gains 239

B. Reactive and Real Powers of the Pickup Coil 241

C. Quantified Secondary Current 242

D. Normalized Reflected Impedance of Compensated Pickup 243

E. Quantified Impedance of the Primary Coil 244

F. Normalized Reactance of the Primary Capacitance for Systems with Compensated Pickup 244

G. Normalized Impedance Functions for Systems with Uncompensated Pickup 245

H. Primary Tuning for Unity DPF at ω_0 246

I. Primary Tuning for Load Independent Unity DPF 250

J. Maximum Allowable Alternating Voltage and Current in Capacitors 252

InductEV, Inc.
Exhibit 1010
Page 101

NOMENCLATURE

Symbol	Description
CCL	Capacitor-capacitor-inductor.
C_1, C_2	Capacitors of inverters.
C_d	dc capacitance.
C_m	Matching capacitance in CCL inverter.
C_p	Primary compensation capacitance.
C_{pn}	Normalized primary compensation capacitance.
C_s	Secondary compensation capacitance.
D, D_1, D_2, D_3, D_4	Diodes of inverters.
DPF	Displacement power factor.
ESR	Equivalent series resistance of capacitors
f, f_0, f_1, f_2	Frequency (Hz).
I	RMS current.
i	Instant current.
$I_{ac,rated}$	Rated ac current of capacitors.
ICPT	Inductively coupled power transfer.
I_{Cs}	Secondary capacitor current.
I_d	dc source current.
I_{dc}	dc load current.
I_{GAIN}	Primary current gain.
i_i, I_i	Inverter output current.
I_{i0}	Inverter output current at ω_0.
Im Z	Imaginary component of the impedance (Z).
i_p, I_p	Primary current.
i_R, I_R	Pickup load current.
i_s, I_s	Secondary current.
$I_{s0,rated}$	Rated secondary current defined at ω_0.

InductEV, Inc.
Exhibit 1010
Page 102

I_{sc}	Short circuit current of the pickup.
I_{sn}	Normalized secondary current.
k	Magnetic coupling coefficient.
k_n	Equivalent coupling coefficient of n pickups.
LCL	Inductor-capacitor-inductor.
L_d	dc inductance.
L_m	Matching inductance in LCL inverter.
L_p	Primary self-inductance.
L_s	Secondary self-inductance.
M	Mutual inductance.
M_n	Equivalent mutual inductance of n pickups.
N_p	Turn number of the primary coil.
N_s	Turn number of the secondary coil.
PP	Parallel-compensated primary and secondary.
PS	Parallel-compensated primary and series-compensated secondary.
P	Power.
P_i	Inverter power delivery.
P_n	Normalized power.
P_{rated}	Rated power defined at ω_0.
Q	Quality factor.
Q_p	Primary quality factor.
Q_{p0}	Primary quality factor at ω_0.
Q_s	Secondary quality factor.
Q_{s0}	Secondary quality factor at ω_0.
$Q_{s0,rated}$	Rated secondary quality factor defined at ω_0.
$Q'_{s0,rated}$	Rated secondary quality factor defined at $\omega_0/\sqrt{1-k^2}$.
R	Pickup ac load (Equivalent ac resistance).
R_{dc}	Pickup dc load.
Re Z	Real component of the impedance (Z).
SP	Series-compensated primary and parallel-compensated secondary.
SS	Series-compensated primary and secondary.
S_s	Apparent power (complex power) of the secondary coil.
S, S_1, S_2, S_3, S_4	Switches of inverters.
T	Period.

InductEV, Inc.
Exhibit 1010
Page 103

t, t_1, t_2, t_3	Time.
$t_n, t_{n1}, t_{n2}, t_{n3}$	Normalized time.
u	Normalized operating frequency.
V	RMS voltage.
v	Instant voltage.
VA_{Cs}	Required VA rating of the secondary compensation capacitor.
VA_s	Required secondary VA rating.
VA_{sn}	Normalized required secondary VA rating.
VA_{s0}	Required secondary VA rating at ω_0.
$VA_{s0,rated}$	Rated secondary VA rating defined at ω_0.
$V_{ac,rated}$	Rated ac voltage of capacitors.
VAR	Reactive power.
VAR_p	Primary reactive power.
VAR_s	Secondary reactive power.
V_{Cs}	Secondary capacitor voltage.
V_d	dc source voltage.
V_{dc}	dc load voltage.
V_{GAIN}	Primary voltage gain.
v_i, V_i	Inverter output voltage.
V_{i0}	Inverter output voltage at ω_0.
V_{oc}	Open circuit voltage of the pickup.
v_p, V_p	Primary voltage (parallel resonant tank voltage).
V_{p0}	Primary voltage at ω_0.
$\hat{V}_p$	Peak primary voltage (parallel resonant tank voltage).
V_{pn}	Normalized primary voltage (parallel resonant tank voltage).
v_R, V_R	Secondary pickup load voltage.
v_s, V_s	Secondary voltage.
$V_{s0,rated}$	Rated secondary voltage defined at ω_0.
V_{sn}	Normalized secondary voltage.
Y_t	Load admittance seen by the power supply.
Y_{tn}	Normalized load admittance seen by the power supply.
Z_p	Impedance of the primary track/coil.
Z_r	Reflected impedance.
Z_{r0}	Reflected impedance at ω_0.

InductEV, Inc.
Exhibit 1010
Page 104

$Z_{r0,rated}$	Rated reflected impedance defined at ω_0.
Z_{rn}	Normalized reflected impedance.
Z_s	Secondary load impedance.
Z_t	Load impedance seen by the power supply.
Z_{t0}	Load impedance seen by the power supply at ω_0.
Z_{tn}	Normalized load impedance seen by the power supply.
ω	Frequency (rad/s).
ω_0	Nominal frequency (Secondary resonant frequency).
θ_1	Phase of the load impedance seen by the power supply.
Φ_1	Phase between the fundamental inverter current and the parallel primary voltage.
ϕ	Phase between the primary and secondary currents.
$\tan \delta$	Dissipation factor of capacitors

InductEV, Inc.
Exhibit 1010
Page 105

LIST OF FIGURES

Fig. 1-1. Application examples from Daifuku (Japan). **2**

Fig. 1-2. Public transport system (New Zealand). **2**

Fig. 1-3. Application examples from Wampfler (Germany). **3**

Fig. 1-4. The block diagram of an ICPT system. **4**

Fig. 2-1. Common configurations of the primary coil. **14**

Fig. 2-2. Common configurations of the secondary core. **15**

Fig. 2-3. Circuit of the mutual inductance transformer model. **15**

Fig. 2-4. The sinusoidal mutual inductance transformer model. **16**

Fig. 2-5. Equivalent secondary circuit supplying power to a linear and resistive load. **17**

Fig. 2-6. The normalized load voltage and current of the uncompensated pickup. **18**

Fig. 2-7. Series-compensated secondary. **20**

Fig. 2-8. Parallel-compensated secondary. **20**

Fig. 2-9. Normalized load voltage and current characteristics of uncompensated as well as series and parallel-compensated pickups. **22**

Fig. 2-10. Series-compensated primary. **23**

Fig. 2-11. Parallel-compensated primary. **23**

Fig. 2-12. Basic compensation topologies of ICPT systems. **24**

Fig. 2-13. The block diagram of a power converter in an ICPT system. **25**

Fig. 2-14. Fundamental types of power source. **26**

Fig. 2-15. Switch configurations. **27**

Fig. 2-16. The voltage-sourced full-bridge power converter. **27**

Fig. 2-17. The voltage-sourced half-bridge power converter. **28**

Fig. 2-18. Voltage-sourced single-switch power converters. **28**

Fig. 2-19. The current-sourced full-bridge power converter. **29**

Fig. 2-20. The current-sourced half-bridge power converter. **29**

Fig. 2-21. Current-sourced single-switch power converters. **29**

InductEV, Inc.
Exhibit 1010
Page 106

Fig. 2-22. The LCL resonant inverter. **30**
Fig. 2-23. The CCL resonant inverter. **30**
Fig. 2-24. The rectangular inverter voltage being in-phase with the current. **33**
Fig. 2-25. The rectangular inverter voltage leading the current. **33**
Fig. 2-26. The rectangular inverter voltage lagging the current. **33**
Fig. 2-27. Pulse-width of the rectangular inverter voltage is less than a full half cycle. **33**
Fig. 2-28. The rectangular inverter current being in-phase with the voltage. **34**
Fig. 2-29. The rectangular inverter current leading the voltage. **34**
Fig. 2-30. The rectangular inverter current lagging the voltage. **34**
Fig. 2-31. Pulse-width of the rectangular inverter current is less than a full half cycle. **34**
Fig. 2-32. Futuristic ICPT applications. **37**

Fig. 3-1. Diagram of the load seen by the power supply. **48**
Fig. 3-2. Full-bridge diode rectifier with inductor output filter. **50**
Fig. 3-3. Full-bridge diode rectifier with capacitor output filter. **50**
Fig. 3-4. Equivalent circuits of the secondary systems. **51**
Fig. 3-5. Quantified secondary current. **57**
Fig. 3-6. Normalized reflected resistance for series and parallel-compensated secondary systems. **60**
Fig. 3-7. Normalized reflected reactance for series and parallel-compensated secondary systems. **61**
Fig. 3-8. Equivalent circuit of the primary coil. **62**
Fig. 3-9. The ratio $Z_p/(j\omega_0 L_p)$ at the secondary resonant frequency ω_0 (u=1). **64**
Fig. 3-10. The ratio $Z_p/(j\omega_0 L_p)$ with k=0.2. ..... **64**
Fig. 3-11. The ratio $Z_p/(j\omega_0 L_p)$ with k=0.6. ..... **65**
Fig. 3-12. Primary resonant circuits with reflected impedance. **67**
Fig. 3-13. Electromagnetic structure of the contact-less battery charger. **72**
Fig. 3-14. The measured coupling parameters (L_p, L_s, M) of the battery charger. **73**
Fig. 3-15. Measured and calculated load admittance (Y_t) of the battery charger. **74**

Fig. 4-1. A design procedure of the ordinary transformer. **79**
Fig. 4-2. A design procedure of ICPT systems. **80**
Fig. 4-3. A block diagram of a pickup regulator. **87**
Fig. 4-4. Examples of current-sourced power supply configurations. **89**

InductEV, Inc.
Exhibit 1010
Page 107

Fig. 4-5. Examples of voltage-sourced power supply configurations. **90**
Fig. 4-6. Sensitivity of DPF to u and k in systems having both the primary and secondary uncompensated. **94**
Fig. 4-7. Sensitivity of DPF to u and k in systems having a compensated primary and an uncompensated secondary. **95**
Fig. 4-8. Sensitivity of DPF to u, k and Q_{s0} in systems having an uncompensated primary and a compensated secondary. **96**
Fig. 4-9. Sensitivity of DPF to u, k and Q_{s0} in systems having both the primary and secondary compensated. **97**
Fig. 4-10. DPF operating with fixed frequency at ω_0. ..... **99**
Fig. 4-11. Required relationship between k and Q_{s0} to achieve unity DPF at ω_0 for the PP topology. **100**
Fig. 4-12. Selection of Q_{s0} to improve DPF when operating at ω_0 over a wider range of k for the PP topology. **100**
Fig. 4-13. Operating frequency with unity DPF. **102**
Fig. 4-14. Frequency shifts for bifurcation-free operations. **104**
Fig. 4-15. DPF and power transfer capability of the contact-less electric vehicle battery charger using a fixed-frequency controller operating at ω_0. ..... **106**
Fig. 4-16. Measured waveforms of the inverter current and the resonant tank voltage for the contact-less electric vehicle battery charger (operating at ω_0=19.7kHz). **107**
Fig. 4-17. Operating frequency and power transfer capability of the contact-less electric vehicle battery charger using a variable-frequency controller operating with unity DPF. ... **108**

Fig. 5-1. Primary tuning for unity DPF at rated load. **116**
Fig. 5-2. SS topology - Operating frequency and power transfer capability under variable-frequency operation. **122**
Fig. 5-3. SP topology - Operating frequency and power transfer capability under variable-frequency operation. **123**
Fig. 5-4. PP topology with loose coupling (k=0.05) - Operating frequency and power transfer capability under variable-frequency operation. **124**
Fig. 5-5. PP topology with middle coupling (k=0.2) - Operating frequency and power transfer capability under variable-frequency operation. **125**
Fig. 5-6. PP topology with good coupling (k=0.4) - Operating frequency and power transfer capability under variable-frequency operation. **126**

InductEV, Inc.
Exhibit 1010
Page 108

Fig. 5-7. PS topology with loose coupling (k=0.05) - Operating frequency and power transfer capability under variable-frequency operation. **127**

Fig. 5-8. PS topology with middle coupling (k=0.2) - Operating frequency and power transfer capability under variable-frequency operation. **128**

Fig. 5-9. PS topology with good coupling (k=0.4) - Operating frequency and power transfer capability under variable-frequency operation. **129**

Fig. 5-10. Normalized load reactance. **132**

Fig. 5-11. Normalized load susceptance. **133**

Fig. 5-12. Normalized function $G(u,Q_{p0},Q_{s0})$. **135**

Fig. 5-13. Analytical bifurcation boundary for the SS and SP topologies. **137**

Fig. 5-14. Numerical algorithm for finding bifurcation boundary. **137**

Fig. 5-15. Numerical bifurcation boundary for the PP and PS topologies. **138**

Fig. 5-16. Bifurcation boundary defined by k and Q_{s0} for the four basic topologies. **139**

Fig. 5-17. A contact-less electric vehicle battery charger with PP topology – Operating frequency and power transfer capability under variable-frequency operation (a comparison of the original and modified tuning schemes). **144**

Fig. 6-1. SP topology - DPF under fixed-frequency operation at ω_0 assuming modified primary tuning to achieve unity DPF at rated load. **151**

Fig. 6-2. PP topology - DPF under fixed-frequency operation at ω_0 assuming modified primary tuning to achieve unity DPF at rated load. **152**

Fig. 6-3. PS topology - DPF under fixed-frequency operation at ω_0 assuming modified primary tuning to achieve unity DPF at rated load. **153**

Fig. 6-4. Influences of k to the required change in C_p to achieve load independent unity DPF. ... **156**

Fig. 6-5. Influence of k to the required change in ω to achieve load independent unity DPF (the PP and PS topologies). **156**

Fig. 6-6. PP topology – System behaviour under fixed-frequency operation ($Q_{s0,rated}$=5). **159**

Fig. 6-7. PS topology – System behaviour under fixed-frequency operation ($Q_{s0,rated}$=5). **160**

Fig. 6-8. Limit of k and $Q_{s0,rated}$ when using the modified tuning to achieve load independent unity DPF. **161**

Fig. 6-9. Changes in the secondary current, secondary voltage, and required secondary VA rating under rated power operation when using the modified tuning to achieve load independent unity DPF. **162**

Fig. 6-10. Power transfer capability under fixed-frequency operation ($Q_{s0,rated}$=2). **163**

InductEV, Inc.
Exhibit 1010
Page 109

Fig. 6-11. A contact-less electric vehicle battery charger with PP topology – DPF under fixed-frequency operation (a comparison of the original and modified tuning schemes). ... **165**

Fig. 6-12. A contact-less electric vehicle battery charger with PP topology – Power transfer capability and required secondary VA rating under fixed-frequency operation (a comparison of the original and modified tuning schemes). **166**

Fig. 6-13. A contact-less electric vehicle battery charger with PS topology – DPF under fixed-frequency operation (a comparison of the original and modified tuning schemes). ... **166**

Fig. 6-14. A contact-less electric vehicle battery charger with PS topology – Power transfer capability and required secondary VA rating under fixed-frequency operation (a comparison of the original and modified tuning schemes). **167**

Fig. 6-15. A contact-less electric vehicle battery charger with PP topology, using the modified tuning to achieve load independent unity DPF (C_{pn}=1, u=1.12) - Measured waveforms of the inverter current (i_i) and the resonant tank voltage (v_p). **168**

Fig. 6-16. A contact-less electric vehicle battery charger with PP topology, using the modified tuning to achieve load independent unity DPF (C_{pn}=1, u=1.12) - Measured and calculated power and secondary VA. **168**

Fig. 6-17. A contact-less electric vehicle battery charger with PS topology, using the modified tuning to achieve load independent unity DPF (C_{pn}=0.8, u=1.12) - Measured waveforms of the inverter current (i_i) and the resonant tank voltage (v_p). **169**

Fig. 6-18. A contact-less electric vehicle battery charger with PS topology, using the modified tuning to achieve load independent unity DPF (C_{pn}=0.8, u=1.12) - Measured and calculated power and secondary VA. **169**

Fig. 7-1. High frequency power capability of capacitors. **174**

Fig. 7-2. Typical frequency dependence of the dissipation factor (tan δ) of capacitors. **175**

Fig. 7-3. Typical temperature dependence of the capacitance. **176**

Fig. 7-4. Typical aging (time dependence of the capacitance) – Class II ceramic capacitors (Source: American Technical Ceramics). **176**

Fig. 7-5. Typical voltage dependence of the capacitance (Source: WIMA) – Polyester plastic film capacitors (PET), Class II ceramic capacitors (X7R/Z5U). **176**

Fig. 7-6. Original tuning (C_{pn}=1, u=1) – The influence of variations in C_p for an electric vehicle battery charger under fixed-frequency operation (k=0.45, $Q_{s0,rated}$=1.8, PP topology, I_p=15A). **178**

InductEV, Inc.
Exhibit 1010
Page 110

Fig. 7-7. Modified tuning for unity DPF at rated load (C_{pn}=1.04, u=1) – The influence of variations in C_p for an electric vehicle battery charger under fixed-frequency operation. **179**

Fig. 7-8. Modified tuning for load independent unity DPF (C_{pn}=1, u=1.12) – The influence of variations in C_p for an electric vehicle battery charger under fixed-frequency operation. **179**

Fig. 7-9. Electromagnetic structure of the monorail material handling system. **180**

Fig. 7-10. The influence of variations in C_p for a monorail material handling system under fixed-frequency operation (k=0.086, $Q_{s0,rated}$=4.7, PP topology, C_{pn}=1, u=1). **181**

Fig. 7-11. Original tuning (C_{pn}=1) – The influence of variations in C_p for an electric vehicle battery charger under variable-frequency operation (k=0.45, $Q_{s0,rated}$=1.8, PP topology, I_p=15A). **183**

Fig. 7-12. Modified tuning for unity DPF at rated load (C_{pn}=1.04) – The influence of variations in C_p for an electric vehicle battery charger under variable-frequency operation. ... **184**

Fig. 7-13. The influence of variations in C_p for a monorail material handling system under variable-frequency operation (k=0.086, $Q_{s0,rated}$=4.7, PP topology, C_{pn}=1, I_p=54A). ... **185**

Fig. 7-14. Original tuning (C_{pn}=1, u=1) – The influence of variations in C_s for an electric vehicle battery charger under fixed-frequency operation (k=0.45, $Q_{s0,rated}$=1.8, PP topology, I_p=15A). **186**

Fig. 7-15. Modified tuning for unity DPF at rated load (C_{pn}=1.04, u=1) – The influence of variations in C_s for an electric vehicle battery charger under fixed-frequency operation. **186**

Fig. 7-16. Modified tuning for load independent unity DPF (C_{pn}=1, u=1.12) – The influence of variations in C_s for an electric vehicle battery charger under fixed-frequency operation. **187**

Fig. 7-17. The influence of variations in C_s for a monorail material handling system under fixed-frequency operation (k=0.086, $Q_{s0,rated}$=4.7, PP topology, C_{pn}=1, u=1). **187**

Fig. 7-18. Original tuning (C_{pn}=1) – The influence of variations in C_s for an electric vehicle battery charger under variable-frequency operation (k=0.45, $Q_{s0,rated}$=1.8, PP topology, I_p=15A). **188**

Fig. 7-19. Modified tuning for unity DPF at rated load (C_{pn}=1.04) – The influence of variations in C_s for an electric vehicle battery charger under variable-frequency operation (k=0.45, $Q_{s0,rated}$=1.8, PP topology, I_p=15A). **189**

InductEV, Inc.
Exhibit 1010
Page 111

Fig. 7-20. The influence of variations in C_s for a monorail material handling system under variable-frequency operation (k=0.086, $Q_{s0,rated}$=4.7, PP topology, C_{pn}=1, I_p=54A). **190**

Fig. 7-21. Misalignment of the contact-less electric vehicle battery charging system. **191**

Fig. 7-22. Measurement of the effects of misalignment on coupling parameters for the contact-less electric vehicle battery charger. **191**

Fig. 7-23. Symmetry of the electromagnetic structure of the battery charger. **192**

Fig. 7-24. Original tuning (C_{pn}=1, u=1) – The influence of variations in L_p for an electric vehicle battery charger under fixed-frequency operation (k=0.45, $Q_{s0,rated}$=1.8, PP topology, I_p=15A). **193**

Fig. 7-25. Modified tuning for unity DPF at rated load (C_{pn}=1.04, u=1) – The influence of variations in L_p for an electric vehicle battery charger under fixed-frequency operation. **193**

Fig. 7-26. Modified tuning for load independent unity DPF (C_{pn}=1, u=1.12) – The influence of variations in L_p for an electric vehicle battery charger under fixed-frequency operation. **194**

Fig. 7-27. Original tuning (C_{pn}=1, u=1) – The influence of variations in L_s for an electric vehicle battery charger under fixed-frequency operation (k=0.45, $Q_{s0,rated}$=1.8, PP topology, I_p=15A). **194**

Fig. 7-28. Modified tuning for unity DPF at rated load (C_{pn}=1.04, u=1) – The influence of variations in L_s for an electric vehicle battery charger under fixed-frequency operation. **195**

Fig. 7-29. Modified tuning for load independent unity DPF (C_{pn}=1, u=1.12) – The influence of variations in L_s for an electric vehicle battery charger under fixed-frequency operation. **195**

Fig. 7-30. Original tuning (C_{pn}=1, u=1) – The influence of variations in M for an electric vehicle battery charger under fixed-frequency operation (k=0.45, $Q_{s0,rated}$=1.8, PP topology, I_p=15A). **196**

Fig. 7-31. Modified tuning for unity DPF at rated load (C_{pn}=1.04, u=1) – The influence of variations in M for an electric vehicle battery charger under fixed-frequency operation. **196**

Fig. 7-32. Modified tuning for load independent unity DPF (C_{pn}=1, u=1.12) – The influence of variations in M for an electric vehicle battery charger under fixed-frequency operation. **197**

InductEV, Inc.
Exhibit 1010
Page 112

Fig. 7-33. The influence of variations in L_p for a monorail material handling system under fixed-frequency operation (k=0.086, $Q_{s0,rated}$=4.7, PP topology, C_{pn}=1, u=1). **197**

Fig. 7-34. The influence of variations in L_s for a monorail material handling system under fixed-frequency operation (k=0.086, $Q_{s0,rated}$=4.7, PP topology, C_{pn}=1, u=1). **198**

Fig. 7-35. The influence of variations in M for a monorail material handling system under fixed-frequency operation (k=0.086, $Q_{s0,rated}$=4.7, PP topology, C_{pn}=1, u=1). **198**

Fig. 7-36. Original tuning (C_{pn}=1) – The influence of variations in L_p for an electric vehicle battery charger under variable-frequency operation (k=0.45, $Q_{s0,rated}$=1.8, PP topology, I_p=15A). **199**

Fig. 7-37. Modified tuning for unity DPF at rated load (C_{pn}=1.04) – The influence of variations in L_p for an electric vehicle battery charger under variable-frequency operation (k=0.45, $Q_{s0,rated}$=1.8, PP topology, I_p=15A). **200**

Fig. 7-38. Original tuning (C_{pn}=1) – The influence of variations in L_s for an electric vehicle battery charger under variable-frequency operation (k=0.45, $Q_{s0,rated}$=1.8, PP topology, I_p=15A). **201**

Fig. 7-39. Modified tuning for unity DPF at rated load (C_{pn}=1.04) – The influence of variations in L_s for an electric vehicle battery charger under variable-frequency operation (k=0.45, $Q_{s0,rated}$=1.8, PP topology, I_p=15A). **202**

Fig. 7-40. Original tuning (C_{pn}=1) – The influence of variations in M for an electric vehicle battery charger under variable-frequency operation (k=0.45, $Q_{s0,rated}$=1.8, PP topology, I_p=15A). **203**

Fig. 7-41. Modified tuning for unity DPF at rated load (C_{pn}=1.04) – The influence of variations in M for an electric vehicle battery charger under variable-frequency operation (k=0.45, $Q_{s0,rated}$=1.8, PP topology, I_p=15A). **204**

Fig. 7-42. The influence of variations in L_p for a monorail material handling system under variable-frequency operation (k=0.086, $Q_{s0,rated}$=4.7, PP topology, C_{pn}=1, I_p=54A). ... **205**

Fig. 7-43. The influence of variations in L_s for a monorail material handling system under variable-frequency operation (k=0.086, $Q_{s0,rated}$=4.7, PP topology, C_{pn}=1, I_p=54A). ... **205**

Fig. 7-44. The influence of variations in M for a monorail material handling system under variable-frequency operation (k=0.086, $Q_{s0,rated}$=4.7, PP topology, C_{pn}=1, I_p=54A). ... **206**

Fig. 8-1. Circuit diagram of an ICPT system driven by an LCL resonant inverter. **212**

Fig. 8-2. Inverter voltage and current waveforms for the LCL resonant inverter. **213**

Fig. 8-3. Switching control of the LCL resonant inverter in discontinuous current mode. **213**

InductEV, Inc.
Exhibit 1010
Page 113

Fig. 8-4. Simplified model of the LCL resonant inverter. **215**
Fig. 8-5. Influences of varying V_{pn} on the inverter current waveform assuming maximum pulse width by setting t_{1n}=0, t_{3n}=0.5. ..... **216**
Fig. 8-6. Influences of V_{pn} and t_{1n} on the inverter current waveform (t_{3n} = 0.5). **217**
Fig. 8-7. Influences of V_{pn} and t_{3n} on the inverter current waveform (t_{1n} = zero). **218**
Fig. 8-8. Influences of increasing t_{1n} on the inverter current phase relationship assuming maximum t_{3n} of 0.5. ..... **220**
Fig. 8-9. Influences of decreasing t_{3n} on the inverter current phase relationship assuming minimum t_{1n} of zero. **221**
Fig. 8-10. Phase angle of the resonant tank admittance at rated load. **222**
Fig. 8-11. Influences of increasing t_{1n} on the operating frequency assuming maximum t_{3n} of 0.5 at rated load. **223**
Fig. 8-12. Resonant tank conductance at rated load. **224**
Fig. 8-13. Effects of t_{1n} on the resonant tank conductance at rated load. **224**
Fig. 8-14. Influences of t_{1n} on resonant tank power absorption capability at rated load. **225**
Fig. 8-15. An analytical procedure for the determination of steady state operation. **226**
Fig. 8-16. Inverter and resonant tank power flow balance at rated load. **227**
Fig. 8-17. Inverter current waveforms at light loads. **229**
Fig. 8-18. Calculated and measured steady state operation. **230**

InductEV, Inc.
Exhibit 1010
Page 114

LIST OF TABLES

TABLE 2-1. PICKUP VOLTAGES, CURRENTS, POWER AND REQUIRED VA RATINGS. **22**

TABLE 3-1. QUANTIFIED PICKUP VOLTAGES, CURRENTS. **58**
TABLE 3-2. LOAD IMPEDANCE OF THE BASIC TOPOLOGIES. **68**
TABLE 3-3. FUNCTIONS OF THE NORMALIZED LOAD IMPEDANCE WITH COMPENSATED PICKUP. ... **70**
TABLE 3-4. PARAMETERS OF THE CONTACT-LESS ELECTRIC VEHICLE BATTERY CHARGER. **72**

TABLE 4-1. ASSUMPTIONS OF THE DESIGN PROCEDURE IN FIG. 4-2. ..... **81**
TABLE 4-2. SUMMARY OF SYSTEM CONFIGURATIONS OF THE DESIGN PROCEDURE. **86**
TABLE 4-3. COMPARISON OF POWER SUPPLY CONFIGURATIONS. **91**
TABLE 4-4. COMPARISON OF FIXED AND VARIABLE FREQUENCY CONTROLLER. **91**
TABLE 4-5. NORMALIZED LOAD IMPEDANCES. **93**
TABLE 4-6. FUNCTIONS OF THE NORMALIZED LOAD IMPEDANCE WITH UNCOMPENSATED PICKUP. **93**
TABLE 4-7. FUNCTIONS OF THE NORMALIZED LOAD IMPEDANCE WITH COMPENSATED PICKUP. ... **94**
TABLE 4-8. DPF OPERATING WITH FIXED FREQUENCY AT ω_0. ..... **98**
TABLE 4-9. BIFURCATION BOUNDARY FOR VARIABLE-FREQUENCY OPERATION WITH UNITY DPF. **103**

TABLE 5-1. PRIMARY TUNING FOR UNITY DPF AT RATED LOAD. **117**
TABLE 5-2. NORMALIZED LOAD IMPEDANCES WITH COMPENSATED PICKUP. **118**
TABLE 5-3. FUNCTIONS OF THE NORMALIZED LOAD IMPEDANCE WITH MODIFIED TUNING. **119**
TABLE 5-4. NORMALIZED FUNCTIONS IN (5-11). **134**
TABLE 5-5. BIFURCATION CRITERIA. **139**
TABLE 5-6. IMPROVEMENT OF THE POWER TRANSFER CAPABILITY WITH THE MODIFIED TUNING FOR A LOOSELY COUPLED SYSTEM (k=0.05)..... **141**
TABLE 5-7. IMPROVEMENT OF THE POWER TRANSFER CAPABILITY WITH THE MODIFIED TUNING FOR A MIDDLE COUPLED SYSTEM (k=0.2)..... **142**

InductEV, Inc.
Exhibit 1010
Page 116

TABLE 5-8. IMPROVEMENT OF THE POWER TRANSFER CAPABILITY WITH THE MODIFIED TUNING FOR A WELL-COUPLED SYSTEM (k=0.4). **142**

TABLE 6-1. A SUMMARY OF C_{pn} FOR THE ORIGINAL TUNING AND THE MODIFIED TUNING FOR UNITY DPF AT RATED LOAD. **151**

TABLE 6-2. NORMALIZED PRIMARY COMPENSATION CAPACITANCE AND OPERATING FREQUENCY REQUIRED TO ACHIEVE LOAD INDEPENDENT UNITY DPF. **155**

TABLE 7-1. TYPICAL CAPACITANCE TOLERANCE OF PLASTIC FILM AND CERAMIC CAPACITORS. ... **175**

TABLE 7-2. LONG TERM CAPACITANCE CHANGE OF PLASTIC FILM CAPACITORS. **176**

TABLE 7-3. TYPICAL CHARACTERISTICS OF PLASTIC FILM AND CERAMIC CAPACITORS (SOURCE: WIMA). **177**

TABLE 7-4. PARAMETERS OF THE MONORAIL MATERIAL HANDLING SYSTEM. **181**

TABLE 7-5. SENSITIVITY OF DPF TO VARIATIONS IN C_P, C_S, L_P, L_S AND M UNDER FIXED-FREQUENCY OPERATION (PP TOPOLOGY). **207**

TABLE 7-6. THE INFLUENCE OF VARIATIONS IN C_S, L_S AND M ON THE POWER TRANSFER CAPABILITY UNDER FIXED-FREQUENCY OPERATION (PP TOPOLOGY). **207**

TABLE 7-7. SENSITIVITY OF THE OPERATING FREQUENCY TO VARIATIONS IN C_P, C_S, L_P, L_S AND M UNDER VARIABLE-FREQUENCY OPERATION (PP TOPOLOGY). **208**

TABLE 7-8. THE INFLUENCE OF VARIATIONS IN C_P, C_S, L_P, L_S AND M ON THE POWER TRANSFER CAPABILITY UNDER VARIABLE-FREQUENCY OPERATION (PP TOPOLOGY). **208**

TABLE 8-1. STEADY STATE OPERATIONS FOR MAXIMUM POWER WITH SELECTIONS OF t_{1n}. **228**

TABLE 8-2. SYSTEM BEHAVIOUR AT LIGHT LOAD. **228**

TABLE 8-3. MEASURED FREQUENCY, PRIMARY CURRENT AND POWER. **230**

InductEV, Inc.
Exhibit 1010
Page 117

This material may be protected by Copyright law (Title 17 U.S. Code)

CHAPTER 1

INTRODUCTION

1-1 Background of ICPT systems
1-2 Fundamental structure of ICPT systems
1-3 Motivations of the research
1-4 Contributions of the thesis
1-5 Scope of the thesis

1-1 BACKGROUND OF ICPT SYSTEMS

Inductively coupled power transfer (ICPT) systems utilize electromagnetic fields to transfer electric power from a stationary primary source to one or more movable secondary loads without contact. Using power electronic technology, ICPT systems with very low magnetic coupling strength have recently been practically realized [1][2] with the number of commercial applications growing every year.

Potential applications of ICPT systems are unlimited. Present applications include material handling, public transport and battery charging. ICPT systems are free of sparking, wear, tear and hazard. They are immune to dirt, moisture, water, snow, ice, and can be used in potentially explosive atmospheres. They are also safe, quiet and highly reliable. This low maintenance requirement improves productivity.

More than a hundred years ago, alternating current at approximately 1-2 kHz was proposed by Hutin and Leblanc [3] to supply power from a track to a railway vehicle across an air gap. Multiple secondary coils with independent circuit breakers were used for regulation of the power transferred to the motor.

In 1974, an ICPT system was suggested by Otto [4] to supply power to a moving vehicle. The suggested operating frequency was 4-10 kHz.

In 1994, Boys and Green suggested an ICPT system operating at 10 kHz for electric vehicles [5-6]. This is probably the first design suitable for practical industrial applications. The application of this invention to material handling systems and in particular to monorail and conveyor systems has since been licensed to Diafuku (Japan), one of the largest manufacturers of conveyors and material handling systems in the world. As shown in Fig. 1-1, successful commercial systems include clean room applications for semiconductor manufacturing industry as well as assembly lines for the car manufacturing industry.

InductEV, Inc.
Exhibit 1010
Page 118



(a) Clean room inter-process transportation. (b) Monorail material handling.

Fig. 1-1. Application examples from Daifuku (Japan).

In 1997, the Electrical and Computer Engineering (ECE) Department at The University of Auckland working with Wampfler AG in Germany through Auckland UniServices developed an ICPT system to provide intervention free battery charging to a specially designed low weight vehicle for use in a public transport system (Fig. 1-2), at the Whakarewarewa thermal park, Rotorua, New Zealand [2]. The charging bay is buried under the ground and the charging process is transparent to the driver. When the driver stops at the loading platform, the charging unit automatically senses the vehicle and begins charging if required. Four charging bays are provided allowing opportunity charging throughout the day. This minimizes the necessary on-board batteries, while still allowing the vehicles to be operated continuously.



Fig. 1-2. Public transport system (New Zealand).

After the success of this public transport system, Wampfler, in cooperation with Auckland UniServices and the ECE Department at The University of Auckland, invested intensively in the commercialisation and marketing of the ICPT technology. Various examples are shown in Fig. 1-3.

InductEV, Inc.
Exhibit 1010
Page 119



(a) Test track for road surfaces, Japan Public Works Research Institute.



(b) BMW-Floor conveying system, BMW AG, Site Dingolfing, Germany.



(c) E-bus, "Porto Antico", Genoa, Italy.



(d) Elevator, "Hermes Tower", Hanover, Germany.



(e) Trolley, "The Grove", Fairfax-District, Los Angeles, U.S.A.

Fig. 1-3. Application examples from Wampfler (Germany).

A recent competitor to Wampfler and Daifuku, VAHLE (Germany), has utilized ICPT technology successfully in its contact-less power transfer systems for material handling. More than 20 systems have been sold mainly to the car manufacturing industry. Its customers include Volkswagen (Germany), Volkswagen (PR China), Ford (Brazil), Volkswagen (Czech Republik), SML/Ford (Belgium), Karmann (Germany), Deckel Maho (Germany), Volkswagen (Poland), Ford (Germany), Gampro (Germany), IHI (Japan), Los Alamos National Laboratory (USA), and Nissan (USA).

In the low power market, there is growing interest in inductive charging of portable consumer products. Inductive charging systems include an electromagnetic or radio frequency coil that generates an electromagnetic field, which is coupled to a receiver coil within the device that includes a battery [7-12]. Scientists are currently researching the possibility of re-charging the battery of the artificial heart through the skin from a coil outside the body [13].

Environmental influences of electromagnetic fields (EMF) are growing fast with advancing technology such as mobile telecommunications. Thus, the anxieties and speculations about the health hazards of EMF exposure are spreading among all populations of the world. The potential health effects of EMF exposure therefore need to be clarified scientifically.

InductEV, Inc.
Exhibit 1010
Page 120

The World Health Organization (WHO) started from 1996 to assess the scientific evidence of possible health effects of EMF exposure in the frequency range from 0 to 300GHz. All reviews conducted so far have indicated that exposures below the limits recommended in the ICNIRP (1998) EMF guidelines [14], covering the full frequency range from 0 to 300GHz, do not produce any known adverse health effect. However, there are gaps in knowledge still needing to be filled before better health risk assessments can be made.

The Medical School of The University of Auckland examined the effect of 10 kHz magnetic fields in an experiment on animals [15-16]. Likewise no health hazard was found.

1-2 FUNDAMENTAL STRUCTURE OF ICPT SYSTEMS

The block diagram of an ICPT system is shown in Fig. 1-4. The system can be separated into six subsystems that include the switching power supply, the primary compensation, the electromagnetic coupling, the secondary compensation, the secondary switching controller and the load.

The power source of an ICPT system is usually the electric utility supplying voltage and current at a line frequency of 50 or 60Hz, single or three phases. For portable applications, the power source can be a battery supplying dc voltage and current.

In order to increase the amount of power transferred via the electromagnetic structure in a practical ICPT system, the power supply is used to provide high frequency voltage and current (normally above the audible range). The reactance of both the primary and secondary windings increases in proportion to increases in the operating frequency, and as such is normally compensated by capacitors. A secondary switched mode controller may be used to control the power flow to the load.

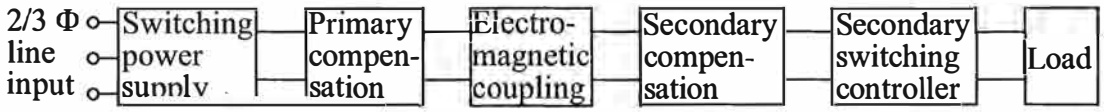


Fig. 1-4. The block diagram of an ICPT system.

1-3 MOTIVATIONS OF THE RESEARCH

This research focuses on the design of ICPT systems for high power applications, where both the primary and secondary are compensated. It is desired to enable increasing air gaps as well as increasing track length and number of pickups, while achieving greater power and better efficiency. The size, weight and cost of such systems are presently much higher than a wired connection. The challenge is to reduce the gap.

InductEV, Inc.
Exhibit 1010
Page 121

The compensated secondary pickup in an ICPT system is normally designed to ensure its tuned frequency is close to the nominal operating frequency of the system. If the operating frequency shifts away from this tuned frequency, the pickup is said to be detuned resulting in significantly lower power transfer capability.

There are two groups of ICPT systems: fixed and variable frequency systems [17]. In fixed-frequency systems, the pickup can be correctly tuned to operate at the maximum power point. In consequence, the size and cost of the pickup are minimized. However, the power supply may operate with a poor displacement power factor (DPF) and needs to be oversized to provide the additional reactive power. This results in an increase in the size and cost of the power supply.

In variable-frequency systems, the operating frequency is allowed to vary so that the power supply operates close to unity DPF. The size and cost of the power supply are therefore minimized. However, pickup frequency detuning is unavoidable and the pickup needs to be oversized to transfer the required power since it does not operate at its "ideal" maximum power point. This increases the size and cost of the pickup.

Under variable-frequency operation, the system may become "unstable" because of the onset of frequency bifurcation with load variation. Here, more than one operating mode is present in the frequency spectrum. If the system can not operate stably at the desired operating load, the required power will be unavailable. The phenomenon of bifurcation has been investigated in selected ICPT systems [1][17]. Further investigation is required to enable general design criteria to ensure system stability.

A direct approach to improve the DPF of the power supply and minimize the frequency detuning of any pickup is dynamic tuning. Here the inductance or capacitance is adjusted dynamically at either the primary or the secondary. In addition to the increased complexity of the controller, dynamically tuned systems have larger size and higher cost. Another approach proposed in [17] has additional resonant circuits consisting of inductors and capacitors at the output stage of the power converter, which significantly maximize the DPF, minimize the pickup frequency detuning, and reduce the influence of bifurcation. Again, the size and cost and complexity of the total system are increased due to additional inductors and capacitors required.

Previous work concentrates on either the primary power supply or the secondary pickups. This research instead investigates the interactions between the power supply and the pickups in order to identify influences of such interactions on the DPF, the power transfer capability, and the operating frequency. Whenever the interactions between the primary and secondary are negligible in comparison to the primary and secondary self-resonance, the primary and secondary resonance can be assumed to be independent of each other. This significantly simplifies the analysis and design of the power supply

InductEV, Inc.
Exhibit 1010
Page 122

as well as the pickups. Here, a constant primary current with a fixed frequency is usually assumed in the pickup design. For the design of the power supply, the loading effect from the pickup is normally assumed to be a variable resistor in series with the primary winding [17]. However, interactions between the primary and secondary resonant circuits become significant when the magnetic coupling strength of the system is improved, the pickup load increases, or more pickups are added [1]. A precise analysis of such systems requires the primary and secondary resonant circuits to be solved simultaneously. This approach is used here.

1-4 CONTRIBUTIONS OF THE THESIS

The contributions of this thesis have emanated mainly from investigations into the interactions between the power supply and the pickup, as well as from exploring suitable design approaches to take into account such interactions.

Quantification of System's Behaviour: Steady state linear high order mathematical model has been developed to represent the load seen by the power supply, which includes the primary compensation capacitor, the electromagnetic structure, the secondary compensation capacitor, and the pickup load. The electromagnetic structure and the primary and secondary compensation capacitors are assumed to be loss-less. The pickup load is assumed to be resistive. Four models have been developed for the four basic compensation topologies (a series compensated primary and secondary, a series compensated primary and parallel compensated secondary, a parallel compensated primary and secondary, a parallel compensated primary and series compensated secondary). The DPF of the power supply, the frequency detuning of the pickup, the bifurcation phenomenon and the power transfer capability are all quantified in terms of the fundamental design parameters, which include the operating frequency, the magnetic coupling coefficient, and the quality factors associated with the primary and secondary resonant circuits. This provides an insight into the system's behaviour at the design stage to assist the choice of the primary and secondary compensation topologies as well as the decision of the fundamental design parameters [18-22].

Description and Evaluation of a Design Methodology: A procedure has been described to illustrate step by step a design approach for ICPT systems. Here the primary and secondary resonances are assumed to be independent. The objective is to minimize the total cost by suitable choices of the operating frequency, the primary current, the electromagnetic structure, the primary and secondary compensation, the pickup regulator, and the high frequency switching power supply. The designed systems are evaluated to determine the degree of system deviation from the desired operating point resulting from loading effects of the pickup on the primary. This investigation shows that systems

InductEV, Inc.
Exhibit 1010
Page 123

designed using the four basic compensation topologies behave quite differently when the secondary loading effects are significant. The necessary design considerations for each topology are identified to ensure power transfer capability and controllability.

New Primary Tuning Schemes for Variable-Frequency Systems: Several new primary tuning schemes are proposed to improve the power transfer capability of variable-frequency systems. The system design approach is kept unchanged, and no additional components are added. The power transfer capability is simply improved by modifying the primary compensation capacitance to minimize frequency variation from the pickup tuned frequency. The necessary modification is determined for each of the four basic compensation topologies. Design criteria are developed for each system to ensure bifurcation is avoided. Significant improvements in power transfer capability are achieved for well-coupled systems where the primary and/or the secondary are parallel compensated, providing the design criteria are satisfied [19-21].

New Primary Tuning Schemes for Fixed-Frequency Systems: Additional primary tuning schemes are proposed to improve the DPF of fixed-frequency systems. Unity DPF is achievable independent of load with suitable choice of the primary compensation capacitance for series tuned primary systems. In the case of parallel tuned primary systems, load independent unity DPF can also be achieved but requires a shift in the ideal operating frequency that in turn affects the power transfer capability of the pickups and the required secondary VA rating. Despite the change in operating frequency, rated power can still be achieved in the majority of ICPT systems, providing (as is the case in practice) they are either loosely coupled systems with reasonable secondary quality factor or well-coupled systems with low secondary quality factor.

Sensitivity Analysis: The proposed new tuning schemes have been investigated further using several sensitivity analyses. Variations in the primary and secondary compensation capacitances as well as misalignment in the electromagnetic structure were considered and evaluated in terms of their influences on power transfer capability, DPF, and operating frequency. Systems designed using the new tuning schemes have similar sensitivities compared with the original tuning.

Investigation of an LCL Resonant Inverter: While the LCL resonant inverter is commonly operated with continuous current, operating under variable frequency control with discontinuous current is able to reduce the required inverter VA rating as well as the turn-on losses. The latter requires a complex design process. To deal with this complexity, a feasible design procedure was detailed to enable the inverter to deliver maximum power to the load [22].

InductEV, Inc.
Exhibit 1010
Page 124

1-5 SCOPE OF THE THESIS

Chapter 2 gives an overview of ICPT systems including the electromagnetic structure, the primary and secondary compensations, the power converters, and control options. The main objective is to clarify the current status of this technology at the on-set of this thesis work and its connections to the work of the thesis.

Chapter 3 develops a general load model as seen by the power supply. This impedance model combines the primary and secondary resonant circuits into a single high order mathematical model allowing the interactions between the primary power supply and the secondary pickups to be well described. The new load model is then normalized to characterise system behaviour in terms of the fundamental design parameters.

Chapter 4 uses the normalized load model to evaluate a design methodology where the primary and secondary resonances are assumed to be independent. A design procedure is described in detail along with a brief review of the design options for pickup regulators and power supplies. Influences of the interactions between the primary and secondary on the DPF of the power supply, the frequency detuning of the pickup, and the bifurcation phenomenon of the controller are investigated.

Chapter 5 proposes new primary tuning schemes for variable-frequency systems taking into account the secondary loading effects on the primary. The objective is to minimize the size and cost of the pickup by reducing frequency detuning. In order to avoid bifurcation, design criteria are developed to identify the boundary where bifurcation occurs.

Chapter 6 proposes alternative primary tuning schemes for fixed-frequency systems. The aim here is to minimize the size and cost of the power supply with better efficiency by improving the DPF of the power supply for all loading conditions.

Chapter 7 compares the relative sensitivity of the various systems described in earlier chapters. The sensitivity analysis focuses on variations in the primary and secondary compensation capacitance as well as misalignment of the electromagnetic structure.

Chapter 8 investigates an LCL resonant inverter using a variable-frequency controller operating under discontinuous current mode. A differential equation model is developed to analyse the capability of the inverter, while the load model describes the capability of the resonant tank. A steady state analysis using power flow balance between the inverter and the resonant tank enables suitable design and control to maximize power transfer.

Chapter 9 concludes the thesis and identifies relevant future work.

InductEV, Inc.
Exhibit 1010
Page 125

REFERENCES

[1]. J. T. Boys, G. A. Covic, A. W. Green, "Stability and control of inductively coupled power transfer systems," *IEE Proc.-Electrical Power Applications*, vol. 147, pp. 37-43, Jan. 2000.

[2]. G. A. Covic, G. Elliott, O. H. Stielau, R. M. Green, J. T. Boys, "The design of a contact-less energy transfer system for a people mover system," in *Proc. International Conference on Power System Technology*, vol. 1, 2000, pp.79-84.

[3]. M. Hutin, M. Leblanc, "Transformer system for electric railways," *United States Patent*, No. 527857, Oct. 23, 1894

[4]. V. D. Otto, "Improvements in or relating to electrified transportation," *New Zealand Patent,* No. 167422, Aug. 14, 1974.

[5]. A. W. Green, J. T. Boys, "10 kHz inductively coupled power transfer-concept and control," in *Proc. Fifth International Conference on Power Electronics and Variable-Speed Drives,* 1994, pp. 694-699.

[6]. J. T. Boys, A. W. Green, "Inductive power distribution system," *United States Patent,* No. 5293308, Mar. 8, 1994.

[7]. T. Bieler, M. Perrottet, V. Nguyen, Y. Perriard, "Contactless power and information transmission," *IEEE Transactions on Industry Applications*, vol. 38, pp. 1266-1272, Sep./Oct. 2002.

[8]. H. Abe, H. Sakamoto, K. Harada, "A noncontact charger using a resonant converter with parallel capacitor of the secondary coil," *IEEE Transactions on Industry Applications*, vol. 36, pp. 444-451, Mar./Apr. 2000.

[9]. Wonseok Lim, Jaehyun Nho, Byungcho Choi, Taeyoung Ahn, "Low-profile contactless battery charger using planar printed circuit board windings as energy transfer device," in *Proc. Power Electronics Specialists Conference*, vol. 2, 2002, pp. 579-584.

[10]. Chang-Gyun Kim, Dong-Hyun Seo, Jung-Sik You, Jong-Hu Park, B. H. Cho, "Design of a contactless battery charger for cellular phone," *IEEE Transactions on Industrial Electronics*, vol. 48, pp. 1238-1247, Dec. 2001.

[11]. Byungcho Choi, Honnyong Cha, Jaehyun Noh, Sangkyu Park, "A new contactless battery charger for portable telecommunication/computing electronics," in *Proc. International Conference on Consumer Electronics*, 2001, pp. 58-59.

[12]. Yungtaek Jang, M. M. Jovanovic, "A contactless electrical energy transmission system for portable-telephone battery chargers," in *Proc. Twenty-second International Telecommunications Energy Conference*, 2000, pp. 726-732.

InductEV, Inc.
Exhibit 1010
Page 126

[13]. Gyu Bum Joun; B. H. Cho, "An energy transmission system for an artificial heart using leakage inductance compensation of transcutaneous transformer," *IEEE Transactions on Power Electronics*, vol. 13, pp. 1013-1022, Nov. 1998.

[14]. International Commission on Non-Ionising Radiation Protection (ICNIRP) "Guidelines for limiting exposure to time-varying electric, magnetic, and electromagnetic fields (up to 300GHz)," *Health Physics*, vol. 74, pp. 494-522, 1998.

[15]. I. G. C. Robertson, W. R. Wilson, B. V. Dawson, L. J. Zwi, A. W. Green, J. T. Boys, "Evaluation of potential health effects of 10 kHz magnetic fields: A short-term mouse toxicology study," *Bioelectromagnetics*, vol. 17, pp. 111-122, 1996.

[16]. B. V. Dawson, I. G. C. Robertson, W. R. Wilson, L. J. Zwi, J. T. Boys, A. W. Green, "Evaluation of potential health effects of 10 kHz magnetic fields: A rodent reproductive study," *Bioelectromagnetics*, vol. 19, pp. 162-171, Dec. 1998.

[17]. A. P. Hu, "Selected resonant converters for IPT power supplies," *PhD thesis*, Oct. 2001, The Electrical and Electronics Engineering Department, The University of Auckland, Auckland, New Zealand.

[18]. Chwei-Sen Wang; Stielau, O.H.; Covic, G.A. "Load models and their application in the design of loosely coupled inductive power transfer systems," in *Proc. International Conference on Power System Technology*, vol. 2, 2000, pp. 1053-1058.

[19]. Chwei-Sen Wang, G. A. Covic, O. H. Stielau, "General stability criterions for zero phase angle controlled loosely coupled inductive power transfer systems," in *Proc. 27th Annual Conference of the IEEE Industrial Electronics Society*, vol. 2, 2001, pp. 1049-1054.

[20]. Chwei-Sen Wang, G. A. Covic, O. H. Stielau, "Power transfer capability and bifurcation phenomenon of loosely coupled inductive power transfer systems," *IEEE Transactions on Industrial Electronics*, vol. 51, pp. 148-157, Feb. 2004.

[21]. Chwei-Sen Wang, O. H. Stielau, G. A. Covic, "Design considerations for a contact-less electric vehicle battery charger," *IEEE Transactions on Industrial Electronics*, (accepted for publication, Feb. 2004).

[22]. Chwei-Sen Wang, G. A. Covic, O. H. Stielau, "Investigating an LCL load resonant inverter for inductive power transfer applications," *IEEE Transactions on Power Electronics*, vol. 19, pp. 995-1002, July 2004.

InductEV, Inc.
Exhibit 1010
Page 127

CHAPTER 2

OVERVIEW OF ICPT SYSTEMS

2-1 Introduction
2-2 Electromagnetic structures
2-3 Compensation
2-4 Power converters
2-5 Controllers
2-6 Future trends
2-7 Conclusions

2-1 INTRODUCTION

This chapter outlines the state-of-the-art ICPT technology. The electromagnetic structure, the primary and secondary compensation, the power supply and controller are all discussed here.

The materials and geometry of the electromagnetic structure commonly used for ICPT applications are introduced first. An electromagnetic coupling model is used to clarify the necessary approaches to boost the power transfer capability of the loosely coupled electromagnetic structures.

The requirements of primary and secondary compensations are then explained, along with the fundamental theory in the analysis of both primary and secondary resonant circuits. This theory is used to characterise the primary and secondary resonances. A summary of the basic compensation topologies is also given.

The necessary capability of power converters used for ICPT applications is then discussed. Suitable voltage and current sourced power converters for both low and high power applications are briefly introduced. Impedance matching between the inverter and primary compensation topologies are also presented.

Finally, the chapter reviews controllers commonly used for both the primary power supply and the secondary pickup, before pointing out future trends of the ICPT technology.

2-2 ELECTROMAGNETIC STRUCTURES

Similar to electromagnetic components such as inductors, transformers and induction motors, the electromagnetic structure of an ICPT system is constructed using magnetic cores surrounded by conductor windings. Magnetic cores concentrate the flux, while conductor windings conduct the

InductEV, Inc.
Exhibit 1010
Page 128

electric currents. This section introduces commonly used materials and geometry, and investigates the coupling and capability of the electromagnetic structure. These are essential in the analysis and design of ICPT systems.

2-2.1 MATERIAL

The materials commonly used for the magnetic cores and the copper windings in an ICPT system are similar to those used in the transformers for high-frequency power electronic applications. A brief summary is given in this section.

2-2.1.1 MAGNETIC CORES

Materials used for magnetic cores can be separated into two groups. In the first group are alloys principally of iron and small amounts of other elements including chrome and silicon. The iron alloy core material has a high electrical conductivity and saturation flux, typically around 1.8 tesla.

Iron alloy core materials can be found in three basic types. The first type is laminated magnetic steel. The objective of introducing laminations is to reduce eddy current losses by insulation between laminated steels. Laminated steel was evaluated in [1] in search of the most suitable materials for ICPT applications. Operating at 10 kHz, it was found that its power transfer capability is substantially limited by its core losses.

The second type of iron alloy core is powdered iron where particles are electrically isolated from each other producing a core with significantly greater resistivity than that obtained by lamination. Because of lower eddy current losses, powdered cores can be used at higher frequencies than laminated cores.

The third group of iron alloy cores, such as 'METGLAS' and 'FINEMET', are manufactured from various amorphous alloys of iron and other transition metals such as cobalt and nickel in combination with boron, silicon, and other glass-forming elements. The electrical resistivity of such alloys is larger than most magnetic steels and thus can be used for higher frequencies.

Due to eddy current loss, iron alloy core materials are usually used only in low frequency applications below 2 kHz, and as such are not suitable for most ICPT applications where the operating frequency is above 10 kHz [2-5].

The other group of materials used for magnetic cores are ferrites. Ferrite materials are basically oxide mixtures of iron and other magnetic elements. They have a high electrical resistivity but rather low saturation flux densities, typically about 0.3 tesla. Because of low eddy current losses, ferrite cores are usually the material of choice for ICPT applications.

InductEV, Inc.
Exhibit 1010
Page 129

2-2.1.2 CONDUCTOR WINDINGS

Presently the common choice of material for the conductor winding is copper because of its high conductivity as well as ductility. The high ductility of the copper makes it easy to bend the conductors into tight windings around a magnetic core and thus minimizes the amount of copper and volume needed. The high conductivity of copper also results in less copper required for the windings and thus decreases the volume and the weight.

The copper conductor may be composed of a single round wire or it may be a special multistranded conductor such as Litz wire in which each strand has a diameter of the order of a few hundred microns or less. Litz wire reduces losses due to skin effect and proximity effect, both of which become significant as the frequency is increased.

2-2.2 GEOMETRY

In a traditional transformer, the primary and secondary are fixed on a common core for tight coupling. However, the secondary in many ICPT systems is allowed to move freely relative to the primary, and as such the magnetic cores of the primary and secondary need to be separated. The magnetic core may be eliminated in the primary and/or the secondary to minimize the weight and cost of the system. In a multiple pickup system, more than one secondary draws power from a common primary. The layout of the electromagnetic structure of an ICPT system is application dependent, and there is virtually no limit to possible configurations. Configuration examples are introduced in this section.

2-2.2.1 PRIMARY ELECTROMAGNETIC STRUCTURES

The primary electromagnetic structure can be classified according to the configuration of the primary coil. For single pickup applications, the primary coil is typically constructed as a lumped coil coupled to a similar lumped coil in the secondary. In multiple pickup systems, the primary coil is usually extended to enable suitable coupling to the lumped coil of each pickup. Common configurations of the primary coil are shown in Fig. 2-1. The extended primary coil is shown in the figure as having a single turn. Multiple turn coils can be set up in the same way.

The primary coil can be extended with the cable and its return constructed in parallel as shown in Fig. 2-1 (a). The cable and its return are in close proximity to concentrate the flux. The secondary is placed between the parallel cables, and is allowed to move freely. This configuration is used in many applications where the vehicles move along linear routes [2].

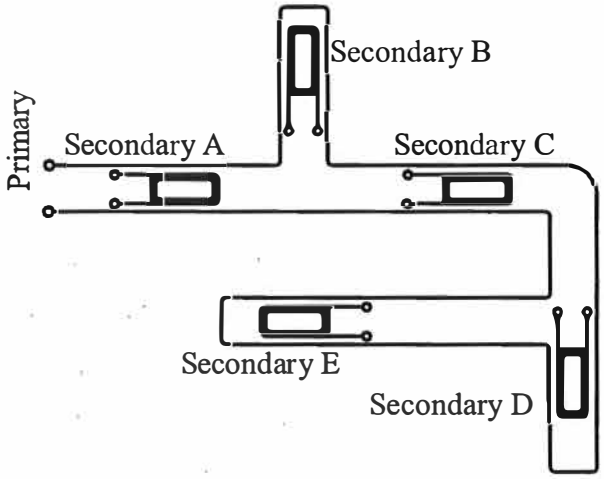
An alteration of the above configuration is to partially twist the parallel cables together as shown in

InductEV, Inc.
Exhibit 1010
Page 130

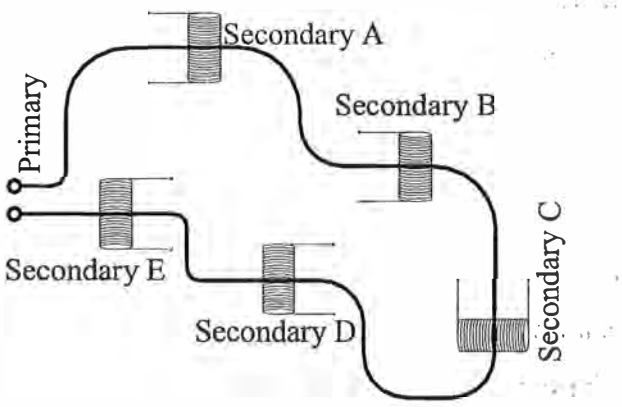
Fig. 2-1 (b). With the cable and its return partially twisted, the primary inductance is reduced. However, the secondary is allowed to draw power only at predetermined locations where the parallel cables are not twisted. A typical application of this configuration is roadway lighting [3].

Alternatively, the primary coil can be extended with the cable and its return constructed to form a loop as shown in Fig. 2-1 (c). The secondary is placed close to the cable, and is also allowed to move freely. This configuration is suitable for automatic guided vehicles.

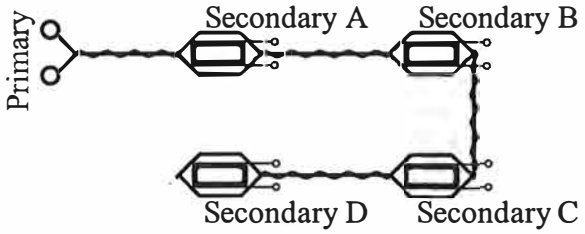
The simplest configuration of the primary coil is a lumped coil as shown in Fig. 2-1 (d). This configuration is commonly used for battery charging of electric vehicles [5-6] and portable electronic devices [7-8].



(a) Extended primary coil with the cable and its return configured in parallel.



(c) Extended primary coil with the cable and its return configured as a loop.



(b) Extended primary coil with the cable and its return configured in parallel and partially twisted.



(d) Lumped primary coil.

Fig. 2-1. Common configurations of the primary coil.

2-2.2.2 SECONDARY ELECTROMAGNETIC STRUCTURES

The secondary electromagnetic structure can be categorized according to the configuration of the secondary core. Common configurations are shown in Fig. 2-2. E-cores and H-cores are used in applications where the vehicles are running on a profile with the cable and its return fitting into each slot respectively. T-cores are used in applications where a guidance slot is given with the cable and its return positioned to the right and left of the guidance slot. Flat cores are used in applications where a

InductEV, Inc.
Exhibit 1010
Page 131

flat floor surface is demanded for full accessibility with the cables embedded in the ground.

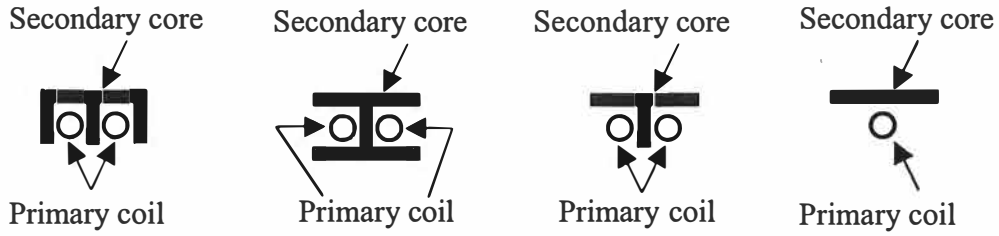


Fig. 2-2. Common configurations of the secondary core.

2-2.3 ELECTROMAGNETIC COUPLING MODEL

There are many approaches that can be used to investigate the coupling between the primary and secondary windings. The most commonly used modeling methodologies are the conventional transformer model [9-14] and the mutual inductance transformer model [15-22]. The conventional transformer model uses the concepts of transformed voltage and reflected current to describe the coupling effect. Both the transformed voltage and reflected current are expressed in terms of the turns ratio. With this model, the magnetizing and leakage inductance must be separated for circuit analysis. The conventional transformer model is therefore well suited for closely coupled systems such as transformers, because the leakage inductance is usually small. In ICPT systems, however, the leakage inductance is usually comparable or much larger than the magnetizing inductance, and the conventional transformer model becomes very complex. In order to simplify the circuit analysis for ICPT systems, the mutual inductance transformer model is used in this thesis because this model does not require the magnetizing and leakage inductance to be separated.

Using the mutual inductance transformer model, as shown in Fig. 2-3, the electromagnetic structure can be presented by three coupling parameters: the primary self-inductance L_p; the secondary self-inductance L_s; and the mutual inductance M between the primary and secondary.

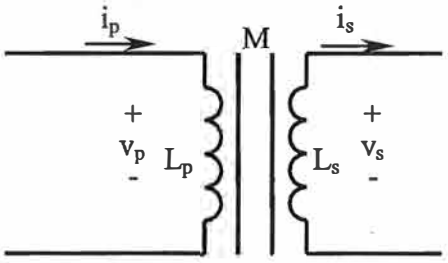


Fig. 2-3. Circuit of the mutual inductance transformer model.

The mutual inductance M is related to the magnetic coupling coefficient k by:

InductEV, Inc.
Exhibit 1010
Page 132

$$k = \frac{M}{\sqrt{L_p L_s}} \tag{2-1}$$

The primary voltage and current are represented as 'v_p' and 'i_p', while the secondary voltage and current are shown as 'v_s' and 'i_s.'

The interactions between the primary and secondary can be represented (under the assumption that no saturation occurs) by:

$$v_p = L_p \frac{di_p}{dt} - M \frac{di_s}{dt} \tag{2-2}$$

and

$$v_s = M \frac{di_p}{dt} - L_s \frac{di_s}{dt} \tag{2-3}$$

Assuming sinusoidal voltages and currents, (2-2) and (2-3) can be simplified to:

$$V_p = j\omega L_p I_p - j\omega M I_s \tag{2-4}$$

and

$$V_s = j\omega M I_p - j\omega L_s I_s \tag{2-5}$$

The equivalent circuit of the sinusoidal mutual inductance transformer model can be derived from (2-4) and (2-5), and is shown in Fig. 2-4. In this circuit, an induced voltage represents the influence of the primary current on the secondary, while the effect of the secondary current on the primary is shown as a reflected voltage. The induced and reflected voltages in this model are specified in terms of the mutual inductance M, the operational frequency ω, the primary current I_p, and the secondary current I_s.

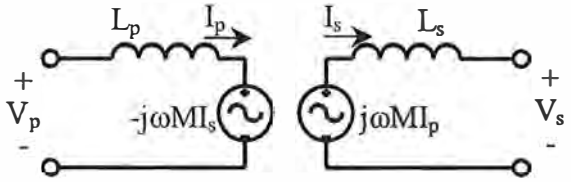


Fig. 2-4. The sinusoidal mutual inductance transformer model.

The mutual inductance M can be determined in a physical system by an open circuit test. The secondary is left open circuit and a sinusoidal primary current I_p with a known frequency ω is made to flow in the primary. The secondary voltage V_s is measured, and is called the open circuit voltage V_{oc} in this thesis. Since the secondary current I_s is zero, (2-5) leads to the open circuit voltage V_{oc} given as:

$$V_{oc} = \omega M I_p \tag{2-6}$$

The mutual inductance determined by the open circuit test is therefore:

$$M = \frac{V_{oc}}{\omega I_p} \tag{2-7}$$

InductEV, Inc.
Exhibit 1010
Page 133

Alternatively, the mutual inductance M can be determined by a short circuit test. A short circuit is placed on the secondary and a sinusoidal primary current I_p is made to flow in the primary. The secondary current I_s is measured, and is called the short circuit current I_{sc} in this thesis. In this case, the secondary voltage V_s is zero and (2-5) leads to the short circuit current I_{sc} given as:

$$I_{sc} = \frac{MI_p}{L_s} \tag{2-8}$$

The mutual inductance determined by the short circuit test is therefore:

$$M = \frac{I_{sc}L_s}{I_p} \tag{2-9}$$

2-2.4 CAPABILITY OF THE ELECTROMAGNETIC STRUCTURE

In this section, the capability of the electromagnetic structure is analyzed using the mutual inductance transformer model developed above. The load voltage and current are characterized for all load conditions. The design factors that need to be optimized to achieve maximum power transfer capability are then determined.

2-2.4.1 LOAD VOLTAGE AND CURRENT

It is assumed in the following analysis that a constant current I_p at a known frequency ω flows in the primary, while the secondary supplies power to a linear and resistive load. The equivalent secondary circuit is shown in Fig. 2-5 using the induced voltage due to the primary current.

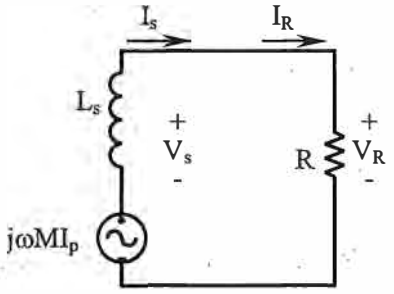


Fig. 2-5. Equivalent secondary circuit supplying power to a linear and resistive load.

The impedance of the secondary as seen by the induced voltage is:

$$Z_s = j\omega L_s + R \tag{2-10}$$

The load current (secondary current) equals the induced voltage divided by the secondary impedance, and is given by:

InductEV, Inc.
Exhibit 1010
Page 134

$$I_R = I_s = \frac{j\omega M I_p}{Z_s} = \frac{j\omega M I_p}{j\omega L_s + R} \tag{2-11}$$

The load voltage (secondary voltage) can be calculated by substituting (2-11) into (2-5) resulting in:

$$V_R = V_s = \frac{j\omega M I_p R}{j\omega L_s + R} \tag{2-12}$$

Eliminating the load resistance R from (2-11) and (2-12), the relation between the amplitudes of the load voltage and current is:

$$V_R^2 = (\omega M I_p)^2 - (\omega L_s)^2 I_R^2 \tag{2-13}$$

The above equation can be normalized using the open-circuit voltage and short-circuit current resulting in:

$$\left(\frac{V_R}{V_{oc}}\right)^2 = 1 - \left(\frac{I_R}{I_{sc}}\right)^2 \tag{2-14}$$

The normalized load voltage and current given by (2-14) are shown in Fig. 2-6 for the complete load range. As the load varies from short circuit (R=0) to open circuit (R=∞), the load current drops from I_{sc} to zero, while the load voltage increases from zero to V_{oc}.

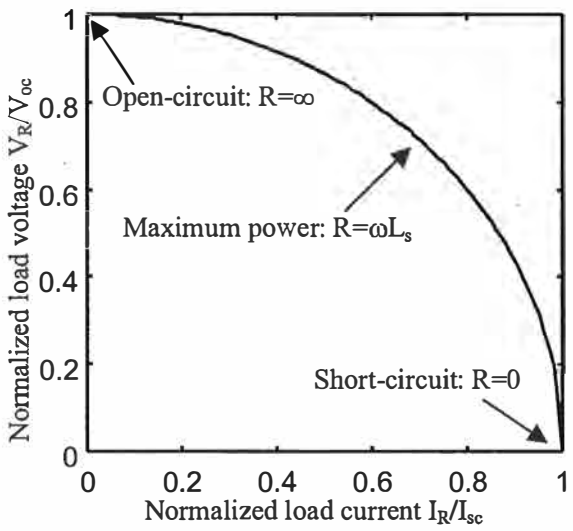


Fig. 2-6. The normalized load voltage and current of the uncompensated pickup.

2-2.4.2 POWER TRANSFER CAPABILITY

The secondary voltage is zero under short-circuit conditions, while the secondary current is zero at open-circuit. Consequently, the power transfer capability is zero under both short-circuit and open-circuit conditions. Maximum power is achieved at a particular load between these two conditions.

The power transfer is the product of the load current and voltage. Since the load current and voltage

InductEV, Inc.
Exhibit 1010
Page 135

in (2-11) and (2-12) are complex variables, the coupling power must be represented by the load current (voltage), multiplied by the conjugate of the load voltage (current) as given by:

$$P = I_R V_R^* = I_R^* V_R = I_R I_R^* R = \frac{V_R V_R^*}{R} \tag{2-15}$$

Substituting (2-10) and (2-12) into (2-15) results in:

$$P = \frac{\omega^2 M^2 R I_p^2}{\omega^2 L_s^2 + R^2} \tag{2-16}$$

The maximum power transfer can be calculated at the following load condition:

$$\frac{\partial P}{\partial R} = 0 \tag{2-17}$$

Solving (2-17) results in:

$$R = \omega L_s \tag{2-18}$$

At this load condition, both the normalized load voltage and current shown in Fig. 2-6 are equal to $1/\sqrt{2}$.

The maximum power transfer calculated using (2-16) and (2-18) is:

$$P_{\max} = \frac{\omega M^2 I_p^2}{2L_s} \tag{2-19}$$

The above equation can be rearranged as:

$$P_{\max} = \frac{V_{oc} I_{sc}}{2} \tag{2-20}$$

Substituting (2-1) into (2-19) results in:

$$P_{\max} = \left(\frac{1}{2}\right)\omega I_p^2 \left(\frac{M^2}{L_s}\right) = \left(\frac{1}{2}\right)\omega I_p^2 \left(k^2 L_p\right) \tag{2-21}$$

According to (2-21), the power transfer capability of an electromagnetic structure is proportional to the operating frequency (ω), the square primary current (I_p^2), and the coupling factor ($k^2L_p=M^2/L_s$). The nominal operating frequency should be chosen as high as possible taking into account practical considerations such as size, cost and efficiency. The limit is determined by switching losses in the semiconductors as well as high frequency losses in the passive components. To fully utilize the capability of the copper windings of an ICPT system, the primary current is normally controlled at the maximum rating to ensure maximum power transfer capability. Improving the magnetic coupling such as reducing the air gap or adding magnetic material results in increases of the three coupling parameters (M, L_p and L_s). A major aim in the design of the electromagnetic structure is to maximise the coupling factor k^2L_p ($=M^2/L_s$) in order to maximise the power transfer, while minimize the weight and cost.

InductEV, Inc.
Exhibit 1010
Page 136

2-3 COMPENSATION

Both the primary and secondary of the electromagnetic structure are often compensated by capacitors to boost the power transfer capability of the pickup, while minimizing the VA rating of the power supply. This section introduces the basic compensation topologies. The compensation level and the resonant behaviour of the primary and secondary resonant circuits are quantified for each topology.

2-3.1 SECONDARY COMPENSATION

To compensate for the secondary inductance (L_s), a capacitor (C_s) can be connected either in series [23-28] or parallel [29-34] with the secondary winding. The equivalent circuits are shown in Fig. 2-7 and 2-8 with the influence of the primary represented by the induced voltage. An equivalent resistance (R) represents the load on the secondary pickup. Under series compensation, the secondary winding, compensation capacitor and the load are all connected in series. For parallel compensation, they are all connected in parallel.

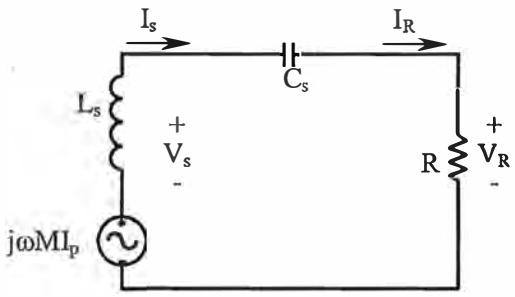


Fig. 2-7. Series-compensated secondary.

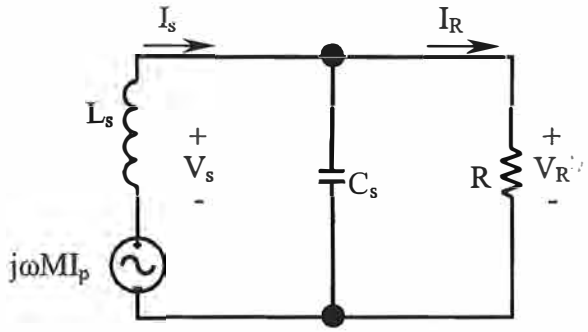


Fig. 2-8. Parallel-compensated secondary.

For maximum power transfer, the secondary resonant frequency (when C_s is in resonance with L_s) is normally designed to equal the nominal frequency (ω_0). In this case, the secondary compensation capacitance is determined as:

$$C_s = \frac{1}{\omega_0^2 L_s} \tag{2-22}$$

The secondary compensation level is quantified in terms of the secondary quality factor (Q_{s0}), defined as the ratio of reactive to real power of the secondary resonant circuit at ω_0. This secondary quality factor derived in Chapter 3 (equation 3-24) is:

$$Q_{s0} = \begin{cases} \dfrac{1}{\omega_0 C_s R} = \dfrac{\omega_0 L_s}{R} & \text{Series secondary} \\ \omega_0 C_s R = \dfrac{R}{\omega_0 L_s} & \text{Parallel secondary} \end{cases} \tag{2-23}$$

InductEV, Inc.
Exhibit 1010
Page 137

2-3.2 SECONDARY RESONANCE

Both series and parallel secondary compensation improve the power transfer capability of the pickup, but present very different characteristics to the load. The circuit equation of the series-compensated pickup (Fig. 2-7) is:

$$j\omega MI_p = \left(j\omega L_s + \frac{1}{j\omega C_s} \right) I_R + V_R \tag{2-24}$$

At ω_0, L_s is in resonance with C_s so that the load voltage V_R derived from (2-24) is identical to the open circuit voltage ($V_R=\omega MI_p=V_{oc}$). The series-compensated pickup therefore exhibits a voltage source to the load. The load current is inversely proportional to the load ($I_R=V_R/R=V_{oc}/R$), and can also be expressed in terms of I_{sc} and Q_{s0} ($I_R=I_{sc}Q_{s0}$).

With series compensation, the pickup power at ω_0 is:

$$P_{series} = V_R I_R = Q_{s0} V_{oc} I_{sc} \tag{2-25}$$

The circuit equation of a parallel-compensated pickup (Fig. 2-8) is:

$$j\omega MI_p = j\omega L_s I_s + \frac{1}{j\omega C_s}(I_s - I_R) = \left(j\omega L_s + \frac{1}{j\omega C_s} \right) I_s - \frac{1}{j\omega C_s} I_R \tag{2-26}$$

At ω_0, the pickup load current derived from (2-26) is equal to the short circuit current ($I_R=\omega^2 C_s MI_p =MI_p/L_s=I_{sc}$). The parallel-compensated pickup therefore exhibits a current source to the load. The pickup load voltage is proportional to the load ($V_R=I_R R=I_{sc}R$), and can be expressed in terms of V_{oc} and Q_{s0} ($V_R=V_{oc}Q_{s0}$).

With parallel compensation, the pickup power at ω_0 is:

$$P_{parallel} = V_R I_R = Q_{s0} V_{oc} I_{sc} \tag{2-27}$$

Comparing (2-20) with (2-25) and (2-27), it can be seen that the pickup power transfer capability is improved by a factor $2Q_{s0}$ with either series or parallel secondary compensation compared to the uncompensated case.

The normalized load voltage and current are shown in Fig. 2-9 for uncompensated as well as series and parallel compensated secondary topologies. In this figure, the load voltage is normalized using the open circuit voltage, while the load current is normalized using the short circuit current.

With series compensation, the normalized load voltage is always unity, while the normalized load current increases with increasing load. With parallel compensation, the normalized load current is always unity, whereas the normalized load voltage increases with increasing load.

InductEV, Inc.
Exhibit 1010
Page 138

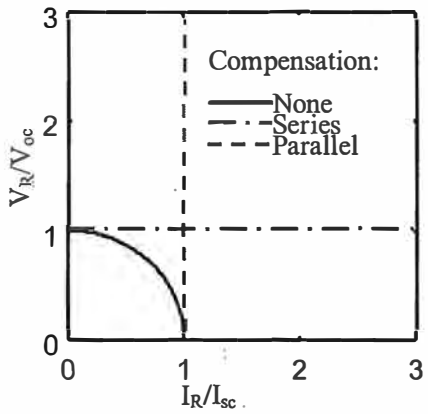


Fig. 2-9. Normalized load voltage and current characteristics of uncompensated as well as series and parallel-compensated pickups.

The pickup voltages, currents, power and required VA ratings at ω_0 are summarized in Table 2-1. In this table, the capability of the pickup at ω_0 is represented in terms of Q_{s0}, V_{oc} and I_{sc}. Although the pickup power transfer capability has been increased by the factor $2Q_{s0}$ over that of an uncompensated pickup, the disadvantage of a compensated pickup is that the required VA rating is significantly higher. The required VA rating of the secondary winding is larger than the real power by a factor of $\sqrt{1+Q_{s0}^2}$, while the required VA rating of the secondary compensation capacitor is Q_{s0} times higher than the real power. These components need to be dimensioned to handle the increased VA requirements.

TABLE 2-1
PICKUP VOLTAGES, CURRENTS, POWER AND REQUIRED VA RATINGS

Pickup topology	Series compensation	Parallel compensation
Load voltage V_R	V_{oc}	$Q_{s0}V_{oc}$
Load current I_R	$Q_{s0}I_{sc}$	I_{sc}
Pickup power P	$Q_{s0}V_{oc}I_{sc}$	$Q_{s0}V_{oc}I_{sc}$
Secondary voltage V_s	$\sqrt{1+Q_{s0}^2}V_{oc}$	$Q_{s0}V_{oc}$
Secondary current I_s	$Q_{s0}I_{sc}$	$\sqrt{1+Q_{s0}^2}I_{sc}$
Required secondary VA rating VA_s	$Q_{s0}\sqrt{1+Q_{s0}^2}V_{oc}I_{sc}$	$Q_{s0}\sqrt{1+Q_{s0}^2}V_{oc}I_{sc}$
Secondary capacitor voltage V_{Cs}	$Q_{s0}V_{oc}$	$Q_{s0}V_{oc}$
Secondary capacitor current I_{Cs}	$Q_{s0}I_{sc}$	$Q_{s0}I_{sc}$
Required secondary capacitor VA rating VA_{Cs}	$Q_{s0}^2V_{oc}I_{sc}$	$Q_{s0}^2V_{oc}I_{sc}$

2-3.3 PRIMARY COMPENSATION

Similar to the secondary compensation, a capacitor (C_p) can be connected in series [35-41] or parallel [42-46] with the primary winding. The equivalent circuits are shown in Fig. 2-10 and 2-11

InductEV, Inc.
Exhibit 1010
Page 139

with the influence of the secondary represented by the reflected voltage in series connection with the primary inductance.

The primary resonant frequency (when C_p is in resonance with L_p) is normally designed to equal the nominal frequency (ω_0). In this case, the primary compensation capacitance is determined as:

$$C_p = \frac{1}{\omega_0^2 L_p} = \frac{C_s L_s}{L_p} \tag{2-28}$$

The primary compensation level can be quantified by the primary quality factor (Q_{p0}) defined as the ratio of reactive to real power associated with the primary coil at the nominal frequency (ω_0). This primary quality factor derived in Chapter 3 (equation 3-51) as a function of the secondary quality factor (Q_{s0}) and the magnetic coupling coefficient (k) is:

$$Q_{p0} = \begin{cases} \dfrac{1}{k^2 Q_{s0}} & \text{series secondary} \\ \dfrac{1-k^2}{k^2 Q_{s0}} = \dfrac{1}{k^2 Q_{s0}} - \dfrac{1}{Q_{s0}} & \text{parallel secondary} \end{cases} \tag{2-29}$$

The primary compensation level is determined intrinsically once the secondary compensation level is selected for a given electromagnetic coupling structure.

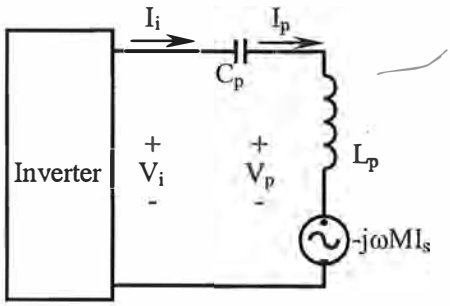


Fig. 2-10. Series-compensated primary.

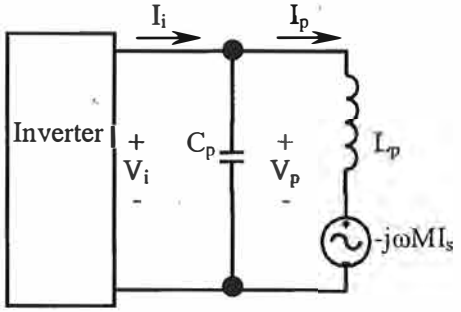


Fig. 2-11. Parallel-compensated primary.

2-3.4 PRIMARY RESONANCE

With a series-compensated primary, the voltage across the primary coil is much larger than the inverter output voltage. This voltage gain is useful for long track systems where the track voltage can be very large. The voltage gain of a series-compensated primary (derived in Appendix A as a function of the primary and secondary quality factors) is:

$$V_{GAIN} = \begin{cases} \sqrt{1+Q_{p0}^2} & \text{Series primary and series secondary} \\ \sqrt{\dfrac{Q_{s0}^2\left(1+Q_{p0}^2\right)}{1+Q_{s0}^2}} & \text{Series primary and parallel secondary} \end{cases} \tag{2-30}$$

InductEV, Inc.
Exhibit 1010
Page 140

In a parallel-compensated primary, the current flowing through the primary coil is much larger than the inverter output current. This current gain is useful when a large current is required for the primary coil. The current gain of a parallel-compensated primary (derived in Appendix A as a function of the primary and secondary quality factors) is:

$$I_{GAIN} = \begin{cases} Q_{p0} & \text{Parallel primary and series secondary} \\ \sqrt{\dfrac{\left(1+Q_{p0}Q_{s0}\right)^2}{1+Q_{s0}^2}} & \text{Parallel primary and parallel secondary} \end{cases} \quad (2\text{-}31)$$

In ICPT systems, the primary and secondary quality factors are usually larger than unity. As a result, the magnitudes of both the voltage and current gains calculated using (2-30) and (2-31) are governed by Q_p. According to (2-29), increasing Q_s or improving k results in lower Q_p, and as such less voltage or current gain.

2-3.5 BASIC COMPENSATION TOPOLOGIES

Three basic compensation choices exist for both the primary and secondary (series compensation, parallel compensation, or uncompensated). Combining the primary and secondary results in nine fundamental compensation topologies [18] as illustrated in Fig. 2-12.

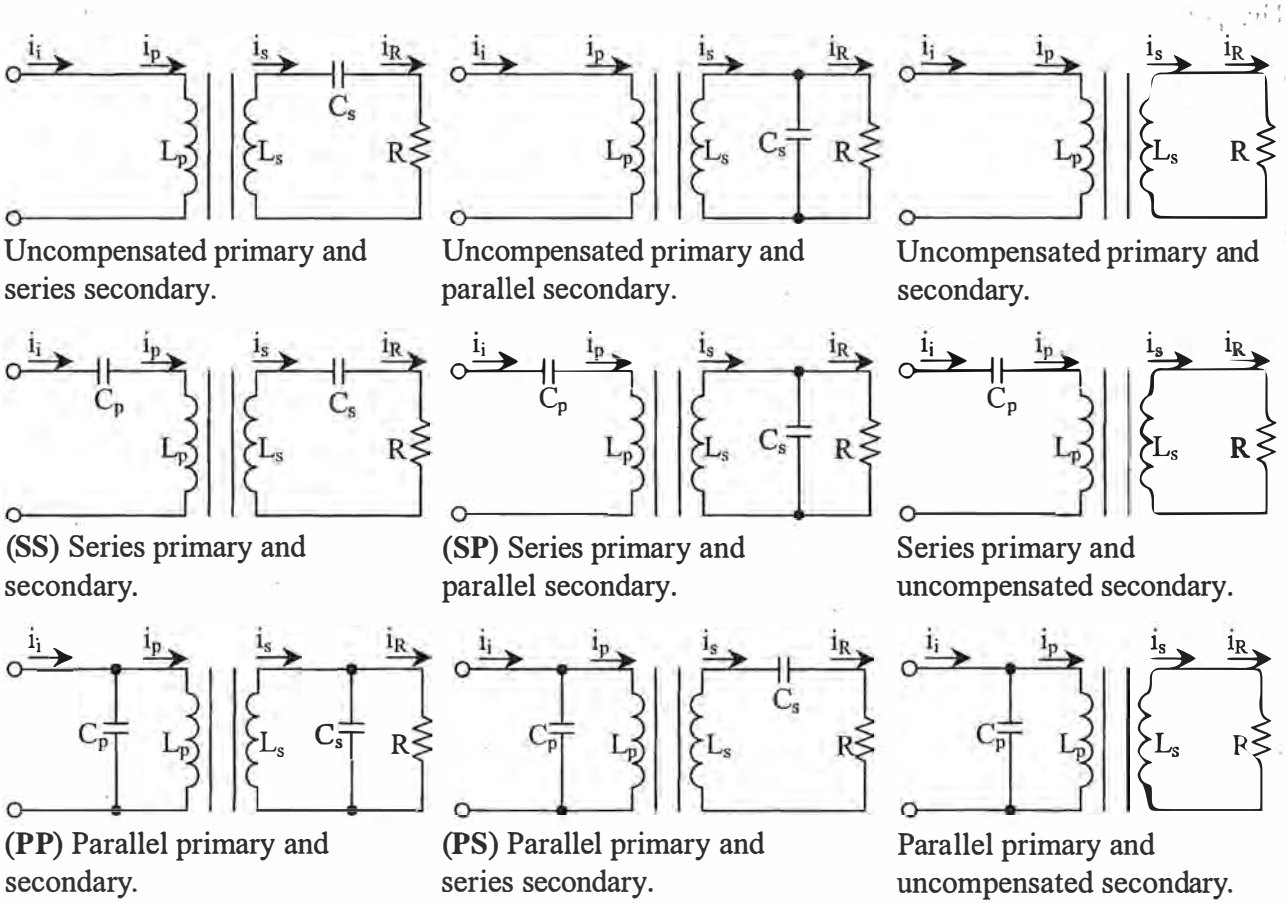


Fig. 2-12. Basic compensation topologies of ICPT systems.

InductEV, Inc.
Exhibit 1010
Page 141

This thesis focuses only on the four basic topologies with both the primary and secondary either series or parallel compensated. They are labelled as SS, SP, PP and PS as shown in Fig. 2-12, where the first S or P stands for series or parallel compensation for the primary winding and the second S or P stands for series or parallel compensation for the secondary winding. Subscripts 'p' and 's' stand for primary and secondary respectively, while the resistance R represents the load on the secondary.

2-4 POWER CONVERTERS

The selection of a suitable power converter depends strongly on the requirements of practical ICPT applications, which include size, cost and power level. Suitable power converters for ICPT applications are identified in this section.

2-4.1 OVERVIEW OF POWER CONVERTERS

ICPT power converters convert incoming utility ac power into dc by rectifiers, and then convert the dc into the required ac power by inverters. Alternatively, the dc power can be supplied from a battery. The power converter can be operated in the linear mode or switch mode. Linear mode power converters have very low efficiencies, typically between 5 and 50%. In this thesis, only switch mode power converters will be considered. The block diagram of a power converter in an ICPT system is shown in Fig. 2-13 as three subsystems: the power source, the high frequency inverter and the resonant tank.

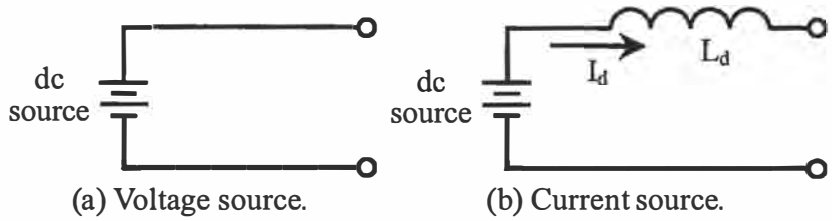


Fig. 2-13. The block diagram of a power converter in an ICPT system.

As shown in Fig. 2-14, two fundamental types of power source are available: voltage sourced and current sourced [47, 48]. The input to a voltage-sourced inverter is assumed to be a constant dc voltage. For a current-sourced inverter, a large inductor is placed in series with the dc voltage source. The input to a current-sourced inverter can thus be assumed to be a constant current. The high frequency inverter can be configured using a single switch, two switches (half-bridge), or four switches (full-bridge) as discussed in the following sections. The full-bridge topology has the highest power capability with various control options, while the single-switch topology has the lowest power capability with limited

InductEV, Inc.
Exhibit 1010
Page 142

control options. The resonant tank consists of the electromagnetic structure, the primary and secondary compensation networks, and the pickup load.



(a) Voltage source. (b) Current source.

Fig. 2-14. Fundamental types of power source.

Power switches can be categorized into three groups. In the first group are diodes with on and off states controlled by the power circuit. In the second group are naturally commutated devices, which can be turned on by a control signal but must be turned off by the power circuit. In the final group are forced commutated switches, which can be turned on and off by control signals.

Diodes can be classified into three categories. Line frequency diodes have large reverse recovery times and as such are not suitable for ICPT applications that typically operate with a frequency above a few kHz. The reverse recovery times of Schottky diodes are negligible. However, the voltage blocking capabilities limits them. Fast recovery diodes have much higher power capabilities with a small reverse recovery time.

Before the appearance of forced commutated switches, naturally commutated devices had been widely used. They still have the highest power capability. Various types of naturally commutated devices are available. The slow switching speed limits the maximum operating frequency to a few kHz.

Forced commutated switches include several device types including gate turn off thyristors (GTOs), MOS controlled thyristors (MCTs), metal-oxide-semiconductor field effect transistors (MOSFETs) and insulated gate bipolar transistors (IGBTs).

GTOs have the highest power capability but lowest switching speed. MCTs have lower power capability but faster switching speed than GTOs. However, they have been taken over by IGBTs. IGBTs with improved characteristics including increased power capability and switching speed have become readily available in recent years. MOSFETs have the lowest power capability but fastest switching speed.

In order to reduce the size and cost of ICPT systems, it is desirable to increase the operating frequency to well above the audible range. This leaves MOSFETs and IGBTs as the most suitable choices for such applications.

Switches can be configured as either reverse conducting or reverse blocking using associated

InductEV, Inc.
Exhibit 1010
Page 143

diodes. The reverse conducting switch configuration has an anti-parallel diode as shown in Fig. 2-15 (a). With this configuration, the current can flow in either direction but the voltage can be blocked in only one direction. The reverse blocking switch configuration has a series diode as shown in Fig. 2-15 (b). This configuration can block voltage in either direction, but the current can flow in one direction only.



(a) Reverse conducting switch configuration. (b) Reverse blocking switch configuration.

Fig. 2-15. Switch configurations.

2-4.2 VOLTAGE-SOURCED POWER CONVERTERS

A voltage-sourced full-bridge power converter, as shown in Fig. 2-16, uses four reverse conducting switches. With the diagonal switch pairs (S_1/S_4 and S_2/S_3) in alternating conduction, the inverter output voltage (v_i) is approximately rectangular. This configuration has been used for ICPT applications such as medical implants [49-54], electric vehicles [55-58] and material handling facilities [59-61]. In this thesis, a voltage-sourced full-bridge power converter is used in a practical example for contact-less electric vehicle battery charging.

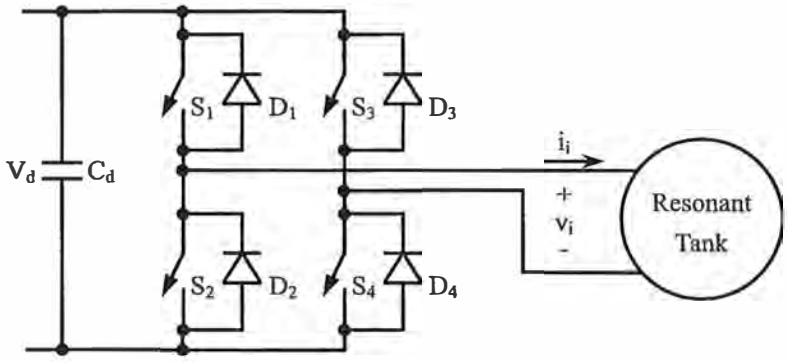


Fig. 2-16. The voltage-sourced full-bridge power converter.

In a voltage-sourced half-bridge power converter, as shown in Fig. 2-17, one leg of the full-bridge is replaced by centre-tapped capacitors. The two switches alternate their conduction resulting in an approximately rectangular inverter output voltage. This inverter utilizes only two switches and therefore is cheaper than the full-bridge topology. However, the amplitude of the rectangular output voltage is only half the dc voltage. This topology has been used for medical implants [62-65], portable

InductEV, Inc.
Exhibit 1010
Page 144

electronics devices [66], electric vehicles [67-71] and material handling facilities [72].

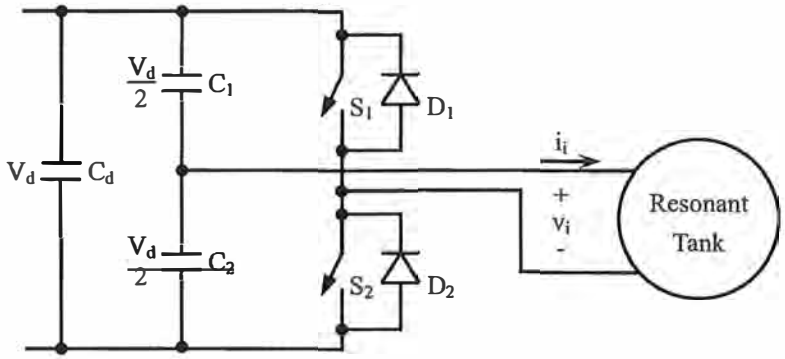
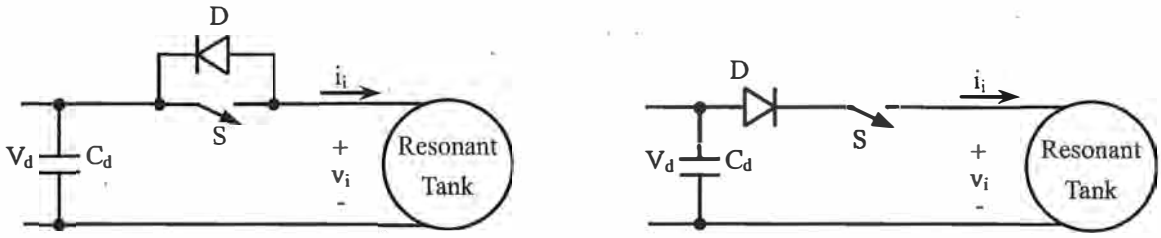


Fig. 2-17. The voltage-sourced half-bridge power converter.

Voltage-sourced single-switch topologies have been investigated in detail in [73-74] for induction heating applications. A common topology for ICPT applications is shown in Fig. 2-18 (a) using a single reverse conducting switch. Low power applications of this topology can be found in [42][75]. Alternatively, a reverse blocking switch can be used as shown in Fig. 2-18 (b).



(a) Reverse conducting switch configuration. (b) Reverse blocking switch configuration.

Fig. 2-18. Voltage-sourced single-switch power converters.

2-4.3 CURRENT-SOURCED POWER CONVERTERS

While current-sourced power converters are not as popular as the voltage-sourced power converters due to the requirement for bulky dc inductors, they have been commonly used in early ICPT systems developed over the past decade [47][76-79]. This is because the current-sourced power converter has the intrinsic ability to maintain constant track/coil current. This is essential to ICPT systems especially for the track-type high power industrial applications with multiple pickups.

A current-sourced full-bridge power converter, as shown in Fig. 2-19, consists of four reverse blocking switches. Diagonal switch pairs conduct in alternate half cycles, producing an inverter output current that is close to a square wave.

In a current-sourced half-bridge power converter as shown in Fig. 2-20, a centre-tapped transformer

InductEV, Inc.
Exhibit 1010
Page 145

replaces the top two switches of the full-bridge.

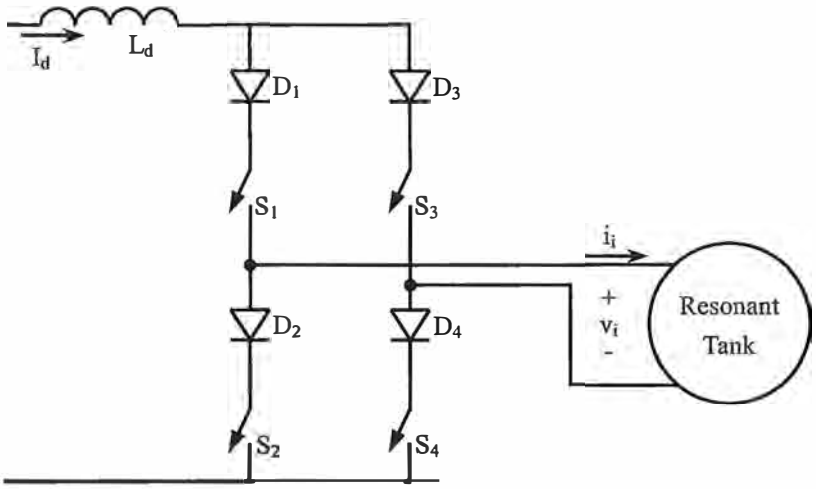


Fig. 2-19. The current-sourced full-bridge power converter.

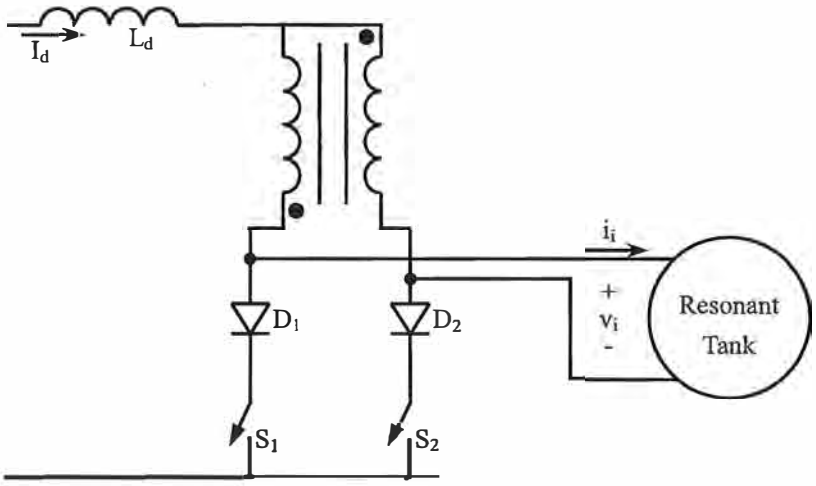
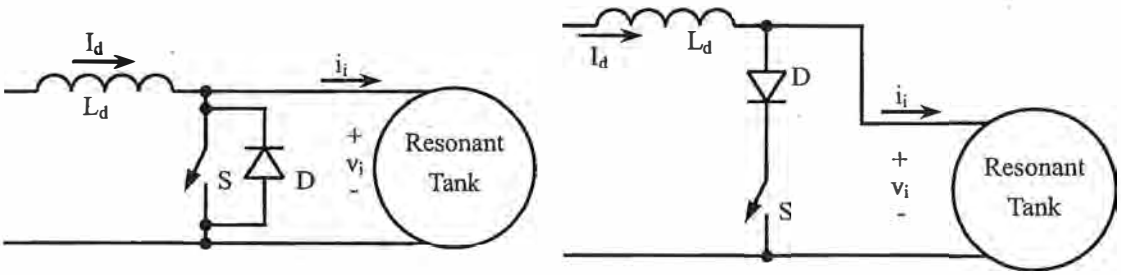


Fig. 2-20. The current-sourced half-bridge power converter.

Current-sourced single-switch topologies have been investigated in detail in [73-74] for induction heating applications. A common configuration for ICPT applications is shown in Fig. 2-21 (a) using a single reverse conducting switch. Low power applications using this topology can be found in [80-81]. Alternatively, the reverse blocking switch can be used as shown in Fig. 2-21 (b).



(a) Reverse conducting switch configuration. (b) Reverse blocking switch configuration.

Fig. 2-21. Current-sourced single-switch power converters.

InductEV, Inc.
Exhibit 1010
Page 146

2-4.4 IMPEDANCE MATCHING

For the voltage-sourced power converter with a rectangular output voltage waveform, a series inductor is required at the inverter output stage in order to avoid current spikes caused by sudden changes in voltage. With a series-compensated primary, the primary winding plays the role of such a series inductor and therefore voltage-sourced inverters can be used directly without additional impedance matching components. An additional series inductor is necessary if a voltage-sourced inverter is used to drive a parallel-compensated primary as shown in Fig. 2-22. This arrangement results in an LCL resonant inverter.

LCL resonant inverters operating with continuous current have been used for both induction heating [82-85] and ICPT applications [47]. In this thesis, an LCL resonant inverter operating in discontinuous current mode is used to supply high frequency voltage and current to a practical ICPT application for contact-less electric vehicle battery charging. Its operation is discussed in detail in Chapter 8.

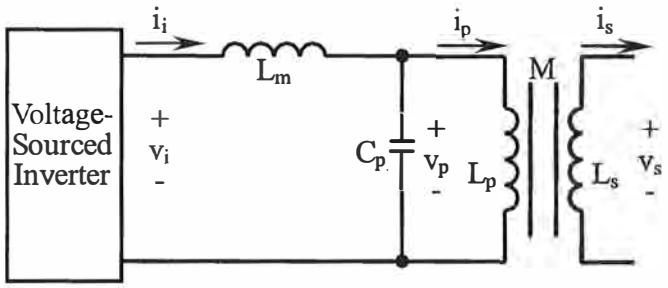


Fig. 2-22. The LCL resonant inverter.

For a current-sourced power converter with a rectangular output current waveform, a parallel capacitor is required across the inverter output stage in order to avoid voltage overshoots caused by sudden changes in the direction of current. With a parallel-compensated primary, the primary capacitor plays the role of the parallel capacitor and therefore current-sourced inverters can be used directly without impedance matching components. An additional parallel capacitor is necessary if a current-sourced inverter is used to drive a series-compensated primary as shown in Fig. 2-23. This arrangement results in a CCL resonant inverter.

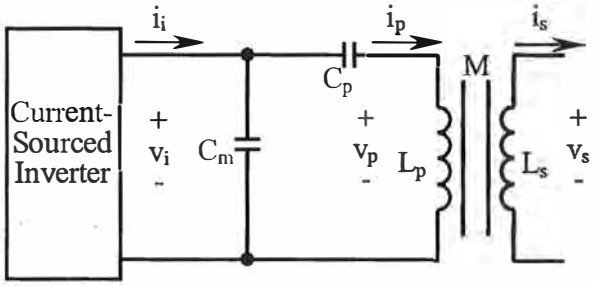


Fig. 2-23. The CCL resonant inverter.

InductEV, Inc.
Exhibit 1010
Page 147

2-5 CONTROLLERS

Various controllers may be used in the primary or the secondary. These are often necessary to accommodate varying operating conditions such as variations in the load, misalignment of the electromagnetic structure, fluctuations in the power source, as well as the tolerance, thermal effects and aging of the circuit components. In this section, control options suitable for ICPT systems are discussed. The bifurcation phenomenon (multiple operating modes in the frequency spectrum) present in variable-frequency systems is also introduced.

2-5.1 POWER FLOW REGULATION

For single pickup applications, power flow regulation can be implemented in the primary or the secondary. Most single pickup low power ICPT applications, such as battery charging for medical implants and portable consumer products, do not employ a secondary controller and as such the primary controller is responsible for providing suitable voltage, current and power to the secondary load. This approach may have the advantage of reduced size and cost of the pickup, but a feedback loop from the secondary to the primary is often necessary. The feedback loop is normally achieved using an additional wireless communication link. When a secondary controller is used to regulate pickup power flow, the feedback communication link may be eliminated. In this case, one of the control objectives of the primary controller is to achieve a constant primary current. In order to fully utilize the capability of the electromagnetic structure, the primary current is normally controlled at the maximum current rating.

In a multiple pickup system, the loading condition on each pickup is almost always different. Since power flow regulation at the primary affects all secondary pickups, it is not a good choice for multiple pickup applications and a secondary controller is required for each individual pickup [1-4][9][14-15] [20][45][47][79]. These secondary controllers normally utilize a switch mode converter to regulate power flow. The pickup regulator will be discussed further in section 4-3.

One option to control power or current in the primary is to regulate the dc voltage [31][48][67] [86]. This approach is suitable for all inverter topologies, but the disadvantage is increased size and cost of the dc-stage. Another option for single pickup applications is to shift the operating frequency around the resonant frequency (ω_0) of the pickup. This approach is applicable for both full-bridge and half-bridge inverters, but the resulting switching losses needs to be considered carefully. For the full-bridge inverter, controlling the duty-cycle of the inverter is a common choice.

InductEV, Inc.
Exhibit 1010
Page 148

2-5.2 FREQUENCY CONTROL

The primary controller can be separated into two major groups respectively with fixed or variable frequency control. A fixed-frequency controller forces the operating frequency to a predetermined value, while a variable-frequency controller allows the operating frequency to vary over a predetermined range.

With a fixed-frequency controller, the secondary resonant frequency is designed to be equal to the operating frequency in order to ensure maximum power transfer to the pickup. Fixed-frequency controllers thus have the advantage that a compensated pickup will always run at its correct tuned frequency. However, the power supplies need to be overrated since the displacement power factor (DPF) will invariably not be unity due to varying operating conditions.

Variable-frequency controllers allow the operating frequency to vary so that the inverter operates close to unity DPF. This ensures that the power supply does not have to be overrated, but frequency-detuning effects within the pickup are unavoidable resulting in reduced power transfer capability.

In this thesis, several new primary tuning approaches are proposed to reduce frequency detuning in variable-frequency systems, and to improve the DPF of fixed-frequency systems.

2-5.3 SWITCHING CONTROL IN VOLTAGE-SOURCED FULL-BRIDGE INVERTERS

In a voltage-sourced full-bridge inverter, switching exactly at the zero crossing of the output current, as shown in Fig. 2-24, results in zero switching losses. Here, the rectangular output voltage is controlled to be in-phase with the current and as such the voltage and current ratings of the inverter are minimized for a given power transfer.

When switching ahead of the zero crossing of the output current, as shown in Fig. 2-25, the switches are turned off with non zero current resulting in turn-off losses. There are, however, no turn-on losses since the switches are turned on with zero voltage as the current is flowing through the anti-parallel diodes. The current flows through the switches when it changes direction and in consequence starts another power transfer period. With this switching strategy, the rectangular output voltage is leading the output current and the voltage and current ratings of the inverter are higher than the transferred power.

When switching occurs after the zero crossing of the current, as shown in Fig. 2-26, the switches are turned off with zero voltage as the current flows through the anti-parallel diodes. This results in zero turn-off loss. When the switches are turned on, the current commutates from the anti-parallel diodes to the switches, resulting in turn-on losses as well as diode reverse recovery. With this switching strategy,

InductEV, Inc.
Exhibit 1010
Page 149

the rectangular output voltage lags the output current and the voltage and current ratings of the inverter are higher than the transferred power.

For the switching controls shown in Fig. 2-24 to 2-26, the pulse-width of the rectangular inverter voltage is identical to a full half cycle. Here, the diagonal switches are controlled at the same time. Many applications control the pulse-width of the rectangular inverter voltage to regulate power flow as shown in Fig. 2-27. With this strategy, both switches of each diagonal switch-pair are controlled with a phase shift. As the current freewheels through the top or bottom bridge legs, the inverter output voltage is zero. With this approach, it is possible that the left-leg of the full-bridge is switched after zero crossing, while the right leg is switched before the zero crossing of the current. As a result, both switches in the left leg have no turn-off loses but turn-on losses and diode reverse recovery exist. On the other hand, both switches in the right-leg have no turn-on losses but turn-off losses exist.

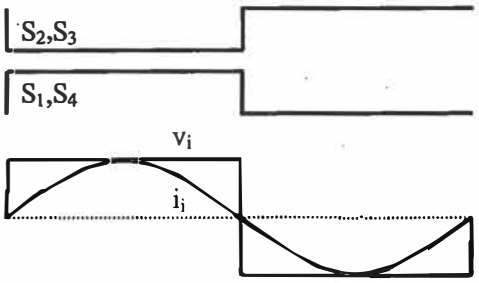


Fig. 2-24. The rectangular inverter voltage being in-phase with the current.

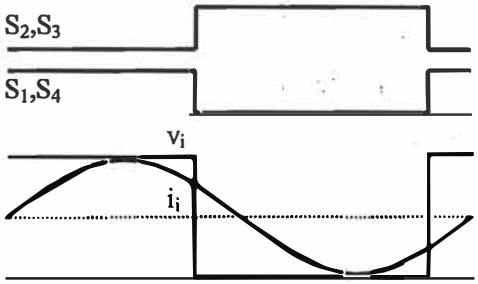


Fig. 2-25. The rectangular inverter voltage leading the current.

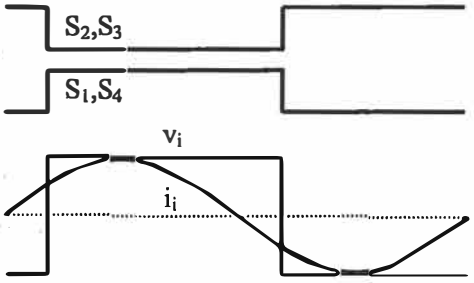


Fig. 2-26. The rectangular inverter voltage lagging the current.

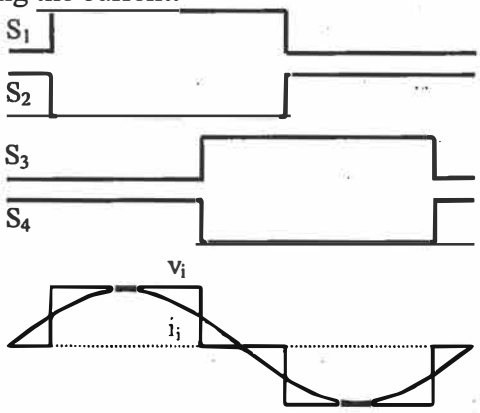


Fig. 2-27. Pulse-width of the rectangular inverter voltage is less than a full half cycle.

2-5.4 SWITCHING CONTROL IN CURRENT-SOURCED FULL-BRIDGE INVERTERS

In a current-sourced full-bridge inverter, switching exactly at the zero crossing of the inverter output voltage, as shown in Fig. 2-28, results in no switching losses since the switches are turned on and off with zero voltage. Moreover, the voltage and current ratings of the inverter are minimized

InductEV, Inc.
Exhibit 1010
Page 150

because the inverter voltage and current are in-phase, eliminating reactive power flow.

When the rectangular inverter current is leading the inverter voltage, as shown in Fig. 2-29, the switches are turned on with the inverter output voltage across them. This results in turn-on losses. But there are no turn-off losses because the switches are turned off with zero voltage and current when the inverter output voltage is blocked by the series diode. With this switching strategy, the voltage and current ratings of the inverter are higher than the transferred power.

If the rectangular inverter current is lagging the voltage, as shown in Fig. 2-30, the switches are turned on with zero voltage and current as the inverter output voltage is blocked by the series diode and therefore there is no turn-on loss. However, the switches are turned off with the inverter output voltage across them, resulting in turn-off losses. With this switching strategy, the voltage and current ratings of the inverter are higher than the transferred power.

When controlling the pulse-width of the rectangular inverter current, as shown in Fig. 2-31, the top two switches have turn-on losses but no turn-off losses, while the bottom two switches have turn-off losses but no turn-on losses.

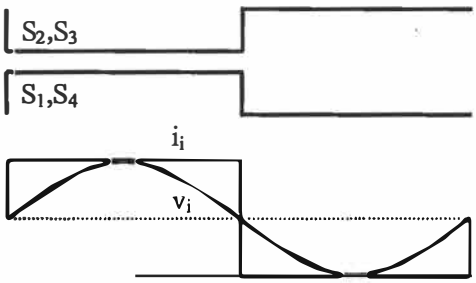


Fig. 2-28. The rectangular inverter current being in-phase with the voltage.

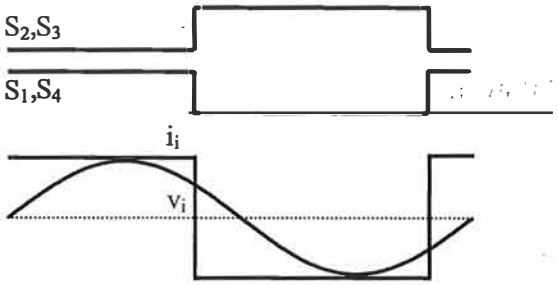


Fig. 2-29. The rectangular inverter current leading the voltage.

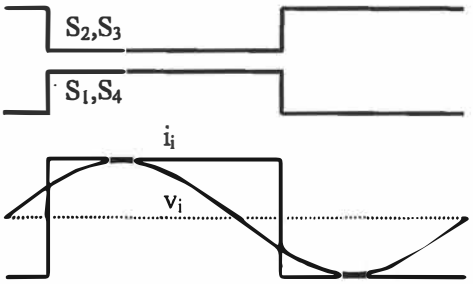


Fig. 2-30. The rectangular inverter current lagging the voltage.

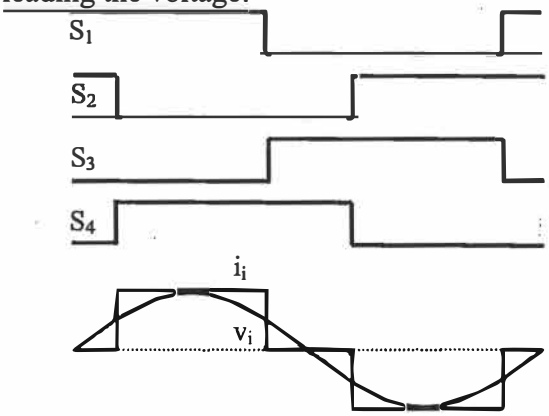


Fig. 2-31. Pulse-width of the rectangular inverter current is less than a full half cycle.

2-5.5 BIFURCATION PHENOMENON

As noted in 2-5.2, a variable-frequency controller allows the frequency to vary so that the power

InductEV, Inc.
Exhibit 1010
Page 151

supply operates with unity DPF. With full-bridge or half-bridge inverters, this is achievable with the inverters switched to track the zero crossing of the inverter output current (in a voltage-sourced power converter) or voltage (in a current-sourced power converter) [2][47][79]. Using this approach, the inverter output voltage and current can be controlled in phase, with the operating frequency varying in response to system variations.

As noted in [2][47][79], there could be more than one operating point in the frequency spectrum, and the variable-frequency controller may jump around these operating modes. Apart from this uncertainty, the operating frequency can shift significantly above or below the secondary resonant frequency resulting in substantial pickup detuning. This phenomenon is termed as a problem of 'frequency stability' in [2][47][79], and is simply labelled as 'bifurcation' in this thesis.

For the design of a variable-frequency system, it is usually required to ensure the system is designed to operate below the bifurcation boundary under all practical operating conditions. If the system needs to operate above the bifurcation boundary, the variable-frequency controller has to be forced to operate at the right operating mode to ensure power transfer capability. In practice, this is difficult.

To date only a limited analysis has been undertaken to determine the bifurcation criterion for selected ICPT systems. In the multiple pickup material handling system [2][79], it was found that bifurcation occurs if the number of pickups is increased such that:

$$n \geq \frac{L_p L_s}{Q_{s0}^2 M^2} \tag{2-32}$$

where n is the number of coupled secondary pickups.

Substituting (2-1) into (2-32) results in:

$$Q_{s0} \geq \frac{1}{\sqrt{n}k} \tag{2-33}$$

As noted in [2][79], this analysis is an approximation assuming high Q_{s0}, and both the parallel-compensated primary and secondary circuits are transformed into series compensated circuits to simplify the analysis. Consequently, the above bifurcation criterion is valid only for ICPT systems with series-compensated primaries and secondaries with high Q_{s0}.

As will be shown in Chapter 9, the equivalent coupling coefficient of a multiple pickup system is found to be proportional to the square root of the number of pickups ($k_n = \sqrt{n}k$). The bifurcation criterion (2-33) expressed in terms of the equivalent coupling coefficient is then:

$$Q_{s0} \geq \frac{1}{k_n} \tag{2-34}$$

With high Q_{s0}, it can be found from (2-23), (2-29) and (2-34) that the bifurcation criterion can be expressed in terms of Q_{p0} and Q_{s0} as:

InductEV, Inc.
Exhibit 1010
Page 152

$$Q_{p0} > Q_{s0} \tag{2-35}$$

As shown the system can achieve bifurcation-free operation when Q_{p0} is larger than Q_{s0}.

A more general bifurcation criterion was developed in [47] for ICPT systems with series-compensated primaries and secondaries. This bifurcation criterion was found to be:

$$Q_{s0} < \frac{\sqrt{1+\sqrt{1-k^2}}}{\sqrt{2}k} \tag{2-36}$$

Using (2-23) and (2-29), the above bifurcation criterion can be expressed in terms of Q_{p0} and Q_{s0} given by:

$$Q_{p0} > \frac{4Q_{s0}^3}{4Q_{s0}^2 - 1} \tag{2-37}$$

At high Q_{s0}, this bifurcation criterion again simplifies to (2-35).

The above bifurcation analysis is again only valid for ICPT systems with series compensated primaries and secondaries. In this thesis, general bifurcation criteria are developed for all basic topologies with the primary and secondary either series or parallel compensated.

2-6 FUTURE TRENDS

Present ICPT technology developments are busy meeting the commercial requirements of industrial applications as well as consumer products. Likely future developments are discussed below.

Wireless Communication Links: Wireless communication between the primary power supply and the secondary pickup is of great importance for many applications where the primary power supply intends to control and/or monitor the secondary pickup. For single pickup coil-type applications such as medical implants, the primary and secondary are very close to each other and communication links have been popularly implemented using radio frequency transceivers on both sides. However, this approach is normally not suitable for multiple pickup track-type applications such as material handling systems in manufacturing sites due to RFI and EMI considerations.

VAHLE (Germany) has been using the slotted microwave guide (SMG) to set up communication links for multiple pickup track-type applications. According to VAHLE, SMG was originally developed by MBB (Messerschmitt-Boelkow-Blohm), now DASA (Deutsche Aerospace), to transmit data to the magnetic levitation train (Transrapid) travelling at speeds of up to 250 mph. VAHLE acquired this technology at the end of 1994 and now has over 1,000 installations worldwide in successful operation.

InductEV, Inc.
Exhibit 1010
Page 153

A favourable approach for communication links in track-type applications would be to use the primary coil to carry radio frequency channels, at a frequency well above that of the power supply. The information transmission is achieved via the same electromagnetic coupling structure used for power transmission, eliminating the additional wave-guide.

New Electromagnetic Materials: Current commercial track-type applications are relatively short (around several hundred meters). The main challenge to enable longer distance is how to overcome conduction losses within the primary coil while limiting voltages. The solution would rely on new materials of conductor windings. Another challenge for long distance track-type applications is that it is economically not acceptable to use expensive magnetic materials such as ferrite along the track to improve magnetic coupling. One possible solution is to utilize cheap magnetic materials such as iron sand.

New Power Electronic Devices and Intelligent Controllers: New semiconductor switches offering better power capability and less loss will enable the operating frequency of high power ICPT industrial applications to be increased, resulting in smaller size magnetic materials. This in turn will extend potential commercial applications. New generations of microprocessors will enable intelligent controllers to be built for very complex multiple pickup applications. In such applications, power and traffic management are critical, requiring low cost high bandwidth wireless communications alongside the contact-less power transfer.

Futuristic Applications: As shown in Fig. 2-32, the aerial cab, the underwater transportation and the electric city bus are among many futuristic projects that are becoming more attractive and realizable with on-going improvements in ICPT technology as well as power electronic and telecommunication techniques.



(a) Aerial cab. (b) Underwater transportation. (c) Electric city bus.

Fig. 2-32. Futuristic ICPT applications.

InductEV, Inc.
Exhibit 1010
Page 154

2-7 CONCLUSIONS

In ICPT systems, the coupling strength of the electromagnetic structure is normally weak and cannot deliver the required power with reasonable size and cost at the line frequency of 50/60 Hz. It is often necessary to increase the frequency to between several kHz and many MHz, depending on the application requirements.

The increased reactance of the primary and secondary windings that arises from these increases in the operating frequency often must be compensated by capacitors connected in series or parallel. Secondary compensation is required for boosting power transfer capability, while primary compensation is introduced to minimize the VA rating of the power supply.

The choice of compensation topologies results in very different circuit characteristics. The series-compensated secondary resembles a voltage source, while the parallel-compensated secondary looks like a current source. The objective of series primary compensation is to achieve a voltage gain between the switching power supply and the primary coil, whereas parallel primary compensation is utilized to obtain a current gain.

Either voltage or current sourced power converters can be used to generate the necessary high frequency voltage and current for ICPT systems. According to the number of switches used, they can be separated into three groups: full-bridge, half-bridge and single switch. Impedance matching must be considered carefully between the selected inverter and primary compensation topology.

Many control strategies can be used to accommodate system variations. For single pickup applications, power control can be implemented at the primary or the secondary. In multiple pickup systems, each pickup needs an individual power regulator.

Both fixed and variable frequency operations can be used for the primary controller. Fixed-frequency operation minimizes pickup detuning, while variable-frequency operation improves the DPF of the power supply. Bifurcation (multiple operating modes) may occur in a variable-frequency system and needs to be considered carefully at the design stage to ensure power transfer capability and controllability.

REFERENCES

[1]. A. Okuno, L. Gamage, M. Nakaoka, "Performance evaluations of high-frequency inverter-linked DC/DC converter with noncontact pickup coil," *IEEE Transactions on Industrial Electronics*, vol. 48, pp. 475-477, Apr. 2001.

[2]. A. W. Green, J. T. Boys, "An inductively coupled high-frequency power system for material handling applications," in *Proc. Int. Power Electronics Conference*, vol. 2, 1993, pp. 821-826.

InductEV, Inc.
Exhibit 1010
Page 155

[3]. A. W. Green, J. T. Boys, "Intelligent Road Studs – Lighting the Paths of the Future," *IPENZ Transactions*, no. 24, pp. 33-40, 1997.

[4]. G. A. Covic, G. Elliott, O. H. Stielau, R. M.Green, J. T. Boys, "The design of a contact-less energy transfer system for a people mover system," in *Proc. International Conference on Power System Technology*, vol. 1, 2000, pp. 79-84.

[5]. Chwei-Sen Wang, G. A. Covic and O. H. Stielau, "Power transfer capability and bifurcation phenomena of loosely coupled inductive power transfer systems," *IEEE Transactions on Industrial Electronics*, vol. 51, pp. 148-157, Feb. 2004.

[6]. R. Laouamer, M. Brunello, J. P. Ferrieux, O. Normand, N. Buchheit, "A multi-resonant converter for non-contact charging with electromagnetic coupling," in *Proc. 23rd International Conference on Industrial Electronics, Control and Instrumentation*, vol. 2, 1997, pp. 792-797.

[7]. Gyu Bum Joun, B. H. Cho, "An energy transmission system for an artificial heart using leakage inductance compensation of transcutaneous transformer," *IEEE Transactions on Power Electronics*, vol. 13, pp. 1013-1022, Nov. 1998.

[8]. Chang-Gyun Kim, Dong-Hyun Seo, Jung-Sik You, Jong-Hu Park, B. H. Cho, "Design of a contactless battery charger for cellular phone," *IEEE Transactions on Industrial Electronics*, vol. 48, pp. 1238-1247, Dec. 2001.

[9]. J. T. Boys, G. A. Covic, G. A. J. Elliott, "Pick-up transformer for ICPT applications," *Electronics Letters*, vol. 38, pp. 1276-1278, Oct. 2002.

[10]. S. C. Tang, S. Y. Hui, Henry Shu-Hung Chung, "Coreless planar printed-circuit-board (PCB) transformers-a fundamental concept for signal and energy transfer," *IEEE Transactions on Power Electronics*, vol. 15, pp. 931-941, Sep. 2000.

[11]. M. Jufer, N. Macabrey, M. Perrottet, "Modeling and test of contactless inductive energy transmission," *Mathematics and computers in simulation*, vol. 46, pp. 197-211, 1998.

[12]. A. Esser, A. Nagel, "Contactless high speed signal transmission integrated in a compact rotatable power transformer," in *Proc. Fifth European Conference on Power Electronics and Applications*, vol. 4, 1993, pp. 409-414.

[13]. M. Eghtesadi, "Inductive power transfer to an electric vehicle-analytical model," in *Proc. IEEE 40th Vehicular Technology Conference*, 1990, pp. 100-104.

[14]. A. W. Kelley, W. R. Owens, "Connectorless power supply for an aircraft-passenger entertainment system," *IEEE Transactions on Power Electronics*, vol. 4, pp. 348-354, July 1989.

[15]. Yong Xiang Xu, J. T. Boys, G. A. Covic, "Modeling and controller design of ICPT pick-ups," in *Proc. International Conference on Power System Technology*, vol. 3, 2002, pp. 1602-1606.

InductEV, Inc.
Exhibit 1010
Page 156

[16]. S. Hussmann, P. A. Hu, "A micro-computer controlled ICPT power pick-up and its EMC considerations for moving sensor applications," in *Proc. International Conference on Power System Technology*, vol. 2, 2002, pp. 1011-1015.

[17]. Chwei-Sen Wang, G. A. Covic, O. H. Stielau, "General stability criterions for zero phase angle controlled loosely coupled inductive power transfer systems," in *Proc. 27th Annual Conference of the IEEE Industrial Electronics Society*, vol. 2, 2001, pp. 1049-1054.

[18]. O. H. Stielau, G. A. Covic, "Design of loosely coupled inductive power transfer systems," in *Proc. International Conference on Power System Technology*, vol. 1, 2000, pp. 85-90.

[19]. Chwei-Sen Wang, O. H. Stielau, G. A. Covic, "Load models and their application in the design of loosely coupled inductive power transfer systems," in *Proc. International Conference on Power System Technology*, vol. 2, 2000, pp. 1053-058.

[20]. G. A. J. Elliott, J. T. Boys, A. W. Green, "Magnetically coupled systems for power transfer to electric vehicles," in *Proc. International Conference on Power Electronics and Drive Systems*, vol. 2, 1995, pp. 797-801.

[21]. H. Matsuki, M. Shiiki, K. Murakami, T. Yamamoto, "Investigation of coil geometry for transcutaneous energy transmission for artificial heart," *IEEE Transactions on Magnetics*, vol. 28 pp. 2406-2408, Sept. 1992.

[22]. W. J. Heetderks, "RF powering of millimeter- and submillimeter-sized neural prosthetic implants," *IEEE Transactions on Biomedical Engineering*, vol. 35, pp. 323-327, May 1988 .

[23]. Yungtaek Jang, M. M. Jovanovic, "A contactless electrical energy transmission system for portable-telephone battery chargers," *IEEE Transactions on Industrial Electronics*, vol. 50, pp. 520-527, June 2003.

[24]. Byungcho Choi, Honnyong Cha, Jaehyun Noh, Sangkyu Park, "A new contactless battery charger for portable telecommunication/computing electronics," in *Proc. International Conference on Consumer Electronics*, 2001, pp. 58-59.

[25]. J. Hirai, Tae-Woong Kim, A. Kawamura, "Study on intelligent battery charging using inductive transmission of power and information," *IEEE Transactions on Power Electronics*, vol. 15, pp. 335-345, March 2000.

[26]. D. A. G. Pedder, A. D. Brown, J. A. Skinner, "A contactless electrical energy transmission system," *IEEE Transactions on Industrial Electronics*, vol. 46, pp. 23-30, Feb. 1999.

[27]. A. Kawamura, K. Ishioka, J. Hirai, "Wireless transmission of power and information through one high-frequency resonant AC link inverter for robot manipulator applications," *IEEE Transactions on Industry Applications*, vol. 32, pp. 503-508, May-June 1996.

InductEV, Inc.
Exhibit 1010
Page 157

[28]. A. Ghahary, B. H. Cho, "Design of transcutaneous energy transmission system using a series resonant converter," *IEEE Transactions on Power Electronics*, vol. 7, pp. 261-269, Apr. 1992.

[29]. J. T. Boys, G. A. Covic, Yongxiang Xu, "DC analysis technique for inductive power transfer pick-ups," *IEEE Power Electronics Letters*, vol. 1, pp. 51-53, June 2003.

[30]. H. Abe, H. Sakamoto, K. Harada, "Load voltage stabilization of noncontact energy transfer using three resonant circuit," in *Proc. Power Conversion Conference*, vol. 2, 2002, pp. 466-471.

[31]. A. P. Hu, Z. J. Chen, S. Hussmann, G. A. Covic, J. T. Boys, "A dynamically on-off controlled resonant converter designed for coalmining battery charging applications," in *Proc. International Conference on Power System Technology*, vol. 2, 2002, pp. 1039-1044.

[32]. D. O'Sullivan, M. Willers, M. G. Egan, J. G. Hayes, P. T. Nguyen, C. P. Henze, "Power-factor-corrected single-stage inductive charger for electric-vehicle batteries," in *Proc. Power Electronics Specialists Conference*, vol. 1, 2000, pp. 509-516.

[33]. J. G. Hayes, M. G. Egan, "A comparative study of phase-shift, frequency, and hybrid control of the series resonant converter supplying the electric vehicle inductive charging interface," in *Proc. Applied Power Electronics Conference and Exposition*, vol. 1, 1999, pp. 450-457.

[34]. L. Juby, A. Green, A. Collinson, "The design of a non-contact charging system for electric vehicles," in *Proc. 32nd Universities Power Engineering Conference*, 1997, pp. 573-576.

[35]. S. Valtchev, B. V. Borges, J. B. Klaassens, "Contactless energy transmission with optimal efficiency," in *Proc. 28th Annual Conference of the Industrial Electronics Society*, vol. 2, 2002, pp. 1330-1335.

[36]. Byeong-Mun Song, R. Kratz, S. Gurol, "Contactless inductive power pickup system for Maglev applications," in *Proc. IEEE Industry Applications Society Annual Meeting*, vol. 3, 2002, pp. 1586-1591.

[37]. Byungcho Choi, Jachyun Nho, "Contactless energy transfer using planar printed circuit board windings," *Electronics Letters*, vol. 37, pp. 1007-1009, Aug. 2001.

[38]. N. H. Kutkut, D. M. Divan, D. W. Novotny, R. H. Marion, "Design considerations and topology selection for a 120-kW IGBT converter for EV fast charging," *IEEE Transactions on Power Electronics*, vol. 13, pp. 169-178, Jan. 1998.

[39]. A. Esser, H.-C. Skudelny, "A new approach to power supplies for robots," *IEEE Transactions on Industry Applications*, vol. 27, pp. 872-875, Sept.-Oct. 1991.

[40]. K. Sylvan, J. R. Jordan, H. W. Whittington, "A shunt-excited inductive power link," *Journal of Medical Engineering and Technology*, vol. 13, pp. 215-219, July/Aug. 1989.

InductEV, Inc.
Exhibit 1010
Page 158

[41]. J. Lukacs, M. Kiss, I. Nagy, G. Gonter, R. Hadik, K. Kaszap, A. Tarsoly, "Inductive energy collection for electric vehicles," in *Proc. Fourth Power Electronics Conference*, 1981, pp. 71-81.

[42]. T. Bieler, M. Perrottet, V. Nguyen, Y. Perriard, "Contactless power and information transmission," *IEEE Transactions on Industry Applications*, vol. 38, pp. 1266-1272, Sep./Oct. 2002.

[43]. H. Abe, H. Sakamoto, K. Harada, "A noncontact charger using a resonant converter with parallel capacitor of the secondary coil," *IEEE Transactions on Industry Applications*, vol. 36, pp. 444-451, Mar.-Apr. 2000.

[44]. A. Hu, J. T. Boys, G. A. Covic, "Dynamic ZVS direct on-line start up of current fed resonant converter using initially forced DC current," in *Proc. IEEE International Symposium on Industrial Electronics*, vol. 1, 2000, pp. 312-317.

[45]. A. W. Green, J. T. Boys, "10 kHz inductively coupled power transfer-concept and control," in *Proc. Fifth International Conference on Power Electronics and Variable-Speed Drives*, 1994, pp. 694-699.

[46]. A. W. Green, "Modelling a push-pull parallel resonant convertor using generalised state-space averaging," *IEE Proc. Electric Power Applications*, vol. 140, pp. 350-356, Nov. 1993.

[47]. A. P. Hu, "Selected resonant converters for IPT power supplies," *PhD thesis*, Oct. 2001, The Electrical and Electronics Engineering Department, The University of Auckland, New Zealand.

[48]. N. H. Kutkut, K. W. Klontz, "Design considerations for power converters supplying the SAE J-1773 electric vehicle inductive coupler," in *Proc. Applied Power Electronics Conference and Exposition*, vol. 2, 1997, pp. 841-847.

[49]. L. Zhao, C. F. Foo, K. J. Tseng, "A new structure transcutaneous transformer for artificial heart system," *IEEE Transactions on Magnetics*, vol. 35, pp. 3550-3552, Sept. 1999.

[50]. G. B. Joung, B. H. Cho, "An energy transmission system for an artificial heart using leakage inductance compensation of transcutaneous transformer," in *Proc. Power Electronics Specialists Conference*, vol. 1, 1996, pp. 898-904.

[51]. H. Matsuki, Y. Yamakata, N. Chubachi, S.-I. Nitta, H. Hashimoto, "Transcutaneous DC-DC converter for totally implantable artificial heart using synchronous rectifier," *IEEE Transactions on Magnetics*, vol. 32, pp. 5118-5120, Sept. 1996.

[52]. C. G. Kim, B. H. Cho, "Transcutaneous energy transmission with double tuned duty cycle control," in *Proc. Energy Conversion Engineering Conference*, vol. 1, 1996, pp. 587-591.

InductEV, Inc.
Exhibit 1010
Page 159

[53]. T. H. Nishimura, T. Eguchi, K. Hirachi, Y. Maejima, K. Kuwana, M. Saito, "A large air gap flat transformer for a transcutaneous energy transmission system," in *Proc. Power Electronics Specialists Conference*, vol.2, 1994, pp. 1323-1329.

[54]. T. H. Nishimura, L. Ding, "Implantable artificial heart system and new actuator control by power electronic system," in *Proc. International Conference on Systems Engineering*, 1989, pp. 289-292.

[55]. Sung-Hun Lim, Seong-Ryong Lee, Byoung-Sung Han, "A novel noncontact electric energy transfer system with regulating AC voltage/frequency," in *Proc. Power Electronics Specialists Conference*, vol. 2, 2001, pp. 713-717.

[56]. H. Sakamoto, K. Harada, S. Washimiya, K. Takehara, Y. Matsuo, F. Nakao, "Large air-gap coupler for inductive charger [for electric vehicles]," *IEEE Transactions on Magnetics*, vol. 35, pp. 3526-3528, Sept. 1999.

[57]. J. G. Hayes, M. G. Egan, J. M. D. Murphy, S. E. Schulz, J. T. Hall, "Wide-load-range resonant converter supplying the SAE J-1773 electric vehicle inductive charging interface," *IEEE Transactions on Industry Applications*, vol. 35, pp. 884-895, July-Aug. 1999.

[58]. K. W. Klontz, D. M. Divan, D. W. Novotny, "An actively cooled 120 kW coaxial winding transformer for fast charging electric vehicles," *IEEE Transactions on Industry Applications*, vol. 31, pp. 1257–1263, Nov.-Dec. 1995.

[59]. J. Hirai, Tae-Woong Kim, A. Kawamura, "Wireless transmission of power and information for cableless linear motor drive," *IEEE Transactions on Power Electronics*, vol. 15, pp. 21-27, Jan. 2000.

[60]. J. M. Barnard, J. A. Ferreira, J. D. van Wyk, "Sliding transformers for linear contactless power delivery," *IEEE Transactions on Industrial Electronics*, vol. 44, pp. 774-779, Dec. 1997.

[61]. Y. Hiraga, J. Hirai, Y. Kaku, Y. Nitta, A. Kawamura, K. Ishioka, "Decentralized control of machines with the use of inductive transmission of power and signal," in *Proc. IEEE Industry Applications Society Annual Meeting*, vol. 2, 1994, pp. 875-881.

[62]. C.-C. Tsai, B.-S. Chen, C.-M. Tsai, "Design of wireless transcutaneous energy transmission system for totally artificial hearts," in *Proc. IEEE Asia-Pacific Conference on Circuits and Systems*, 2000, pp. 646-649.

[63]. T. Inoue, T. H. Nishimura, M. Saito, M. Nakaoka, "A transcutaneous energy transmission system for an artificial organ by using a novel resonant converter," in *Proc. IEEE International Conference on Systems Engineering*, 1992, pp. 294-297.

InductEV, Inc.
Exhibit 1010
Page 160

[64]. A. Djemouai, M. Sawan, M. Slamani, "An efficient RF power transfer and bidirectional data transmission to implantable electronic devices," in *Proc. International Symposium on Circuits and Systems*, vol. 2, 1999, pp. 259-262.

[65]. J. S. Mueller, R. S. Gyurcsik, "Two novel techniques for enhancing powering and control of multiple inductively-powered biomedical implants," in *Proc. International Symposium on Circuits and Systems*, vol. 1, 1997, pp. 289-292.

[66]. Wonseok Lim, Jaehyun Nho, Byungcho Choi, Taeyoung Ahn, "Low-profile contactless battery charger using planar printed circuit board windings as energy transfer device," in *Proc. Power Electronics Specialists Conference*, vol. 2, 2002, pp. 579-584.

[67]. A. Esser, "Contactless charging and communication for electric vehicles," *IEEE Industry Applications Magazine*, vol. 1, pp. 4-11, Nov.-Dec. 1995.

[68]. H. Sakamoto, K. Harada, K. Yamasaki, "A novel high power converter for non-contact charging with magnetic coupling," in *Proc. International Conference on Power Electronics and Drive Systems*, vol. 1, 1995, pp. 461-464.

[69]. K. W. Klontz, A. Esser, P. J. Wolfs, D. M. Divan, "Converter selection for electric vehicle charger systems with a high-frequency high-power link," in *Proc. Power Electronics Specialists Conference*, 1993, pp. 855-861.

[70]. A. Esser, "Contactless charging and communication system for electric vehicles," in *Proc. IEEE Industry Applications Society Annual Meeting*, vol. 2, 1993, pp. 1021-1028.

[71]. K. W. Klontz, A. Esser, R. R. Bacon, D. M. Divan, D. W. Novotny, R. D. Lorenz, "An electric vehicle charging system with 'universal' inductive interface," in *Proc. Power Conversion Conference*, 1993, pp. 227-232.

[72]. J. I. Rodriguez, D. K. Jackson, S. B. Leeb, "Capability analysis for an inductively coupled power transfer system," in *Proc. 7th Workshop on Computers in Power Electronics*, 2000, pp. 59-63.

[73]. O. H. Stielau, "High frequency, high power resonant electronic converters for induction heating," *PhD thesis*, Jan. 1991, The Electrical and Electronics Engineering Department, Rand Afrikaans University, South Africa

[74]. H. W. E. Koertzen, "Varying load induction heating by medium frequency power electronic converters," *PhD thesis*, Nov. 1994, The Electrical and Electronics Engineering Department, Rand Afrikaans University, South Africa

[75]. Y. Kanai, M. Mino, T. Sakai, T. Yachi, "A non-contact power-supply card powered by solar cells for mobile communications," in *Proc. Applied Power Electronics Conference and Exposition*, vol. 2, 2000, pp. 1157-1162.

InductEV, Inc.
Exhibit 1010
Page 161

[76]. A. P. Hu, J. T. Boys, G. A. Covic, "ZVS frequency analysis of a current-fed resonant converter," in *Proc. IEEE International Power Electronics Congress*, 2000, pp. 217-221.

[77]. A. P. Hu, J. T. Boys, G. A. Covic, "Frequency analysis and computation of a current-fed resonant converter for ICPT power supplies," in *Proc. International Conference on Power System Technology*, vol. 1, 2000, pp. 327-332.

[78]. J. T. Boys, A. P. Hu, G. A. Covic, "Critical Q analysis of a current-fed resonant converter for ICPT applications," *Electronics Letters*, vo. 36, pp. 1440-1442, Aug. 2000.

[79]. J. T. Boys, G. A. Covic, A. W. Green, "Stability and control of inductively coupled power transfer systems," *IEE Proc. Electric Power Applications*, vol. 147, pp. 37-43, Jan. 2000.

[80]. P. R. Troyk, M. A. K. Schwan, "Closed-loop class E transcutaneous power and data link for MicroImplants," *IEEE Transactions on Biomedical Engineering*, vol. 39, pp. 589-599, June 1992.

[81]. C. M. Zierhofer, E. S. Hochmair, "The Class-E Concept For Efficient Wide-Band Coupling-Insensitive Transdermal Power And Data Transfer," in *Proc. Annual International Conference of the IEEE Engineering in Medicine and Biology Society*, vol.2, 1992, pp. 382-383.

[82]. S. Dieckerhoff, M. J. Ruan, R. W. De Doncker, "Design of an IGBT-based LCL-resonant inverter for high-frequency induction heating," in *Proc. IEEE Industry Applications Society Annual Meeting*, vol. 3, 1999, pp. 2039-2045.

[83]. J. M. Espi, E. J. Dede, E. Navarro, E. Sanchis, A. Ferreres, "Features and design of the voltage-fed L-LC resonant inverter for induction heating," in *Proc. Power Electronics Specialists Conference*, vol. 2, 1999, pp. 1126-1131.

[84]. G. L. Fischer, H. Doht, "An inverter system for inductive tube welding utilizing resonance transformation," in *Proc. IEEE Industry Applications Society Annual Meeting*, vol. 2, 1994, pp. 833-840.

[85]. J. M. Espi, A. E. Navarro, J. Maicas, J. Ejea, S. Casans, "Control circuit design of the L-LC resonant inverter for induction heating," in *Proc. Power Electronics Specialists Conference*, vol. 3, 2000, pp. 1430-1435.

[86]. K. W. Klontz, D. M. Divan, D. W. Novotny, R. D. Lorenz, "Contactless power delivery system for mining applications," *IEEE Transactions on Industry Applications*, vol. 31, pp. 27-35, Jan.-Feb. 1995.

InductEV, Inc.
Exhibit 1010
Page 162

InductEV, Inc.
Exhibit 1010
Page 163

CHAPTER 3

DEVELOPMENT OF A GENERAL LOAD MODEL

3-1 Introduction
3-2 Overview of the load model
3-3 The pickup load
3-4 The secondary resonant circuit
3-5 The secondary quality factor
3-6 The reflected impedance
3-7 Pickup behaviour and influences on the primary
3-8 The primary coil
3-9 The primary quality factor
3-10 The power supply load model
3-11 Verification of the load model
3-12 Conclusions

3-1 INTRODUCTION

ICPT systems are normally designed to deliver power from a stationary primary source to one or more movable secondary loads (pickups) over large air gaps via magnetic coupling. Both the primary and pickup secondary are often compensated using capacitors connected in series or parallel to boost the power transfer capability while minimizing the VA rating of the power supply. In such a system, the primary resonant circuit is magnetically coupled with one or more secondary resonant circuits that supply power to a load. Consequently, the load seen by the power supply is a high order load resonant tank consisting of both the primary and secondary resonant circuits. The behaviour of this load resonant tank is mathematically complex and highly sensitive to variations in system parameters such as the operating frequency, the load, as well as misalignment in the electromagnetic structure.

To better facilitate the design of an ICPT system, this chapter develops a model to generally quantify the characteristics of the load resonant tank. The behaviour of the pickup and its influences on the primary are investigated to identify the influences of the operating frequency, the load, and the electromagnetic coupling structure. This chapter focuses on single pickup applications. Multiple pickup systems are discussed later in this thesis. The developed power supply load model is verified by a practical example.

3-2 OVERVIEW OF THE LOAD MODEL

In an ICPT system, the primary and secondary can be either series or parallel compensated or remain un-compensated. This results in nine basic topologies. To simplify the discussion, this thesis

InductEV, Inc.
Exhibit 1010
Page 164

only focuses on the analysis and design of the four topologies with both primary and secondary compensations as this reflects the majority of such systems in the medium-high power range. In practice, topologies without primary and/or secondary compensations can be analysed using a similar approach.

Sinusoidal steady state analysis is used for modelling the load resonant tank. The electromagnetic structure and the primary and secondary compensation capacitors (C_p and C_s) are assumed to be loss-less. The pickup load is assumed to be linear and resistive. The electromagnetic structure is modelled using the transformer mutual inductance coupling model (as noted in section 2.2.3). Here the coupling parameters include the primary self-inductance L_p, the mutual inductance M between the primary and secondary, and the secondary self-inductance L_s. Linear and frequency dependent impedances are used to represent the reactive elements (C_p, L_p, M, L_s and C_s) within the load resonant tank.

The load seen by the power supply, as shown in Fig. 3-1, consists of the primary compensation, an electromagnetic structure, the secondary compensation and a load. In this figure, the electromagnetic coupling between the primary and secondary is represented by an induced voltage and a reflected voltage (as has been noted in section 2-2.3). The load seen by the power supply can be separated into two interrelated resonant circuits: the primary and secondary. The primary resonant circuit includes the primary compensation, the primary inductance (L_p) and the reflected voltage ($-j\omega MI_s$). The secondary resonant circuit is formed by the induced voltage ($j\omega MI_p$), the secondary inductance (L_s), the secondary compensation and the load.

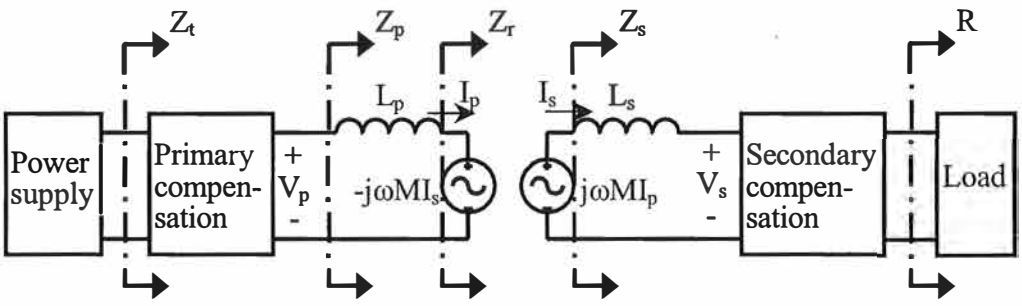


Fig. 3-1. Diagram of the load seen by the power supply.

The voltages and currents of a resonant circuit with a high quality factor are close to sinusoidal. As such, a sinusoidal ac analysis is suitable. With this approach, the circuit model of the load seen by the power supply can be transformed into an impedance model as shown in Fig. 3-1. The pickup load normally consists of a rectifier and a filter supplying power to a dc load with or without a switched-mode controller. To facilitate the linear sinusoidal ac analysis, this controlled dc load is

InductEV, Inc.
Exhibit 1010
Page 165

represented as an equivalent variable ac load (R). A secondary load impedance (Z_s) is used to represent the impedance seen by the induced voltage. The secondary load impedance is formed by the secondary inductance, the secondary compensation and an equivalent ac load. A reflected impedance (Z_r) is also used to represent the loading effect of the secondary resonant circuit on the primary. The reflected impedance is defined as the reflected voltage divided by the primary current. The impedance of the primary coil (Z_p) is a combination of the reactance of the self-inductance of the primary coil and the reflected impedance. Combining the impedance of the primary coil with the primary compensation results in the total load impedance (Z_t) seen by the power supply.

3-3 THE PICKUP LOAD

The high frequency ac voltage and current of the pickup may be used to supply power to a simple resistive load, a low frequency ac load such as an ac motor, or a dc load such as a dc motor or battery charger. When supplying power to a low frequency ac load, a frequency conversion device such as an ac-ac converter is required. To power up a dc load, a rectifier is commonly used to transform the ac voltage and current into a dc voltage and current, the harmonics of which can then be reduced by employing an output filter.

To simplify the resonant circuit analysis of the pickup, an equivalent resistive load can be developed to represent the pickup loading system. Two common examples are discussed in this section. Other pickup loading systems can be analysed using a similar approach.

For a diode bridge rectifier with an inductor output filter as shown in Fig. 3-2, the average current of the dc load capacitor at steady state is zero. As such the average of the inductor current equals the dc load current. Assuming a significantly large inductor output filter, the variation of the inductor current is negligible. In consequence, the input current (i_R) to the rectifier is approximately rectangular with a magnitude of the dc load current (I_{dc}) [1]. The fundamental component of this rectangular current is:

$$I_R = \frac{2\sqrt{2}I_{dc}}{\pi} \tag{3-1}$$

Assuming the input voltage (v_R) to the rectifier is sinusoidal in a resonant circuit, at steady state, the average voltage across the inductor is zero and as such the average of the rectified input voltage equals the dc load voltage (V_{dc}) [1]. As a result, the RMS value of v_R is:

$$V_R = \frac{\pi V_{dc}}{2\sqrt{2}} \tag{3-2}$$

The equivalent ac load found from (3-1)&(3-2) is therefore:

$$R = \frac{V_R}{I_R} = \frac{\pi^2 V_{dc}}{8I_{dc}} = \frac{\pi^2 R_{dc}}{8} \tag{3-3}$$

InductEV, Inc.
Exhibit 1010
Page 166

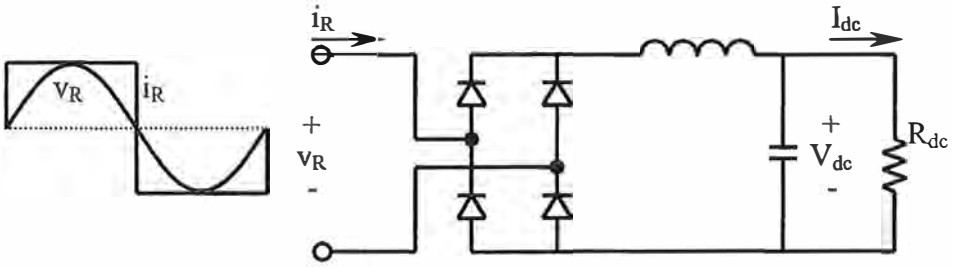


Fig. 3-2. Full-bridge diode rectifier with inductor output filter.

For a diode bridge rectifier with a capacitor output filter as shown in Fig. 3-3, the variation of the load voltage is negligible, assuming a substantially large capacitor. In consequence, the input voltage (v_R) to the rectifier is approximately rectangular with a magnitude of the dc load voltage (V_{dc}) [1]. The fundamental component of this rectangular voltage is:

$$V_R = \frac{2\sqrt{2}V_{dc}}{\pi} \tag{3-4}$$

Assuming the input current (i_R) to the rectifier is sinusoidal in a resonant circuit, at steady state, the average capacitor current is zero and as such the average of the rectified input current equals the dc load current (I_{dc}) [1]. As a result, the RMS value of i_R is:

$$I_R = \frac{\pi I_{dc}}{2\sqrt{2}} \tag{3-5}$$

The equivalent ac load found from (3-4)&(3-5) is thus:

$$R = \frac{V_R}{I_R} = \frac{8V_{dc}}{\pi^2 I_{dc}} = \frac{8R_{dc}}{\pi^2} \tag{3-6}$$

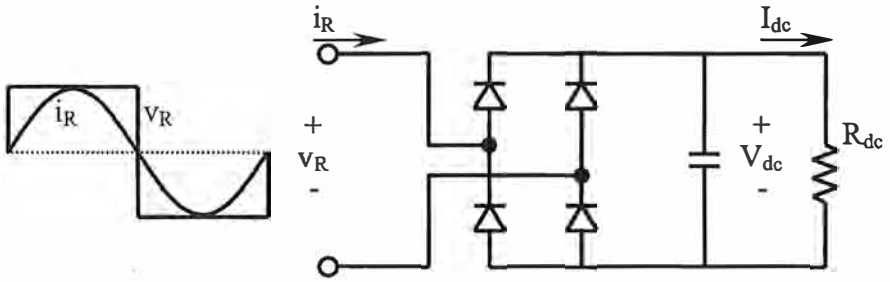


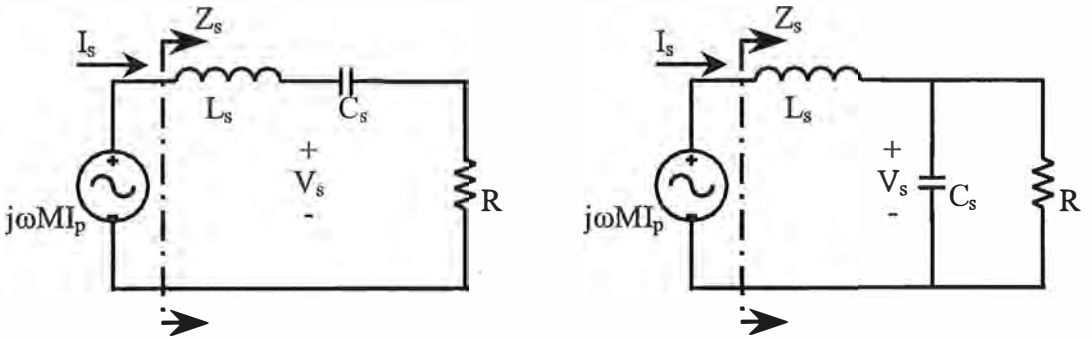
Fig. 3-3. Full-bridge diode rectifier with capacitor output filter.

3-4 THE SECONDARY RESONANT CIRCUIT

With the pickup loading system represented as an equivalent resistor, the equivalent circuits of series and parallel compensated secondary systems are shown respectively in Fig. 3-4 (a) and (b). In these circuits, the induced voltage ($j\omega MI_p$) in the secondary coil is represented as a voltage source in

InductEV, Inc.
Exhibit 1010
Page 167

series connection with the secondary inductance. The induced voltage arises from the magnetic coupling (M) between the primary and secondary and is dependent on the operating frequency of the primary power supply as well as the primary current flowing through the primary coil.



(a) Series compensated secondary. (b) Parallel compensated secondary.

Fig. 3-4. Equivalent circuits of the secondary systems.

To simplify the analysis, the secondary resonant circuit can be represented as a lumped impedance (Z_s) driven by the induced voltage. As shown in Fig. 3-4, the lumped secondary impedance depends on the compensation topology. With a series compensated secondary system, the secondary impedance consists of an inductor, a capacitor and a load in series connection. For a parallel-compensated secondary, the secondary impedance is formed by an inductor in series connection with the parallel-connected capacitor and load. The secondary impedances derived respectively from the circuits of series and parallel compensated secondary systems in Fig. 3-4 (a) and (b) are:

$$Z_s = \begin{cases} j\omega L_s + \dfrac{1}{j\omega C_s} + R & \text{series secondary} \\ j\omega L_s + \dfrac{1}{j\omega C_s + \dfrac{1}{R}} & \text{parallel secondary} \end{cases} \tag{3-7}$$

3-5 THE SECONDARY QUALITY FACTOR

The secondary resonance can be quantified by the quality factor (Q_s) associated with the secondary resonant circuit. The quality factor of a resonant circuit is defined as the ratio of reactive to real power as:

$$Q = \frac{VAR}{P} \tag{3-8}$$

In either series or parallel-compensated pickups, the reactive power of the pickup coil equals the reactive power of the secondary compensation capacitor (C_s), while the real power transferred by the pickup coil equals the power going to the load (R) as noted in Appendix B. They are calculated below

InductEV, Inc.
Exhibit 1010
Page 168

to determine the secondary quality factor.

Series compensated secondary: When the secondary is series compensated, the secondary current (I_s) flows through the pickup coil, the secondary compensation capacitor (C_s) and the load (R). The following analysis of series compensated secondary resonant circuit refers to the secondary current.

The reactive power of the secondary compensation capacitor is:

$$VAR_s = \frac{I_s^2}{\omega C_s} \tag{3-9}$$

The real power of the load is:

$$P = I_s^2 R \tag{3-10}$$

The secondary quality factor of a series-compensated pickup is then:

$$Q_s = \frac{VAR_s}{P} = \frac{1}{\omega C_s R} \tag{3-11}$$

Parallel-compensated secondary: When the secondary is parallel compensated, the secondary voltage (V_s) appears across the pickup coil, the secondary compensation capacitor and the load. The following analysis of parallel-compensated secondary resonant circuit refers to the secondary voltage.

The real power of the load R is:

$$P = \frac{V_s^2}{R} \tag{3-12}$$

The reactive power of the secondary capacitor is:

$$VAR_s = V_s^2 \omega C_s \tag{3-13}$$

The secondary quality factor of a parallel-compensated pickup is then:

$$Q_s = \frac{VAR_s}{P} = \omega C_s R \tag{3-14}$$

3-6 THE REFLECTED IMPEDANCE

Using the mutual inductance coupling model, as noted in section 2-2.3, a reflected voltage ($-j\omega MI_s$) can be used to represent the loading effects of the secondary resonant circuit on the primary coil. This reflected voltage in the primary coil arises from the magnetic coupling between the primary and secondary and is dependent on the operating frequency of the primary power supply as well as the secondary current flowing through the secondary coil. Equivalently, this can be regarded as a voltage source in series connection with the primary inductance.

With the secondary impedance given in (3-7), the secondary current is then:

InductEV, Inc.
Exhibit 1010
Page 169

$$I_s = \frac{j\omega M I_p}{Z_s} \tag{3-15}$$

The reflected voltage from the secondary to the primary calculated using (3-15) is:

$$-j\omega M I_s = -j\omega M\left(\frac{j\omega M I_p}{Z_s}\right) = \frac{\omega^2 M^2 I_p}{Z_s} \tag{3-16}$$

In order to simplify the analysis of the loading effects of the secondary resonant circuit, a reflected impedance can be calculated by dividing the reflected voltage given in (3-16) by the primary current as:

$$Z_r = \frac{-j\omega M I_s}{I_p} = \frac{\omega^2 M^2}{Z_s} \tag{3-17}$$

As shown above, the reflected impedance is dependent on the operating frequency, the mutual inductance, and the secondary impedance.

Substituting (3-7) into (3-17), the reflected resistance and reactance can be derived for the specified secondary compensation as:

$$\mathrm{Re}\,Z_r = \begin{cases} \dfrac{\omega^4 C_s^2 M^2 R}{\left(\omega^2 C_s L_s - 1\right)^2 + \omega^2 C_s^2 R^2} & \text{series secondary} \\ \dfrac{\omega^2 M^2 R}{R^2\left(\omega^2 C_s L_s - 1\right)^2 + \omega^2 L_s^2} & \text{parallel secondary} \end{cases} \tag{3-18}$$

and

$$\mathrm{Im}\,Z_r = \begin{cases} \dfrac{-\omega^3 C_s M^2\left(\omega^2 C_s L_s - 1\right)}{\left(\omega^2 C_s L_s - 1\right)^2 + \omega^2 C_s^2 R^2} & \text{series secondary} \\ \dfrac{-\omega^3 M^2\left[C_s R^2\left(\omega^2 C_s L_s - 1\right) + L_s\right]}{R^2\left(\omega^2 C_s L_s - 1\right)^2 + \omega^2 L_s^2} & \text{parallel secondary} \end{cases} \tag{3-19}$$

where the operators 'Re' and 'Im' represent the real and imaginary components of the corresponding complex variable respectively.

The power transferred from the primary to the secondary is the reflected resistance multiplied by the square of the primary current as given by:

$$P = (\mathrm{Re}\,Z_r) I_p^2 \tag{3-20}$$

The primary current I_p is normally controlled constant in ICPT systems especially for high power applications [2-3]. With such systems, the power transfer capability is proportional to the reflected resistance according to (3-20).

The required VA rating of the secondary compensation capacitor is:

$$VA_{Cs} = VAR_s = Q_s P \tag{3-21}$$

InductEV, Inc.
Exhibit 1010
Page 170

The secondary VA rating required for the pickup coil is then:

$$VA_s = \sqrt{P^2 + (VAR_s)^2} = \left(\sqrt{1+Q_s^2}\right)P \tag{3-22}$$

3-7 PICKUP BEHAVIOUR AND INFLUENCES ON THE PRIMARY

In this section, the steady state behaviour of both series and parallel-compensated pickups are quantified, which in turn enables their influences on the primary circuit to be determined. The pickups in the system are normally designed to operate at or near their resonant frequency. Consequently, this section initially focuses on the influence of the pickup when operating at this frequency. However, under variable-frequency control, the operating frequency may shift from the secondary resonant frequency. Alternatively, in some applications the operating frequency may be deliberately changed to regulate power flow. In either case, this frequency shift dramatically influences the system operation. As such a general analysis is undertaken across the frequency spectrum to quantify this effect.

3-7.1 OPERATION AT THE SECONDARY RESONANT FREQUENCY

The secondary resonant frequency ω_0 (the frequency where L_s is in resonance with C_s) is given by:

$$\omega_0 = \frac{1}{\sqrt{L_s C_s}} \tag{3-23}$$

The voltages, currents, power and VAs of the secondary resonant circuit when operated at the secondary resonant frequency have been investigated in section 2-3.2, with a summary of these results given in Table 2-1.

The quality factor of the pickup at ω_0 can be derived from (3-11), (3-14) and (3-23) as:

$$Q_{s0} = Q_s(\omega = \omega_0) = \begin{cases} \dfrac{1}{\omega_0 C_s R} = \dfrac{\omega_0 L_s}{R} & \text{series secondary} \\ \omega_0 C_s R = \dfrac{R}{\omega_0 L_s} & \text{parallel secondary} \end{cases} \tag{3-24}$$

Since Q_{s0} is a function of the load, this dimensionless parameter is used in the thesis as a fundamental design parameter representing the pickup load. It equals the secondary quality factor when operating at ω_0. At other operating frequencies (ω), it relates to the operating secondary quality factor (Q_s) as:

$$Q_s = \begin{cases} \dfrac{Q_{s0}}{\omega/\omega_0} & \text{series secondary} \\ (\omega/\omega_0)Q_{s0} & \text{parallel secondary} \end{cases} \tag{3-25}$$

InductEV, Inc.
Exhibit 1010
Page 171

To investigate the loading effects of the secondary resonant circuit on the primary coil when operated at ω_0, the reflected resistance and reactance at ω_0 can be calculated from (3-18) and (3-19) for the specified secondary compensation as:

$$\mathrm{Re}Z_{r0} = \mathrm{Re}Z_r(\omega=\omega_0) = \begin{cases} \dfrac{\omega_0^2 M^2}{R} = \left(\dfrac{\omega_0 M^2}{L_s}\right) Q_{s0} & \text{series secondary} \\ \dfrac{M^2 R}{L_s^2} = \left(\dfrac{\omega_0 M^2}{L_s}\right) Q_{s0} & \text{parallel secondary} \end{cases} \tag{3-26}$$

and

$$\mathrm{Im}Z_{r0} = \mathrm{Im}Z_r(\omega=\omega_0) = \begin{cases} 0 & \text{series secondary} \\ -\dfrac{\omega_0 M^2}{L_s} & \text{parallel secondary} \end{cases} \tag{3-27}$$

As shown in (3-26), if the system operates at ω_0, both the reflected resistance and the power transfer capability (assuming a constant primary current) in a series compensated secondary increase to infinity when the load R is reduced to zero ($Q_{s0}=\infty$). A similar result arises for a parallel-compensated secondary as the load R increases to infinity ($Q_{s0}=\infty$). When expressed in terms of the secondary quality factor (Q_{s0}), the reflected resistance at ω_0 for series compensation becomes identical to that determined with parallel compensation.

As can be seen in (3-27), a series compensated secondary has zero reflected reactance, whereas a parallel-compensated system reflects a capacitive load that is independent of the loading conditions on the pickup. This is one of the major differences between series and parallel-compensated secondary systems.

The power transfer capability at ω_0 can be calculated by substituting the reflected resistance given in (3-26) into (3-20). The result is identical to (2-25) and (2-27) respectively for series and parallel-compensated secondary systems.

Equating (3-20) with (2-25) and (2-27), the reflected resistance at ω_0 can be expressed in terms of the open circuit voltage and the short circuit current as:

$$\mathrm{Re}Z_{r0} = \frac{P}{I_p^2} = \frac{Q_{s0} V_{oc} I_{sc}}{I_p^2} \tag{3-28}$$

According to the above equation, this reflected resistance is strongly related to the capability of the electromagnetic structure (the open circuit voltage and the short circuit current) as well as the secondary compensation level (the secondary quality factor).

InductEV, Inc.
Exhibit 1010
Page 172

3-7.2 NORMALIZATION OF THE IMPEDANCE MODEL

The loading effect of the secondary pickup on the primary coil is represented as a reflected impedance (Z_r) in section 3-6. Similarly (as discussed later in section 3-10.1) the loading effect of the load resonant tank, consisting of both the primary and secondary resonant circuits, on the power supply is represented as a load impedance (Z_t). Analysis of these impedance models is complex. The pickup reflected impedance is a function of the operating frequency (ω), the mutual inductance (M), the secondary self-inductance (L_s), the secondary compensation capacitance (C_s), and the pickup load (R). In addition to these parameters (ω, M, L_s, C_s and R), the power supply load impedance also depends on the primary self-inductance (L_p) and the primary compensation capacitance (C_p).

For a general analysis across the frequency spectrum, both the pickup reflected impedance and the power supply load impedance models can be simplified using normalization methods. Since the pickup is generally designed to operate at ω_0, this frequency is therefore selected as a base parameter in the normalization process. The normalized frequency (u) is defined as:

$$u = \frac{\omega}{\omega_0} \tag{3-29}$$

When operating above or below ω_0, u varies from unity indicating the percentage of frequency detuning within the pickup. To ensure power transfer capability of the pickup, it is normally desirable to minimize this frequency detuning.

For a general analysis of the load, another useful base parameter for normalization is Re Z_{r0} (as noted in section 3-7.1) as this represents the designed power transfer capability of the system operating with constant primary current. Using this parameter, the normalized pickup reflected impedance (Z_{rn}) and power supply load impedance (Z_{tn}) are defined as:

$$Z_{rn,tn} = \frac{Z_{r,t}}{\mathrm{Re}\, Z_{r0}} \tag{3-30}$$

With this approach, Z_{rn} represents the pickup loading effects on the primary coil relative to the designed power transfer capability of the pickup, while Z_{tn} indicates the loading effects seen by the power supply scaled to the designed power transfer capability of the pickup.

3-7.3 INFLUENCE OF FREQUENCY ON THE PICKUP BEHAVIOUR

The ratio of the secondary current (I_s) given in (3-15) to the short circuit current (I_{sc}) given in (2-8) is:

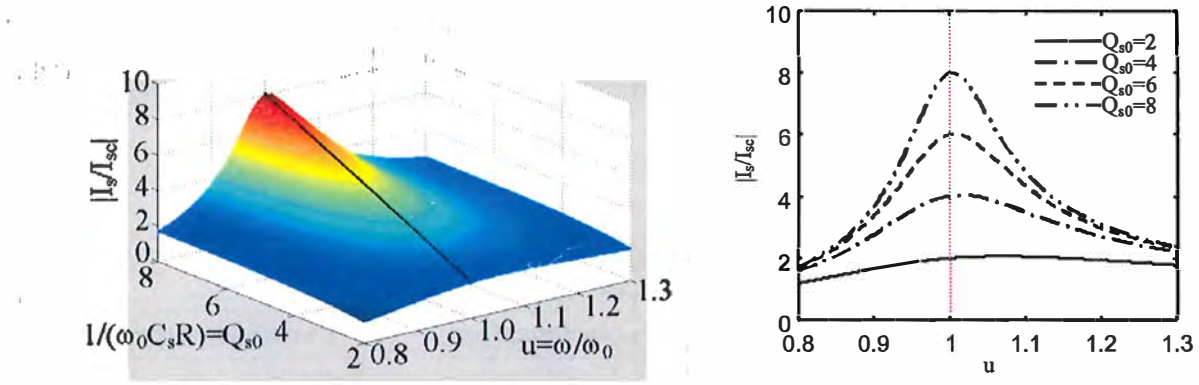
$$\frac{I_s}{I_{sc}} = \frac{j\omega L_s}{Z_s} \tag{3-31}$$

InductEV, Inc.
Exhibit 1010
Page 173

This ratio (as derived in Appendix C) is a function of the normalized frequency (u) and the secondary quality factor at ω_0 (Q_{s0}) for the specified secondary compensation as:

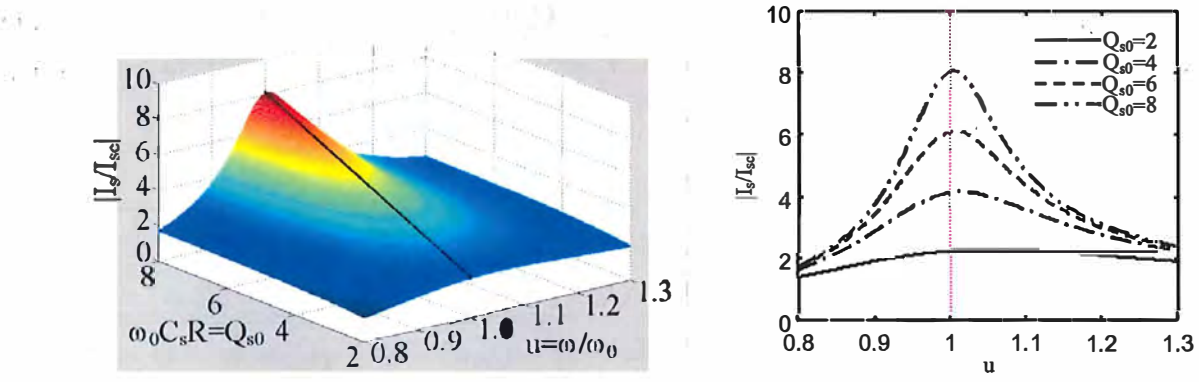
$$\left|\frac{I_s}{I_{sc}}\right| = \begin{cases} \dfrac{\sqrt{Q_{s0}^4 u^4 \left(u^2-1\right)^2 + Q_{s0}^2 u^6}}{u^2 + Q_{s0}^2\left(u^2-1\right)^2} & \text{series secondary} \\ \dfrac{\sqrt{\left[Q_{s0}^2 u^2\left(u^2-1\right)+u^2\right]^2 + Q_{s0}^2 u^2}}{u^2 + Q_{s0}^2\left(u^2-1\right)^2} & \text{parallel secondary} \end{cases} \tag{3-32}$$

Equation (3-32) can be used to investigate variations in the secondary current as the pickup is detuned from the design frequency ω_0, or when the secondary quality factor changes with the load. They are compared in Fig. 3-5 for series and parallel-compensated secondary systems. In this figure, the selected range of Q_{s0} is from 2 to 8 and u is chosen to be around unity (the secondary resonant frequency ω_0), since typical ICPT systems are normally designed to operate close to ω_0 (u close to unity) with Q_{s0} below 10 [1-2]. The cross-sections of these surfaces are also drawn at selected Q_{s0} of 2, 4, 6 and 8 to clarify corresponding features.



(i) Surface function. (ii) Cross sections of the surface.

(a) Series compensated secondary.



(i) Surface function. (ii) Cross sections of the surface.

(b) Parallel compensated secondary.

Fig. 3-5. Quantified secondary current.

InductEV, Inc.
Exhibit 1010
Page 174

Both series and parallel-compensated secondary systems have similar features. The maximum secondary current occurs close to ω_0, and drops quickly when the operating frequency shifts away. This sensitivity increases as the secondary quality factor becomes larger with increasing load.

Using a similar approach, the ratio of the load current (I_R) and the secondary capacitor current (I_{Cs}) to the short circuit current (I_{sc}) can be derived as functions of only the normalized operating frequency (u) and the secondary quality factor (Q_{s0}). Similarly, the ratio of the secondary voltage (V_s), the load voltage (V_R) and the secondary capacitor voltage (V_{Cs}) to the open circuit voltage (V_{oc}) can also be derived as functions of only u and Q_{s0}. The open circuit voltage is calculated using (2-6) with the frequency (ω) set equal to the secondary resonant frequency (ω_0). A summary of these functions is given in Table 3-1. The ratio of the power transfer, the required VA rating of the secondary coil and the required VA rating of the secondary capacitor to the product of open circuit voltage and short circuit current can be derived using functions of relevant voltages and currents. The results are once again functions of only u and Q_{s0}.

An analysis of these functions in Table 3-1 across the frequency spectrum for selected Q_{s0} shows they are similar to the results shown in Fig. 3-5 for the secondary current. In consequence, maximum voltages, currents, power and VAs of both series and parallel compensated pickups all occur when the system operates at or close to the secondary resonant frequency, and becomes substantially lower with large frequency detuning.

TABLE 3-1
QUANTIFIED PICKUP VOLTAGES, CURRENTS

Pickup topology	Series compensation	Parallel compensation
Secondary current $\lvert I_s / I_{sc}\rvert$	$\frac{\sqrt{Q_{s0}^4 u^4 \left(u^2-1\right)^2 + Q_{s0}^2 u^6}}{u^2 + Q_{s0}^2\left(u^2-1\right)^2}$	$\frac{\sqrt{\left[Q_{s0}^2 u^2\left(u^2-1\right)+u^2\right]^2 + Q_{s0}^2 u^2}}{u^2 + Q_{s0}^2\left(u^2-1\right)^2}$
Secondary voltage $\lvert V_s / V_{oc}\rvert$	$\frac{\sqrt{Q_{s0}^2 u^8 + u^2\left[u^2 - Q_{s0}^2\left(u^2-1\right)\right]^2}}{u^2 + Q_{s0}^2\left(u^2-1\right)^2}$	$\frac{\sqrt{Q_{s0}^2 u^4 + Q_{s0}^4 u^2\left(u^2-1\right)^2}}{u^2 + Q_{s0}^2\left(u^2-1\right)^2}$
Load current $\lvert I_R / I_{sc}\rvert$	$\frac{\sqrt{Q_{s0}^4 u^4 \left(u^2-1\right)^2 + Q_{s0}^2 u^6}}{u^2 + Q_{s0}^2\left(u^2-1\right)^2}$	$\frac{\sqrt{u^4 + Q_{s0}^2 u^2\left(u^2-1\right)^2}}{u^2 + Q_{s0}^2\left(u^2-1\right)^2}$
Load voltage $\lvert V_R / V_{oc}\rvert$	$\frac{\sqrt{Q_{s0}^2 u^4 \left(u^2-1\right)^2 + u^6}}{u^2 + Q_{s0}^2\left(u^2-1\right)^2}$	$\frac{\sqrt{Q_{s0}^2 u^4 + Q_{s0}^4 u^2\left(u^2-1\right)^2}}{u^2 + Q_{s0}^2\left(u^2-1\right)^2}$
Secondary capacitor current $\lvert I_{Cs} / I_{sc}\rvert$	$\frac{\sqrt{Q_{s0}^4 u^4 \left(u^2-1\right)^2 + Q_{s0}^2 u^6}}{u^2 + Q_{s0}^2\left(u^2-1\right)^2}$	$\frac{\sqrt{Q_{s0}^4 u^4 \left(u^2-1\right)^2 + Q_{s0}^2 u^6}}{u^2 + Q_{s0}^2\left(u^2-1\right)^2}$
Secondary capacitor voltage $\lvert V_{Cs} / V_{oc}\rvert$	$\frac{\sqrt{Q_{s0}^2 u^4 + Q_{s0}^4 u^2\left(u^2-1\right)^2}}{u^2 + Q_{s0}^2\left(u^2-1\right)^2}$	$\frac{\sqrt{Q_{s0}^2 u^4 + Q_{s0}^4 u^2\left(u^2-1\right)^2}}{u^2 + Q_{s0}^2\left(u^2-1\right)^2}$

InductEV, Inc.
Exhibit 1010
Page 175

3-7.4 INFLUENCE OF FREQUENCY ON THE REFLECTED IMPEDANCE

According to the above investigation, the electric characteristics of the secondary resonant circuit are sensitive to variations in the operating frequency and the load. In consequence, the loading effects of the second resonant circuit on the primary will exhibit a similar sensitivity. To enable a general analysis of the pickup loading effects, a normalized reflected impedance is calculated using (3-30) as:

$$Z_{rn} = \frac{Z_r}{\mathrm{Re}\, Z_{r0}} = \frac{\mathrm{Re}\, Z_r}{\mathrm{Re}\, Z_{r0}} + j\frac{\mathrm{Im}\, Z_r}{\mathrm{Re}\, Z_{r0}} = \mathrm{Re}\, Z_{rn} + j\,\mathrm{Im}\, Z_{rn} \tag{3-33}$$

The resistive and reactive components of Z_m (as derived in Appendix D) are both functions of the secondary quality factor (Q_{s0}) and the normalized operating frequency (u) as stated below for the specified secondary compensation:

$$\mathrm{Re}\, Z_{rn} = \frac{\mathrm{Re}\, Z_r}{\mathrm{Re}\, Z_{r0}} = \begin{cases} \dfrac{u^4}{\left(u^2-1\right)^2 Q_{s0}^2 + u^2} & \text{series secondary} \\ \dfrac{u^2}{\left(u^2-1\right)^2 Q_{s0}^2 + u^2} & \text{parallel secondary} \end{cases} \tag{3-34}$$

and

$$\mathrm{Im}\, Z_{rn} = \frac{\mathrm{Im}\, Z_r}{\mathrm{Re}\, Z_{r0}} = \begin{cases} \dfrac{-u^3\left(u^2-1\right)Q_{s0}}{\left(u^2-1\right)^2 Q_{s0}^2 + u^2} & \text{series secondary} \\ \dfrac{-u^3\left[\left(u^2-1\right)Q_{s0} + \dfrac{1}{Q_{s0}}\right]}{\left(u^2-1\right)^2 Q_{s0}^2 + u^2} & \text{parallel secondary} \end{cases} \tag{3-35}$$

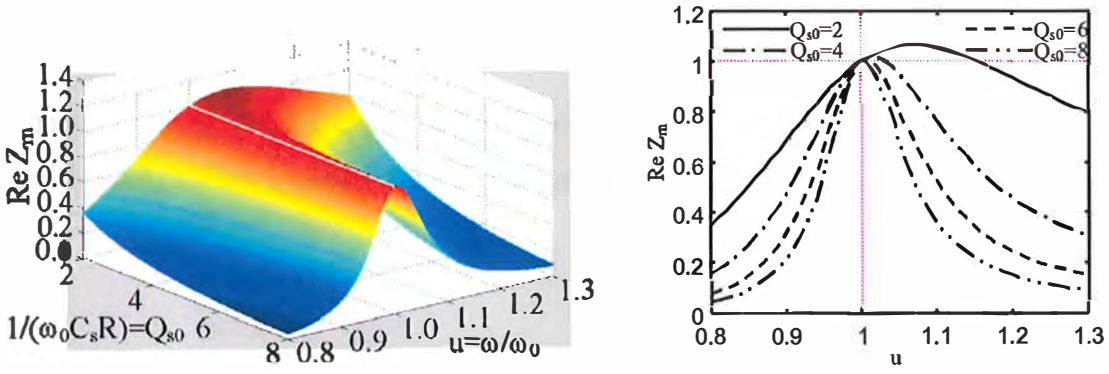
The normalized reflected resistance and reactance are compared in Fig. 3-6 and Fig. 3-7 for series and parallel compensated secondary systems respectively. They are shown as functions of the secondary quality factors (Q_{s0}) and the normalized operating frequency (u). Cross-sections of the surfaces at selected Q_s of 2, 4, 6 and 8 are drawn to show the influences of u and Q_{s0}.

The normalized reflected resistance at ω_0 is shown as white lines on the surfaces in Fig. 3-6 (a-i)&(b-i). The normalized reflected reactance at ω_0 is shown as black lines on the surfaces in Fig. 3-7 (a-i)&(b-i). The reflected resistance and reactance of the series and parallel-compensated secondary systems once again have similar features. As with the electric characteristic of the pickup, both the reflected resistance and reactance are highly sensitive to variations in the operating frequency. This sensitivity increases as the secondary quality factor increases.

For both series and parallel compensated secondary systems, maximum reflected resistance and

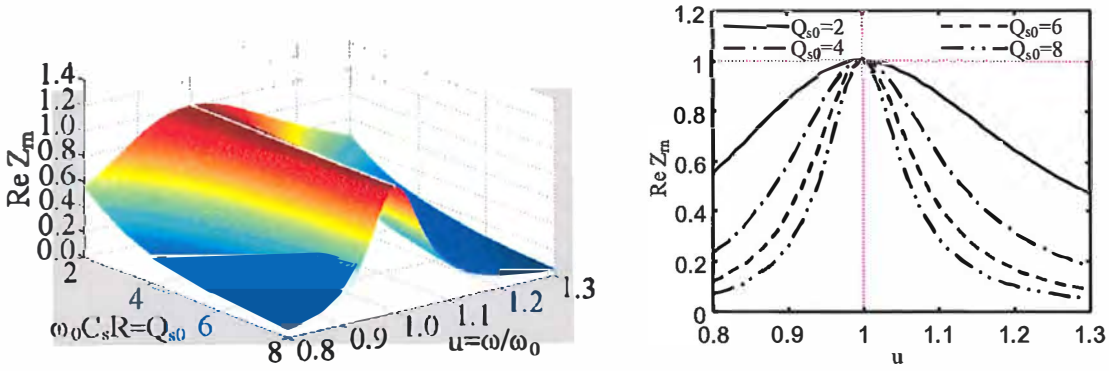
InductEV, Inc.
Exhibit 1010
Page 176

power transfer capability under constant primary current control, is achieved when operated close to ω_0. As the operating frequency shifts away, both the reflected resistance and power transfer capability quickly drop. Assuming a secondary quality factor of 5, if u is 0.9 (representing a 10% drop below ω_0), the power transfer capability decreases by 62% for series compensated pickups, and 53% for parallel-compensated pickups. Whereas a 10% frequency increase (u=1.1) results in decreases in power of 37% and 48% for series and parallel-compensated pickups respectively.



(i) Surface function. (ii) Cross sections of the surface.

(a) Series compensated secondary.



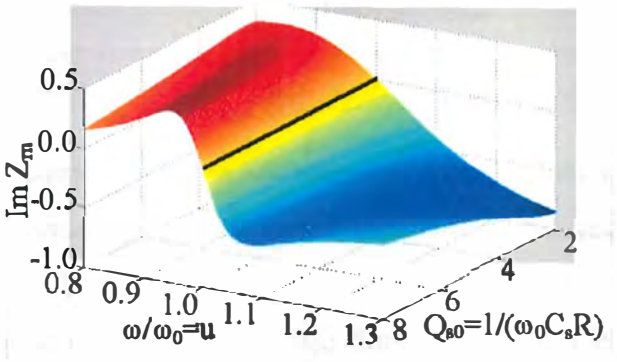
(i) Surface function. (ii) Cross sections of the surface.

(b) Parallel compensated secondary.

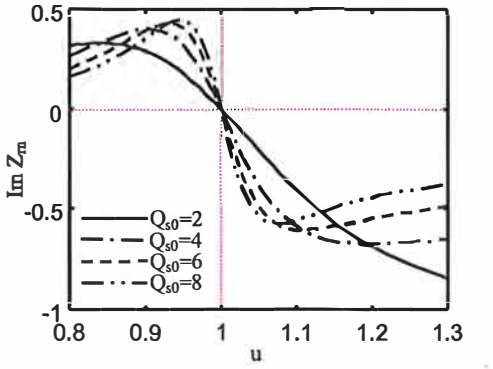
Fig. 3-6. Normalized reflected resistance for series and parallel-compensated secondary systems.

The reflected reactance from a series compensated secondary is always zero at ω_0. This reflected reactance is inductive (positive) below ω_0, and capacitive (negative) above ω_0. The parallel-compensated secondary system, however, reflects a capacitive reactance at ω_0. This reflected reactance becomes less capacitive and eventually inductive as the operating frequency moves below ω_0. It becomes more capacitive as the operating frequency shifts above ω_0.

InductEV, Inc.
Exhibit 1010
Page 177

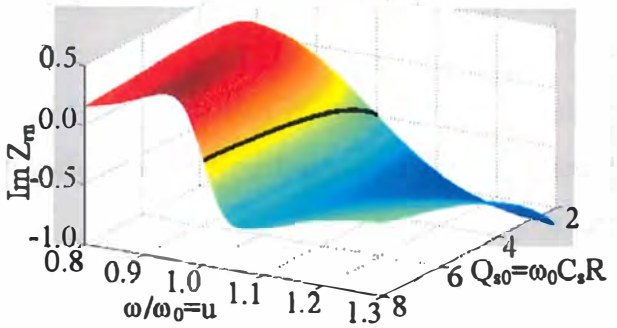


(i) Surface function.

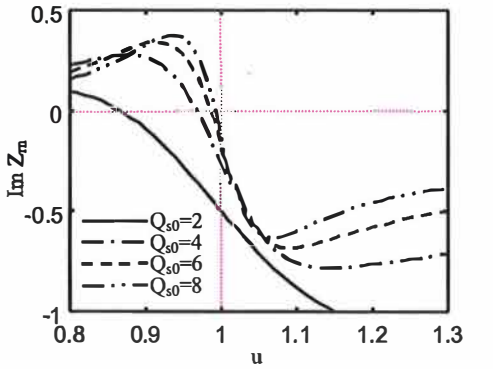


(ii) Cross sections of the surface.

(a) Series compensated secondary.



(i) Surface function.



(ii) Cross sections of the surface.

(b) Parallel compensated secondary.

Fig. 3-7. Normalized reflected reactance for series and parallel-compensated secondary systems.

3-7.5 OPERATING CONDITIONS FOR MAXIMUM POWER TRANSFER

According to (3-20), the power transfer from the primary to the secondary depends on the reflected resistance and the primary current. Assuming constant primary current, the power transfer is then proportional to the reflected resistance. In this case, the operating frequency for maximum power transfer can be determined by:

$$\frac{\partial\left(\dfrac{\mathrm{Re}\,Z_r}{\mathrm{Re}\,Z_{r0}}\right)}{\partial u}=0 \tag{3-36}$$

The result is found to be:

$$u=\begin{cases}\sqrt{\dfrac{2Q_{s0}^2}{2Q_{s0}^2-1}} & \text{series secondary}\\ 1 & \text{parallel secondary}\end{cases} \tag{3-37}$$

Substituting (3-37) into (3-34) results in:

InductEV, Inc.
Exhibit 1010
Page 178

$$\frac{\mathrm{Re}\,Z_r}{\mathrm{Re}\,Z_{r0}} = \begin{cases} \dfrac{4Q_{s0}^2}{4Q_{s0}^2 - 1} & \text{series secondary} \\ 1 & \text{parallel secondary} \end{cases} \tag{3-38}$$

With a series compensated secondary system, the operating frequency for maximum power transfer is higher than the secondary resonant frequency. This maximum power transfer, however, is only slightly higher than the available power at the secondary resonant frequency. With Q_{s0} of 2, the difference in both frequency and power transfer is about 7%. Such differences become negligible as the secondary quality factor increases (with Q_{s0} of 5, the difference in both frequency and power transfer is only 1%). Consequently, the usual approach is to design the pickup to operate at the secondary resonant frequency rather than the maximum power frequency, which is load dependent and as such difficult for a pickup design to follow.

For a parallel-compensated secondary system, the operating frequency for maximum power transfer is identical to the secondary resonant frequency under all loading conditions. The secondary resonant frequency is therefore a logical choice for the pickup design.

3-8 THE PRIMARY COIL

With the loading effects of the secondary resonant circuit represented by the reflected impedance, the equivalent circuit of the primary coil consists of its self-inductance (L_p) in series with the secondary pickup reflected impedance (Z_r) as shown in Fig. 3-8.

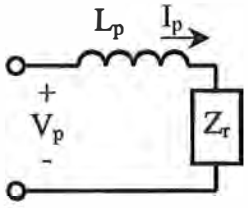


Fig. 3-8. Equivalent circuit of the primary coil.

The impedance of the primary coil calculated from the circuit in Fig. 3-8 is:

$$Z_p = j\omega L_p + Z_r \tag{3-39}$$

The first term in (3-39) is inductive, corresponding to the self-inductance of the primary coil. It is proportional to the operating frequency and independent of the load. The second term in (3-39) is the reflected impedance. As noted in section 3-7.4, it can be either capacitive or inductive as the frequency varies across the frequency spectrum, and is a non-proportional function of the operating frequency and the load.

InductEV, Inc.
Exhibit 1010
Page 179

The impedance of the primary coil is analysed relative to the reactance of its self-inductance at the secondary resonant frequency thereby enabling the influence of Z_r (representing the secondary loading effect) to be easily seen. This ratio is determined to be:

$$\frac{Z_p}{j\omega_0 L_p} = \frac{\omega}{\omega_0}\left(1 - \frac{jk^2\omega L_s}{Z_s}\right) \tag{3-40}$$

Substituting (3-29)&(3-31) into (3-40) results in:

$$\frac{Z_p}{j\omega_0 L_p} = u\left(1 - \frac{k^2 I_s}{I_{sc}}\right) \tag{3-41}$$

This ratio (as derived in Appendix E) is a function of the secondary quality factor (Q_{s0}), the normalized operating frequency (u), as well as the magnetic coupling coefficient (k), and is given for the specified secondary compensation as:

$$\left|\frac{Z_p}{j\omega_0 L_p}\right| = \begin{cases} \dfrac{\sqrt{k^4 Q_{s0}^2 u^8 + u^2\left\{u^2 + Q_{s0}^2\left(u^2-1\right)\left[u^2\left(1-k^2\right)-1\right]\right\}^2}}{u^2 + Q_{s0}^2\left(u^2-1\right)^2} & \text{series secondary} \\ \dfrac{\sqrt{k^4 Q_{s0}^2 u^4 + u^2\left\{u^2\left(1-k^2\right) + Q_{s0}^2\left(u^2-1\right)\left[u^2\left(1-k^2\right)-1\right]\right\}^2}}{u^2 + Q_{s0}^2\left(u^2-1\right)^2} & \text{parallel secondary} \end{cases} \tag{3-42}$$

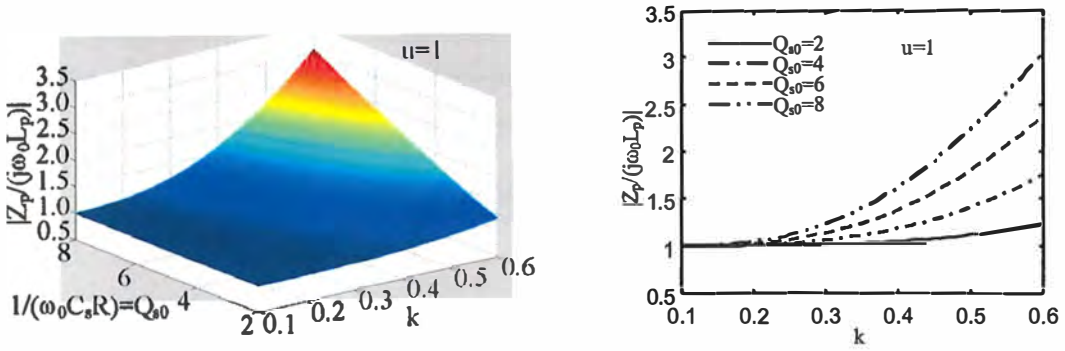
To further clarify the effects of the magnetic coupling strength and the secondary quality factor, the ratio $Z_p/(j\omega_0 L_p)$ at the secondary resonant frequency (u=1) can be derived from (3-42) as:

$$\left|\frac{Z_p(u=1)}{j\omega_0 L_p}\right| = \begin{cases} \sqrt{k^4 Q_{s0}^2 + 1} & \text{series secondary} \\ \sqrt{k^4 Q_{s0}^2 + \left(1-k^2\right)^2} & \text{parallel secondary} \end{cases} \tag{3-43}$$

The result is a function of Q_{s0} and k, and is shown in Fig. 3-9. As can be seen, the ratio $Z_p/(j\omega_0 L_p)$ at the secondary resonant frequency is close to unity at low secondary quality factor or magnetic coupling, but increases with increasing secondary quality factor or magnetic coupling due to loading effects of the secondary. As shown, the effects due to the secondary quality factor are nearly linear, while the effects due to the magnetic coupling are close to following a square law. These characteristics can be verified from (3-43).

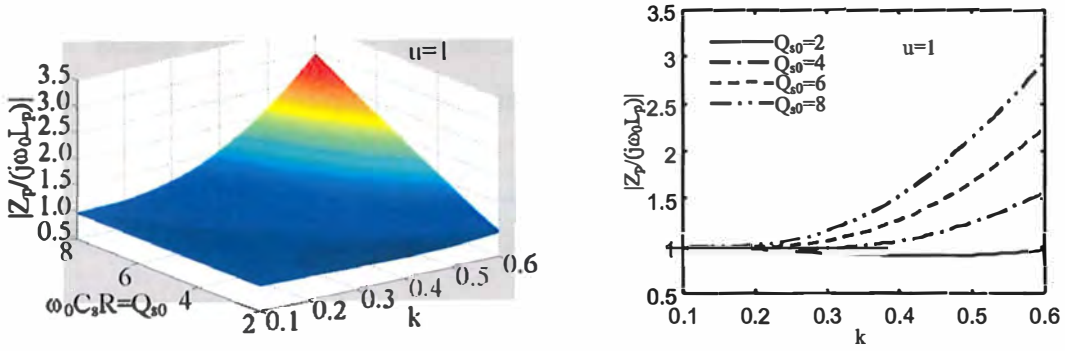
In order to investigate the effects of frequency variations, the ratio $Z_p/(j\omega_0 L_p)$ is compared in Fig. 3-10 and Fig. 3-11 for series and parallel compensated secondary systems. It is shown as a function of Q_{s0} and u at selected k. The values at selected Q_{s0} of 2, 4, 6 and 8 are also drawn to clarify the features in each case. Once again, series and parallel compensations exhibit similar features.

InductEV, Inc.
Exhibit 1010
Page 180



(i) Surface function. (ii) Cross sections of the surface.

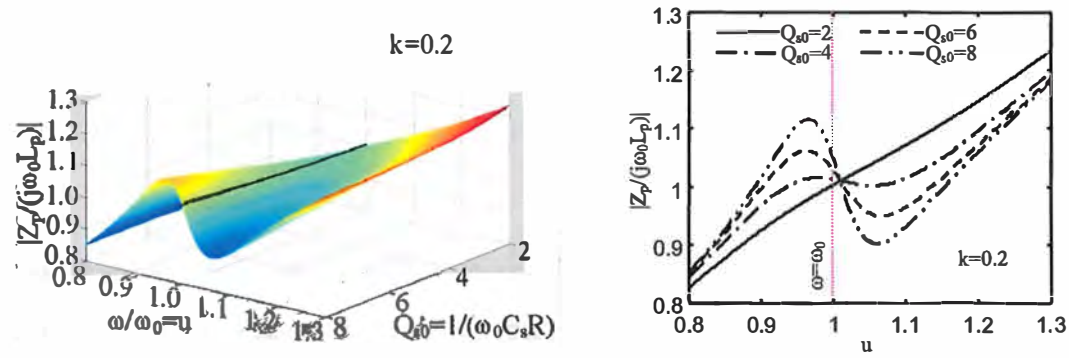
(a) Series compensated secondary.



(i) Surface function. (ii) Cross sections of the surface.

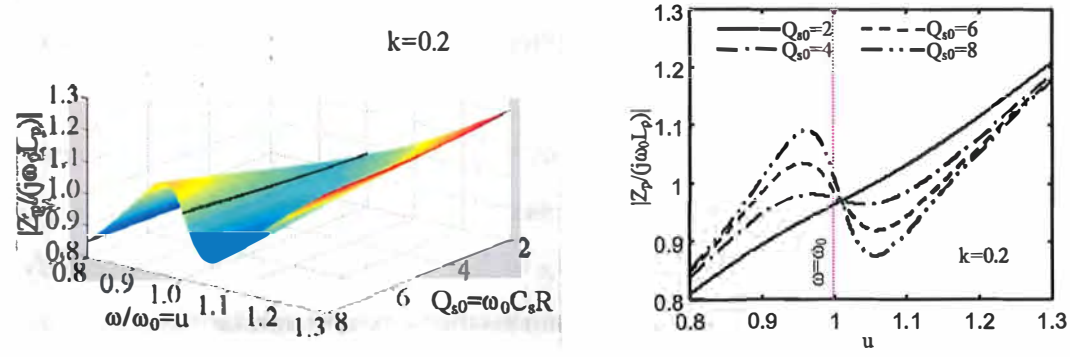
(b) Parallel compensated secondary.

Fig. 3-9. The ratio $Z_p/(j\omega_0L_p)$ at the secondary resonant frequency ω_0 (u=1).



(i) Surface function. (ii) Cross sections of the surface.

(a) Series compensated secondary.

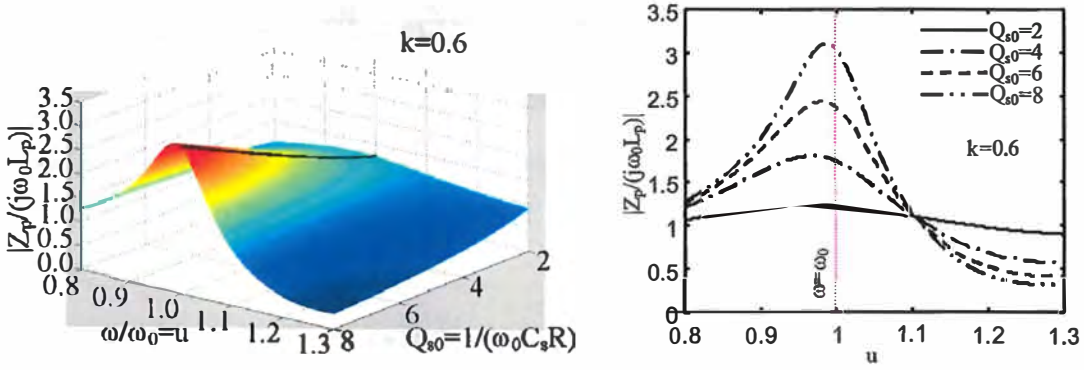


(i) Surface function. (ii) Cross sections of the surface.

(b) Parallel compensated secondary.

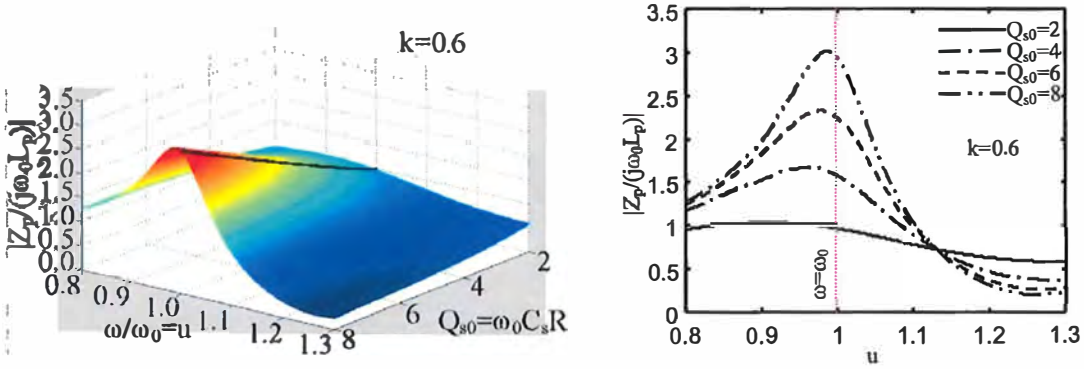
Fig. 3-10. The ratio $Z_p/(j\omega_0L_p)$ with k=0.2.

InductEV, Inc.
Exhibit 1010
Page 181



(i) Surface function. (ii) Cross sections of the surface.

(a) Series compensated secondary.



(i) Surface function. (ii) Cross sections of the surface.

(b) Parallel compensated secondary.

Fig. 3-11. The ratio $Z_p/(j\omega_0 L_p)$ with k=0.6.

As can be seen, in loosely coupled systems (low k) with low compensation levels (low Q_s) the impedance of the primary coil increases with the frequency. The relationship is closely linear because the loading effects of the secondary on the primary are negligible. With improved magnetic coupling and increased compensation level, the secondary loading effects gradually dominate the impedance of the primary coil.

3-9 THE PRIMARY QUALITY FACTOR

The primary quality factor (Q_p) associated with the primary coil is calculated in this section. The reactive power of the primary coil is:

$$VAR_p = (\omega L_p + \mathrm{Im}\, Z_r) I_p^2 \tag{3-44}$$

The real power transferred by the primary coil was calculated in (3-20). The primary quality factor defined as the ratio of reactive to real power is then:

InductEV, Inc.
Exhibit 1010
Page 182

$$Q_p = \frac{VAR_p}{P} = \frac{(\omega L_p + \mathrm{Im}Z_r)I_p^2}{(\mathrm{Re}Z_r)I_p^2} = \frac{\frac{\omega L_p}{\mathrm{Re}Z_{r0}} + \frac{\mathrm{Im}Z_r}{\mathrm{Re}Z_{r0}}}{\frac{\mathrm{Re}Z_r}{\mathrm{Re}Z_{r0}}} = \frac{\frac{\omega L_p}{\mathrm{Re}Z_{r0}} + \mathrm{Im}Z_{rn}}{\mathrm{Re}Z_{rn}} \tag{3-45}$$

The normalized reactance of the self-inductance (L_p) of the primary coil can be derived from (3-26) and (3-29):

$$\frac{\omega L_p}{\mathrm{Re}Z_{r0}} = \frac{\omega L_p}{\left(\frac{\omega_0 M^2}{L_s}\right)Q_{s0}} = \frac{uL_pL_s}{M^2Q_{s0}} \tag{3-46}$$

The relation of the mutual inductance (M) and the coupling coefficient (k) derived from (2-1) is:

$$M^2 = k^2 L_p L_s \tag{3-47}$$

Substituting (3-47) into (3-46) results in:

$$\frac{\omega L_p}{\mathrm{Re}Z_{r0}} = \frac{u}{k^2 Q_{s0}} \tag{3-48}$$

Substituting (3-48) into (3-45) results in:

$$Q_p = \frac{\frac{u}{k^2 Q_{s0}} + \mathrm{Im}Z_{rn}}{\mathrm{Re}Z_{rn}} \tag{3-49}$$

Substituting (3-34) and (3-35) into (3-49), the primary quality factor is determined to be functions of k, u and Q_{s0} for the specified secondary compensation as:

$$Q_p = \begin{cases} \dfrac{u^2 + Q_{s0}^2(u^2-1)\left[(1-k^2)u^2-1\right]}{k^2u^3Q_{s0}} & \text{series secondary} \\ \dfrac{(1-k^2)u^2 + Q_{s0}^2(u^2-1)\left[(1-k^2)u^2-1\right]}{k^2uQ_{s0}} & \text{parallel secondary} \end{cases} \tag{3-50}$$

The primary quality factor at ω_0 derived from (3-50) is then:

$$Q_{p0} = Q_p(\omega=\omega_0) = Q_p(u=1) = \begin{cases} \dfrac{1}{k^2Q_{s0}} & \text{series secondary} \\ \dfrac{1-k^2}{k^2Q_{s0}} = \dfrac{1}{k^2Q_{s0}} - \dfrac{1}{Q_{s0}} & \text{parallel secondary} \end{cases} \tag{3-51}$$

Normally, ICPT systems are designed to operate close to ω_0. In such systems, the fundamental design parameters k, Q_{p0} and Q_{s0} are related. The primary quality factor reduces when the secondary quality factor increases or the electromagnetic structure improves.

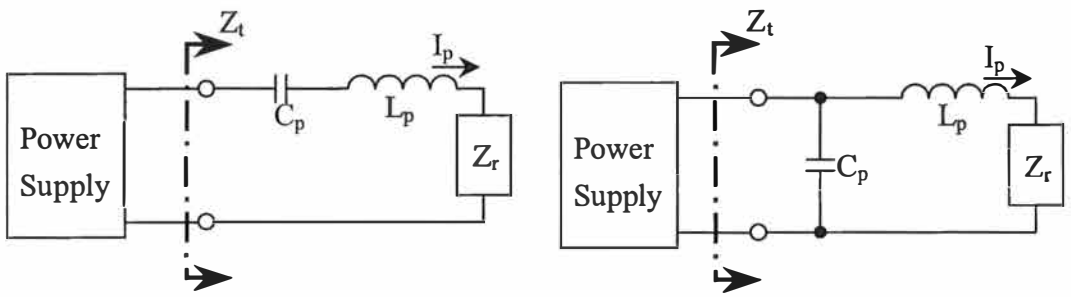
InductEV, Inc.
Exhibit 1010
Page 183

3-10 THE POWER SUPPLY LOAD MODEL

According to above analysis, when the magnetic coupling is weak and the secondary quality factor is low, the loading effect of the secondary on the primary is negligible comparing to the self-inductance of the primary coil. In this case, the primary and secondary resonance can be assumed to be independent and as such significantly simplifies the design process. For such systems, a constant primary current at the secondary resonant frequency can be assumed in the design of the secondary pickup, and the secondary loading effect can be assumed to be a resistance in the design of the primary power supply [2-4]. However, a common trend in the design of ICPT systems is to improve magnetic coupling and increase secondary quality factor in order to transfer more power. The primary and secondary resonances thus become strongly interlinked. For optimal design of these systems, the simplified design approach is not accurate enough. It is necessary to consider all of the interactions between the primary and secondary. This section develops a mathematical model to represent the complete load resonant tank consisting of both the primary and secondary resonant circuits. The resulting power supply load models of commonly used compensation topologies are compared. They are then normalized to simplify the analysis and used as a design tool in following chapters.

3-10.1 MODELLING OF THE POWER SUPPLY LOAD IMPEDANCE

Both series and parallel-compensated primary resonant circuits are shown in Fig. 3-12 with the loading effects of the secondary represented by the reflected impedance (Z_r) in series connection with the primary self-inductance. To simplify the analysis of the load seen by the power supply, the primary resonant circuits can be represented as a lumped impedance (Z_t). As noted in Fig. 3-12, this lumped load impedance seen by the power supply depends on the primary compensation topologies. With a series compensated primary, it consists of the primary capacitance in series connection to the primary coil (formed by the self-inductance and the reflected impedance). For a parallel-compensated primary, it is formed by the primary capacitance in parallel connection with the primary coil.



(a) Series compensated primary. (b) Parallel compensated primary.

Fig. 3-12. Primary resonant circuits with reflected impedance.

InductEV, Inc.
Exhibit 1010
Page 184

The power supply load impedance (Z_t) is derived for the specified primary compensation as:

$$Z_t = \begin{cases} \dfrac{1}{j\omega C_p} + Z_p = \dfrac{1}{j\omega C_p} + j\omega L_p + Z_r & \text{series primary} \\ \dfrac{1}{j\omega C_p + \dfrac{1}{Z_p}} = \dfrac{1}{j\omega C_p + \dfrac{1}{j\omega L_p + Z_r}} & \text{parallel primary} \end{cases} \tag{3-52}$$

The real part of the load impedance (Re Z_t) is the load resistance and represents real power transfer. The imaginary part (Im Z_t) is the load reactance and dictates reactive power flow.

As noted above, the load impedance seen by the supply is a function of the reflected impedance (Z_r), which in turn depends on the secondary compensation topology. In consequence, the load impedance seen by the power supply depends on not only the primary but also the secondary compensation topology. Since both the primary and secondary can be either series or parallel compensated, there are four basic topologies labelled as SS, SP, PP and PS (as noted in section 2-3.5). A summary of the load impedance is given in Table 3-2 for each topology.

TABLE 3-2
LOAD IMPEDANCE OF THE BASIC TOPOLOGIES

Topology	Load impedance
SS	$Z_t = \dfrac{1}{j\omega C_p} + j\omega L_p + \dfrac{\omega^2 M^2}{j\omega L_s + \dfrac{1}{j\omega C_s} + R}$
SP	$Z_t = \dfrac{1}{j\omega C_p} + j\omega L_p + \dfrac{\omega^2 M^2}{j\omega L_s + \dfrac{1}{j\omega C_s + \dfrac{1}{R}}}$
PP	$Z_t = \dfrac{1}{j\omega C_p + \dfrac{1}{j\omega L_p + \dfrac{\omega^2 M^2}{j\omega L_s + \dfrac{1}{j\omega C_s + \dfrac{1}{R}}}}}$
PS	$Z_t = \dfrac{1}{j\omega C_p + \dfrac{1}{j\omega L_p + \dfrac{\omega^2 M^2}{j\omega L_s + \dfrac{1}{j\omega C_s} + R}}}$

InductEV, Inc.
Exhibit 1010
Page 185

3-10.2 THE NORMALIZED LOAD IMPEDANCE

Similar to the normalization process of the reflected impedance (Z_r) in section 3-7.4, the load impedance (Z_t) is normalized in this section with respect to the reflected resistance at the secondary resonant frequency ($\mathrm{Re}\, Z_{r0}$) using (3-30), while the operating frequency (ω) is normalized with respect to the secondary resonant frequency (ω_0) using (3-29). The normalised load impedance is calculated as:

$$Z_{tn} = \frac{Z_t}{\mathrm{Re}\, Z_{r0}} = \frac{\mathrm{Re}\, Z_t}{\mathrm{Re}\, Z_{r0}} + j\frac{\mathrm{Im}\, Z_t}{\mathrm{Re}\, Z_{r0}} = \mathrm{Re}\, Z_{tn} + j\,\mathrm{Im} Z_{tn} \tag{3-53}$$

This definition is suitable for series compensated primary systems, however it is often much easier to describe the load impedance in terms of its admittance value (conductance and susceptance) when dealing with parallel compensated primary systems, so that:

$$Z_{tn} = \frac{1}{Y_t(\mathrm{Re}\, Z_{r0})} = \frac{1}{(\mathrm{Re}\, Y_t)(\mathrm{Re}\, Z_{r0}) + j(\mathrm{Im}\, Y_t)(\mathrm{Re}\, Z_{r0})} = \frac{1}{\mathrm{Re}\, Y_{tn} + j\,\mathrm{Im} Y_{tn}} = \frac{1}{Y_{tn}} \tag{3-54}$$

Substituting (3-52) into (3-53), the normalized load resistance and reactance for series compensated primary systems are given by:

$$\mathrm{Re}\, Z_{tn} = \mathrm{Re}\, Z_{rn} \tag{3-55}$$

and

$$\mathrm{Im} Z_{tn} = -\frac{1}{\omega C_p(\mathrm{Re}\, Z_{r0})} + \frac{\omega L_p}{\mathrm{Re}\, Z_{r0}} + \mathrm{Im} Z_{rn} \tag{3-56}$$

Substituting (3-52) into (3-54), the normalized load conductance and susceptance for parallel compensated primary systems are derived as:

$$\mathrm{Re}\, Y_{tn} = \frac{\mathrm{Re}\, Z_{rn}}{(\mathrm{Re}\, Z_{rn})^2 + \left(\frac{\omega L_p}{\mathrm{Re}\, Z_{r0}} + \mathrm{Im} Z_{rn}\right)^2} \tag{3-57}$$

and

$$\mathrm{Im}\, Y_{tn} = \omega C_p(\mathrm{Re}\, Z_{r0}) - \frac{\frac{\omega L_p}{\mathrm{Re}\, Z_{r0}} + \mathrm{Im} Z_{rn}}{(\mathrm{Re}\, Z_{rn})^2 + \left(\frac{\omega L_p}{\mathrm{Re}\, Z_{r0}} + \mathrm{Im} Z_{rn}\right)^2} \tag{3-58}$$

As shown above, for a series compensated primary the load resistance is identical to the reflected resistance. The load reactance, however, depends on the primary capacitance and inductance, and also the reflected reactance. For a parallel-compensated primary the load conductance depends on the primary inductance, and also the reflected resistance and reactance, while the load susceptance depends on the primary capacitance and inductance as well as the reflected resistance and reactance.

InductEV, Inc.
Exhibit 1010
Page 186

Equations (3-55) to (3-58) can be simplified if they are written in terms of the normalized operating frequency ($u=\omega/\omega_0$), and the quality factors (Q_{p0} and Q_{s0}) associated to the primary and secondary resonant circuits at ω_0. These equations consist of the normalized reactance of the self-inductance of the primary coil, the normalized reactance of the primary compensation capacitance, and the normalized reflected resistance and reactance as summarized in Table 3-3. This simplification process of the normalized load impedance is discussed following.

TABLE 3-3
FUNCTIONS OF THE NORMALIZED LOAD IMPEDANCE WITH COMPENSATED PICKUP

$\dfrac{1}{\omega C_p(\mathrm{Re}Z_{r0})}$	$\begin{cases} \dfrac{Q_{p0}}{u}=\dfrac{1}{uk^2Q_{s0}} \\ \left(\dfrac{1}{u}\right)\left(Q_{p0}+\dfrac{1}{Q_{s0}}\right)=\dfrac{1}{uk^2Q_{s0}} \end{cases}$	Series secondary. Parallel secondary.
$\dfrac{\omega L_p}{\mathrm{Re}Z_{r0}}$	$\begin{cases} uQ_{p0}=\dfrac{u}{k^2Q_{s0}} \\ u\left(Q_{p0}+\dfrac{1}{Q_{s0}}\right)=\dfrac{u}{k^2Q_{s0}} \end{cases}$	Series secondary. Parallel secondary.
$\mathrm{Re}Z_{rn}=\dfrac{\mathrm{Re}Z_r}{\mathrm{Re}Z_{r0}}$	$\begin{cases} \dfrac{u^4}{(u^2-1)^2Q_{s0}^2+u^2} \\ \dfrac{u^2}{(u^2-1)^2Q_{s0}^2+u^2} \end{cases}$	Series secondary. Parallel secondary.
$\mathrm{Im}Z_{rn}=\dfrac{\mathrm{Im}Z_r}{\mathrm{Re}Z_{r0}}$	$\begin{cases} \dfrac{-u^3(u^2-1)Q_{s0}}{(u^2-1)^2Q_{s0}^2+u^2} \\ \dfrac{-u^3\left[(u^2-1)Q_{s0}+1/Q_{s0}\right]}{(u^2-1)^2Q_{s0}^2+u^2} \end{cases}$	Series secondary. Parallel secondary.

The normalized reflected resistance and reactance depend on the secondary compensation topology (either series or parallel) and are derived in section 3-7.4 with the results given in (3-34) and (3-35). They are functions of u and Q_{s0} only.

The normalized reactance of the self-inductance of the primary coil given in (3-48) can be rearranged using (3-51) as a function of u, Q_{p0} and Q_{s0} given by:

$$\frac{\omega L_p}{\mathrm{Re}Z_{r0}}=\begin{cases} uQ_{p0} & \text{series secondary} \\ u\left(Q_{p0}+\dfrac{1}{Q_{s0}}\right) & \text{parallel secondary} \end{cases} \tag{3-59}$$

The primary compensation capacitance is normally selected using (2-28). With this conventional choice, the normalized reactance of the primary compensation capacitance as derived in Appendix F is

InductEV, Inc.
Exhibit 1010
Page 187

also a function of u, Q_{p0} and Q_{s0} given by:

$$\frac{1}{\omega C_p(\mathrm{Re}Z_{r0})} = \begin{cases} \dfrac{Q_{p0}}{u} & \text{series secondary} \\ \left(\dfrac{1}{u}\right)\left(Q_{p0} + \dfrac{1}{Q_{s0}}\right) & \text{parallel secondary} \end{cases} \tag{3-60}$$

As noted in section 3-9, the primary quality factor depends on the magnetic coupling coefficient and the secondary quality factor. Consequently, these functions can be expressed alternatively in terms of the normalized frequency (u), the magnetic coupling coefficient (k), and the secondary quality factor (Q_{s0}) as given also in Table 3-3. This enables the identification of the influence of the magnetic coupling structure and the pickup compensation level on the load seen by the power supply.

3-11 VERIFICATION OF THE LOAD MODEL

In order to validate the theoretical load model, a contact-less electric vehicle battery charging system was designed using the design methodology proposed in the following chapter. This system delivers 30kW across a 45mm air gap at a nominal frequency of 20 kHz with a primary current I_p of 150A. The loading system (load resonant tank) on the power supply consists of the electromagnetic structure, the primary and secondary compensation capacitances, and the pickup load that is formed by a rectifier, a filter and a dc regulator. In this test system, the pickup load is replaced by a linear resistor to simplify the verification process. With the power supply disconnected, the load impedance seen by the power supply was measured at the input to the load resonant tank. This measured impedance was then compared with the theoretical calculation using the load model developed in section 3-10.1.

The electromagnetic structure of this system is given in Fig. 3-13. Here the primary and secondary windings are identical, each having concentrated coils with distributed ferrites. It is assumed that the secondary winding is attached to the underside of an electric vehicle, while the primary winding is buried in the ground. Once an electric vehicle has stopped over the charging station, electric power is transferred to the vehicle across an air gap via magnetic coupling between the primary coil in the ground and secondary coil on the vehicle.

For compensation, a PP topology was chosen since it is commonly used for high power industrial applications [2]. The current source characteristic of the parallel-compensated secondary is well suited for battery charging, whereas the parallel-compensated primary is used to generate a large primary current.

The measured coupling and compensation parameters, along with other key system parameters used for the above design, are given in Table 3-4. A variable-frequency Fluke PM 6306 RLC meter was used to measure the coupling parameters of the electromagnetic structure. The primary self-inductance

InductEV, Inc.
Exhibit 1010
Page 188

(L_p) was measured with the secondary left open circuit, while the secondary self-inductance (L_s) was measured with the primary left open circuit. The mutual inductance (M) was determined by measuring the change of the primary inductance (ΔL_p) with a short-circuited secondary. This change occurs due to the reflected impedance from the secondary, and the relationship is given by:

$$Z_r = j\omega(\Delta L_p) \tag{3-61}$$

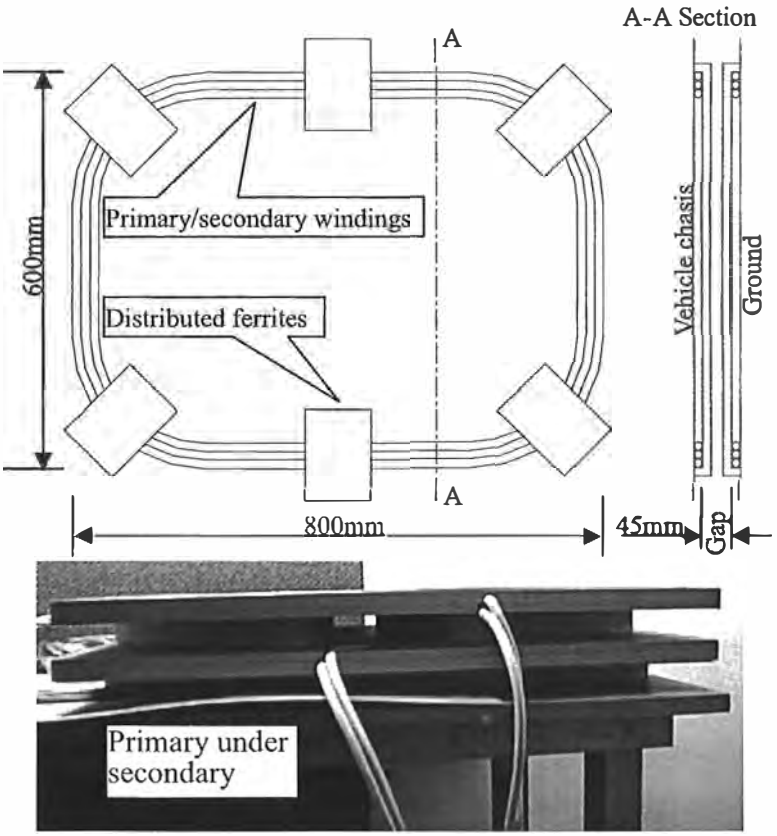


Fig. 3-13. Electromagnetic structure of the contact-less battery charger.

TABLE 3-4
PARAMETERS OF THE CONTACT-LESS ELECTRIC VEHICLE BATTERY CHARGER

Nominal resonant frequency (f)	20kHz
Rated power (P)	30kW
Primary rated current (I_p)	150A
Rated load (R)	6Ω
Primary inductance (L_p)	29.6μH
Primary capacitance (C_p)	2.21μF
Mutual inductance (M)	12.7μH
Secondary inductance (L_s)	26.9μH
Magnetic coupling coefficient (k)	0.45
Secondary capacitance (C_s)	2.42μF

With the secondary placed under short circuit (R=0, uncompensated secondary), the secondary impedance derived from (3-7) is:

InductEV, Inc.
Exhibit 1010
Page 189

$$Z_s = j\omega L_s \tag{3-62}$$

Substituting (3-62) into (3-17), the reflected impedance calculated using the mutual inductance (M) is:

$$Z_r = -j\frac{\omega M^2}{L_s} \tag{3-63}$$

From (3-61) and (3-63), the mutual inductance is determined as:

$$M = \sqrt{-(\Delta L_p)L_s} \tag{3-64}$$

Substituting (3-64) into (2-1), the magnetic coupling coefficient is determined as:

$$k = \sqrt{-\frac{\Delta L_p}{L_p}} \tag{3-65}$$

As shown, the magnetic coupling strength of an electromagnetic coupling structure can be determined by simply measuring the rate of change in the primary inductance when the secondary is placed in a short circuit.

The measured coupling parameters (L_p, M, L_s) of the electromagnetic structure are shown in Fig. 3-14 for selected frequency range from 15kHz to 25kHz around the nominal frequency of 20kHz. As shown, variations with frequency are negligible.

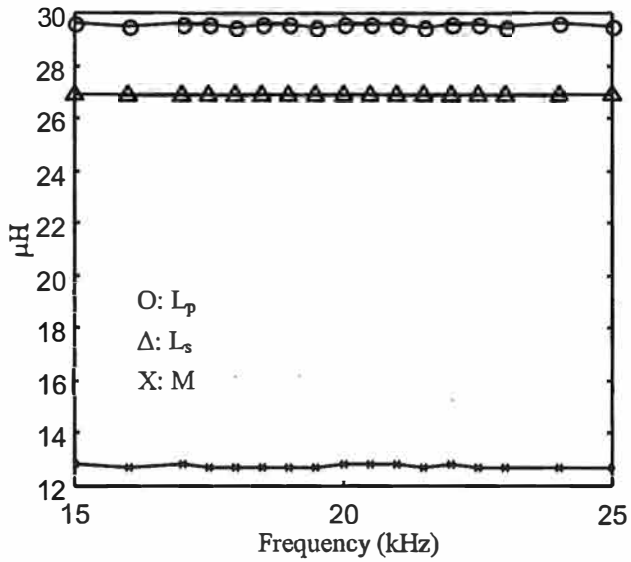


Fig. 3-14. The measured coupling parameters (L_p, L_s, M) of the battery charger.

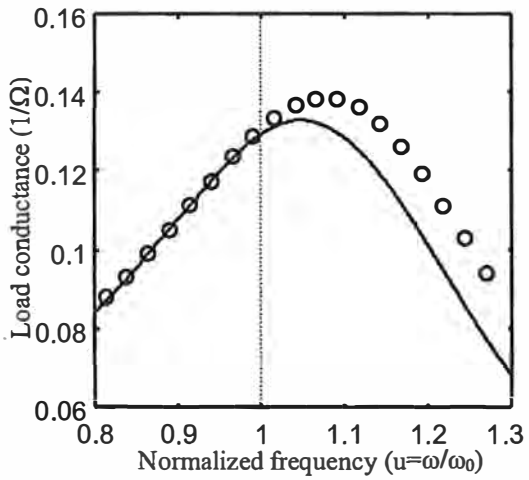
Both the primary and secondary compensation capacitances in Table 3-4 are designed for the nominal frequency using (2-22) and (2-28). With the selected secondary compensation capacitance (C_s=2.42 μF), the secondary resonant frequency (f_0) calculated by (2-22) is 19.7 kHz, which is slightly lower than the nominal resonant frequency (20 kHz). The primary compensation capacitance (C_p) calculated by (2-28) is 2.20 μF. The measured value of C_p as shown in Table 3-4 is 2.21 μF, which is

InductEV, Inc.
Exhibit 1010
Page 190

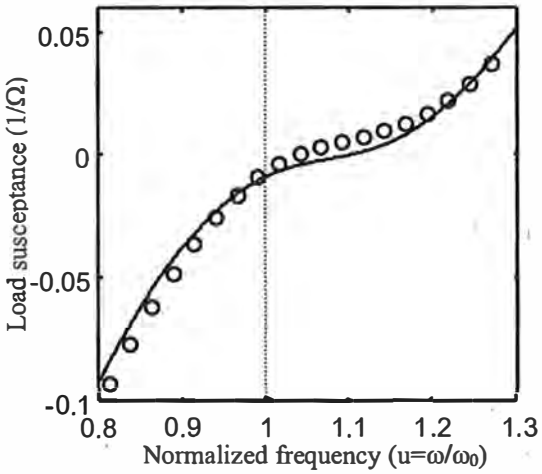
slightly higher than the theoretical value. In order to compare the experimental measurements with the analytical load model, the measured values of both the primary and secondary capacitances are used in the theoretical calculations.

The variable-frequency Fluke PM 6306 RLC meter was also used to measure the power supply load impedance (Z_t). The coupling parameters (L_p, M, L_s) of the electromagnetic structure and the primary and secondary compensation capacitances (C_p, C_s) were kept unchanged at the values given in Table 3-4. Firstly, Z_t was measured at rated load (6Ω) and various frequencies around f_0. Secondly, Z_t was measured by fixing the frequency at the secondary resonant frequency (f_0=19.7 kHz), while varying the load about its rated value.

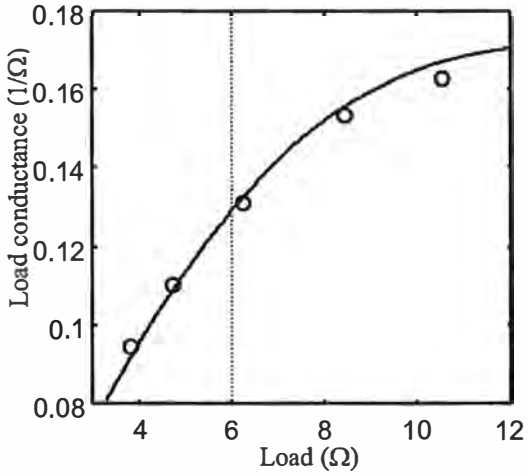
The measured load impedance was recalculated in terms of a load admittance (Y_t=1/Z_t), and compared with the theoretical values as shown in Fig. 3-15. Here, the measured values are shown as circles, whereas solid lines are used to indicate the theoretical values.



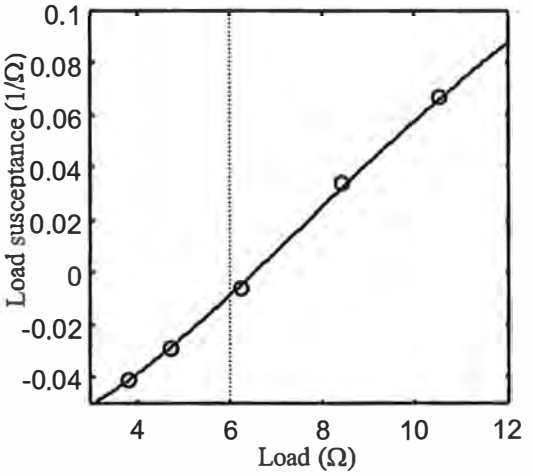
(a) Load conductance (Re Y_t) with R=6Ω.



(b) Load susceptance (Im Y_t) with R=6Ω.



(c) Load conductance (Re Y_t) with u=ω/ω0=1.



(d) Load susceptance (Im Y_t) with u=ω/ω0=1.

Fig. 3-15. Measured and calculated load admittance (Y_t) of the battery charger.

InductEV, Inc.
Exhibit 1010
Page 191

As previously discussed, Fig. 3-15 (a) and (b) show comparisons with the load (R) fixed at its rated value of 6Ω while varying the frequency about f_0, whereas Fig. 3-15 (c) and (d) show comparisons at f_0 while varying R about its rated value. As can be seen, the measured values follow the theoretical predictions closely despite simplifications in the model that assumes sinusoidal voltages and currents, and ignores losses in the inductors and capacitors. The differences are most notable in Fig. 3-15 (a) but are still within 10% across the selected range of frequencies, and mainly arise because the rated load used in the test system is slightly larger than 6Ω and has a stray inductance of about 2.4μH. The influence of the stray inductance increases with increasing frequency.

3-12 CONCLUSIONS

A general load impedance model as seen by the power supply is developed in this chapter to investigate steady state operation of an ICPT system. The developed load model was verified by comparing measured and calculated values in a practical contact-less electric vehicle battery charging system. The measured values follow theoretical calculations within practical limitations. The models therefore can be used confidently in the analyses and designs of ICPT systems.

A major assumption in developing the load model is that the pickup load is linear and resistive. In practice, the pickup load is often a non-linear system, and an equivalent linear resistive load needs to be developed when applying the load model. The electromagnetic structure and the primary and secondary compensation capacitors (C_p and C_s) are assumed to be loss-less. The electromagnetic structure is modelled using the transformer mutual inductance coupling model. The coupling parameters include the primary self-inductance L_p, the mutual inductance M between the primary and secondary, and the secondary self-inductance L_s. The reactive elements (C_p, L_p, M, L_s and C_s) are modelled as impedances that are assumed to be linear functions of the frequency.

The load model is then used to investigate the system behaviour of each topology. The resonant frequency of the pickup (the frequency when L_s is in resonance with C_s) is a key parameter called the secondary resonant frequency (ω_0). To generally quantify system characteristics, the developed impedance models can be expressed in terms of the normalized frequency ($u=\omega/\omega_0$), the quality factors (Q_{p0} and Q_{s0}) associated with the primary and secondary resonant circuits at ω_0, and the magnetic coefficient (k) of the electromagnetic structure. These dimensionless parameters (u, k, Q_{p0} and Q_{s0}) have major influences on system performance, and need to be chosen carefully when designing and optimising the systems.

The frequency for maximum power transfer capability is found to be exactly at ω_0 when the pickup is parallel compensated. However, if the pickup uses series compensation, this frequency is

InductEV, Inc.
Exhibit 1010
Page 192

unexpectedly higher (although the variation from ω_0 becomes negligible as Q_s gets large). The secondary quality factor can be increased to improve the power transfer, however, it also increases its sensitivity to frequency variations. In such systems, the power transfer capability of the pickup drops substantially as the frequency shifts away from the secondary resonant frequency. This pickup frequency detuning has to be minimized in a practical system. The loading effects of the secondary pickup on the primary are also found to increase with increases in Q_s and k, and consequently need to be carefully considered in the design of ICPT systems.

REFERENCES

[1]. N. Mohan, T. M. Undeland, W. P. Robbins, *Power electronics: converters, applications, and design.* New York: John Wiley & Sons, second edition, 1995.

[2]. O. H. Stielau, G. A. Covic, "Design of loosely coupled inductive power transfer systems," in *Proc. 2000 Int. Conf. Power System Technology*, vol. 1, Dec. 2000, pp. 85-90.

[3]. J. T. Boys, G. A. Covic, A. W. Green, "Stability and control of inductively coupled power transfer systems," *Proc. IEE -Elect. Power Applicat.*, vol. 147, no. 1, pp. 37-43, Jan. 2000.

[4]. A. P. Hu, *Selected resonant converters for IPT power supplies*. PhD thesis. The Electrical and Electronics Engineering Department, The University of Auckland, New Zealand, 2001.

InductEV, Inc.
Exhibit 1010
Page 193

CHAPTER 4

EVALUATION OF A DESIGN METHODOLOGY FOR ICPT SYSTEMS

4-1 Introduction
4-2 A design procedure
4-3 Design options for the pickup regulator
4-4 Design options for the power supply
4-5 Design evaluations
4-6 A practical design example
4-7 Conclusions

4-1 INTRODUCTION

Many design examples of ICPT systems have been described in the literature [1-12], but each is dependent on its particular application. Currently, the optimisation and design of an ICPT system relies strongly on experience and experimental verification. This requires suitable design choices for the operating frequency, the primary current, the electromagnetic structure, the primary and secondary compensation, the pickup regulator, and the high frequency switching power supply. This chapter briefly reviews design options used in these areas in terms of their advantages and disadvantages. Since the design choices are inter-related, a design procedure is described with the aim of achieving a controllable power transfer capability over a specified operating range with minimum total cost. As an integrated tool with the design procedure, the normalized load model (developed in chapter 3) is used to evaluate the system behaviour under fixed and variable frequency control in order to determine its sensitivity to the fundamental design parameters u (the normalized frequency), k (the magnetic coupling coefficient) and Q_s (the secondary quality factor).

4-2 A DESIGN PROCEDURE

The power transfer capability of a compensated pickup in an ICPT system (developed in section 2-3.2) was determined as:

$$P = V_{oc} I_{sc} Q_{s0} = \omega_0 I_p^2 \left(k^2 L_p\right) Q_{s0} = \omega_0 I_p^2 \left(\frac{M^2}{L_s}\right) Q_{s0} \tag{4-1}$$

with the required secondary VA rating given by:

InductEV, Inc.
Exhibit 1010
Page 194

$$VA_{s0} = V_{oc} I_{sc} Q_{s0} \sqrt{1+Q_{s0}^2} = P\sqrt{1+Q_{s0}^2} \tag{4-2}$$

As shown to achieve the desired power there are four major design factors: the operating frequency (ω_0), the primary current (I_p), the magnetic design factor ($k^2L_p=M^2/L_s$) and the secondary quality factor (Q_{s0}). The operating frequency and the primary current are restricted by the primary power supply as well as the primary track/coil. The magnetic design factor is restricted by the application layout as well as the geometry and material of the electromagnetic structure. The pickup VA rating as well as stability considerations of the controller restrict the secondary quality factor. Since these design factors are interrelated, an iterative design procedure is introduced in this section to optimise the cost distribution of the total system.

It is assumed in this design procedure that if compensated both the primary and secondary resonance are designed by:

$$\omega_0 = \frac{1}{\sqrt{C_p L_p}} = \frac{1}{\sqrt{C_s L_s}} \tag{4-3}$$

The secondary quality factor at ω_0 (developed in section 3-5) is given by:

$$Q_{s0} = Q_s(\omega=\omega_0) = \begin{cases} \dfrac{1}{\omega_0 C_s R} = \dfrac{\omega_0 L_s}{R} & \text{series secondary} \\ \omega_0 C_s R = \dfrac{R}{\omega_0 L_s} & \text{parallel secondary} \end{cases} \tag{4-4}$$

System stability under variable-frequency control is considered in the design procedure in terms of the magnetic coupling coefficient (k) and the quality factors (Q_{p0} and Q_{s0}) associated with the primary and secondary resonant circuits at ω_0. These three parameters (as noted in section 3-9) are related by:

$$Q_{p0} = \begin{cases} \dfrac{1}{k^2 Q_{s0}} & \text{series secondary} \\ \dfrac{1-k^2}{k^2 Q_{s0}} = \dfrac{1}{k^2 Q_{s0}} - \dfrac{1}{Q_{s0}} & \text{parallel secondary} \end{cases} \tag{4-5}$$

An ICPT system is essentially a transformer with the additional flexibility of relative movement between the primary and secondary. The design procedure of an ICPT system therefore is more complex than an ordinary transformer. This section describes a design procedure to deal with the additional complexities.

4-2.1 DESIGN OF ORDINARY TRANSFORMERS

The design of the ordinary transformer is a well-known procedure. A simplified design methodology for ordinary transformers is shown in Fig. 4-1. The main consideration is a suitable

InductEV, Inc.
Exhibit 1010
Page 195

choice of the geometries and sizes of the magnetic cores. Normally an iterative process is followed that results in the optimum core size. For a given core geometry, the winding parameters are calculated. If the primary and secondary windings do not fit into the chosen common magnetic core, a larger core is necessary. If the window area is not fully utilised, a smaller core should be used.

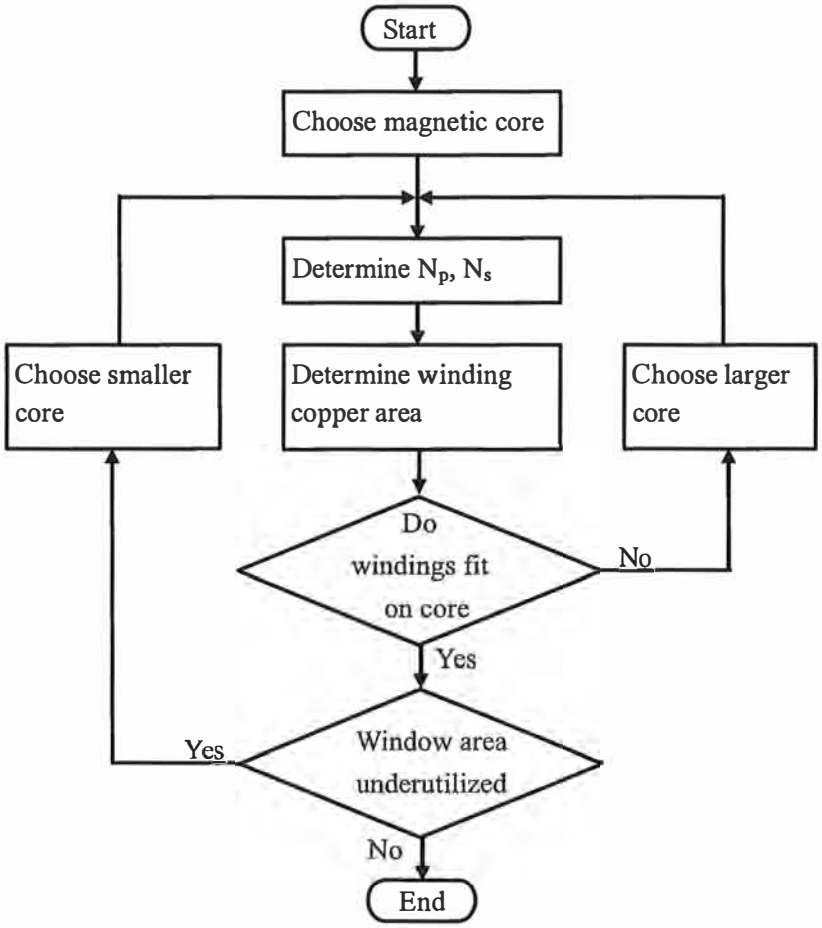


Fig. 4-1. A design procedure of the ordinary transformer.

4-2.2 DESIGN OF ICPT SYSTEMS

To deal with the additional complexities of ICPT systems, a design methodology has been proposed in [12]. This design methodology is extended here to include primary compensation considerations as well as control options (either fixed or variable frequency control). System behaviour under fixed and variable frequency control is quantified in terms of u, k, Q_{p0} and Q_{s0} using the normalized load model seen by the power supply (as developed in chapter 3). This design procedure is shown in Fig. 4-2, and is discussed step by step below. Many choices need to be made throughout the design process, influenced mainly by the cost distribution of the various components in the system.

InductEV, Inc.
Exhibit 1010
Page 196

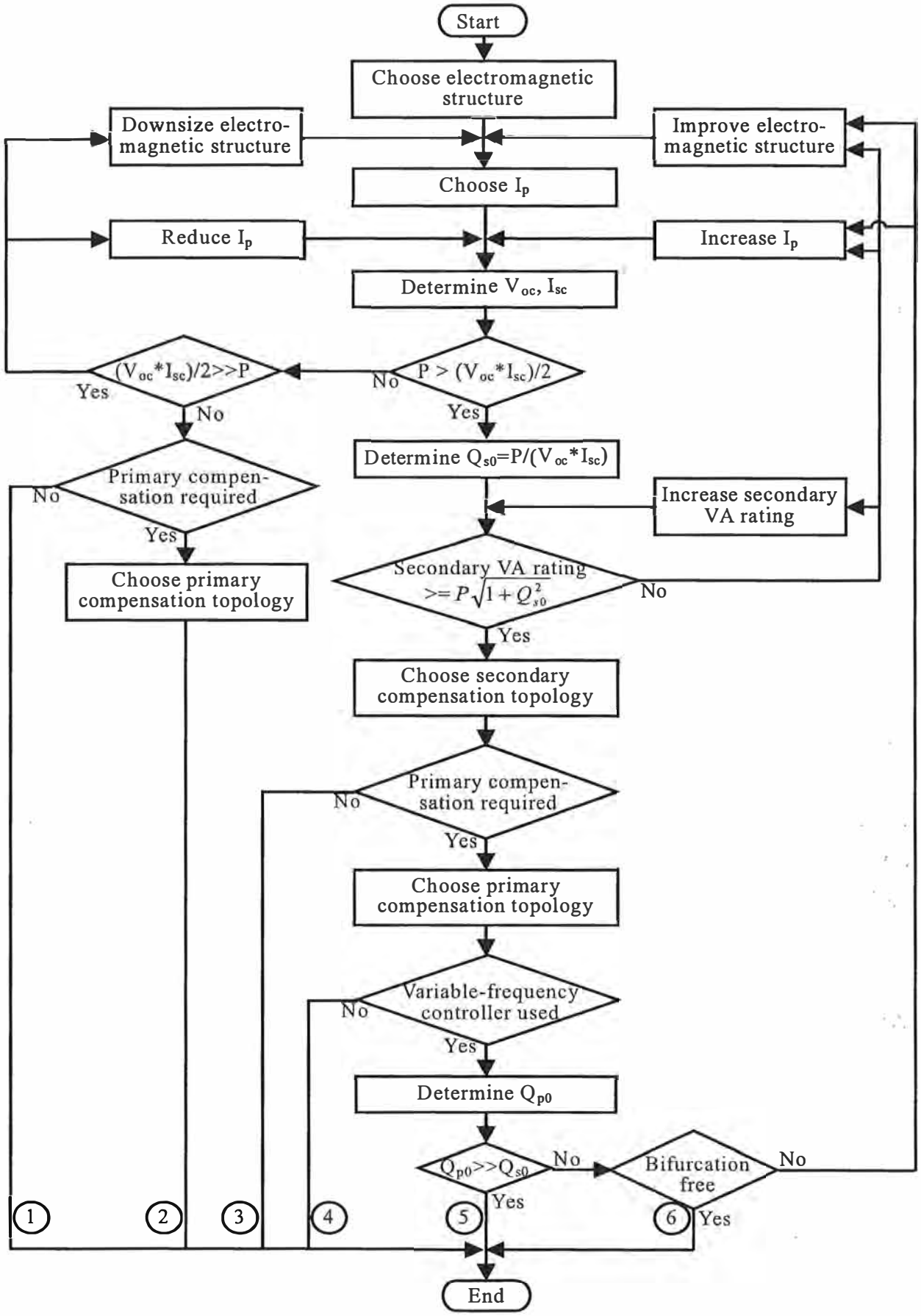


Fig. 4-2. A design procedure of ICPT systems.

InductEV, Inc.
Exhibit 1010
Page 197

Due to the complexity involved in the design procedure, it is necessary to make some assumptions. A summary of the assumptions is given in Table 4-1 and is discussed following. One important assumption is that the desired operating frequency (nominal frequency) ω_0 is known. The power transfer capability of any ICPT system is a strong function of ω_0. In theory increasing ω_0 reduces the size, weight and cost of the total system for the same power transfer capability. However, the choice of ω_0 is limited by practical restrictions in the system components that include the choice of the power switch and the electromagnetic structure.

TABLE 4-1
ASSUMPTIONS OF THE DESIGN PROCEDURE IN FIG. 4-2

1.	Known operating frequency (nominal frequency): ω_0.
2.	Primary and secondary resonant design: $\omega_0 = \frac{1}{\sqrt{C_p L_p}} = \frac{1}{\sqrt{C_s L_s}}$.
3.	Linear and resistive pickup load.
4.	Constant primary current.
5.	Known power supply VA rating.

The capability of commercially available power switches plays a crucial role in the determination of ω_0. Two major considerations are the switching speed and power handling capability. Suitable power switches for ICPT applications are MOSFETs and IGBTs. The switching speeds of MOSFETs are much faster than IGBTs, while the power handling capabilities of IGBTs are much higher than MOSFETs. In consequence, MOSFETs are usually used for low power applications with an operating frequency of up to tens of MHz, while IGBTs are normally selected for high power applications with an operating frequency of up to tens of kHz.

As shown in section 2-2.4, the power transfer capability of an electromagnetic structure increases linearly with frequency. Practically, the core and copper losses also increase with frequency due to hysteresis as well as skin and proximity effects. As a result, the power does not increase linearly with frequency. Increasing core and copper losses result in increasing temperatures, which may exceed the thermal limits of the materials used. The maximum operating frequency of an ICPT system is therefore also limited by the thermal capability of the electromagnetic components, which can be improved by using better materials or additional heat dissipation devices.

The choice of ω_0 thus involves a trade-off between the complexity of the power supply and the power transfer capability of the electromagnetic structure. The power transfer capability of an

InductEV, Inc.
Exhibit 1010
Page 198

electromagnetic structure increases with frequency. However, the complexity of the power supply also increases with increasing frequency. An iterative process is necessary to determine the most cost effective operating frequency.

In compensated systems, it is assumed that the primary and secondary compensation capacitances are calculated by (4-3). The primary compensation minimizes the power supply VA rating, while the secondary compensation boosts the power transfer capability to the pickup. In applications where frequency is adjusted to regulate power flow, operation above or below ω_0 (the secondary resonant frequency) may be preferred in order to improve the controllability [1] because in such applications the relationship between frequency and power has been found to be approximately linear over the operating frequency range. For most applications, however, operation at or near ω_0 is a logical choice because maximum power transfer capability can be achieved at this point.

The primary and secondary compensation capacitors need to work with significant amount of apparent power. A major consideration when choosing these capacitors is their high frequency power handling capability as well as temperature and lifetime stability. The capacitance stability is particularly necessary in high Q systems where the resonant circuit and power transfer capability are highly sensitive to small variations. Such design considerations are discussed later in chapter 7, whereas here it is assumed that accurate tuning can be achieved for normal Q_s from 1 to 10.

In this design procedure, the secondary load is assumed to be linear which simplifies the determination of the power transfer capability and the secondary VA rating. Practical design options for the pickup regulator are discussed in section 4-3.

On the primary side, it is assumed that the primary current is controlled constant at the rated value to fully utilize the electromagnetic structure. The electromagnetic structure of an ICPT system is again dependent on the practical applications for which the ICPT system is being designed as discussed in section 2-2. The design considerations are thus very different to a traditional high frequency transformer. Those aspects that are similar include the material of the electromagnetic structure and its ratings, which are dominated by the core and copper losses. The voltage rating is normally determined by core losses, while the current rating is usually determined by copper losses. Where they differ is that both the primary and secondary windings of a conventional transformer surround a common magnetic core. To utilize the magnetic core fully, the primary is usually operated at rated voltage corresponding to rated flux density while the current is allowed to change with the load. However, the primary and secondary magnetic cores in an ICPT system are separate allowing the pickup to move relative to the primary. As such a major portion of the magnetomotive force will be situated across a substantial air gap. Consequently, it is advantageous to fully utilize the primary by operating at rated current, while allowing the voltage to change with the load.

InductEV, Inc.
Exhibit 1010
Page 199

Finally the power supply configuration is assumed to have been chosen with a specified VA rating. Design options for the power supply are discussed in section 4-4.

The design process starts with a choice of the electromagnetic structure, which is application-oriented. The structure for an ordinary transformer is limited to available magnetic cores, but the possibilities for ICPT systems are virtually unlimited. Systems of all shapes and sizes have been built, and a good first choice relies strongly on experience. As noted in section 2-2.2, typical configurations of the primary coil (Fig. 2-1) are: (a) an extended primary coil with the cable and its return configured in parallel; (b) an extended primary coil with the cable and its return configured in parallel and partially twisted; (c) an extended primary coil with the cable and its return configured as a loop; (d) a lumped primary coil. Typical configurations of the secondary core (Fig. 2-2) are: (a) an E-core; (b) a T-core; (c) a Flat-core. A major design consideration of the electromagnetic structure is to maximize the magnetic design factor k^2L_p ($=M^2/L_s$) for power transfer capability. This is normally done using magnetic design methods often by modelling the system taking into account practical constraints as well as the cost and weight. Simulation techniques such as finite element analysis can be used.

Under normal operating conditions, the coupling parameters (L_p, L_s and M) can be assumed to be constant for ordinary transformers due to fixed relative position between the primary and secondary. In ICPT systems, however, the relative position between the primary and secondary can vary resulting in variations in the coupling parameters. The power transfer capability in an ICPT system is a strong function of these coupling parameters. In practice, the misalignment in the electromagnetic structure is constrained mechanically or controlled electrically to a reasonable range such that system operations in the worst case are acceptable. Influences of this misalignment can be determined using the load model developed in chapter 3 and are investigated later in chapter 7. Here, it is assumed that the electromagnetic structure is properly aligned.

The next step is to choose a primary current. Since the cost of the primary is a strong function of this current, the first choice should be to choose a low current. If the system cannot transfer the required power, the current can be progressively increased. With the given electromagnetic structure and primary current, the voltage across the primary winding can be calculated and the primary VA rating is determined.

With a selected primary current, the measured or predicted (by simulation) values of open circuit voltage (V_{oc}) and short circuit current (I_{sc}) can be used to determine the power transfer capability of the electromagnetic structure. The maximum power transfer capability without secondary compensation is equal to half the value of the product of the open circuit voltage and short circuit current ($V_{oc}*I_{sc}/2$) as noted in section 2-2.

If the power to be transferred is less than $V_{oc}*I_{sc}/2$, the selected electromagnetic structure and

InductEV, Inc.
Exhibit 1010
Page 200

primary current is able to deliver the required power so that the secondary can be left uncompensated. However, it is necessary to ensure the primary current is not much larger than necessary and the electromagnetic structure is not oversized. In this case, the primary current and the electromagnetic structure needs to be reduced to make the required power transfer only slightly lower than $V_{oc}*I_{sc}/2$.

The design process then considers the primary compensation. If the primary VA rating does not exceed the VA rating of the selected power supply, the primary can be left uncompensated. This resulting system configuration is noted as design '1' in Fig. 4-2 and Table 4-1, with both the primary and secondary uncompensated. When the VA rating of the power supply is exceeded, either series or parallel compensation can be used to reduce the necessary power supply VA rating, resulting in a system configuration noted as design '2' with a compensated primary and an uncompensated secondary.

The series compensated primary provides voltage amplification between the power supply and the primary coil, and is suitable for long track applications. A parallel-compensated primary provides current amplification between the power supply and the primary coil, and is attractive for applications where a large primary current is required. The choice is also related to the configuration of the selected high frequency switching power supply as discussed in section 4-4.

If the power to be transferred to the pickup exceeds $V_{oc}*I_{sc}/2$ (assuming the electromagnetic structure is sufficiently well designed), then the secondary needs to be compensated by a capacitor connected either in series or parallel. Here a series compensated secondary has a voltage source characteristic. A parallel-compensated secondary has a current source characteristic. The choice is related to the configurations of the pickup regulator as well as the requirements of the applications as discussed in section 4-3.

Once compensated, the power transfer capability of the secondary is increased by the factor $2Q_{s0}$. As such, the magnitude of Q_{s0} required to provide the necessary power (P) is determined by the ratio: $P/(V_{oc}*I_{sc})$. However, secondary compensation also increases the required secondary VA rating of the pickup by the factor $\sqrt{1+Q_{s0}^2}$. If the actual VA rating of the secondary, given by the selected material and components, is more than this value, the system will be able to transfer the power. If not, the chosen configuration will need to be modified to increase the power transfer capability in one of the following three ways.

(a) Increasing the secondary VA rating by adding more copper or magnetic material.

(b) Increasing the primary current.

(c) Improving the coupling of the electromagnetic structure.

The first option increases the cost of the secondary, the second option increases the cost of the primary, and the third option increases the cost of the coupling structure. To optimise the system

InductEV, Inc.
Exhibit 1010
Page 201

design, a few iterations might be necessary to achieve the highest benefit to cost distribution.

It is also necessary to consider whether primary compensation is required by comparing the primary VA rating with the VA rating of the selected power supply using a similar approach discussed above. If primary compensation is not necessary, the design is complete, resulting in a system configuration noted as design '3' having an uncompensated primary and a compensated secondary.

If primary compensation is required, the resulting design is more complex with the primary and secondary either series or parallel compensated. In this case, the choice of either a fixed-frequency controller or variable-frequency controller needs to be considered. When a fixed-frequency controller is used, the design is complete resulting in a system configuration noted as design '4'. In this case, the operating frequency can be fixed at ω_0, but the power supply may operate with a displacement power factor less than unity. Consequently, the required VA rating of the power supply becomes higher. This can be evaluated in terms of k and Q_s using the normalized load model as shown later in this chapter.

If a variable-frequency controller is used, the frequency can be controlled to ensure the displacement power factor of the power supply is close to unity. In this case, the necessary VA rating of the power supply is minimized, but the pickup does not operate at the maximum power point due to frequency detuning. Such influences on power transfer capability once again can be evaluated in terms of k and Q_s using the normalized load model as shown later in this chapter.

When operation with variable-frequency control, it is also necessary to ensure that the system is stable and controllable under all reasonable loading conditions. This depends on the relationship between the primary and secondary quality factors (Q_p and Q_s). Stable and controllable operation can be assured if Q_p is much larger than Q_s ($Q_p >> Q_s$, where the primary reactive energy is much larger than the secondary reactive energy) as has been noted in section 2-5.5. The resulting system configuration is noted as design '5'.

With the given electromagnetic structure and secondary quality factor, the primary quality factor can be calculated using (4-5). Typical values of Q_s in practical circuits range from about 2 to 10, while typical values of Q_p lie between 2 and 30. Using (4-5), the stability requirement $Q_p >> Q_s$ can be expressed alternatively as $Q_s << 1/k$. To ensure $Q_p > Q_s$ in a loosely coupled system with a k of 0.1, the maximum Q_s is about 10. In a well-coupled system with a k of 0.5, this maximum Q_s drops to about 2.

If Q_p is close to Q_s, it is necessary to identify the bifurcation boundary. This can be done using the normalized load model developed in chapter 3, and will be explained later in this chapter. If the system design falls within the bifurcation boundary, stable and controllable operation is available. The design is thus complete, resulting in a system configuration noted as design '6'. If the system design is outside the bifurcation boundary, the design has to be modified to increase the power transfer capability by the following two ways.

InductEV, Inc.
Exhibit 1010
Page 202

(a) Increasing the primary current.

(b) Improving the coupling of the electromagnetic structure.

Table 4-2 summarizes system configurations resulting from the design procedure. The sensitivity of the system behaviour is compared in each case. Such sensitivities may result in a poor power supply displacement power factor when using a fixed-frequency controller operating at the secondary resonant frequency, or significant pickup frequency detuning when using a variable-frequency controller operating with unity displacement power factor. In each case, the system may be unable to deliver the required power. For system configurations '1', '2' and '3' within Table 4-2, the power supply is less sensitive to system variations as part of the system is left uncompensated. The remaining system configurations have both the primary and secondary either series or parallel compensated and therefore are more sensitive to system variations. The sensitivity in this case depends on k and Q_s and will be investigated later in this chapter.

TABLE 4-2
SUMMARY OF SYSTEM CONFIGURATIONS OF THE DESIGN PROCEDURE

System configurations*	Secondary compensation	Primary compensation	Fixed/variable-frequency controller	System sensitivity
1.	None	None	Fixed/variable	Small
2.	None	Series/parallel	Fixed/variable	Small
3.	Series/parallel	None	Fixed/variable	Small
4.	Series/parallel	Series/parallel	Fixed	Medium/High
5.	Series/parallel	Series/parallel	Variable	Medium
6.	Series/parallel	Series/parallel	Variable	High

*: these numbers represent system configurations as shown in Fig. 4-2.

4-3 DESIGN OPTIONS FOR THE PICKUP REGULATOR

A pickup may be used to supply power directly to a linear resistive load, however when it is used to supply power to a dc load such as a dc motor or a battery charger, a rectifier and a filter are necessary. If the load requires a low frequency ac supply such as an ac motor, frequency conversion is required. Although an ac-ac converter may be used, it is often necessary to use a two-stage process with an intermediate dc-bus to ensure stable output voltage and current.

Power flow regulation is often necessary to accommodate system variations such as misalignment of the electromagnetic structure and variations in the load. For single pickup applications, this could be controlled at either the primary or the secondary. With multiple pickup systems, the required power of

InductEV, Inc.
Exhibit 1010
Page 203

each pickup is often different. Since primary regulation affects all secondary pickups, it is not a good choice for multiple pickup applications. For these systems, power flow regulation needs to be implemented on the secondary pickup.

A block diagram of a pickup regulator that utilizes switching controllers to regulate power flow to a dc load is shown in Fig. 4-3. The switching control can be configured on either the ac or dc side (before or after the rectifier). Various configurations are possible [13-19]. The topology of the switching controller depends on the secondary compensation. Parallel compensation has current source characteristics requiring a controller that can work with a current source input. Series compensation requires a controller operating off a voltage source input.

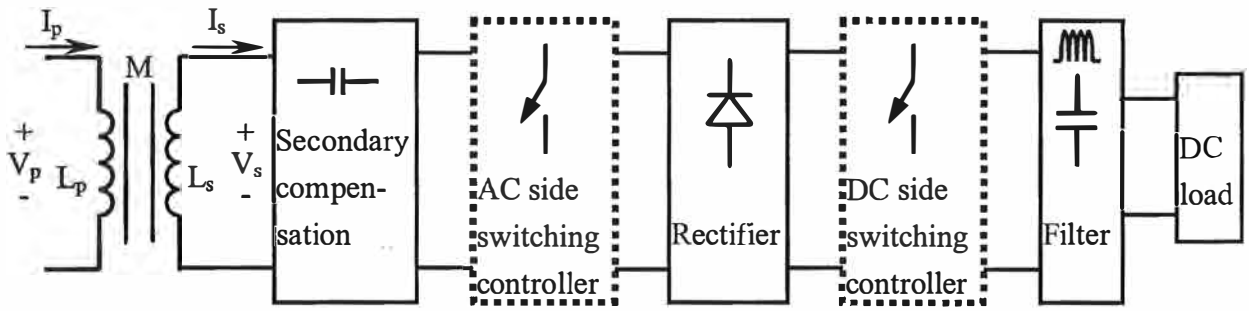


Fig. 4-3. A block diagram of a pickup regulator.

The real and reactive power transferred to the pickup can be calculated using the induced voltage ($j\omega MI_p$) and the secondary current (I_s) as:

$$\text{Real power} = P = \omega M I_p I_s \sin\phi \tag{4-6}$$

and

$$\text{Reactive power} = \omega M I_p I_s \cos\phi \tag{4-7}$$

where ϕ is the phase angle between the primary and secondary currents.

According to (4-6), the parameters that are controllable by the pickup regulator are the magnitude of the secondary current (I_s) and the phase relationship (ϕ) between the primary and secondary currents. In practice, this may be achieved indirectly via controlling other parameters such as V_s. Consequently, there are two fundamental strategies for the pickup regulator to control power. One strategy is to control the magnitude of I_s and the other strategy is to control ϕ. These two strategies can also be combined.

When controlling ϕ, it is desirable that the magnitude of I_s is kept at the maximum value to ensure maximum power transfer. The phase angle ϕ is controlled close to 90° for rated load, and reduced for light load operations. With this strategy, the reactive power flow is negligible at rated load condition,

InductEV, Inc.
Exhibit 1010
Page 204

but increases as ϕ is reduced with decreasing load. Because of this reactive power flow, the power loss in the secondary winding and the influence of the pickup on the primary are larger in comparison to the strategy of controlling the magnitude of I_s as discussed below. An example of this strategy can be found in [13].

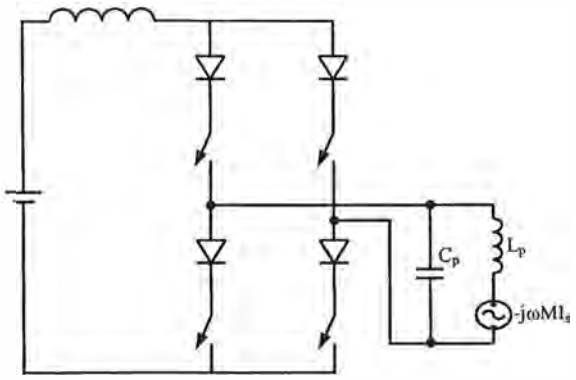
When controlling the magnitude of I_s, it is desirable that ϕ is kept close to the maximum value of 90° as this assures maximum power transfer with negligible reactive power flow as can be seen in (4-6) and (4-7). The secondary current is controlled at the maximum value for rated load, and reduced for light load operations. In consequence, the power loss in the secondary winding is minimized as I_s drops with decreasing load. This strategy has been applied to many industrial applications [15-19].

The actual switching frequency that can be used in a pickup regulator is restricted [18]. A low frequency (slow switching) option allows better transient response but a high frequency (fast switching) option gives lower output ripple. With slow switching, the switch is either closed or open for a relatively long period of time so that the switching transient actually dies out completely before the switch changes state again. In this case, the regulator essentially switches between two states, one at full power and the other at zero power. When the switching speed is much lower than the operating frequency of an ICPT system, the transition times are negligible. The average power output is the maximum possible power output moderated by the duty cycle of the switch. With fast switching, the averaging process happens so quickly that the power flow is quasi stable and the resonant voltage and current of the pickup are stable at the same average value as for slow switching under steady state conditions. Both slow and fast switching systems are therefore mathematically identical in terms of output power and average Q_s versus switch duty cycle. In this thesis, an equivalent resistance represents this average load.

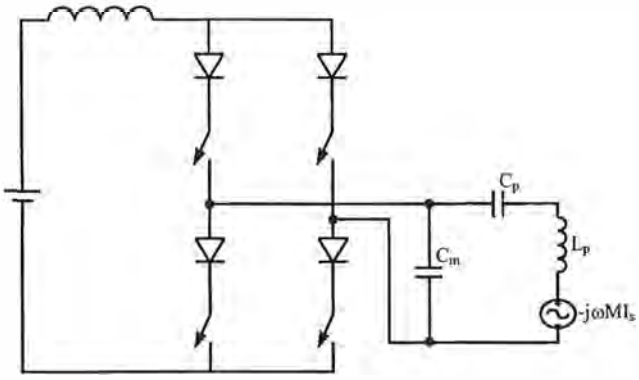
4-4 DESIGN OPTIONS FOR THE POWER SUPPLY

The configuration of the power supply is normally classified according to the input source as well as the inverter and resonant tank topologies. The input can be either voltage or current-sourced. The topology of the inverter can be single-switch, half-bridge, or full-bridge. The fundamental resonant tank topologies use either series or parallel-resonance. One or more reactive elements may be added to the resonant tank. The common configurations for ICPT applications are summarized in Fig. 4-4 and Fig. 4-5 respectively when using either a current or voltage source. In these figures, a reflected voltage ($-j\omega MI_s$) in series with the primary inductance is used to represent the loading effects of all the secondary pickups on the primary track/coil. The strength and weakness of these configurations are compared in Table 4-3.

InductEV, Inc.
Exhibit 1010
Page 205

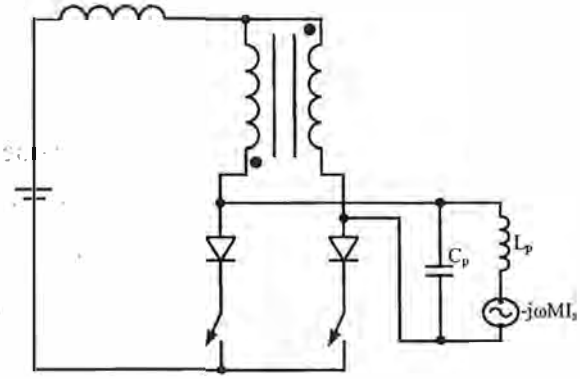


Current-sourced, full-bridge, parallel-resonant

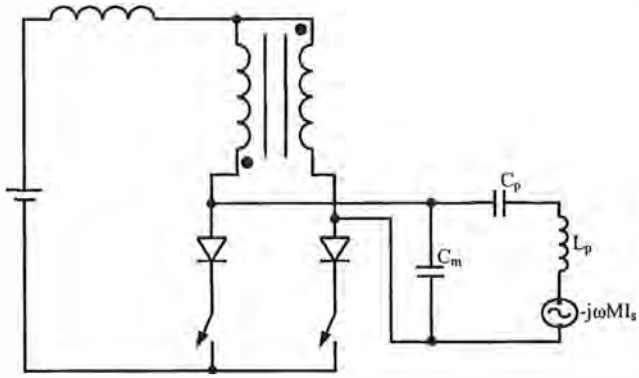


Current-sourced, full-bridge, CCL-resonant

(a) Full-bridge.

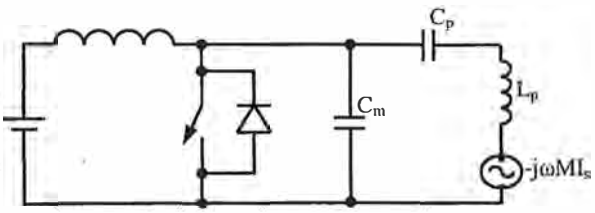


Current-sourced, half-bridge, parallel-resonant

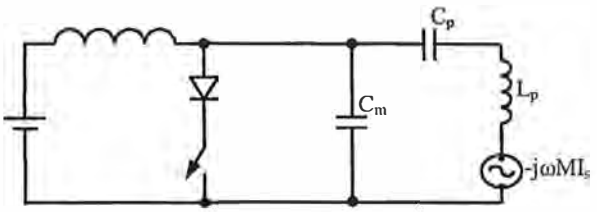


Current-sourced, half-bridge, CCL-resonant

(b) Half-bridge.



Current-sourced, single-reverse-conducting-switch, CCL-resonant



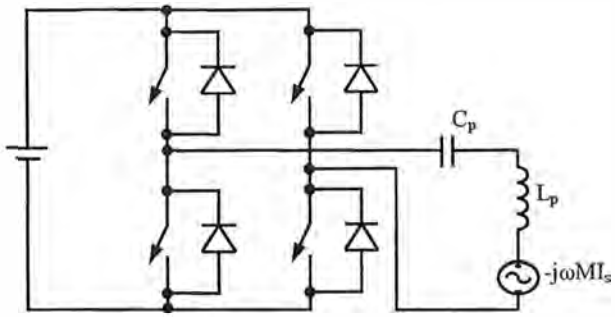
Current-sourced, single-reverse-blocking-switch, CCL-resonant

(c) Single-switch.

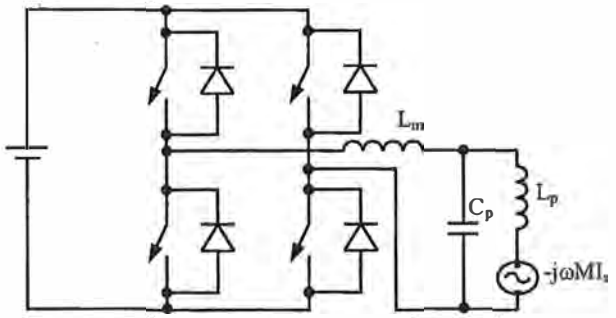
Fig. 4-4. Examples of current-sourced power supply configurations.

For both the voltage-sourced and current-sourced configurations, the power capability as well as the cost and size are mainly determined by the inverter topologies. The full-bridge inverter has the largest power capability with the highest cost and size, while the single-switch inverter has the least power capability with the lowest cost and size. The primary current (track current) and the track length are dependent on the resonant tank topologies. Parallel resonance enables a large primary current, while series resonance allows a long track length. In practice, many series capacitors may be distributed along the track.

InductEV, Inc.
Exhibit 1010
Page 206

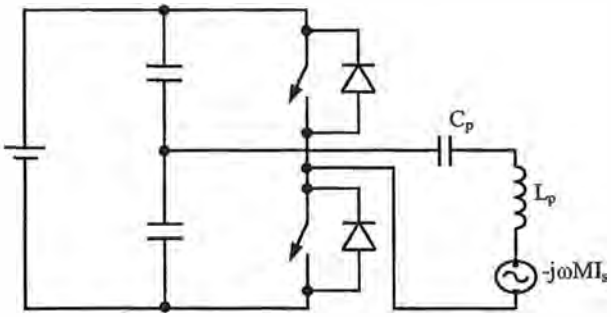


Voltage-sourced, full-bridge, series-resonant

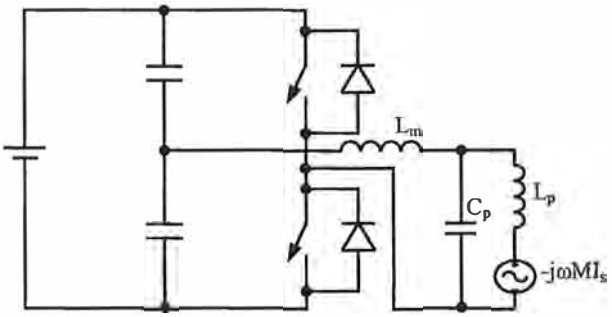


Voltage-sourced, full-bridge, LCL-resonant

(a) Full-bridge.

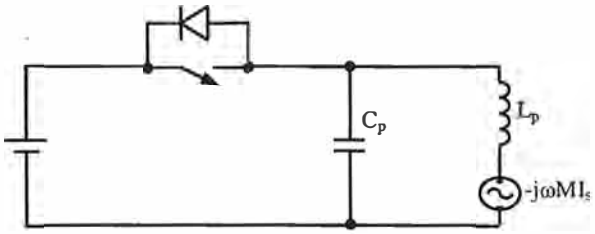


Voltage-sourced, half-bridge, series-resonant

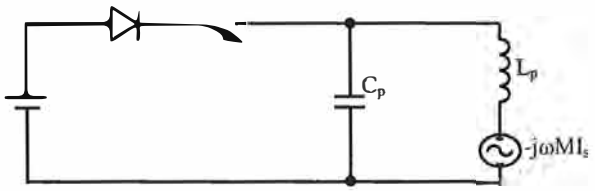


Voltage-sourced, half-bridge, LCL-resonant

(b) Half-bridge.



Voltage-sourced,
single-reverse-conducting-switch,
parallel-resonant



Voltage-sourced, single-reverse-blocking-switch,
parallel-resonant

(c) Single-switch.

Fig. 4-5. Examples of voltage-sourced power supply configurations.

As noted in section 2-5, both fixed and variable-frequency controllers can be used to control the power supply in ICPT systems. The advantages and disadvantages are compared in Table 4-4. Fixed-frequency controllers normally operate at the tuned frequency of the pickup for maximum power transfer. Since the operating frequency is fixed, there are no bifurcation problems in the frequency domain. However, it is unavoidable that the power supply will operate with a displacement power factor less than unity. Consequently, the power supply needs to be oversized and the efficiency is reduced.

Variable-frequency controllers usually operate with unity displacement power factor to minimize the VA rating of the power supply and to improve the efficiency. However, the power transfer

InductEV, Inc.
Exhibit 1010
Page 207

capability of the system is reduced due to frequency detuning effects in the pickup. Moreover, operation may become unstable or uncontrollable if frequency bifurcation occurs.

TABLE 4-3
COMPARISON OF POWER SUPPLY CONFIGURATIONS

Power supply configurations			Power capability	Track length	Primary current	System sensitivity	Cost	Size
Voltage-sourced	Full-bridge	Series-resonant	H	H	L	M	H	H
		LCL-resonant	H	L	H	H	H	H
	Half-bridge	Series- resonant	M	H	L	M	M	M
		LCL- resonant	M	L	H	H	M	M
	Single-switch	Reverse-conducting, parallel-resonant	L	L	L	M	L	L
		Reverse-blocking, parallel-resonant	L	L	L	M	L	L
Current-sourced	Full-bridge	Parallel-resonant	H	L	H	M	H	H
		CCL-resonant	H	H	H	H	H	H
	Half-bridge	Parallel-resonant	M	L	H	M	M	M
		CCL-resonant	M	H	H	H	M	M
	Single-switch	Reverse-conducting, CCL-resonant	L	L	L	H	L	L
		Reverse-blocking, CCL-resonant	L	L	L	H	L	L

H=High, M=Medium, L=Low

TABLE 4-4
COMPARISON OF FIXED AND VARIABLE FREQUENCY CONTROLLER

Controller	Advantages	Disadvantages
Fixed-frequency controller	1. Operation at the tuned frequency of the pickup for maximum power transfer. 2. No bifurcation problems.	1. Reduced displacement power factor. 2. Oversized power supply. 3. Reduced efficiency.
Variable-frequency controller	1. Operation with unity displacement power factor. 2. Minimized VA rating of the power supply. 3. Improved efficiency.	1. Pickup frequency detuning. 2. Reduced power transfer. 3. Unstable or uncontrollable operation due to bifurcation.

InductEV, Inc.
Exhibit 1010
Page 208

4-5 DESIGN EVALUATIONS

In this section the normalized load model developed in chapter 3 is used to evaluate system designs resulting from the design procedure described in section 4-2. The sensitivity of the displacement power factor to the fundamental design parameters u, k and Q_s are evaluated generally for all possible configurations where the primary and secondary can be either series, parallel or uncompensated. Here u varies across the operating frequency spectrum, while Q_s changes over the operating load range.

The thesis then focuses on systems with compensated primary and secondary because this is the usual case for high power applications. The system behaviour under fixed and variable frequency control is investigated. Such analysis is essential when the fundamental design parameters are determined. As noted in chapter 3, the loading effects of the secondary pickup on the primary may have significant influences on the behaviour of the load resonant tank (seen by the power supply) when the secondary quality factor or the magnetic coupling coefficient is increased. When designing ICPT systems, it is necessary to identify such influences on the displacement power factor of the power supply, the power transfer capability to the pickup, and the stability and controllability of the controller.

4-5.1 SENSITIVITY OF THE DISPLACEMENT POWER FACTOR

As the cost of the power supply depends on its VA rating, it is desirable that the power supply operates with unity displacement power factor to minimize this. The phase angle between the fundamental components of the output voltage and current of the power supply can be calculated using the normalized load impedance as:

$$\tan\theta_1 = \frac{\mathrm{Im}\,Z_{in}}{\mathrm{Re}\,Z_{in}} = \frac{-\mathrm{Im}\,Y_{in}}{\mathrm{Re}\,Y_{in}} \tag{4-8}$$

The displacement power factor (DPF) of the power supply can then be determined from this phase angle as:

$$\text{Displacement Power Factor (DPF)} = \cos\theta_1 \tag{4-9}$$

The normalized load impedance (defined in section 3-10.2) depends on the primary compensation topology and is summarized in Table 4-5.

When the secondary is left uncompensated, maximum power transfer to the pickup is achieved when '$\omega_0 L_s$' and R are equal (as shown in section 2-2.4.2). In this case, the normalized load impedance given in Table 4-5 is a function of u and k as derived in Appendix G. A summary of the normalized function for each term within this normalized load impedance is given in Table 4-6.

InductEV, Inc.
Exhibit 1010
Page 209

TABLE 4-5
NORMALIZED LOAD IMPEDANCES

Uncompensated primary: $Z_{tn} = \frac{Z_t}{\mathrm{Re}\,Z_{r0}} = \mathrm{Re}\,Z_{tn} + j\,\mathrm{Im}\,Z_{tn}$	$\mathrm{Re}\,Z_{tn} = \mathrm{Re}\,Z_{rn}$
	$\mathrm{Im}\,Z_{tn} = \frac{\omega L_p}{\mathrm{Re}\,Z_{r0}} + \mathrm{Im}\,Z_{rn}$
Series primary: $Z_{tn} = \frac{Z_t}{\mathrm{Re}\,Z_{r0}} = \mathrm{Re}\,Z_{tn} + j\,\mathrm{Im}\,Z_{tn}$	$\mathrm{Re}\,Z_{tn} = \mathrm{Re}\,Z_{rn}$
	$\mathrm{Im}\,Z_{tn} = -\frac{1}{\omega C_p(\mathrm{Re}\,Z_{r0})} + \frac{\omega L_p}{\mathrm{Re}\,Z_{r0}} + \mathrm{Im}\,Z_{rn}$
Parallel primary: $Z_{tn} = \frac{1}{Y_{tn}} = \frac{1}{\mathrm{Re}\,Y_{tn} + j\,\mathrm{Im}\,Y_{tn}}$	$\mathrm{Re}\,Y_{tn} = \frac{\mathrm{Re}\,Z_{rn}}{(\mathrm{Re}\,Z_{rn})^2 + \left(\frac{\omega L_p}{\mathrm{Re}\,Z_{r0}} + \mathrm{Im}\,Z_{rn}\right)^2}$
	$\mathrm{Im}\,Y_{tn} = \omega C_p(\mathrm{Re}\,Z_{r0}) - \frac{\frac{\omega L_p}{\mathrm{Re}\,Z_{r0}} + \mathrm{Im}\,Z_{rn}}{(\mathrm{Re}\,Z_{rn})^2 + \left(\frac{\omega L_p}{\mathrm{Re}\,Z_{r0}} + \mathrm{Im}\,Z_{rn}\right)^2}$

TABLE 4-6
FUNCTIONS OF THE NORMALIZED LOAD IMPEDANCE WITH UNCOMPENSATED PICKUP

$\frac{1}{\omega C_p(\mathrm{Re}\,Z_{r0})} = \frac{2}{uk^2}$	$\frac{\omega L_p}{\mathrm{Re}\,Z_{r0}} = \frac{2u}{k^2}$
$\mathrm{Re}\,Z_{rn} = \frac{\mathrm{Re}\,Z_r}{\mathrm{Re}\,Z_{r0}} = \frac{2u^2}{1+u^2}$	$\mathrm{Im}\,Z_{rn} = \frac{\mathrm{Im}\,Z_r}{\mathrm{Re}\,Z_{r0}} = \frac{-2u^3}{1+u^2}$

With the secondary compensated, the normalized load impedance has been developed in section 3-10.2 as a function of u, k and Q_{s0}. A summary of the normalized function for each term within the normalized load impedance has been shown in Table 3-3, and is given again in Table 4-7 for convenience.

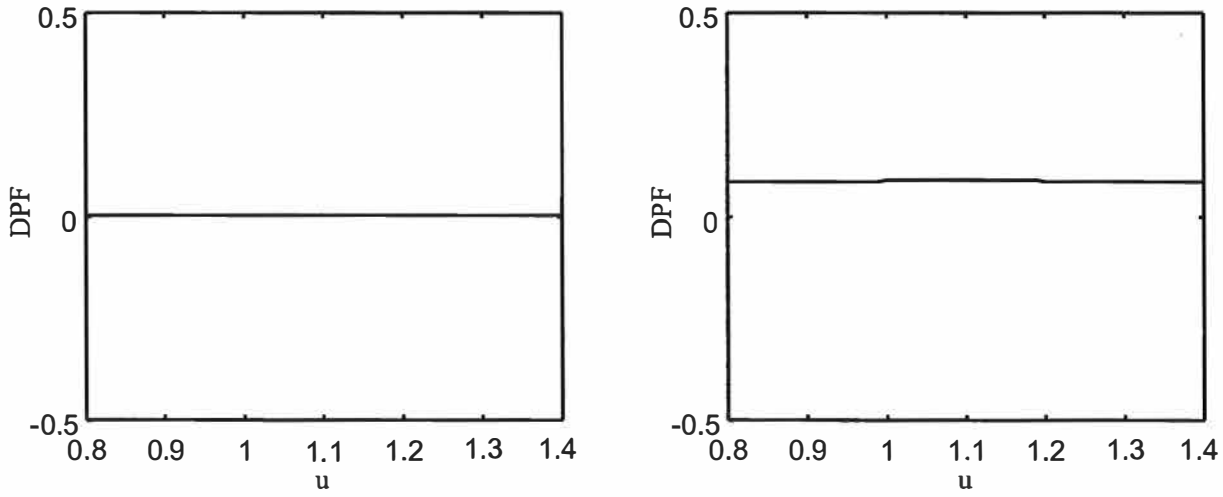
Since the normalized load impedance is again simply a function of u, k and Q_{s0}, the DPF determined from (4-9) is also a function of these parameters. The sensitivity of the DPF to these parameters is discussed below.

InductEV, Inc.
Exhibit 1010
Page 210

TABLE 4-7
FUNCTIONS OF THE NORMALIZED LOAD IMPEDANCE WITH COMPENSATED PICKUP

$\frac{1}{\omega C_p(\mathrm{Re}\,Z_{r0})}=\frac{1}{k^2Q_{s0}u}$	Series/parallel secondary
$\frac{\omega L_p}{\mathrm{Re}Z_{r0}}=\frac{u}{k^2Q_{s0}}$	Series/parallel secondary
$\mathrm{Re}\,Z_{rn}=\frac{\mathrm{Re}\,Z_r}{\mathrm{Re}Z_{r0}}=\begin{cases}\frac{u^4}{(u^2-1)^2Q_{s0}^2+u^2}\\ \frac{u^2}{(u^2-1)^2Q_{s0}^2+u^2}\end{cases}$	Series secondary Parallel secondary
$\mathrm{Im}\,Z_{rn}=\frac{\mathrm{Im}\,Z_r}{\mathrm{Re}Z_{r0}}=\begin{cases}\frac{-u^3(u^2-1)Q_{s0}}{(u^2-1)^2Q_{s0}^2+u^2}\\ \frac{-u^3[(u^2-1)Q_{s0}+1/Q_{s0}]}{(u^2-1)^2Q_{s0}^2+u^2}\end{cases}$	Series secondary Parallel secondary

Systems having both the primary and secondary uncompensated: The DPF of systems with both primary and secondary uncompensated is shown in Fig. 4-6 as a function of u for selected k. As can be seen, the power supply operates with poor DPF. In both loosely and well-coupled systems (low and high k), the DPF is close to zero as the power transfer of an uncompensated pickup is small in comparison to the reactive power of the primary winding.



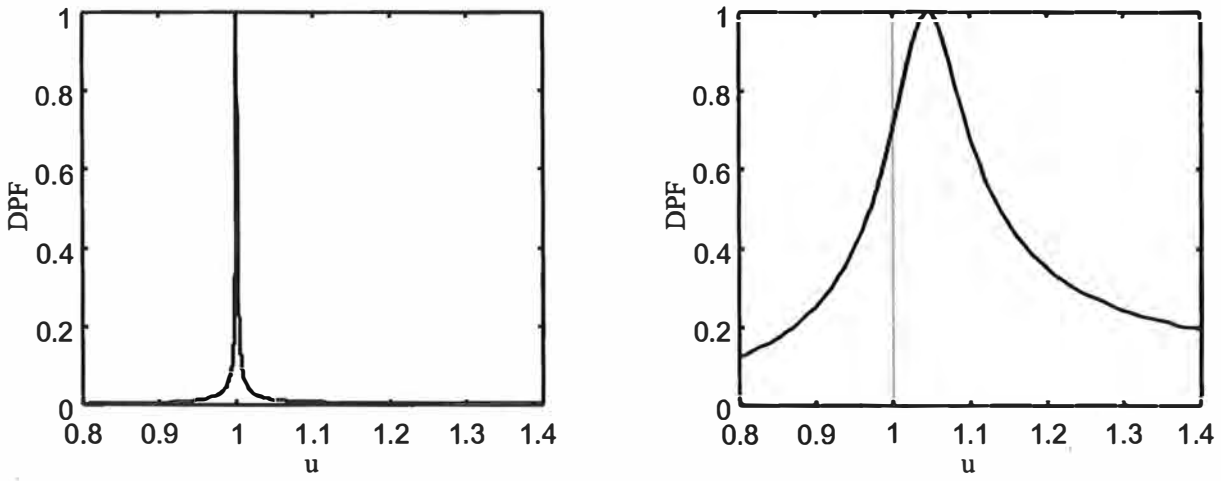
(a) k=0.05. (b) k=0.4.

Fig. 4-6. Sensitivity of DPF to u and k in systems having both the primary and secondary uncompensated.

Systems having a compensated primary and an uncompensated secondary: The poor DPF

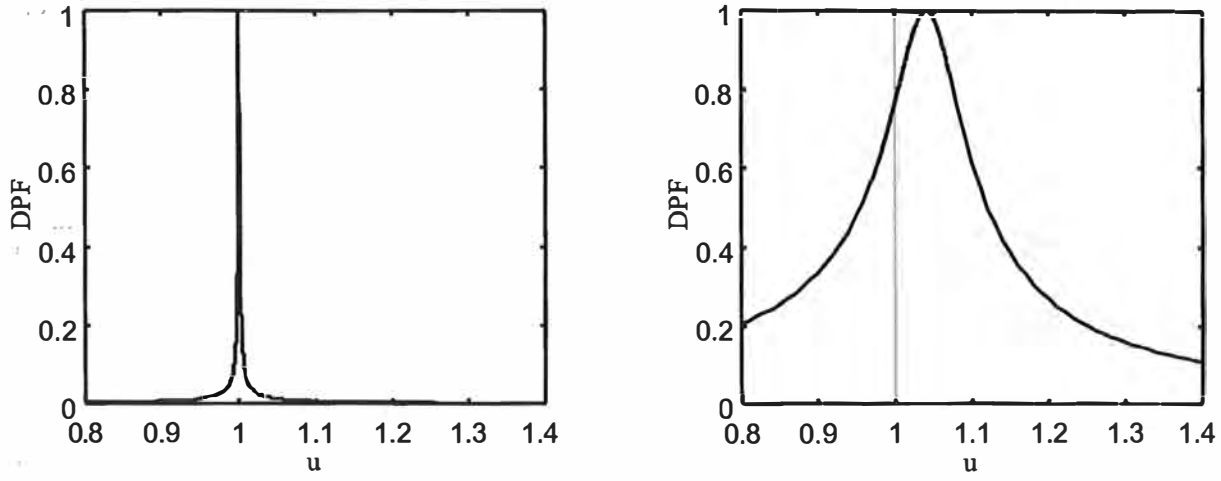
InductEV, Inc.
Exhibit 1010
Page 211

discussed above can be improved using primary compensation (as shown in Fig. 4-7). Both series and parallel-compensated primary topologies show similar effects. In loosely coupled systems, unity DPF can be achieved close to ω_0 (u=1). For well-coupled systems, the DPF at ω_0 is about 0.7 only due to the influence of the secondary pickup loading. In this case, unity DPF is achieved at a single frequency above ω_0 (u>1).



(i) k=0.05. (ii) k=0.4.

(a) Series primary.



(i) k=0.05. (ii) k=0.4.

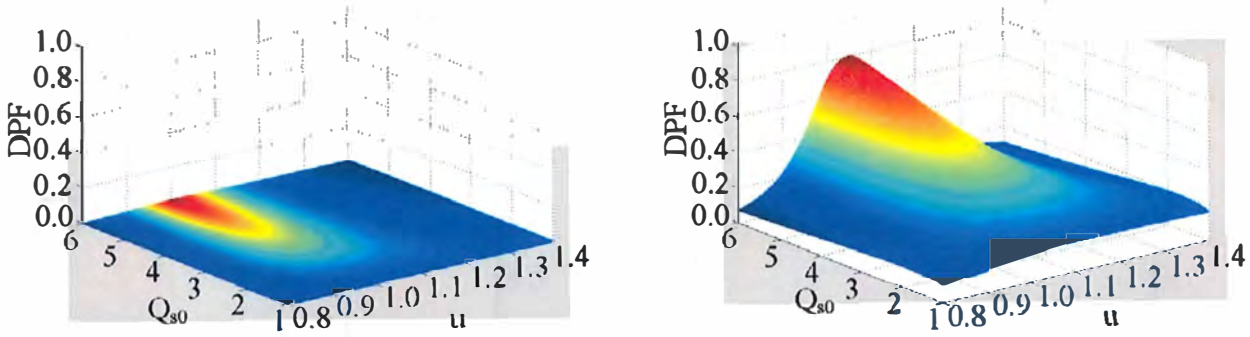
(b) Parallel primary.

Fig. 4-7. Sensitivity of DPF to u and k in systems having a compensated primary and an uncompensated secondary.

Systems having an uncompensated primary and a compensated secondary: The DPF of systems with an uncompensated primary and a compensated secondary are shown in Fig. 4-8 as a function of u and Q_{s0} for selected k. As expected, the power supply operates with a DPF less than unity. Once again, series and parallel secondary topologies exhibit similar features. In loosely coupled systems, the DPF is very close to zero as the power transfer is small. For well-coupled systems with high Q_s, the DPF

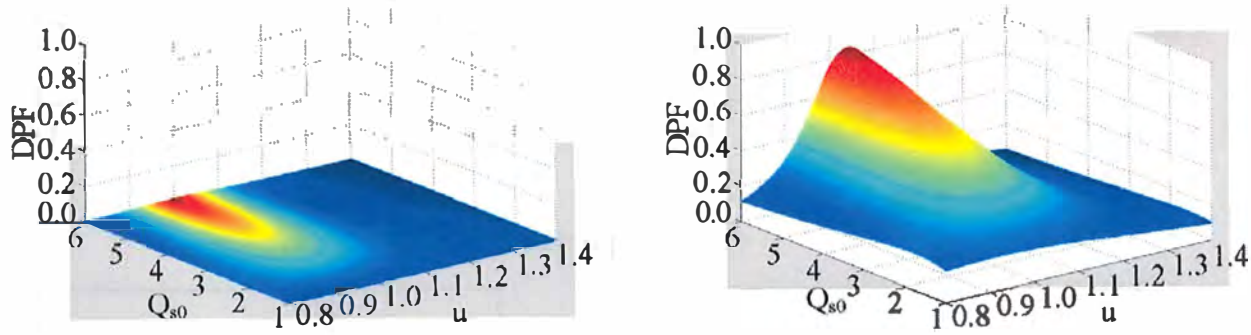
InductEV, Inc.
Exhibit 1010
Page 212

becomes higher because more power is transferred.



(i) k=0.05. (ii) k=0.4.

(a) Series secondary.



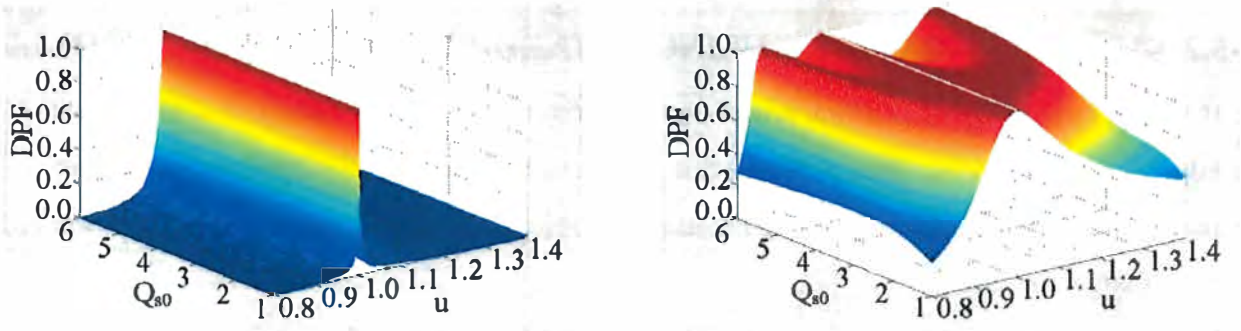
(i) k=0.05. (ii) k=0.4.

(b) Parallel secondary.

Fig. 4-8. Sensitivity of DPF to u, k and Q_{s0} in systems having an uncompensated primary and a compensated secondary.

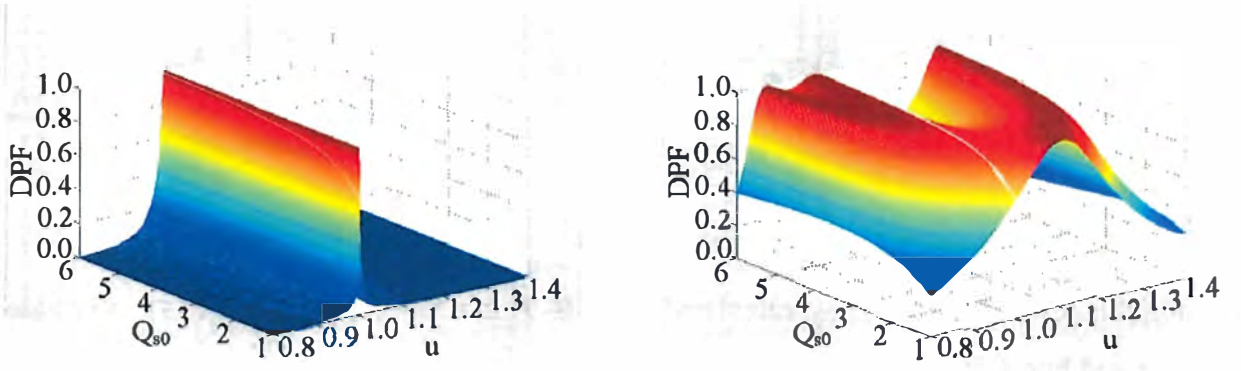
Systems having both the primary and secondary compensated: Poor DPF as shown in earlier systems can be improved with primary compensation. The four basic topologies (SS, SP, PP and PS) are compared in Fig. 4-9. In this figure, the DPF at ω_0 (u=1) is shown on the surfaces as a white line. Theoretically, the SS topology achieves the best results compared with the other topologies. The DPF of the SS topology at ω_0 is unity and independent of Q_s and k, but those of other three topologies are below unity and dependent on both Q_s and k. In addition, unity DPF is achieved only at one operating frequency if Q_s is low. When Q_s is high, unity DPF can be achieved at three operating frequencies. This bifurcation occurs at lower Q_s values as the magnetic coupling improves (high k). Furthermore, the operating frequency with unity DPF is not at ω_0 when either the primary or the secondary is parallel compensated (SP, PP and PS topologies).

InductEV, Inc.
Exhibit 1010
Page 213



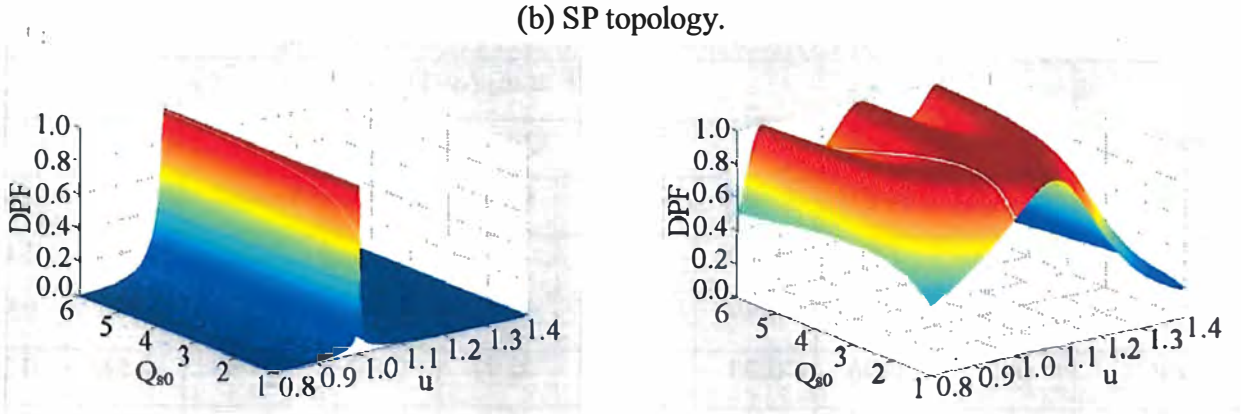
(i) k=0.05. (ii) k=0.4.

(a) SS topology.



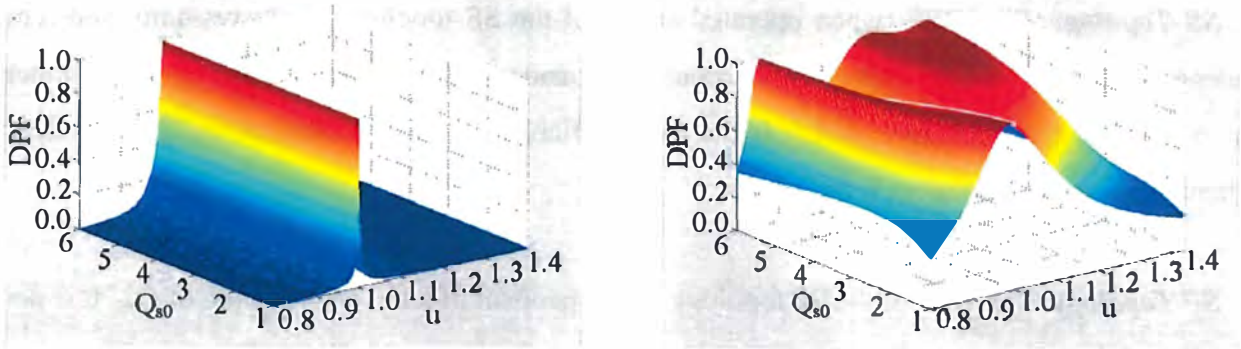
(i) k=0.05. (ii) k=0.4.

(b) SP topology.



(i) k=0.05. (ii) k=0.4.

(c) PP topology.



(i) k=0.05. (ii) k=0.4.

(d) PS topology.

Fig. 4-9. Sensitivity of DPF to u, k and Q_{s0} in systems having both the primary and secondary compensated.

InductEV, Inc.
Exhibit 1010
Page 214

4-5.2 SYSTEM BEHAVIOUR USING A FIXED-FREQUENCY CONTROLLER

If the operating frequency of the power supply is fixed at ω_0, the frequency detuning effects of the pickup are minimized. As shown above, this may result in a poor DPF if either the primary or the secondary is parallel compensated (SP, PP and PS topologies). A poor DPF requires the power supply to have a large VA rating.

For fixed-frequency operation at ω_0 (u=1), equation (4-8) can be calculated as:

$$\tan\theta_1(u=1)=\begin{cases}0 & \text{SS topology}\\ -\dfrac{1}{Q_{s0}} & \text{SP topology}\\ -k^2Q_{s0}+\dfrac{1-k^2}{Q_{s0}} & \text{PP topology}\\ -k^2Q_{s0} & \text{PS topology}\end{cases} \tag{4-10}$$

Using this result, the DPF at ω_0 calculated using (4-9) is a function of k and Q_{s0} as illustrated in Table 4-8 and Fig. 4-10.

TABLE 4-8
DPF OPERATING WITH FIXED FREQUENCY AT ω_0

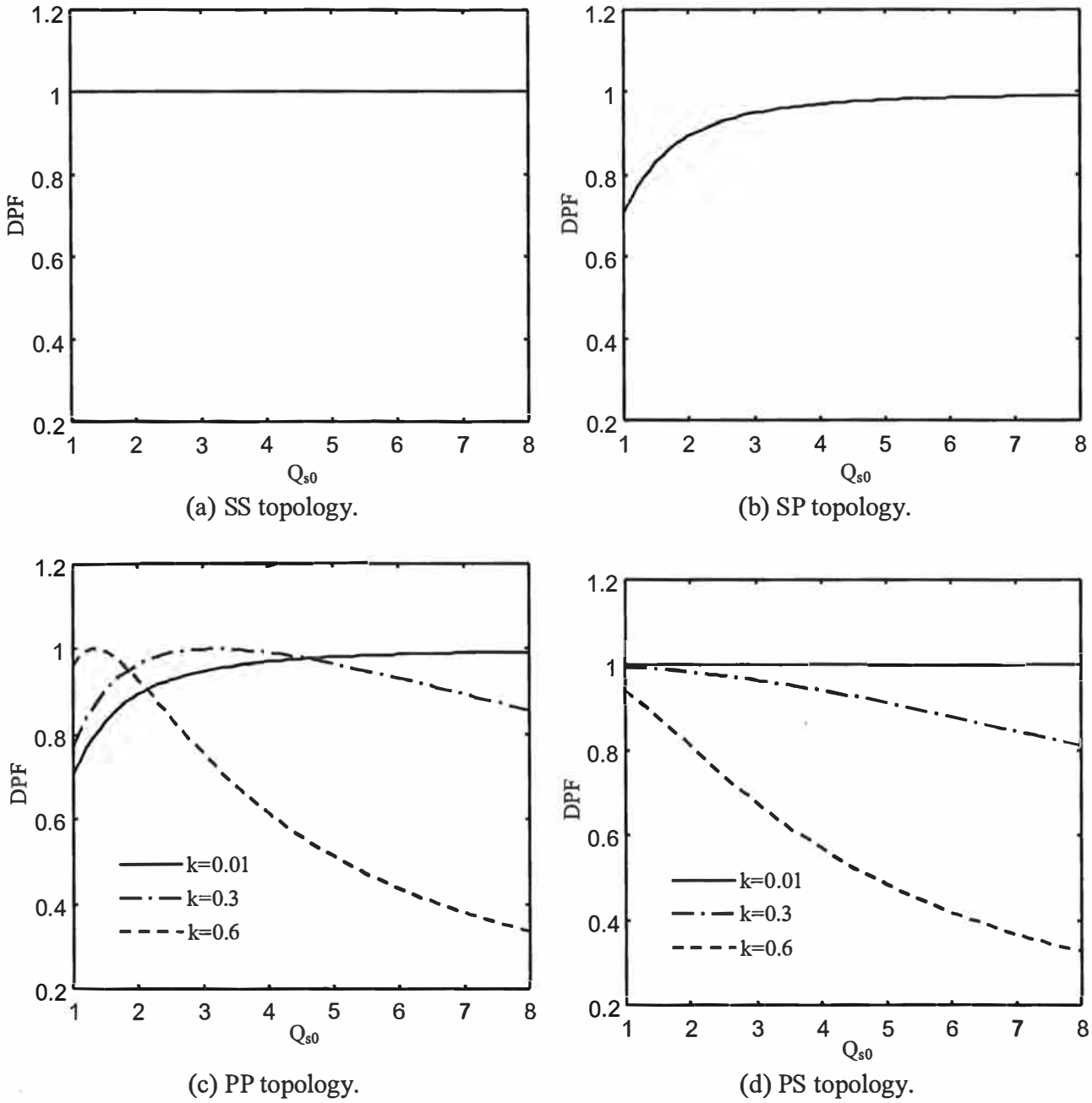
Topology	DPF at ω_0 (u=1)								
	Q_{s0}=2			Q_{s0}=5			Q_{s0}=8		
	k=0.01	k=0.3	k=0.6	k=0.01	k=0.3	k=0.6	k=0.01	k=0.3	k=0.6
SS	1.00	1.00	1.00	1.00	1.00	1.00	1.00	1.00	1.00
SP	0.89	0.89	0.89	0.98	0.98	0.98	0.99	0.99	0.99
PP	0.89	0.96	0.93	0.98	0.97	0.51	0.99	0.86	0.34
PS	1.00	0.98	0.81	1.00	0.91	0.49	1.00	0.81	0.33

SS Topology: The DPF (when operated at ω_0) of the SS topology is always unity and remains independent of k and Q_{s0}. This allows system performance to be maintained during misalignment of the electromagnetic structure, which is the most difficult parameter to control in ICPT applications where mechanical alignment is not used.

SP Topology: The DPF of the SP topology is independent ofk but is a function of Q_{s0}. It is poor at low Q_s, and becomes ever closer to unity as Q_s increases. Similar to the SS topology, the SP topology is independent of k allowing misalignment of the electromagnetic structure. Consequently, the performance of the SP topology is comparable to the SS topology providing Q_s is about 2 or larger that

InductEV, Inc.
Exhibit 1010
Page 215

is almost always true.



(a) SS topology. (b) SP topology.

(c) PP topology. (d) PS topology.

Fig. 4-10. DPF operating with fixed frequency at ω_0.

PP Topology: The DPF of the PP topology depends on both k and Q_s. The effects of Q_s and k are very complex. From (4-10) it can be seen that unity DPF can be achieved when:

$$k = \frac{1}{\sqrt{Q_{s0}^2 + 1}} \qquad \text{PP topology} \qquad (4\text{-}11)$$

This relationship is shown in Fig. 4-11 as a curve. As the magnetic coupling improves, Q_s must decrease to maintain unity DPF. The power transfer capability of an ICPT system can be improved by

InductEV, Inc.
Exhibit 1010
Page 216

enhancing k or increasing Q_s. However, to ensure good DPF in this case, a trade-off between k and Q_s is necessary.

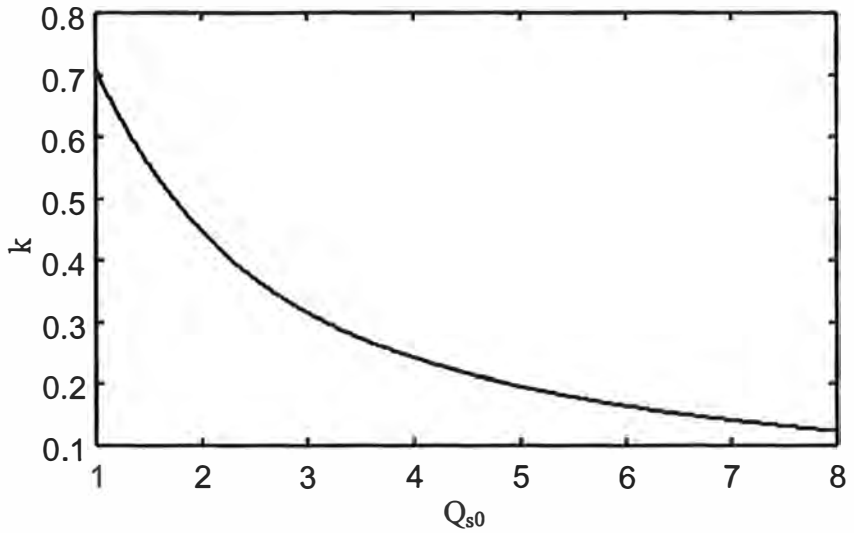


Fig. 4-11. Required relationship between k and Q_{s0} to achieve unity DPF at ω_0 for the PP topology.

Interestingly with low Q_s (around 2), as illustrated in Fig. 4-12, the DPF is close to unity across a wide range of k. At this condition, unity DPF is achieved when k is about 0.45. With higher Q_s, the DPF drops rapidly as k increases. For well-coupled systems where the variation of the magnetic coupling is large, it may be desirable to design the system with low Q_s. The contact-less electric vehicle battery charger discussed later in this thesis is designed with this in mind.

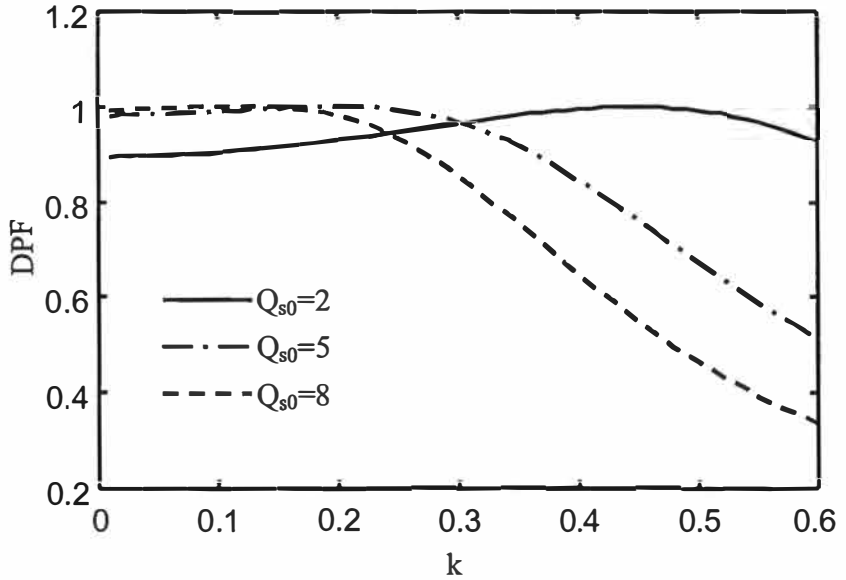


Fig. 4-12. Selection of Q_{s0} to improve DPF when operating at ω_0 over a wider range of k for the PP topology.

InductEV, Inc.
Exhibit 1010
Page 217

PS Topology: The DPF of the PS topology is the most sensitive of the topologies listed here to Q_s and k. The DPF becomes worse with increasing Q_s or improving k. This topology is thus a poor choice for well-coupled systems with high Q_s.

4-5.3 SYSTEM BEHAVIOUR USING A VARIABLE-FREQUENCY CONTROLLER

If the operating frequency of the power supply is controlled to achieve unity DPF, the necessary VA rating can be minimized. However, in such systems the pickup does not operate at the tuned frequency when either the primary or the secondary is parallel compensated (SP, PP and PS topologies) as stated earlier. If the frequency-detuning effect is large, the pickup may not be able to transfer enough power.

Under variable-frequency control, all of the four basic compensation topologies exhibit frequency bifurcation when Q_s is large. As a result, the system may shift between any of the possible operating frequencies. Naturally the controller operates at the frequency extremes (either the lowest or the highest operating point) where pickup frequency detuning can be very large resulting in significant loss of power transfer capability.

For variable-frequency operation with unity DPF, the operating frequency is the zero phase angle frequency of the load impedance and can be calculated by:

$$\mathrm{Im}\, Z_{in}(u,k,Q_{s0}) = 0 \quad \textbf{or} \quad \mathrm{Im}\, Y_{in}(u,k,Q_{s0}) = 0 \tag{4-12}$$

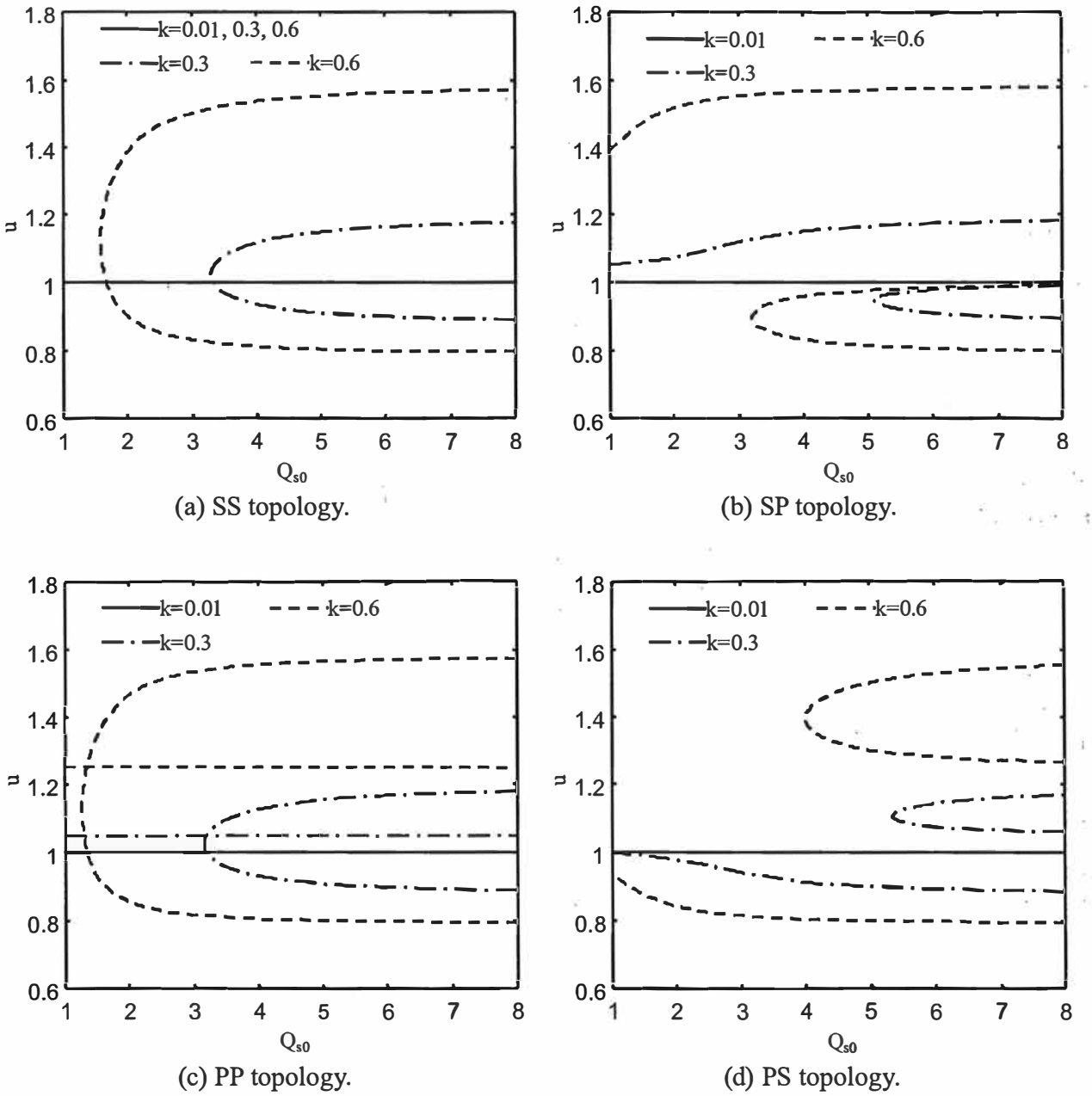
The operating frequency determined by (4-12) is a function of k and Q_{s0}. These topology dependent results are compared in Fig. 4-13. As expected, in all four basic topologies the operating frequency is closely at ω_0 for loosely coupled systems (low k), and bifurcation phenomenon is evident for well-coupled systems (high k) with high Q_s. In all cases, improving k results in the occurrence of bifurcation at lower Q_s.

SS topology: The SS topology once again is the most desirable as it can theoretically operate at ω_0 and as such assures maximum power transfer to the pickup. Moreover, this is achieved independent of k and Q_{s0}. Once bifurcation occurs there exists two additional operating modes above and below ω_0. Their frequency shifts from ω_0 increase with increasing k and Q_s, and may result in substantial frequency detuning of the pickup and as such a major drop in power transfer capability. It is necessary to avoid these two operating modes.

SP topology: All the three operating modes of the SP topology are dependent on k and Q_{s0}. This

InductEV, Inc.
Exhibit 1010
Page 218

topology has the worst light load behaviour (low Q_s in the bifurcation-free region) as the operating frequency can shift well above ω_0. In the region where bifurcation occurs, one of the three operating modes remains close to ω_0. If the system could be controlled to operate at this operating mode, detuning of the pickup would be minimized. Once again, the frequency shifts of the other two operating modes increase with increasing k and Q_s, and should be avoided.



(a) SS topology. (b) SP topology.

(c) PP topology. (d) PS topology.

Fig. 4-13. Operating frequency with unity DPF.

PP topology: In the bifurcation-free area, the operating frequency of the PP topology is independent of Q_{s0}. It can be shown that this frequency is a function of k given by:

InductEV, Inc.
Exhibit 1010
Page 219

$$u = \frac{1}{\sqrt{1-k^2}} \tag{4-13}$$

Consequently, the frequency shift increases with increasing k. This operating mode extends into the bifurcation region. The frequency shifts of the other two operating modes in the bifurcation region are normally larger and should be avoided.

PS topology: All the three operating modes of the PS topology also depend on k and Q_{s0}. The frequency shifts at light load (low Q_s in the bifurcation-free area) is comparable to the PP topology and less than that of the SP topology. Once bifurcation occurs, frequency shifts are significant in all three operating modes. It is desirable to avoid operation in this region.

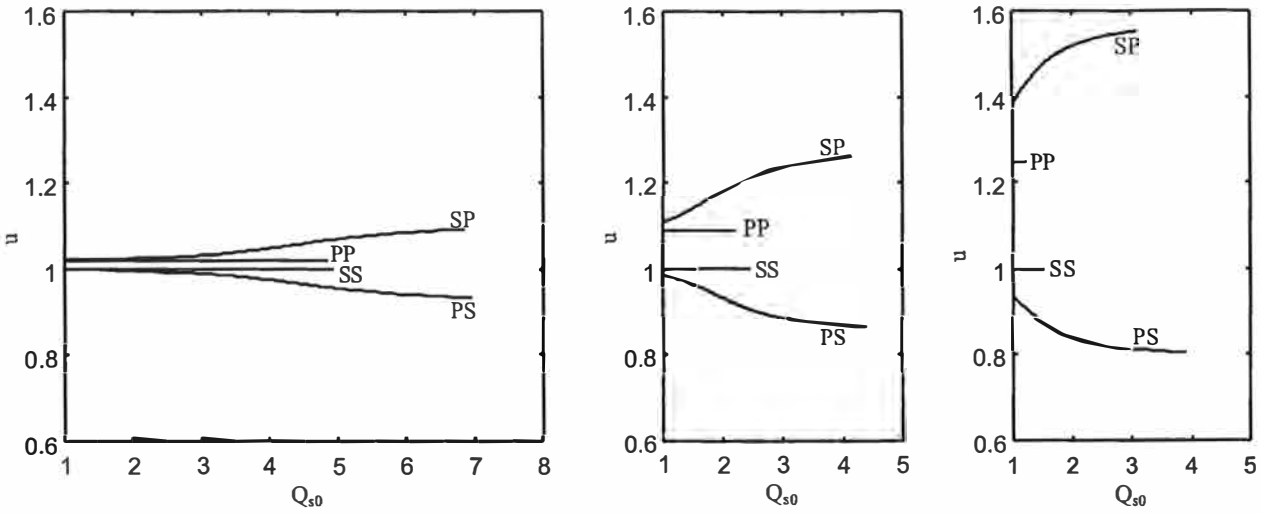
The bifurcation boundaries of the basic topologies are compared in Table 4-9 for selected k of 0.2, 0.4 and 0.6. Bifurcation appears when Q_{s0} is larger than the boundary value given in this table in each case. The corresponding primary quality factor (Q_{p0}) determined by (4-5) is also shown in the table. When the primary and secondary have the same compensation topology (SS and PP topologies), as can be seen in this table, the bifurcation boundary is very close to the simplified bifurcation criterion of $Q_{p0}>Q_{s0}$ (as discussed in section 2-5.5). For the other two topologies (SP and PS topologies), however, this simplified bifurcation criterion is not suitable, and bifurcation only occurs at a much larger Q_{s0}.

TABLE 4-9
BIFURCATION BOUNDARY FOR VARIABLE-FREQUENCY OPERATION WITH UNITY DPF

Topology	k=0.2	k=0.4	k=0.6
SS	Q_{p0}=5.05, Q_{s0}=4.95	Q_{p0}=2.55, Q_{s0}=2.45	Q_{p0}=1.79, Q_{s0}=1.55
SP	Q_{p0}=3.48, Q_{s0}=6.90	Q_{p0}=1.27, Q_{s0}=4.15	Q_{p0}=0.56, Q_{s0}=3.15
PP	Q_{p0}=4.95, Q_{s0}=4.85	Q_{p0}=2.39, Q_{s0}=2.20	Q_{p0}=1.42, Q_{s0}=1.25
PS	Q_{p0}=3.55, Q_{s0}=7.05	Q_{p0}=1.39, Q_{s0}=4.50	Q_{p0}=0.70, Q_{s0}=3.95

For bifurcation-free operation, the frequency shifts relative to ω_0 are compared in Fig. 4-14 for selected k. The SS topology as shown has no frequency shift. The SP topology has the largest frequency shift above ω_0. The PP topology also has a frequency shift above the ω_0, but is less than that of the SP topology. The PS topology has a frequency shift below ω_0. The absolute frequency shift of the PS topology at low Q_s is less than that of the PP topology. To minimize the pickup frequency detuning effects, the SS topology is the best choice, while the SP topology should be avoided, and the PS topology is a better choice than the PP topology.

InductEV, Inc.
Exhibit 1010
Page 220



(a) k=0.2. (b) k=0.4. (c) k=0.6.

Fig. 4-14. Frequency shifts for bifurcation-free operations.

4-5.4 DESIGN CONSIDERATIONS

It is usually assumed that a variable-frequency controlled ICPT system requires bifurcation-free operation, as it is very difficult for a standard variable-frequency controller to distinguish the different operating modes in the bifurcation region due to the fact that the operating frequency of each mode is load dependent. Using the load model developed in chapter 3, the bifurcation boundary can be determined to ensure bifurcation-free operation when a variable-frequency controller operating with unity DPF is used. The bifurcation boundary is a relation between k and Q_{s0}. With a given Q_{s0}, bifurcation occurs as k is improved over this boundary. For a given k, bifurcation occurs when Q_{s0} is increased across this boundary. The bifurcation boundary is topology dependent. With a given k, the maximum Q_{s0} of the SP and PS topologies for bifurcation-free operation is much higher than the SS and PP topologies.

The primary resonance design determined by (4-3) assumes the primary and secondary resonance is independent of each other. However, with improved k and increased Q_s the interactions between the primary and secondary resonant circuits may affect system behaviour significantly. This does not present a problem to the SS topology, but does for the other topologies. A series-compensated secondary reflects no reactance when operating at ω_0 as noted in section 3-7.1, and the primary can be completely tuned with the selected primary capacitance in series connection. However, a parallel-compensated secondary reflects a capacitive reactance when operating at this frequency, and this reflected reactance is not tuned by the selected primary capacitance. Both series and parallel-compensated secondary systems reflect a resistance representing the power transfer. Since this reflected resistance is in series with the primary coil, the selected primary capacitance is unable to tune

InductEV, Inc.
Exhibit 1010
Page 221

the reactance of the primary coil completely in a parallel-compensated primary system. The only exception is the PP topology, where complete tuning can be achieved if k and Q_s are carefully selected as explained in section 4-5.2.

Since the load resonant tank is not properly tuned, system operation will deviate from the design point. With a fixed-frequency controller operating at ω_0, the power supply will operate with a DPF less than unity. Using a variable-frequency controller operating with unity DPF, the operating frequency will shift away from ω_0 and bifurcation may occur. Such deviations are small when the loading effects of the secondary resonant circuit on the primary are negligible. This is true in loosely coupled system (low k) with low Q_s (no bifurcation).

With increased Q_s or improved k, the interactions between the primary and secondary resonant circuits can result in large frequency detuning of the pickup or poor DPF of the power supply. With a large frequency detuning, the assumption of operation about ω_0 is not valid. With a poor DPF, the desired constant primary current is not available when the required VA rating exceeds the capability of the selected power supply. In either case, the system will be unable to deliver the required power.

4-6 A PRACTICAL DESIGN EXAMPLE

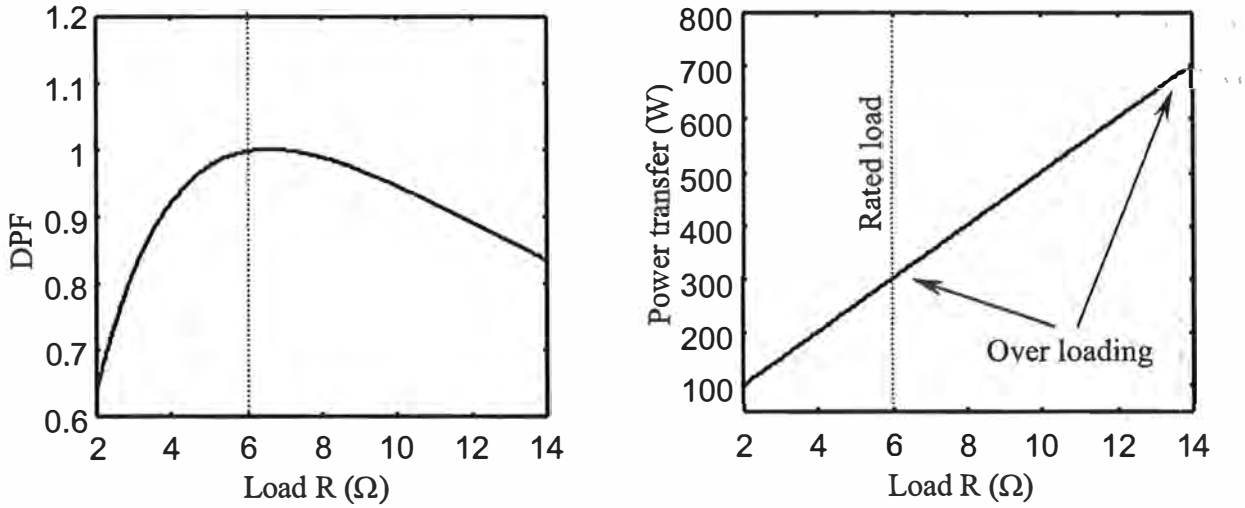
The contact-less electric vehicle battery charger discussed in section 3-11 was designed using the design methodology described in this chapter. The electromagnetic structure, the compensation topology, and the system parameters have been given in section 3-11. Using these parameters, the open circuit voltage (V_{oc}) was calculated as 239V, while the short circuit current (I_{sc}) was determined to be 71A. The maximum power transfer capability without secondary compensation is therefore given by $V_{oc}*I_{sc}/2$ to be 8.5kW. As this value is less than the required power transfer (P) of 30kW, secondary compensation is necessary. The compensation level (the secondary quality factor, Q_{s0}) as determined by $P/(V_{oc}*I_{sc})$ is about 1.8. The rated load is then calculated using (2-23) to be 6Ω. The secondary VA rating as determined by $\sqrt{1+Q_{s0}^2}$ *P is thus 62kVA.

The primary compensation capacitance (C_p) is calculated by (4-3). This primary capacitance is determined to compensate only the self-inductance of the primary coil. Without compensating the loading effects of the secondary resonant circuit on the primary coil, as noted in section 4-5, the system operation will deviate from the design point. For fixed-frequency operation at ω_0, the power supply will operate with a DPF less than unity. For variable-frequency operation with unity DPF, the operating frequency will shift away from ω_0. This section investigates and verifies such deviations for the above battery charger.

With a fixed-frequency controller operating at ω_0 (19.7 kHz), the DPF of the power supply and the

InductEV, Inc.
Exhibit 1010
Page 222

power transfer capability of the pickup assuming constant primary current are shown respectively in Fig. 4-15 (a) and (b). In these figures, the load is extended above rated load to illustrate complete system characteristics, but operation above rated load may be not possible due to the limit of the actual pickup VA rating. The DPF is determined from the phase relationship between the power supply output voltage and current. This phase relationship is calculated using the power supply load impedance developed in section 3-10.1 for the PP topology. The power transfer capability of the pickup when operated at ω_0 is calculated by (3-20). The power curve in this figure and the following similar figures were calculated assuming the primary current was controlled at 15A instead of the rated value of 150A for practical reasons, as this enables the theoretical curves to be verified in the laboratory. Although the primary current is reduced, all the system characteristics presented are identical except that the power level is scaled down by one-hundredth. Since the pickup operates at ω_0, the power curve shows a linear relationship to the load, and rated power of 300W is achieved at rated load.



(a) DPF (b) Power transfer capability (I_p=15A)

Fig. 4-15. DPF and power transfer capability of the contact-less electric vehicle battery charger using a fixed-frequency controller operating at ω_0.

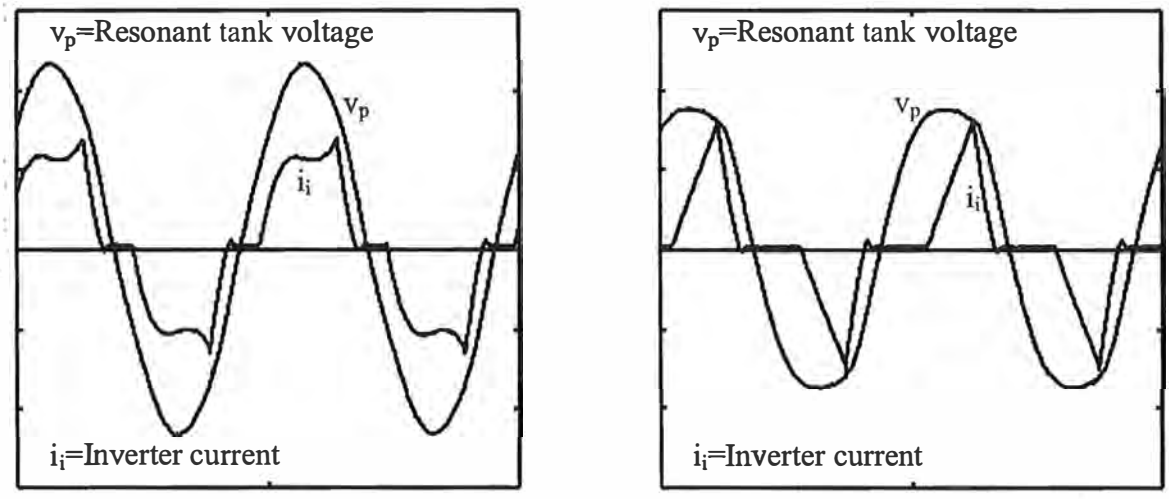
Since the choice of Q_{s0} is close to 2, as noted in section 4-5.2, the DPF of the power supply will be close to unity over a wide range of k allowing a larger tolerance to misalignment between the primary and secondary coils. The magnetic coupling coefficient (k) of the battery charger calculated by (2-1) is 0.45. The necessary Q_{s0} to achieve unity DPF for this coupling condition determined by (4-11) is 1.98 corresponding to a load of 6.6Ω, which is slightly larger than rated load of 6Ω as can be seen in Fig. 4-15 (a). At rated load, the DPF is slightly lower than unity. Due to a suitable choice of k and Q_{s0} for the selected PP topology, the interactions of the primary and secondary resonant circuits do not affect

InductEV, Inc.
Exhibit 1010
Page 223

the DPF of the power supply substantially for rated operation. However, the DPF of the power supply at light load conditions becomes very poor due to such interactions as Q_{s0} drops with the decreasing load.

As part of the experimental set-up, a voltage-fed full-bridge LCL-resonant inverter operating in discontinuous current mode was used to drive the designed system. This inverter will be investigated thoroughly in chapter 8. To simplify the discussion of the PP topology, the series inductor between the inverter and the primary parallel resonant tank is regarded as part of the power supply. As such, the system configuration is formed by a PP topology driven by this power supply. The DPF of the power supply is then determined by measuring the phase relationship between the discontinuous inverter current and the resonant tank voltage.

With the operating frequency controlled at ω_0 (19.7kHz, by manually adjusting the switching instant of the inverter), the measured waveform of the discontinuous inverter current (i_i) and the resonant tank voltage (v_p) are shown in Fig. 4-16 for rated load (6Ω) and a reduced load (3.8Ω). As shown, the fundamental inverter current and the resonant tank voltage are closely in phase at rated load, indicating a DPF close to unity. At the reduced load, there exists a significant phase angle, indicating a DPF less than unity. The inverter current waveform will be investigated further in chapter 8.



(a) Rated load (R=6Ω) (b) A reduced load (R=3.8Ω)

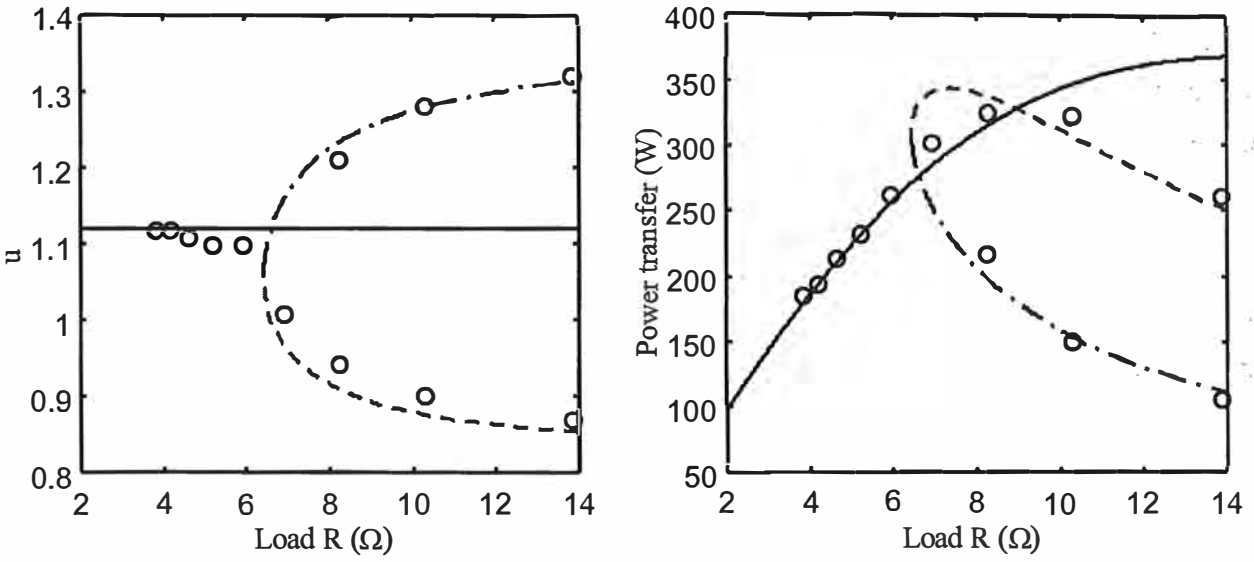
Fig. 4-16. Measured waveforms of the inverter current and the resonant tank voltage for the contact-less electric vehicle battery charger (operating at ω_0=19.7kHz).

Variable-frequency operation with unity DPF (zero-phase angle of the power supply load impedance) was achieved by controlling the inverter current (i_i) to follow the voltage (v_p) across the parallel-compensated primary winding. With this system, operating frequencies can be calculated from the power supply load impedance using:

InductEV, Inc.
Exhibit 1010
Page 224

$$\mathrm{Im}\, Z_t(\omega, R) = 0 \tag{4-14}$$

As shown in Fig. 4-17 (a), the frequencies at which zero-phase angle occurs are actually functions of the load. The power transfer capability when operated along these zero-phase angle frequency profiles can be calculated from (3-20) and are shown in Fig. 4-17 (b). As can be seen, bifurcation occurs as the load is increased slightly above rated load. The measured frequencies and power transfers are shown in Fig. 4-17 as circles at each of the measured loads. In practice, control perturbations and transients affect the operating frequency of the variable-frequency controller in the bifurcation region. In order to investigate and measure the system operating at the three different zero phase angle frequencies and thereby verify the theory, the converter was made to operate in this region by increasing the load beyond rated value while adjusting the turn-on interval of the inverter manually to force a shift between these operating frequencies. Under steady state conditions, the system was found to operate stably at either the lowest or highest zero phase angle frequency since perturbations that give a large positive phase angle will shift operation to the lowest zero phase angle frequency and perturbations that give a large negative phase angle will shift operation to the highest zero phase angle frequency. Stable operation at the middle zero phase angle frequency is not feasible without forcing the frequency (which was not possible with the controller used). As shown, the measured results closely follow the theoretical curves despite simplifications in the model that assume sinusoidal voltages and currents, and ignore losses in the capacitors and inductors.



(a) Operational frequency (b) Power transfer capability (I_p=15A)

Fig. 4-17. Operating frequency and power transfer capability of the contact-less electric vehicle battery charger using a variable-frequency controller operating with unity DPF.

Due to interactions between the primary and secondary resonant circuits, the operating frequency at

InductEV, Inc.
Exhibit 1010
Page 225

rated load (6Ω) is about 10% higher than ω_0. Since the pickup is detuned, the available power at rated load is only 266W. This is more than 10% lower than rated power of 300W.

4-7 CONCLUSIONS

A design methodology is described in this chapter for determination of the operating frequency, the primary current, the electromagnetic structure, the compensation requirement and the secondary quality factor. These design factors are inter-related and have to be selected properly to deliver the required power with minimum total cost.

The load model developed in chapter 3 was then used to evaluate system sensitivity to fundamental design parameters. When the primary compensation does not consider the interactions between the primary and secondary resonant circuits, it is found that the system deviates from design expectations due to influences of the secondary pickup on the primary. These influences depend on the compensation topology (SS, SP, PP and PS), the magnetic coupling coefficient (k) and the secondary quality factor (Q_s).

The influence of the interactions between the primary and secondary resonant circuits is not a problem for the SS topology (series primary and secondary), as the load resonant tank can be properly tuned. However, care must be taken when other topologies are used. With loose magnetic coupling (low k) and low Q_s, the loading effects of the secondary on the primary are negligible in comparison to the primary reactance. In this case, the system works very well since the primary and secondary resonant behaviour are virtually independent of each other. With improved magnetic coupling (high k) and increased Q_s, the secondary loading effect affects the primary resonant behaviour substantially. As a result, the system may operate with a poor displacement power factor under a fixed-frequency controller designed to operate at ω_0. For a variable-frequency controlled system operating with unity displacement power factor, the system may have significant pickup frequency detuning. With poor displacement power factor, the system operation may exceed the VA rating of the power supply. With large frequency detuning, the pickup may have a substantial drop in power transfer capability. In both cases, the system may be unable to deliver the required power.

Moreover, under variable-frequency control three operating modes may exist in the frequency spectrum, and as such the system may become uncontrollable. Bifurcation occurs when either the secondary quality factor or the magnetic coupling coefficient increase. Bifurcation limits are once again topology dependent. For well-coupled system (high k), bifurcation may occur with a Q_s less than 2.

The design methodology was applied to a practical example for contact-less electric vehicle battery

InductEV, Inc.
Exhibit 1010
Page 226

charging, and verified under fixed and variable frequency control respectively. The system behaviour is predicable, and clearly shows where improvements can be made.

REFERENCES

[1]. Gyu Bum Joun, B. H. Cho, "An energy transmission system for an artificial heart using leakage inductance compensation of transcutaneous transformer," *IEEE Transactions on Power Electronics,* vol. 13, pp. 1013-1022, Nov. 1998.

[2]. J. Lukacs, M. Kiss, I. Nagy, G. Gonter, R. Hadik, K. Kaszap, A. Tarsoly, "Inductive energy collection for electric vehicles," in *Conf. Rec. Fourth Power Electronics Conference*, 1981, pp. 71-81.

[3]. J. M. Barnard, J. A. Ferreira, J. D. van Wyk, "Sliding transformers for linear contactless power delivery," *IEEE Transactions on Industrial Electronics*, vol. 44, pp. 774-779, Dec. 1997.

[4]. A. Esser, H.-C. Skudelny, "A new approach to power supplies for robots," *IEEE Transactions on Industry Applications*, vol. 27, pp. 872-875, 1991.

[5]. A. Kawamura, K. Ishioka, J. Hirai, "Wireless transmission of power and information through one high-frequency resonant AC link inverter for robot manipulator applications," *IEEE Transactions on Industry Applications*, vol. 32, pp. 503-508, May-June 1996.

[6]. D. A. G. Pedder, A. D. Brown, J. A. Skinner, "A contactless electrical energy transmission system," *IEEE Transactions on Industrial Electronics*, vol. 46, pp. 23-30, Feb. 1999.

[7]. J. T. Boys, G. A. Covic, A. W. Green, "Stability and control of inductively coupled power transfer systems," *IEE Proceedings-Electric Power Applications*, vol. 147, pp. 37-43, Jan. 2000.

[8]. G. A. Covic, G. Elliott, O. H. Stielau, R. M. Green, J. T. Boys, "The design of a contact-less energy transfer system for a people mover system," in *Conf. Rec. International Conference on Power System Technology*, vol. 1, Dec. 2000, pp. 79-84.

[9]. Chwei-Sen Wang, G. A. Covic, O. H. Stielau, "General stability criterions for zero phase angle controlled loosely coupled inductive power transfer systems," in *Conf. Rec. The 27th Annual Conference of the IEEE Industrial Electronics Society,* vol. 2, 2001, pp. 1049-1054.

[10]. A. P. Hu, *Selected resonant converters for IPT power supplies*, PhD thesis, The Electrical and Electronics Engineering Department, The University of Auckland, Auckland, New Zealand, 2001, pp. 151-167.

[11]. A. W. Green, "Modelling a push-pull parallel resonant converter using generalised state-space averaging," *IEE Proceedings-Electric Power Applications*, vol. 140, pp. 350-356, Nov. 1993.

InductEV, Inc.
Exhibit 1010
Page 227

[12]. O. H. Stielau, G. A. Covic, "Design of loosely coupled inductive power transfer systems," in *Conf. Rec. International Conference on Power System Technology*, vol. 1, Dec. 2000, pp. 85-90.

[13]. J. B. Turner, G. W. Roth, "Regulator for inductively coupled power distributions system," *US-Patent No. 4914539*, Apr. 3, 1990.

[14]. A. W. Kelley, W. R. Owens, "Connectorless power supply for an aircraft-passenger entertainment system," *IEEE Transactions on Power Electronics*, vol. 4, pp. 348-354, July 1989.

[15]. J. T. Boys, A. W. Green, "Inductive power distribution system," *US-Patent No. 5293308*, Mar. 8, 1994.

[16]. A. W. Green, J. T. Boys, "An inductively coupled high-frequency power system for material handling applications," in *Conf. Rec. International Power Electronics*, vol. II, 1993, pp. 821-826.

[17]. J. T. Boys, G. A. Covic, Yongxiang Xu, "DC analysis technique for inductive power transfer pick-ups," *IEEE Power Electronics Letters*, vol. 1, pp. 51-53, June 2003.

[18]. J. T. Boys, G. A. Covic, J. E. James, "Switching frequencies in inductively coupled power transfer systems,' in C*onf. Rec. International Power Engineering Conference*, Nov. 2003.

[19]. J. T. Boys, G. A. Covic, G. A. J. Elliott, "Pick-up transformer for ICPT applications," *Electronics Letters*, vol. 38, pp. 1276-1278, Oct. 2002.

InductEV, Inc.
Exhibit 1010
Page 228

InductEV, Inc.
Exhibit 1010
Page 229

CHAPTER 5

TUNING TO IMPROVE POWER TRANSFER FOR VARIABLE-FREQUENCY SYSTEMS

5-1 Introduction
5-2 Primary tuning for unity DPF at rated load
5-3 Power transfer capability and bifurcation phenomenon
5-4 Bifurcation criteria
5-5 Discussion
5-6 Verification
5-7 Conclusions

5-1 INTRODUCTION

In variable-frequency systems, the operating frequency can vary from the desired pick-up tuned frequency (ω_0) with changes in load, thereby affecting the power transfer capability of the system. In this chapter, improvements in the system's power transfer capability are investigated by modifying the primary tuning assumed with the design methodology described in Chapter 4.

Modifying the secondary compensation capacitance also affects the system's power transfer characteristics, however this modification results in a change to the secondary resonant frequency. This is undesirable under the design methodology described in Chapter 4 since the required power transfer to the pickup can only be guaranteed whenever the secondary resonant circuit is tuned to the nominal operating frequency (ω_0). As previously shown, the load resonant tank tuning has a marked effect on the system's frequency deviations, consequently the focus of this chapter is the appropriate selection of the primary compensation capacitance (C_p) to minimise variations from ω_0 (over the operating load range).

Theoretically, an ideal solution could be achieved if C_p were able to be dynamically tuned [1]. However, this is normally not preferred in a practical system due to the complexity and cost of the control means necessary to achieve this. In this chapter, the aim is then to first select the best C_p that improves the tuning of the load resonant tank when operating at rated load. Following this the power transfer capability and bifurcation phenomenon under variable-frequency operation are investigated to find out the influences of the compensation topologies (SS, SP, PP and PS) as well as the fundamental parameters k (the magnetic coupling coefficient) and $Q_{s0,rated}$ (the secondary quality factor at ω_0 and rated load) determined with the design methodology described in Chapter 4. A general bifurcation

InductEV, Inc.
Exhibit 1010
Page 230

criterion is developed for each topology to ensure the system can deliver the necessary power stably over the full operating range. Finally the theory is verified using a practical design example. System behaviour under fixed-frequency operation is analysed in the following chapter.

5-2 PRIMARY TUNING FOR UNITY DPF AT RATED LOAD

In this chapter, all of the design parameters are assumed to be determined following the standard design process outlined in chapter 4 except the primary compensation capacitance (C_p). Thus the focus here is on using the load impedance model developed in section 3-10 to determine a suitable modification to C_p.

In order to minimize the VA rating of the power supply, it is desirable to operate at the zero phase angle frequency of the load impedance (Z_t). At this frequency, the load reactance (Im Z_t) seen by the power supply is zero, and the DPF of the power supply is unity. This zero phase angle frequency must be designed to equal ω_0 to ensure maximum power meets the required power. The design solution to achieve this objective can be determined using:

$$\operatorname{Im} Z_{t0} = \operatorname{Im} Z_t(\omega = \omega_0) = 0 \tag{5-1}$$

To meet this condition, C_p is designed here to compensate not only the self-inductance of the primary coil (L_p) but also the reflected impedance (Z_r). The necessary C_p as derived in Appendix H is:

$$C_p = \begin{cases} \dfrac{C_s L_s}{L_p} & \text{SS topology} \\ \dfrac{C_s L_s}{L_p}\left(\dfrac{1}{1-k^2}\right) & \text{SP topology} \\ \dfrac{C_s L_s}{L_p}\left(\dfrac{1-k^2}{Q_{s0}^2 k^4 + (1-k^2)^2}\right) & \text{PP topology} \\ \dfrac{C_s L_s}{L_p}\left(\dfrac{1}{Q_{s0}^2 k^4 + 1}\right) & \text{PS topology} \end{cases} \tag{5-2}$$

For a general analysis, a normalized primary compensation capacitance (C_{pn}) is defined here using the C_p assumed earlier with the design methodology described in chapter 4 (equation 4-3). Thus:

$$C_{pn} = \frac{C_p}{\dfrac{C_s L_s}{L_p}} \tag{5-3}$$

Substituting (5-2) into (5-3) results in:

InductEV, Inc.
Exhibit 1010
Page 231

$$C_{pn}=\begin{cases}1 & \text{SS topology}\\ \dfrac{1}{1-k^2} & \text{SP topology}\\ \dfrac{1-k^2}{Q_{s0}^2k^4+\left(1-k^2\right)^2} & \text{PP topology}\\ \dfrac{1}{Q_{s0}^2k^4+1} & \text{PS topology}\end{cases} \tag{5-4}$$

The value of C_{pn} as shown depends on three factors: the compensation topologies (SS, SP, PP and PS), the magnetic coupling coefficient (k) and the secondary quality factor (Q_{s0}) at ω_0. As expected, C_{pn} is unity when an SS topology is used and there is no need to modify C_p from the original tuning because the load resonant tank has been properly tuned (as noted in section 4-5). However, a different C_p ($C_{pn}\neq 1$) is necessary when the other three topologies are used.

As can be seen in (5-4), the selected primary and secondary compensation topologies play a large role in the correct choice of C_p. Since a series-compensated secondary reflects no reactance at ω_0, the primary inductance can be "tuned out" (independent of either k or Q_{s0}) using a series-connected capacitance in the primary network. Although this SS topology seems to be the best choice regarding primary resonance design, parallel compensation may be preferred in the primary and/or secondary resonant circuits for practical reasons [2-8]. The required C_p in these topologies (SP, PP and PS) is dependent on k. As a parallel-compensated secondary reflects a load-independent capacitive reactance at ω_0, the required C_p for a series tuned primary in this case (the SP topology) is independent of Q_{s0}. However, the required C_p for a parallel tuned primary (the PP and PS topologies) is a function of Q_{s0} and consequently load. The reflected impedance contains a real component representing the load in series with the primary self-inductance, and consequently parallel tuning of the primary coil is load dependent. It is impractical to allow C_p to vary with the load, thus C_p must be chosen for a selected load point. Given that the designer must ensure maximum power can be delivered, the logical choice is to select C_p for the rated power point. The required C_{pn} is thus:

$$C_{pn}=\begin{cases}1 & \text{SS topology}\\ \dfrac{1}{1-k^2} & \text{SP topology}\\ \dfrac{1-k^2}{Q_{s0,rated}^2k^4+\left(1-k^2\right)^2} & \text{PP topology}\\ \dfrac{1}{Q_{s0,rated}^2k^4+1} & \text{PS topology}\end{cases} \tag{5-5}$$

With this approach, the designed power should be delivered for all loading (Q_{s0}) variations within the design range.

InductEV, Inc.
Exhibit 1010
Page 232

As shown above, k and/or $Q_{s0,rated}$ must be included in the choice of C_p. In order to investigate the effects of k and $Q_{s0,rated}$ on the proposed primary resonance design, C_{pn} (as determined by (5-5)) is shown in Fig. 5-1 as a function of k, for $Q_{s0,rated}$ of 2, 5 and 10. While no change to the original tuning is required for the SS topology, the SP topology is shown to require a larger C_p with better coupling. The PP topology requires a slightly larger C_p for loose coupling with low $Q_{s0,rated}$, but needs a smaller C_p if the coupling is improved or $Q_{s0,rated}$ is increased. A smaller C_p is always required for the PS topology and the change becomes larger with better coupling or higher $Q_{s0,rated}$.

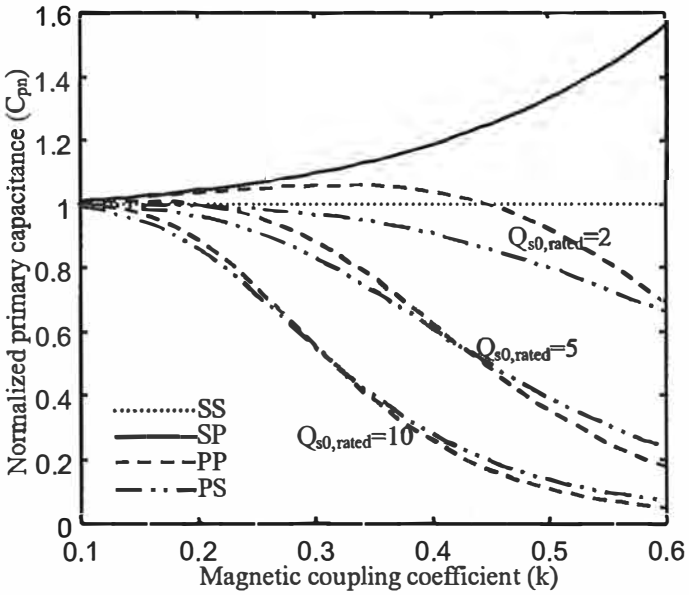


Fig. 5-1. Primary tuning for unity DPF at rated load.

To increase the power transfer capability of ICPT systems, effort has gone into improving the magnetic coupling between the primary and secondary, and coupling coefficients for single pickup applications of between 0.3 and 0.6 are often achievable [2], [8]. For multiple pickup applications, system constraints usually result in coupling coefficients of less than 0.1 per pickup [6], [7]. However, as discussed later in Chapter 9, the effect of all pickups together is often again equivalent to a single pickup with a coupling coefficient of about 0.2 to 0.5.

As shown in Fig 5-1, systems with such high coupling coefficients behave very differently to loosely coupled systems. For coupling coefficients of less than 0.2, the system can be considered loosely coupled and the original tuning gives a good result. However, as the coupling improves the system characteristics change substantially. This change is a strong function of both the system topology as well as $Q_{s0,rated}$ that could present a problem in SP, PP and PS topologies. With a $Q_{s0,rated}$ equal to 10, the PP and PS topologies start deviating from the loosely coupled theory at coupling coefficients exceeding about 0.2, while for lower $Q_{s0,rated}$ values of 2 the deviation only occurs at coupling coefficients exceeding about 0.5.

InductEV, Inc.
Exhibit 1010
Page 233

Practical ICPT systems are normally either loosely-middle coupled with medium-high Q_s or middle-well coupled with low-medium Q_s. Examples of C_{pn} are given in Table 5-1 for both systems assuming $Q_{s0,rated}$ of 10 (high Q_s) and 5 (medium Q_s). For loosely coupled high Q_s systems (k=0.1, $Q_{s0,rated}$=10), the required C_p is close to the original tuning (C_{pn}=1) as the reflected impedance is negligible. For middle coupled high Q_s systems (k=0.2, $Q_{s0,rated}$=10), the design can change by as much as 4% for an SP topology, 11% for a PP topology and 14% for a PS topology. For middle coupled medium Q_s systems (k=0.2, $Q_{s0,rated}$=5), the required C_p for the PP topology is again close to the original tuning, while the required change to C_p for the SP and PS topologies is about 4%. The well coupled medium Q_s systems (k=0.4, $Q_{s0,rated}$=5) change the design significantly by 19% for an SP topology, 38% for a PP topology and 39% for a PS topology.

TABLE 5-1
PRIMARY TUNING FOR UNITY DPF AT RATED LOAD

Topology	C_{pn}			
	$Q_{s0,rated}$=10		$Q_{s0,rated}$=5	
	k=0.1	k=0.2	k=0.2	k=0.4
SS	1	1	1	1
SP	1.01	1.04	1.04	1.19
PP	1.00	0.89	1.00	0.62
PS	0.99	0.86	0.96	0.61

From the above it can be seen that the original tuning works well for the SS topology, and for other topologies with low $Q_{s0,rated}$ (less than 2) or coupling coefficients less than 0.2. Special care needs to be taken when designing systems with either PP or PS topologies.

5-3 POWER TRANSFER CAPABILITY AND BIFURCATION PHENOMENON

In order to investigate the effects of the modified tuning on the power transfer capability, here the power transfer is normalized using the rated power determined at rated load ($Q_{s0,rated}$) and ω_0 (u=1). As noted in section 3-6 (equation 3-20), the power transfer to a secondary pickup is given by the square of the primary current (I_p) multiplied by the reflected resistance (Re Z_r). Assuming constant primary current, the normalized power P_n is then:

$$P_n = \frac{P}{P_{rated}} = \frac{(\mathrm{Re}\,Z_r)I_p^2}{(\mathrm{Re}\,Z_{r0,rated})I_p^2} = \frac{\mathrm{Re}\,Z_r}{\mathrm{Re}\,Z_{r0,rated}} = \left(\frac{\mathrm{Re}\,Z_r}{\mathrm{Re}\,Z_{r0}}\right)\left(\frac{\mathrm{Re}\,Z_{r0}}{\mathrm{Re}\,Z_{r0,rated}}\right) = (\mathrm{Re}\,Z_{rn})\left(\frac{\mathrm{Re}\,Z_{r0}}{\mathrm{Re}\,Z_{r0,rated}}\right) \qquad (5\text{-}6)$$

where (Re Z_{rn}) is the normalized reflected resistance, (Re Z_{r0}) is the reflected resistance at ω_0, and (Re

InductEV, Inc.
Exhibit 1010
Page 234

$Z_{r0,rated}$) is the rated reflected resistance at ω_0. These parameters are defined in section 3-7.

Substituting (3-26) into (5-6) results in:

$$P_n = (\mathrm{Re}\,Z_{rn})\left(\frac{\mathrm{Re}\,Z_{r0}}{\mathrm{Re}\,Z_{r0,rated}}\right) = (\mathrm{Re}\,Z_{rn})\left(\frac{\left(\frac{\omega_0 M^2}{L_s}\right)Q_{s0}}{\left(\frac{\omega_0 M^2}{L_s}\right)Q_{s0,rated}}\right) = (\mathrm{Re}\,Z_{rn})\left(\frac{Q_{s0}}{Q_{s0,rated}}\right) \tag{5-7}$$

Since (Re Z_{rn}) is a function of u and Q_{s0} as shown in (3-34), P_n is also a function of u and Q_{s0}. In addition, it is related to the specified rated load ($Q_{s0,rated}$).

To calculate P_n for variable-frequency systems, the operating frequency needs to be determined. Here it is assumed the power supply operates with unity DPF by allowing the frequency to vary with the load (Q_{s0}). At this frequency the phase angle of the load impedance (Z_t) is zero. Similar to the analysis in section 4-5.3, this operating frequency can be calculated using the normalized load impedance (Z_{tn}) by:

$$\mathrm{Im}\,Z_{tn}(u,k,Q_{s0}) = 0 \ \textbf{or}\ \mathrm{Im}\,Y_{tn}(u,k,Q_{s0}) = 0 \tag{5-8}$$

The normalized load impedance developed in section 3-10.2 can be reused providing the normalized reactance for C_p (defined as "$1/[\omega C_p(\mathrm{Re}\,Z_{r0})]$") is modified to include the changes proposed to C_p in this chapter. For convenience, the normalized load impedance is summarized in Table 5-2 with the function of each term given in Table 5-3. Here C_{pn} is unity for systems tuned using the approach described in Chapter 4 (hereafter labelled as "original tuning"). For systems using the modified tuning methodology proposed in section 5-2 (hereafter labelled as "modified tuning"), it is topology dependent as given by (5-5).

TABLE 5-2
NORMALIZED LOAD IMPEDANCES WITH COMPENSATED PICKUP

Series primary: $Z_{tn} = \frac{Z_t}{\mathrm{Re}\,Z_{r0}} = \mathrm{Re}\,Z_{tn} + j\,\mathrm{Im}\,Z_{tn}$	$\mathrm{Re}\,Z_{tn} = \mathrm{Re}\,Z_{rn}$
	$\mathrm{Im}\,Z_{tn} = -\frac{1}{\omega C_p(\mathrm{Re}\,Z_{r0})} + \frac{\omega L_p}{\mathrm{Re}\,Z_{r0}} + \mathrm{Im}\,Z_{rn}$
Parallel primary: $Z_{tn} = \frac{1}{Y_{tn}} = \frac{1}{\mathrm{Re}\,Y_{tn} + j\,\mathrm{Im}\,Y_{tn}}$	$\mathrm{Re}\,Y_{tn} = \frac{\mathrm{Re}\,Z_{rn}}{(\mathrm{Re}\,Z_{rn})^2 + \left(\frac{\omega L_p}{\mathrm{Re}\,Z_{r0}} + \mathrm{Im}\,Z_{rn}\right)^2}$
	$\mathrm{Im}\,Y_{tn} = \omega C_p(\mathrm{Re}\,Z_{r0}) - \frac{\frac{\omega L_p}{\mathrm{Re}\,Z_{r0}} + \mathrm{Im}\,Z_{rn}}{(\mathrm{Re}\,Z_{rn})^2 + \left(\frac{\omega L_p}{\mathrm{Re}\,Z_{r0}} + \mathrm{Im}\,Z_{rn}\right)^2}$

InductEV, Inc.
Exhibit 1010
Page 235

TABLE 5-3
FUNCTIONS OF THE NORMALIZED LOAD IMPEDANCE WITH MODIFIED TUNING

$\dfrac{1}{\omega C_p(\mathrm{Re}Z_{r0})} = \begin{cases} \dfrac{Q_{p0}}{uC_{pn}} = \dfrac{1}{uk^2Q_{s0}C_{pn}} \\ \left(\dfrac{1}{uC_{pn}}\right)\left(Q_{p0}+\dfrac{1}{Q_{s0}}\right) = \dfrac{1}{uk^2Q_{s0}C_{pn}} \end{cases}$	Series secondary. Parallel secondary.
$\dfrac{\omega L_p}{\mathrm{Re}Z_{r0}} = \begin{cases} uQ_{p0} = \dfrac{u}{k^2Q_{s0}} \\ u\left(Q_{p0}+\dfrac{1}{Q_{s0}}\right) = \dfrac{u}{k^2Q_{s0}} \end{cases}$	Series secondary. Parallel secondary.
$\mathrm{Re}\,Z_{rn} = \dfrac{\mathrm{Re}\,Z_r}{\mathrm{Re}Z_{r0}} = \begin{cases} \dfrac{u^4}{(u^2-1)^2Q_{s0}^2+u^2} \\ \dfrac{u^2}{(u^2-1)^2Q_{s0}^2+u^2} \end{cases}$	Series secondary. Parallel secondary.
$\mathrm{Im}\,Z_{rn} = \dfrac{\mathrm{Im}\,Z_r}{\mathrm{Re}Z_{r0}} = \begin{cases} \dfrac{-u^3(u^2-1)Q_{s0}}{(u^2-1)^2Q_{s0}^2+u^2} \\ \dfrac{-u^3[(u^2-1)Q_{s0}+1/Q_{s0}]}{(u^2-1)^2Q_{s0}^2+u^2} \end{cases}$	Series secondary. Parallel secondary.

With k and $Q_{s0,rated}$ determined using the design methodology described in Chapter 4, the normalized operating frequency (u) determined using (5-8) is a function of Q_{s0} (load) as shown in Fig. 5-2 to 5-9 for all four basic topologies (SS, SP, PP and PS). The normalized power transfer capability (P_n) when operating at this frequency calculated using (5-7) is also shown in Fig. 5-2 to 5-9. Here, the modified tuning is shown as solid lines, while dashed lines represent the original tuning. Bifurcation as shown is a common phenomenon in all topologies. Bifurcation occurs when Q_s is high, and improving k simply results in the appearance of bifurcation at lower Q_s.

In the analysis of each topology, the value of k is assumed to be 0.05, 0.2 and 0.4 to represent systems that are loosely coupled, middle coupled or well coupled. Typical loosely coupled systems are track-type ICPT systems, where the secondary pickup moves along a long track, and couples only with a small portion of the primary cable extended along the track. If in such systems, the primary is required to supply power to many secondary pickups distributed along the track, the coupling will increase and equivalently become mid-coupled or well-coupled systems (as noted later in Chapter 9). Typical mid-coupled or well-coupled systems are coil-type ICPT systems used in battery charging applications, where often both the primary and secondary are concentrated coils.

As expected, the frequency and power curves when tuned using the approach described in Chapter 4 ("original tuning") are independent of $Q_{s0,rated}$ in each topology as C_p is not load dependent. For the SS

InductEV, Inc.
Exhibit 1010
Page 236

topology, the modified tuning proposed in this chapter and the original tuning are identical. With the SP topology, the frequency and power curves for the modified tuning are also independent of $Q_{s0,rated}$. Here the independency to $Q_{s0,rated}$ arises from the fact that the required C_p is independent of load. In order to draw the power curves, $Q_{s0,rated}$ is arbitrary assumed to be close to, but still within the bifurcation boundary. Other values can be used for $Q_{s0,rated}$ but this only changes the scale of the power curves.

The PP and PS topologies with the modified tuning are more complex as the required C_p is load dependent. The frequency and power curves strongly depend on C_p, and it is assumed here that C_p is designed to achieve unity DPF at $Q_{s0,rated}$. The analysis here investigates three systems with different values of $Q_{s0,rated}$. The first system assumes $Q_{s0,rated}$ is well within the bifurcation boundary. The second system has $Q_{s0,rated}$ close to, but still within the bifurcation boundary. The third system has a value of $Q_{s0,rated}$ slightly higher so that bifurcation occurs at rated load. This later system is neither desirable nor practical and should be avoided as demonstrated by the effect this has a poor power transfer capability due to large frequency detuning.

The possible improvements in the power transfer capability that arise from the modified tuning depends on the system topology as well as k, Q_{s0} and $Q_{s0,rated}$ as discussed following.

SS Topology: As noted in section 4-5.3, the SS topology is theoretically the most desirable and there is no need to change C_p. Here operating at ω_0 is achievable for all loading conditions (any Q_s). In theory, there is no pickup frequency detuning providing the operation is constrained to the bifurcation-free region, and the power transfer capability increases linearly with the load as shown in Fig. 5-2. For the selected k of 0.05, 0.2 and 0.4, bifurcation occurs at Q_{s0} of about 20, 5 and 2.5, and as such $Q_{s0,rated}$ is selected as 18, 4.5 and 2.2 respectively to ensure maximum and stable power transfer.

SP Topology: Since the required change in C_p for the SP topology is independent of Q_{s0}, operating at ω_0 is achievable for all loading conditions (any Q_{s0}) as shown in Fig. 5-3. It is noted that the influences of k and Q_s on the operating frequency and the bifurcation phenomenon of the SS and SP topologies are similar. Both are able to operate at ω_0 under all loading conditions, which is a major improvement for the SP topology. The bifurcation boundary of the SP topology is slightly lower than that of the SS topology. For the selected k of 0.05, 0.2 and 0.4, bifurcation occurs at Q_{s0} of about 20, 4.9 and 2.3, and as such $Q_{s0,rated}$ is selected as 18, 4.5 and 2.2 respectively to ensure maximum and stable power transfer. Rated power is achieved (P_n=1) at $Q_{s0,rated}$ with the modified tuning, while the original tuning is unable to deliver rated power (P_n<1) due to pickup frequency detuning. The improvement in power transfer capability strongly depends on Q_{s0} and k. With a Q_{s0} much lower than $Q_{s0,rated}$, the improvement is negligible but becomes significant at $Q_{s0,rated}$ when k is high. With a k of

InductEV, Inc.
Exhibit 1010
Page 237

0.05, it is about 4% only and increases to 28% when k is 0.2, and 64% if k is 0.4.

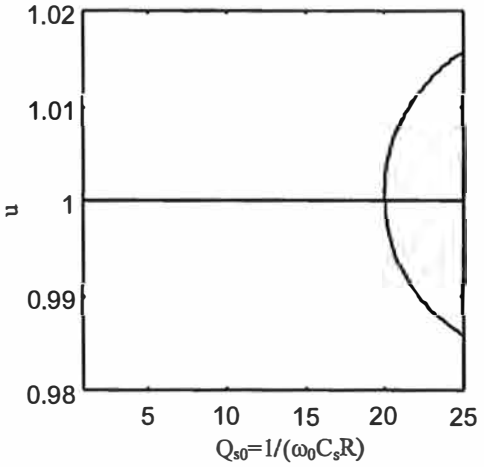
With the SS and SP topologies, one of the three operating modes in the bifurcation region shows no pickup frequency detuning. This could be exploited to deliver greater power providing a suitable variable-frequency controller could utilize this feature to enable stable operation within the bifurcation region and providing the VA rating of the secondary is not exceeded. However, pickup frequency detuning is unavoidable if the system chooses to operate in either of the other two operating modes.

PP Topology: Because C_p of the PP topology is selected to achieve unity DPF at rated load, operating at ω_0 is achievable only at $Q_{s0,rated}$ as shown in Fig. 5-4 to 5-6. In addition to k and Q_{s0}, the value of $Q_{s0,rated}$ affects the operating frequency and power transfer capability because the required C_p is dependent on $Q_{s0,rated}$. If $Q_{s0,rated}$ is within the bifurcation boundary, the modified tuning is able to reduce pickup frequency detuning, resulting in improved power transfer capability for all loading conditions up to and including rated load. With $Q_{s0,rated}$ at or within the bifurcation region, the modified tuning undesirably increases the pickup frequency detuning at all loading conditions within the bifurcation boundary and as such the pickup power transfer capability becomes lower. It is necessary to avoid this situation when using the modified tuning proposed in this chapter. To achieve this objective, a general bifurcation criterion is developed in section 5-4.

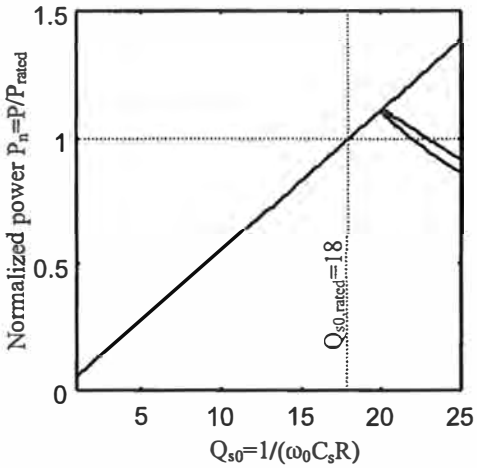
For this topology, the load (Q_{s0}) at which bifurcation occurs is higher than the original tuned system, resulting in a larger safety margin. This improvement is significant if the selected $Q_{s0,rated}$ is well within the bifurcation boundary. The bifurcation boundary of the PP topology is similar to the SP topology discussed above. For the selected k of 0.05, 0.2 and 0.4, bifurcation occurs also at Q_{s0} of about 20, 4.9 and 2.3. If $Q_{s0,rated}$ is well within the bifurcation boundary, the difference in the operating frequency and power transfer capability between the modified tuning and the original tuning is small or negligible below rated load. Once again the improvement in power transfer capability becomes significant when $Q_{s0,rated}$ is close to but within the bifurcation boundary in high k systems. With k of 0.05, this improvement is negligible. As k improves to 0.2, it is 3% only. At a k of 0.4, the improvement increases to about 15%.

PS Topology: Similar to the PP topology, the C_p of the PS topology is modified to achieve unity DPF at rated load and as such operating at ω_0 is only achieved at $Q_{s0,rated}$ as shown in Fig. 5-7 to 5-9. With $Q_{s0,rated}$ within the bifurcation boundary, the modified tuning is able to improve the power transfer capability under all loading conditions up to and including rated load. With systems where bifurcation occurs at $Q_{s0,rated}$, rated power is only available in the bifurcation area where the controller is normally unstable, thus this design should be avoided. A general bifurcation criterion is developed in section 5-4 to enable suitable values of k and $Q_{s0,rated}$ to be determined such that the system design is within the bifurcation boundary.

InductEV, Inc.
Exhibit 1010
Page 238

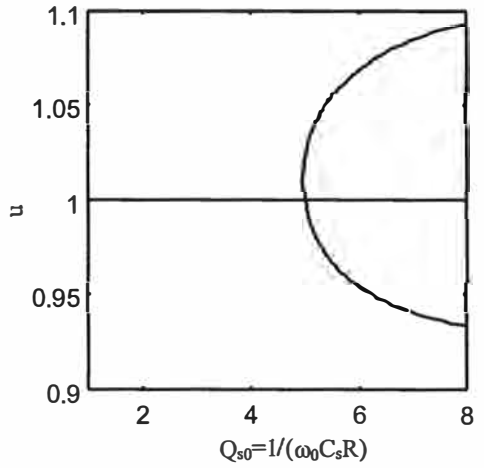


(i) Operating frequency.

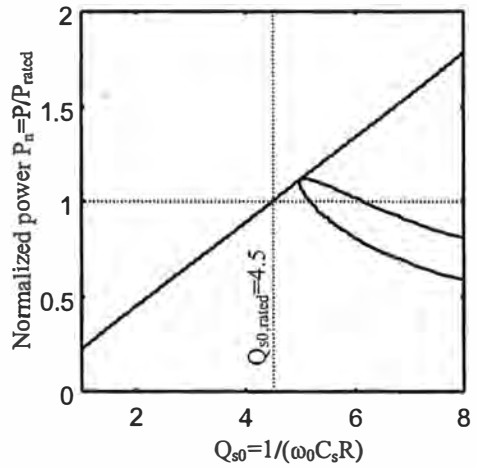


(ii) Power transfer capability.

(a) A loosely coupled system (k=0.05).

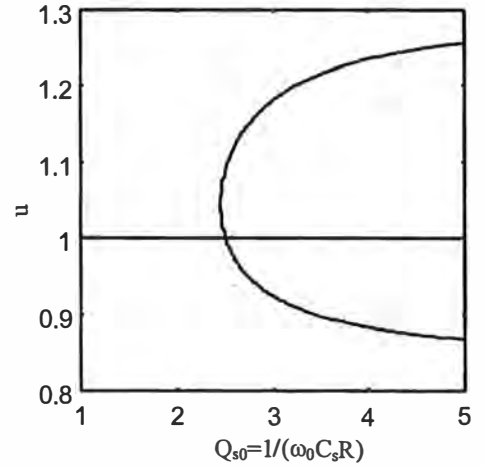


(i) Operating frequency.

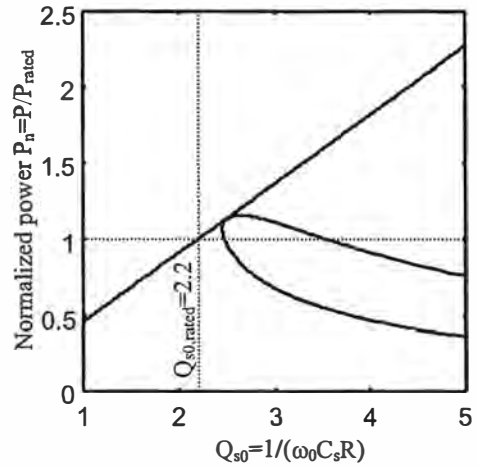


(ii) Power transfer capability.

(b) A mid-coupled system (k=0.2).



(i) Operating frequency.

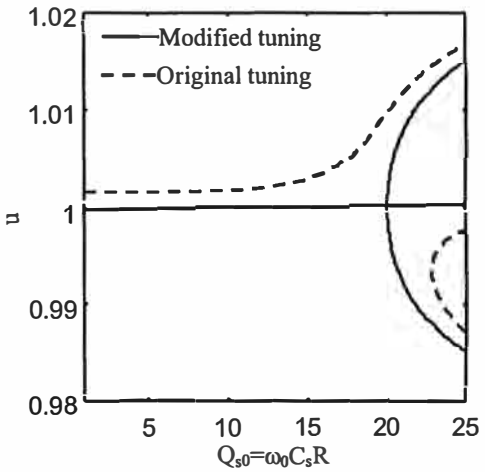


(ii) Power transfer capability.

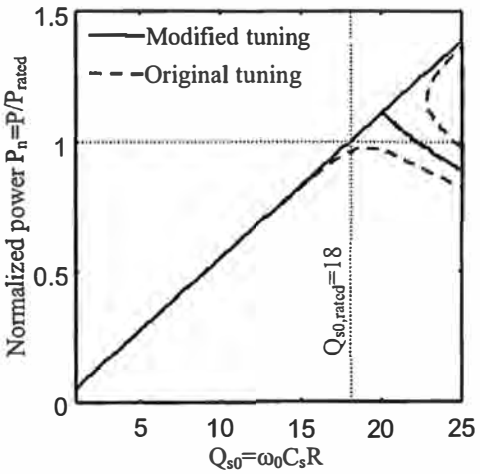
(c) A well-coupled system (k=0.4).

Fig. 5-2. SS topology - Operating frequency and power transfer capability under variable-frequency operation.

InductEV, Inc.
Exhibit 1010
Page 239

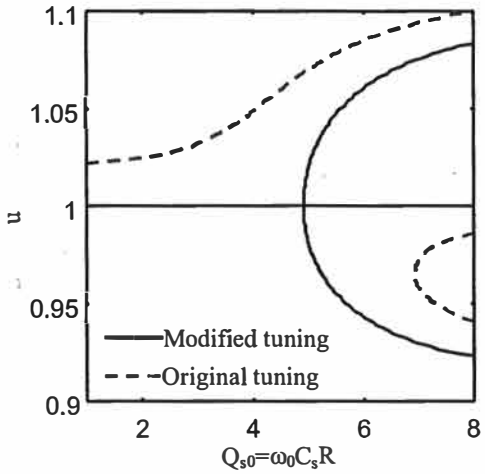


(i) Operating frequency.

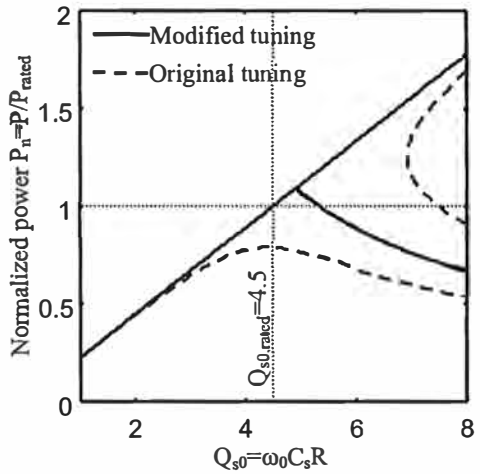


(ii) Power transfer capability.

(a) A loosely coupled system (k=0.05).

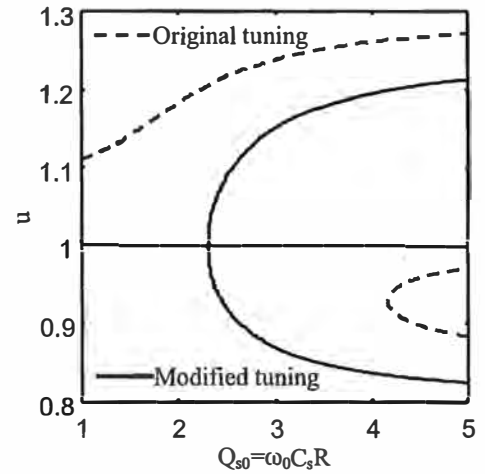


(i) Operating frequency.

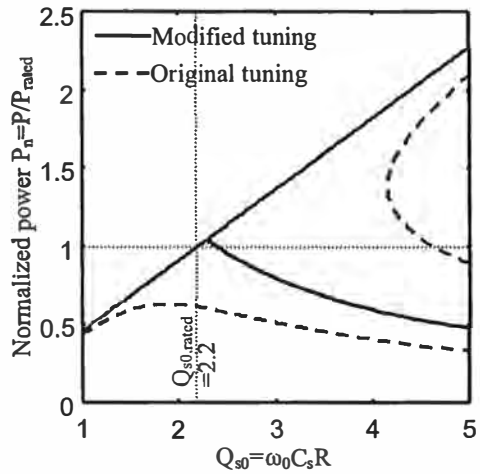


(ii) Power transfer capability.

(b) A mid-coupled system (k=0.2).



(i) Operating frequency.

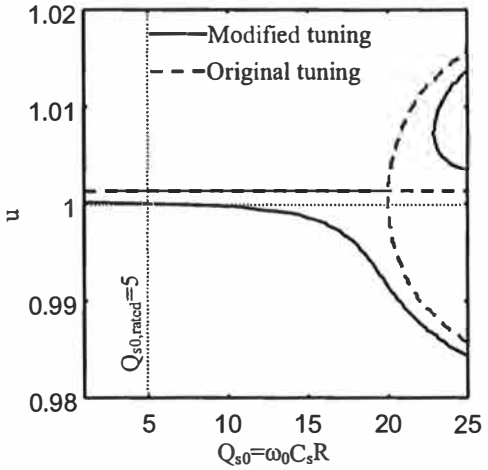


(ii) Power transfer capability.

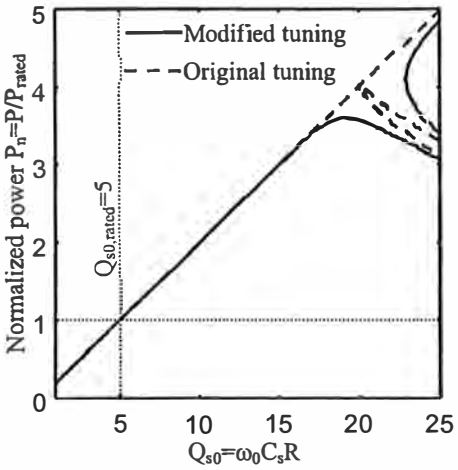
(c) A well-coupled system (k=0.4).

Fig. 5-3. SP topology - Operating frequency and power transfer capability under variable-frequency operation.

InductEV, Inc.
Exhibit 1010
Page 240

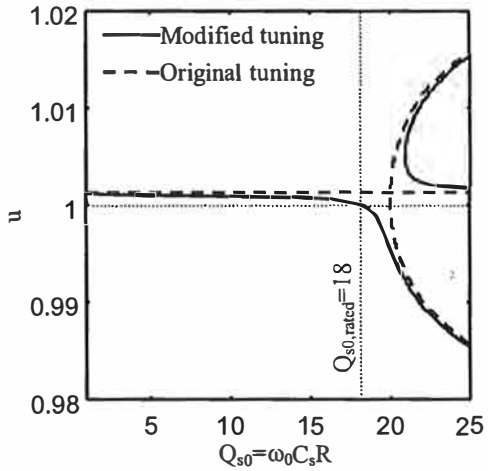


(i) Operating frequency.

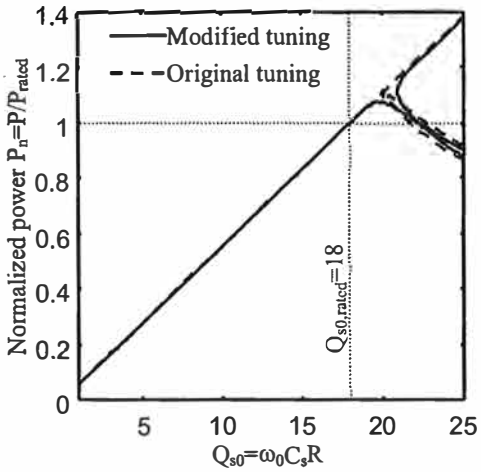


(ii) Power transfer capability.

(a) A system with $Q_{s0,rated}$ well within the bifurcation boundary.

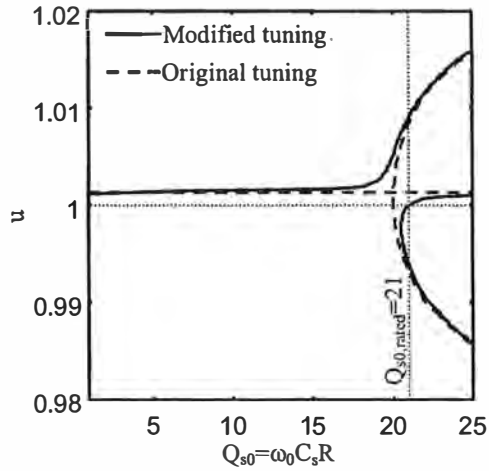


(i) Operating frequency.

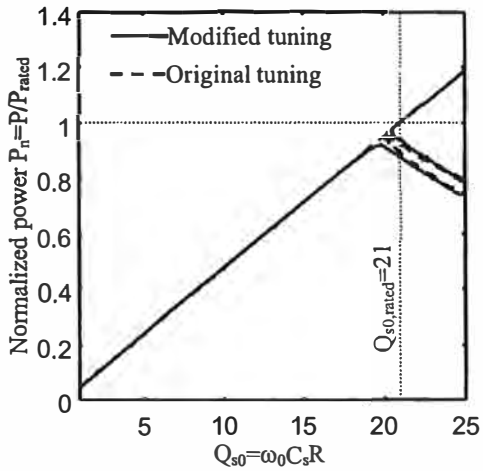


(ii) Power transfer capability.

(b) A system with $Q_{s0,rated}$ close to, but still within the bifurcation boundary.



(i) Operating frequency.

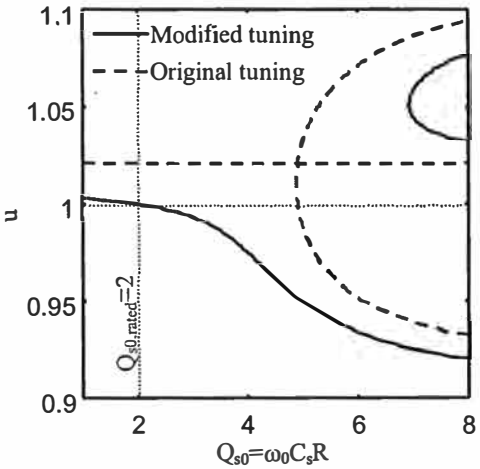


(ii) Power transfer capability.

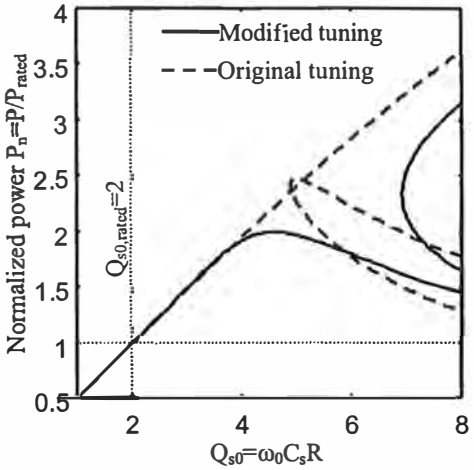
(c) A system where bifurcation occurs at $Q_{s0,rated}$.

Fig. 5-4. PP topology with loose coupling (k=0.05) - Operating frequency and power transfer capability under variable-frequency operation.

InductEV, Inc.
Exhibit 1010
Page 241

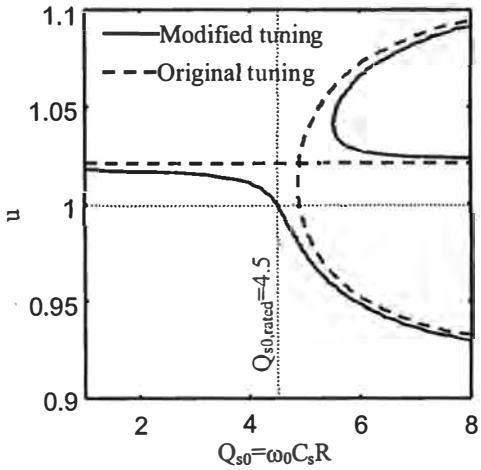


(i) Operating frequency.

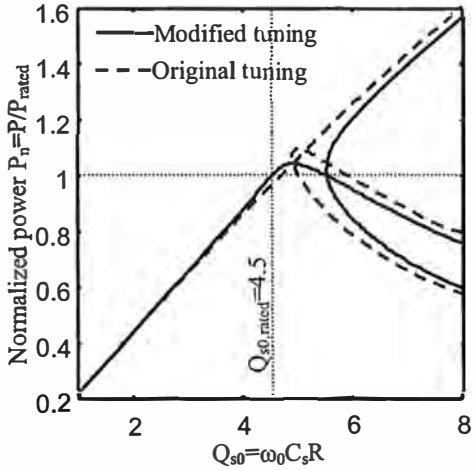


(ii) Power transfer capability.

(a) A system with $Q_{s0,rated}$ well within the bifurcation boundary.

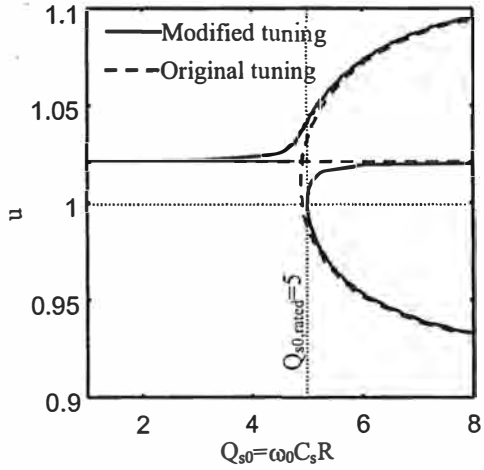


(i) Operating frequency.

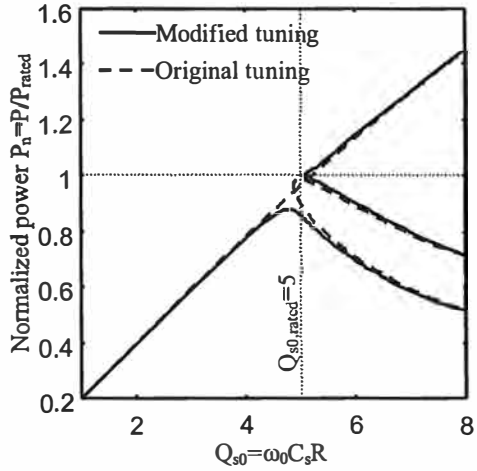


(ii) Power transfer capability.

(b) A system with $Q_{s0,rated}$ close to, but still within the bifurcation boundary.



(i) Operating frequency.

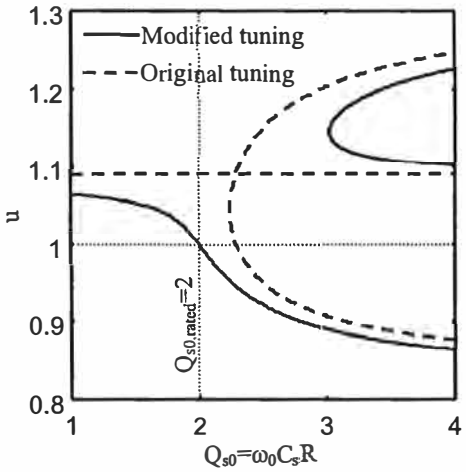


(ii) Power transfer capability.

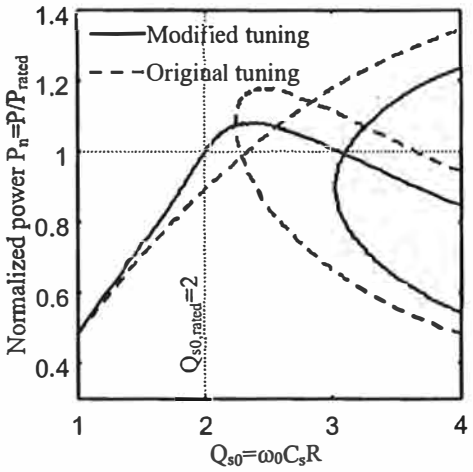
(c) A system where bifurcation occurs at $Q_{s0,rated}$.

Fig. 5-5. PP topology with middle coupling (k=0.2) - Operating frequency and power transfer capability under variable-frequency operation.

InductEV, Inc.
Exhibit 1010
Page 242

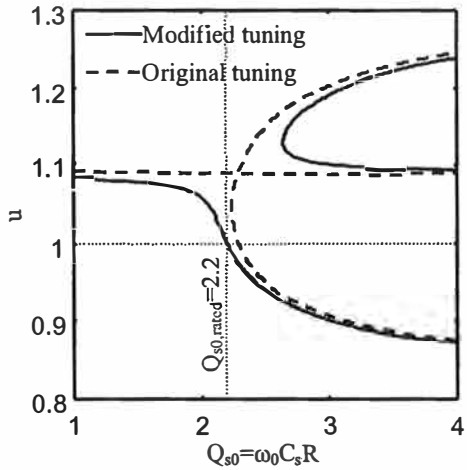


(i) Operating frequency.

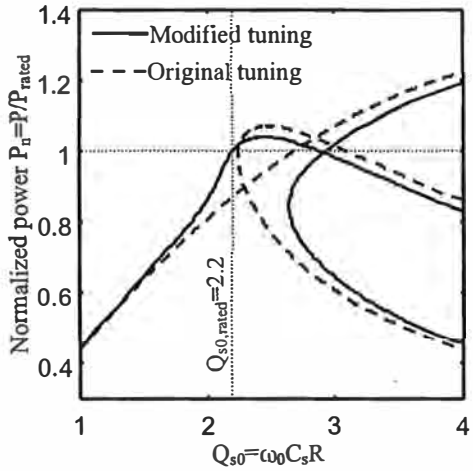


(ii) Power transfer capability.

(a) A system with $Q_{s0,rated}$ well within the bifurcation boundary.

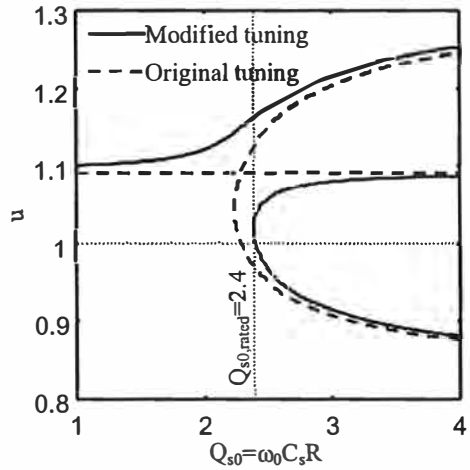


(i) Operating frequency.

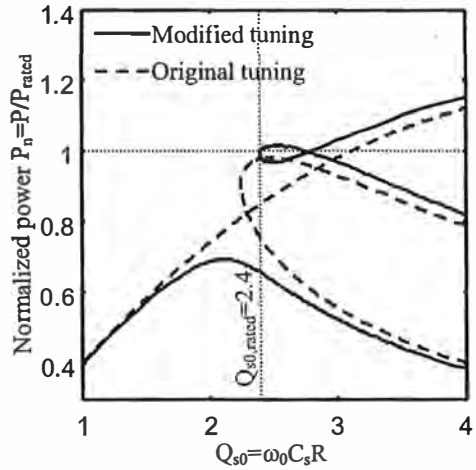


(ii) Power transfer capability.

(b) A system with $Q_{s0,rated}$ close to, but still within the bifurcation boundary.



(i) Operating frequency.

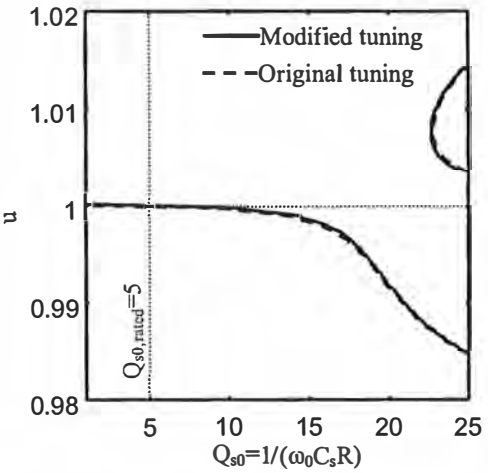


(ii) Power transfer capability.

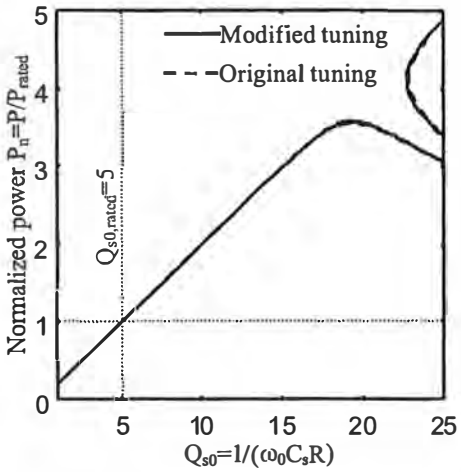
(c) A system where bifurcation occurs at $Q_{s0,rated}$.

Fig. 5-6. PP topology with good coupling (k=0.4) - Operating frequency and power transfer capability under variable-frequency operation.

InductEV, Inc.
Exhibit 1010
Page 243

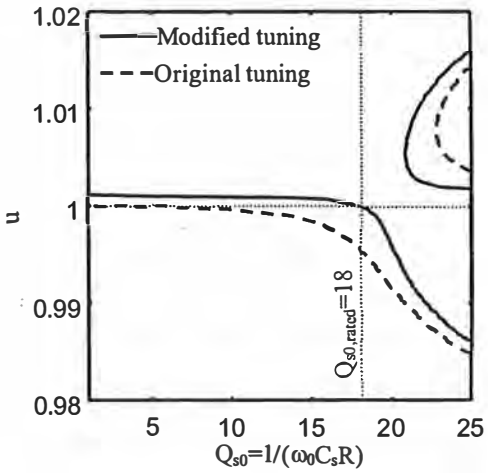


(i) Operating frequency.

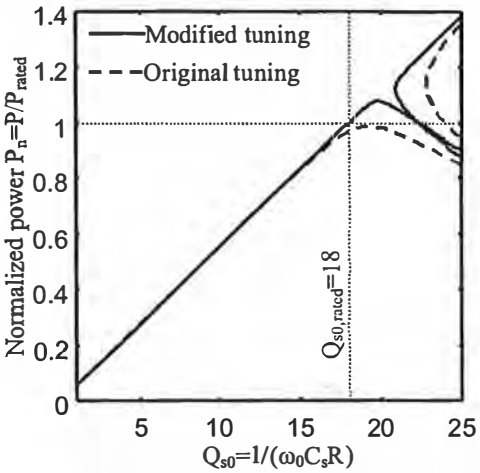


(ii) Power transfer capability.

(a) A system with $Q_{s0,rated}$ well within the bifurcation boundary.

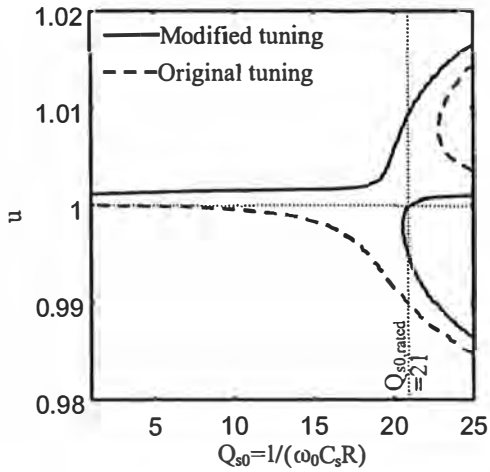


(i) Operating frequency.

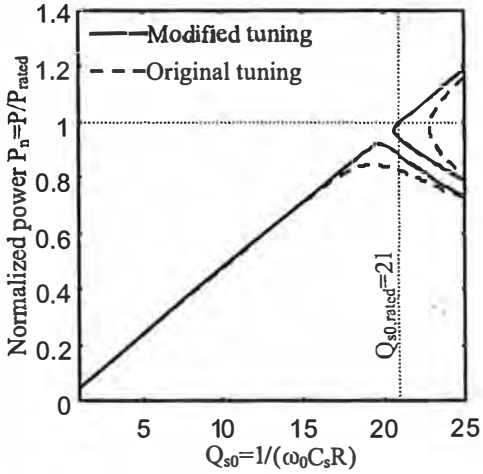


(ii) Power transfer capability.

(b) A system with $Q_{s0,rated}$ close to, but still within the bifurcation boundary.



(i) Operating frequency.

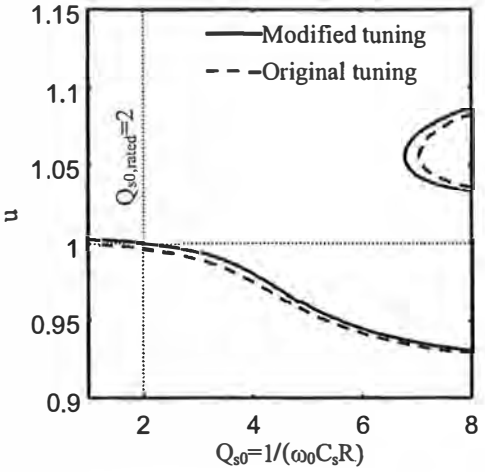


(ii) Power transfer capability.

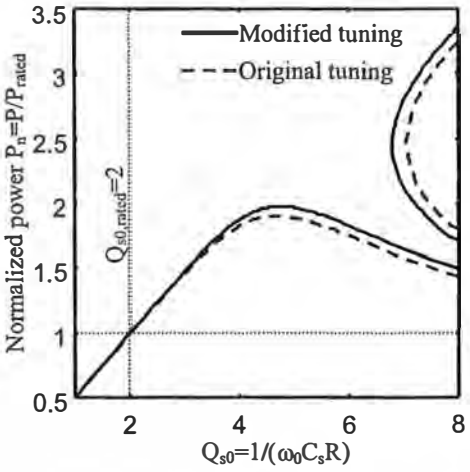
(c) A system where bifurcation occurs at $Q_{s0,rated}$.

Fig. 5-7. PS topology with loose coupling (k=0.05) - Operating frequency and power transfer capability under variable-frequency operation.

InductEV, Inc.
Exhibit 1010
Page 244

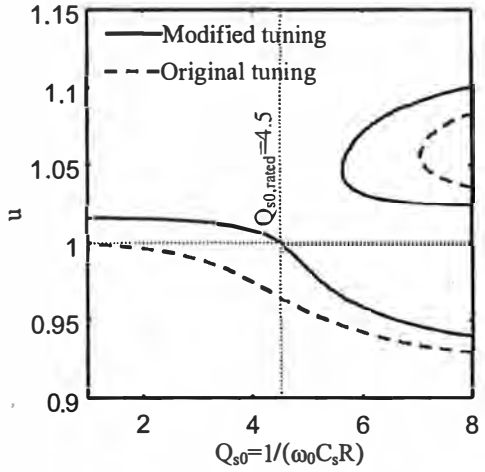


(i) Operating frequency.

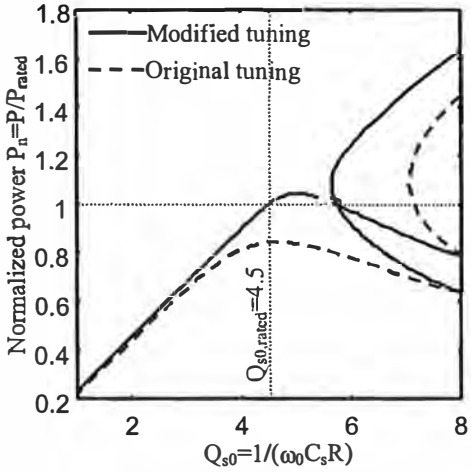


(ii) Power transfer capability.

(a) A system with $Q_{s0,rated}$ well within the bifurcation boundary.

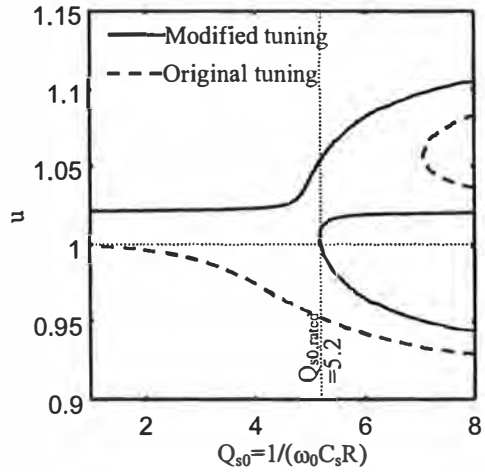


(i) Operating frequency.

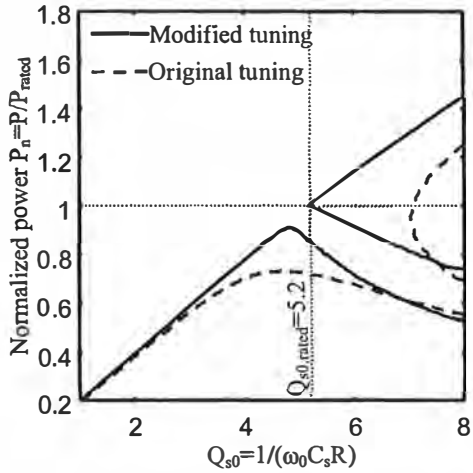


(ii) Power transfer capability.

(b) A system with $Q_{s0,rated}$ close to, but still within the bifurcation boundary.



(i) Operating frequency.

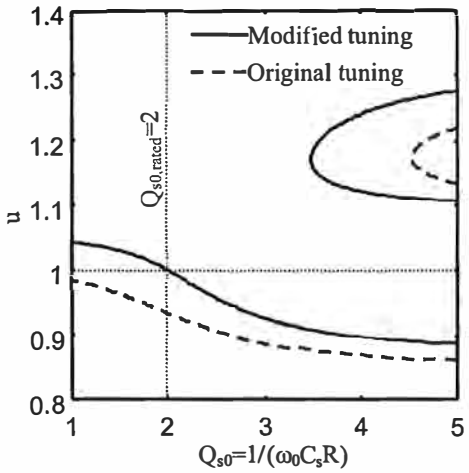


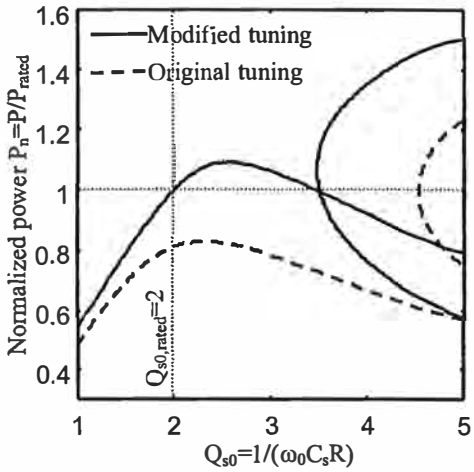
(ii) Power transfer capability.

(c) A system where bifurcation occurs at $Q_{s0,rated}$.

Fig. 5-8. PS topology with middle coupling (k=0.2) - Operating frequency and power transfer capability under variable-frequency operation.

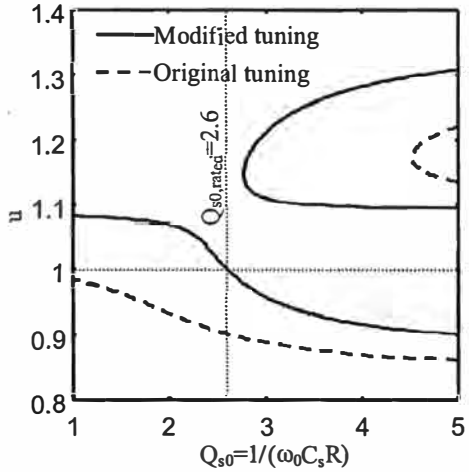
InductEV, Inc.
Exhibit 1010
Page 245

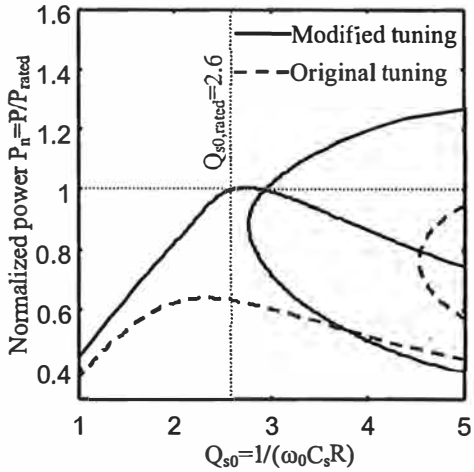




(i) Operating frequency. (ii) Power transfer capability.

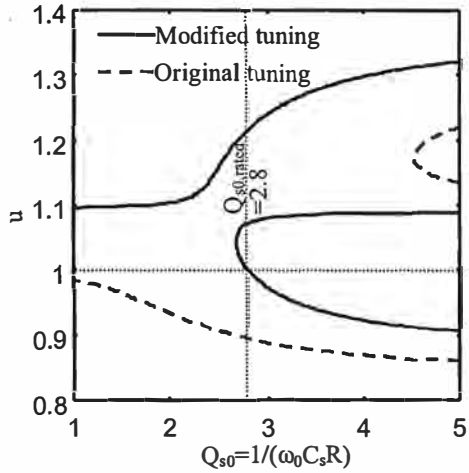
(a) A system with $Q_{s0,rated}$ well within the bifurcation boundary.

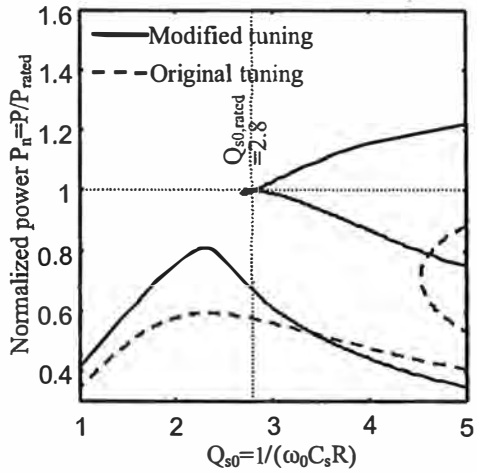




(i) Operating frequency. (ii) Power transfer capability.

(b) A system with $Q_{s0,rated}$ close to, but still within the bifurcation boundary.





(i) Operating frequency. (ii) Power transfer capability.

(c) A system where bifurcation occurs at $Q_{s0,rated}$.

Fig. 5-9. PS topology with good coupling (k=0.4) - Operating frequency and power transfer capability under variable-frequency operation.

InductEV, Inc.
Exhibit 1010
Page 246

The bifurcation boundary of the PS topology is slightly higher than SP and PP topologies. For the selected k of 0.05, 0.2 and 0.4, bifurcation occurs at Q_{s0} of about 20, 5.1 and 2.7. If $Q_{s0,rated}$ is well within the bifurcation boundary, the improvement in power transfer capability is negligible below rated load in low k systems. This improvement becomes significant when $Q_{s0,rated}$ is close to but within the bifurcation boundary in high k systems. With a k of 0.05, 0.2 and 0.4, the improvement in power transfer capability under this condition is about 4%, 18% and 59% respectively.

With the SP and PS topologies, bifurcation appears at a lower Q_s in comparison to the original tuning. While this appears to be a disadvantage under variable-frequency control as the safety margin before bifurcation is reduced, the original tuning cannot transfer more power despite larger Q_s in the pickup design due to increased pickup frequency detuning. The maximum available power with the original tuning actually occurs at a Q_s below the bifurcation boundary of the modified tuning. Further increase of Q_s results in a drop of the power transfer.

5-4 BIFURCATION CRITERIA

According to above analysis, it is crucial to ensure the system design is within the bifurcation boundary when applying the modified tuning proposed in this chapter. In order to develop simple design criteria to identify the bifurcation boundary, it is assumed in this section that C_p is given by (5-2) and therefore changes with the load when the primary is parallel compensated. In consequence, the developed bifurcation criteria are valid for all loading conditions if the primary is series compensated (the SS and SP topologies) where the required C_p is independent of the load, but is applicable only at rated load in parallel compensated primary systems (the PP and PS topologies) since here C_p is selected at rated load as it is impractical to allow C_p to vary with the load. Because bifurcation only occurs with increasing load, it is shown in section 5-6 that designing the system to meet the bifurcation criterion at rated load (with a small safety margin) can ensure bifurcation-free operation for all loading conditions up to and including rated load.

As shown earlier in Fig. 5-2 to 5-9, the bifurcation criteria are topology dependent functions of k and Q_s. The theoretical analysis in this section investigates the full range of k and Q_s to develop general bifurcation criteria that can be used for any practical system design. For a given k (a specified electromagnetic structure), Q_s is allowed to vary in theory from a low value to a high value, and bifurcation appears if Q_s is greater than a boundary value determined by the bifurcation criteria. This process can be repeated with varying k values. The objective is to identify all theoretical k and Q_s where bifurcation occurs. The results can then be applied to any design where practical values of k and Q_s are known. Theoretically, a suitable trade-off between k and Q_s can be determined according to the

InductEV, Inc.
Exhibit 1010
Page 247

bifurcation criteria. In most designs, the electromagnetic structure is optimised to achieve the best k and here the bifurcation criteria can be used to determine the maximum allowable Q_s.

As noted in section 3-9, the fundamental design parameters k, Q_{p0} and Q_{s0} are related as:

$$Q_{p0} = \begin{cases} \dfrac{1}{k^2 Q_{s0}} & \text{series secondary} \\ \dfrac{1}{k^2 Q_{s0}} - \dfrac{1}{Q_{s0}} & \text{parallel secondary} \end{cases} \tag{5-9}$$

The bifurcation criteria can therefore be expressed in terms of Q_{p0} and Q_{s0} as well. In this section, the bifurcation criteria are developed first as relationships between Q_{p0} and Q_{s0}. They are then re-expressed in terms of k and Q_{s0} using (5-9).

Under ideal conditions, C_p can be assumed to be given by (5-2) so that pickup frequency detuning is eliminated at all loading conditions. Thus the normalized reactance of C_p (as derived in Appendix H) is a function of u, Q_{p0} and Q_{s0} given by:

$$\frac{1}{\omega C_p (\mathrm{Re}\, Z_{r0})} = \begin{cases} \dfrac{Q_{p0}}{u} & \text{series primary} \\ \dfrac{1+Q_{p0}^2}{uQ_{p0}} & \text{parallel primary} \end{cases} \tag{5-10}$$

When operating at the desired frequency that ensures unity DPF, the fundamental inverter output voltage and current of the power supply are in phase. This zero phase angle frequency can be calculated by determining the point at which the normalized load reactance is zero (Im Z_{tn}=0). However, for parallel-compensated primary systems, it is often mathematically easier to look at the normalized load susceptance (Im Y_{tn}=0). The normalized load impedance in Table 5-2 and 5-3 is once again used in this analysis with the normalized reactance of C_p replaced by (5-10).

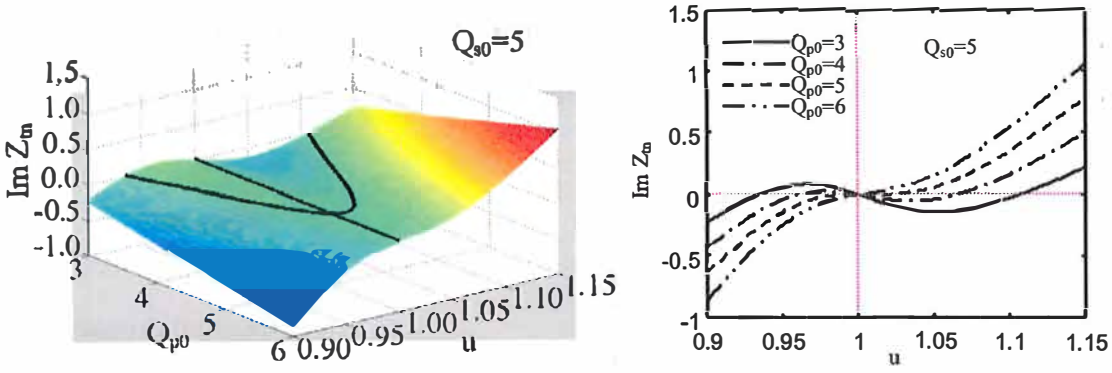
The normalized load reactance of series compensated primary systems (the SS and SP topologies) is shown in Fig. 5-10 as a function of u and Q_{p0}, with Q_{s0} fixed at 5. Similar graphs can be drawn for other values of Q_{s0}. The zero phase angle frequencies are shown as black lines on the surfaces. The cross-sections of these surfaces at selected values of Q_{p0} are also shown for comparison.

Generally, the SS and SP topologies exhibit similar features. The zero phase angle frequency is unique and identical to the secondary resonant frequency (u=1) if the primary quality factor is much larger than the secondary quality factor ($Q_p >> Q_s$). However, there are three zero phase angle frequencies when the primary quality factor is much lower than the secondary quality factor ($Q_p << Q_s$). One of these zero phase angle frequencies is identical to the secondary resonant frequency. The differences between these three zero phase angle frequencies increases as the primary quality factor Q_p

InductEV, Inc.
Exhibit 1010
Page 248

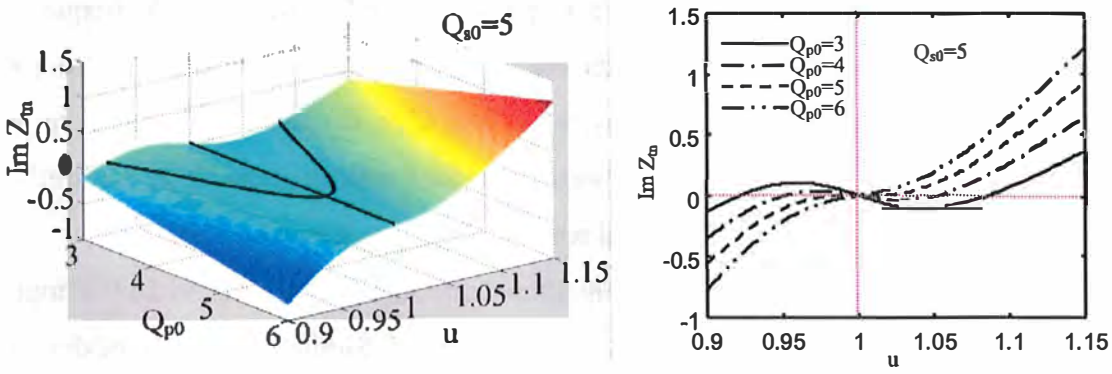
is reduced.

The normalized load susceptance of parallel-compensated primary systems is shown in Fig. 5-11. As shown, the PP and PS topologies have similar features to the afore mentioned SS and SP topologies. For all basic topologies, not only are the zero phase angle frequency curves similar, but also the normalized load reactance surfaces of series compensated primary systems are similar to the normalized load susceptance surfaces of parallel-compensated primary systems. Consequently, it is possible to develop a general analysis of the zero phase angle frequencies for all basic topologies (SS, SP, PP and PS). This approach is used in this section to develop general bifurcation criteria thereby enabling the bifurcation boundary conditions to be precisely specified.



(i) Surface function. (ii) Cross sections of the surface.

(a) SS topology.



(i) Surface function. (ii) Cross sections of the surface.

(b) SP topology.

Fig. 5-10. Normalized load reactance.

InductEV, Inc.
Exhibit 1010
Page 249